# MECHANISMS OF INTESTINAL PHOSPHATE ABSORPTION AND THE EFFECT OF DIET-INDUCED IRON DEFICIENCY ON PHOSPHATE HOMEOSTASIS

**By**

**Evans Ohenhen Asowata**

**Thesis submitted for the degree of Doctor of Philosophy in the Division of Biosciences, School of Life and Medical Sciences University College London, London, United Kingdom**

**Epithelial Physiology Group**
**Department of Neuroscience, Physiology & Pharmacology**
**University College London**
**Royal Free Campus**
**Rowland Hill Street**
**London**
**NW3 2PF**

**2019**

## Declaration

I, Evans Ohenhen Asowata, confirm that the work presented in this thesis is my own. Where information has been derived from other sources, I confirm that this has been indicated in the thesis.

**Abstract**

Intestinal phosphate absorption occurs via a sodium-dependent mechanism, known to be NaPi-IIb-mediated, and a sodium-independent mechanism, thought to be mediated via the paracellular pathway. Emerging evidence suggests that the paracellular pathway is likely to be more dominant and that this pathway is regulated by NHE3. Studies in rats, mice and humans have shown some species differences in the efficacy of both NaPi-IIb and NHE3 inhibitors on intestinal phosphate absorption, thus, the suitability of rodents as experimental models to study phosphate absorption is uncertain. Furthermore, recent reports suggest that alterations in iron levels influence phosphate homeostasis, although there are conflicting reports regarding how it affects intestinal phosphate absorption. In this study, the mechanisms of phosphate absorption in the small intestine of rats, mice and humans were compared, and the effect of diet-induced iron deficiency on these mechanisms was investigated. The result showed a similar profile for intestinal NHE3 in rats and humans, suggesting that the rat is a more appropriate model to study the mechanisms of paracellular phosphate absorption. Using *in vivo* and *in vitro* uptake experiments, iron deficiency was demonstrated to significantly inhibit phosphate absorption in the duodenum and jejunum of rats. The findings of this study demonstrated that NaPi-IIb expression or activity was unaffected by iron deficiency. However, while the sodium-independent phosphate transport pathway was most affected in the duodenum, NHE3 activity was inhibited in the jejunum, in response to iron deficiency. Interestingly, iron deficiency resulted in increased expression of duodenal claudin 3, while also causing the expected upregulation of DMT1 in the duodenum and jejunum. It is therefore hypothesised that increased DMT1 expression, in addition to the inhibition of jejunal NHE3 activity by iron deficiency, may locally impact phosphate

absorption by a mechanism involving the accumulation of intracellular protons leading to the sealing of the paracellular pathway.

**Impact statement**

This study aims to improve our understanding of intestinal phosphate absorption and address the potential discrepancies in the efficacy of NaPi-IIb and NHE3 inhibitors in the inhibition of intestinal phosphate absorption in rodents and humans. The recently reported negative clinical outcomes from the use of NaPi-IIb inhibitors in the treatment of hyperphosphataemia in CKD patients may be because this transporter was found to be most highly expressed in the shortest segment of the human small intestine, the duodenum, known to have the shortest sojourn time of food. In addition, under normal phosphate concentration in the intestinal lumen, NaPi-IIb would likely become saturated and therefore, its function would be limited.

NHE3 has recently been linked to paracellular phosphate transport, and the findings of this study confirm its role in mediating phosphate absorption in rats, but not in mice. Interestingly, this is the first study to show that the regional expression of NHE3 in the small intestine of rats and humans are similar. This may explain why the findings that tenapanor, an NHE3 inhibitor that effectively inhibits phosphate absorption in rats translate into improved management of hyperphosphataemia in humans with CKD. Based on these findings, pre-clinical studies and future experiments aimed at discovering new compounds for inhibiting intestinal phosphate absorption in patients with hyperphosphataemia should be carried out using rats.

This study is the first to show that diet-induced iron deficiency inhibits intestinal phosphate absorption, and this is potentially why iron deficiency, the most common micronutrient deficiency globally, has recently been linked to bone disease. The reduction of intestinal phosphate absorption in iron deficient

conditions may cause a potential dip in postprandial serum phosphate levels and this may result in the breakdown of bone mineral to buffer the change in serum phosphate. Increased bone resorption may be one of the causes of bone disease in iron deficient individuals. Therefore, it is important to educate the public to consume iron-rich diets to prevent not only iron deficiency anaemia, but also rickets in children or osteoporosis in adults.

The findings of this study provide the first evidence that diet-induced iron deficiency inhibits intestinal phosphate absorption by a mechanism that potentially involves the upregulation of DMT1 and claudin 3 in the duodenum. In addition, diet-induced iron deficiency also causes jejunal DMT1 upregulation and inhibits NHE3-regulated paracellular phosphate absorption in this intestinal segment. The hypothesis is that DMT1 not only mediates iron absorption, but also activates mechanisms that result in the inhibition of intestinal phosphate absorption. These findings linking DMT1 and the inhibition of intestinal phosphate absorption may present a significant breakthrough in the management of hyperphosphataemia in CKD patients. To bring about the impact of this potential breakthrough, further studies in collaboration with pharmaceutical companies should be aimed at identifying compounds that can increase DMT1 levels in the small intestine of CKD patients. These compounds, if identified, will potentially increase intestinal iron absorption and reduce that of phosphate, thus, correcting two major clinical problems in CKD patients, iron deficiency anaemia and hyperphosphataemia.

**Acknowledgement**

I wish to express my profound gratitude to my supervisors, Dr Joanne Marks and Professor Robert Unwin for accepting me into your group. I am extremely grateful for training me in Physiology research and for the knowledge you both imparted in me throughout my PhD programme. My inestimable thanks go to Dr Joanne Marks for the confidence you have instilled into me, and the fact that I have more belief in myself now is a clear indication of how much you have improved me. I sincerely thank you both for the financial support you granted me to continue my research. I would also like to thank Professor Kaila Srai for his contribution to the design of this study and the suggestions going forward.

I would like to thank Professor Antonio Di Sabatino from IRCCS San Matteo Hospital, Pavia, Italy, and Professor Lars Fandriks and Dr Anna Casselbrant from the University of Gothenburg, Gothenburg, Sweden, for providing the human intestinal biopsies for this study.

I would also like to thank all staff and colleagues of the first-floor division of Nephrology for creating the enabling environment for me to carry out my research. Many thanks to Dr Barbara Jensen, Dr Gregory Jacquillet and Dr Felice Leung for their support in the laboratory. To Tobi Olusanya, my lab colleague and dearest friend, words alone cannot describe how thankful I am for the times you listened and encouraged me during difficult moments. Special thanks to Dr Anselm Zdebik for the invaluable advice and technical support in times of technical difficulty.

Many Thanks to the Nigerian government for granting me a scholarship to embark on this academic journey.

Finally, a huge thank you to my mum and every member of my family for the financial support and continuous encouragements, especially when I doubted whether I would ever be able to complete this PhD research programme.

**Abbreviations**

| | |
|---|---|
| $1,25(OH)_2D_3$ | 1, 25-dihydroxycholecalciferol |
| ADHR | Autosomal dominant hypophosphataemic rickets |
| ANOVA | Analysis of variance |
| ANP | Atrial natriuretic factor |
| ATP | Adenosine triphosphate |
| BBE | Brush border epithelia |
| BBM | Brush border membrane |
| cAMP | Cyclic adenosine monophosphate |
| cDNA | Complementary deoxyribonucleic acid |
| cGMP | Cyclic guanosine monophosphate |
| CKD | Chronic kidney disease |
| DMT | Divalent metal transporter |
| DNA | Deoxyribonucleic acid |
| EDTA | Ethylenediaminetetraacetic acid |
| EGTA | Ethylene glycol-bis (2-aminoethyl)-N,N,N',N'-tetraacetic acid |
| ELISA | Enzyme-linked immunosorbent assay |
| ER | Estrogen receptor |
| ERK | Extracellular signal-regulated kinase |
| ESRD | End-stage renal disease |
| FGF | Fibroblast growth factor |
| FGFR | Fibroblast growth factor receptor |
| GABA | Gamma aminobutyric acid |
| GABARAP | Gamma aminobutyric acid receptor-associated protein |
| GLUT | Glucose transporter |
| GTP | Guanosine triphosphate |
| HEPES | 4-(2-hydroxyethyl)-1-piperazineethanesulfonic acid |

| | |
|---|---|
| HNF | Hepatocyte nuclear factor |
| HRP | Horseradish peroxidase |
| IGF | Insulin-like growth factor |
| JAK | Janus kinase |
| JNK | c-Jun N-terminal kinase |
| $K_m$ | Affinity constant |
| MAPK | Mitogen-activated protein kinase |
| MDCK | Madin-Darby canine kidney |
| MEPE | Matrix extracellular phosphoglycoprotein |
| mRNA | Messenger ribonucleic acid |
| NaPi | Sodium-dependent phosphate cotransporter |
| NHE3 | Sodium/hydrogen exchanger |
| NHERF | Sodium/hydrogen exchanger regulatory factor |
| OSR | Oxidative stress-responsive kinase |
| PBS | Phosphate buffered saline |
| PBS-T | Phosphate buffered saline and tween 20 |
| PDZ | Post-synaptic density protein (P), Drosophila disc large tumour suppressor (D), zonular occludens-1 protein (Z) |
| PFA | Phosphonoformic acid |
| PiT | Phosphate transporter |
| PKA | Protein kinase A |
| PKC | Protein kinase C |
| PKG | Protein kinase G |
| PLC | Phospholipase C |
| PMSF | Phenylmethylsulfonyl fluoride |
| PTH | Parathyroid hormone |
| PTHR | Parathyroid hormone receptor |
| PVDF | Polyvinylidene difluoride |

| | |
|---|---|
| RANKL | Receptor activator of nuclear factor kB ligand |
| RNA | Ribonucleic acid |
| RTase | Reverse transcriptase |
| RT-PCR | Real-time polymerase chain reaction |
| SEM | Standard error of mean |
| sFRP | Secreted frizzled-related protein |
| SGK | Serum glucocorticoid-regulated kinase |
| SGLT | Sodium glucose cotransporter |
| SLC | Solute carrier |
| SPAK | SPS1-related proline/alanine-rich kinase |
| TAE | Tris-acetate-EDTA |
| TEER | Transepithelial electrical resistance |
| TIBC | Total iron-binding capacity |
| TMBZ | 3,3’,5,5’-Tetramethylbenzidine |
| TMD | Transmembrane domain |
| UIBC | Unsaturated iron-binding capacity |
| VDR | 1, 25-dihydroxycholecalciferol receptor |
| WNK | With-no-lysine protein kinase |

**Table of content**

**List of Tables and Figures**

# Chapter One

## 1.0. Introduction

## 1.0. Introduction to phosphate homeostasis and mechanisms of phosphate transport

Inorganic phosphate is essential for the following physiological processes: generation of adenosine triphosphate (ATP), biosynthesis of nucleotides and proteins, cell signalling and bone mineralisation. Phosphate is also known to be a major component of the phospholipid bilayer of cell membranes. Because of these important functions, the maintenance of phosphate balance is necessary for survival. Phosphate imbalance is seen in inherited disorders such as X-linked hypophosphataemic rickets and tumoral calcinosis [1], and in acquired disorders like chronic kidney disease (CKD) [2,3]. In addition, consistent consumption of excess phosphate from natural and processed food may increase serum phosphate levels, and this poses significant risks to the health of the general population. High serum phosphate levels (hyperphosphataemia) in healthy individuals and CKD patients have been linked to increased risk of cardiovascular diseases [2,4]. With the high global prevalence of CKD [5], a condition associated with hyperphosphataemia, studies into understanding the mechanisms of phosphate homeostasis are gaining significant attention. A better understanding of these mechanisms will be invaluable in generating new management therapies for the management of phosphate imbalance.

### 1.1. Phosphate homeostasis

Phosphate homeostasis is the maintenance of extracellular phosphate levels within narrow physiological limits. In healthy adults, serum phosphate ranges from 0.8 – 1.45 mmol/l (2.5 – 4.5 mg/dl) [6]. It is generally accepted that three key systems regulate phosphate balance: the bone-phosphate buffering system, the gastrointestinal system and the renal system, and the interaction between these

systems is regulated by a complex hormonal axis [7–11]. While the bone rapidly buffers acute changes in serum phosphate, the renal system plays a more significant role in the long-term regulation of phosphate levels. The gastrointestinal system is involved in the digestion of phosphate-containing food and the subsequent absorption of phosphate into the circulation. Therefore, this system contributes to phosphate homeostasis by replenishing the extracellular phosphate pool during negative phosphate balance. The renal system acts as the major regulator of phosphate homeostasis by adjusting the levels of phosphate in the extracellular fluid in response to changes in phosphate absorption by the small intestine and phosphate shuttling from bone (Figure 1.1).

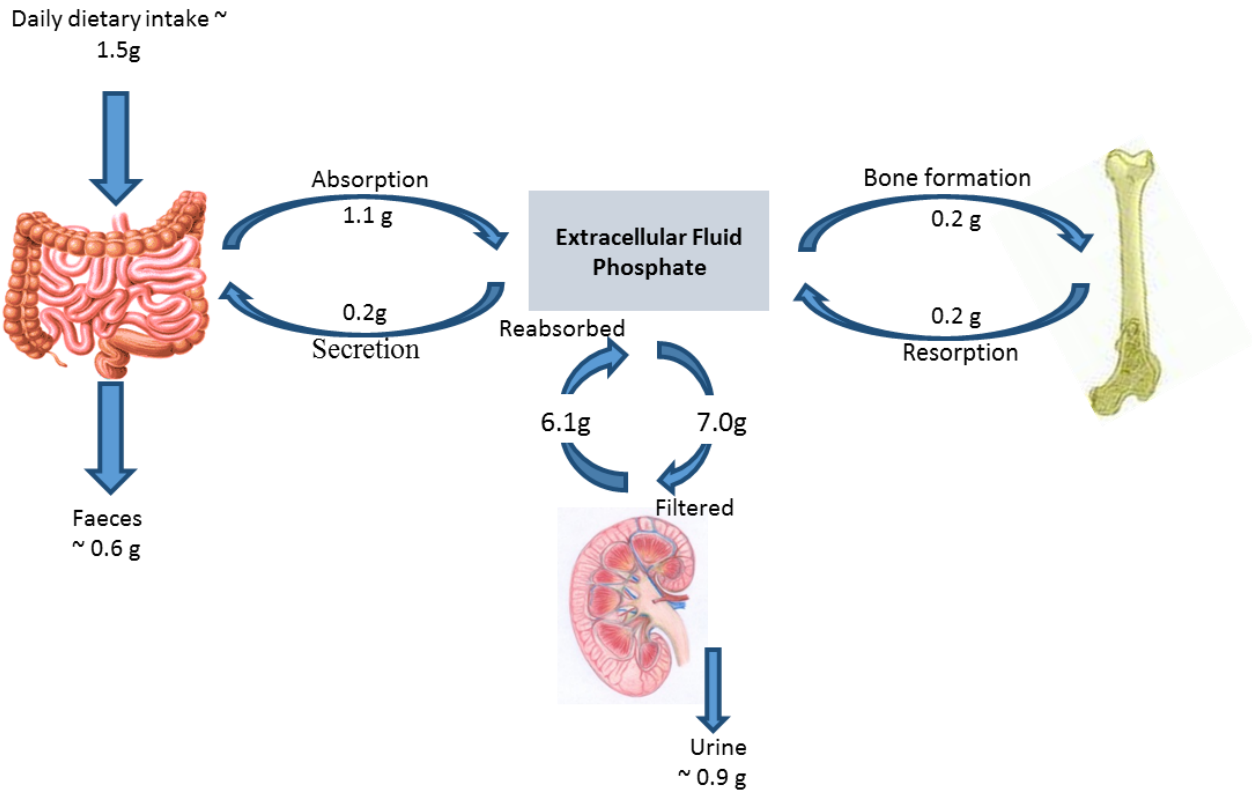


**Figure 1.1. Systems involved in phosphate homeostasis**. To maintain phosphate homeostasis, dietary phosphate intake is the same as the sum of the amount of phosphate excreted in urine and faeces. Bone acts as a reservoir for phosphate, where it is deposited and subsequently mobilised into the extracellular fluid when necessary.

The regulation of phosphate balance by the renal system involves changes in the expression of specific membrane transporters that facilitate proximal tubular reabsorption of phosphate. Two families of transporters mediate the transport of phosphate in the renal proximal tubule, of which the solute carrier, SLC34 family or type II phosphate transporters are known to be the major players, while the SLC20 or type III phosphate transporters only play a minor role (reviewed in [12,13]). During positive phosphate balance, which could result from excessive intake of dietary phosphate, the expression of these transporters is downregulated resulting in an increase in urinary phosphate excretion. In contrast, these transporters are upregulated to conserve phosphate when extracellular phosphate levels are below normal physiological limits, or when intestinal phosphate absorption is significantly reduced during the intake of a low phosphate diet [14–17].

Intestinal phosphate absorption is mediated by both transcellular and paracellular mechanisms [18]. Like the renal system, transcellular or active phosphate transport in the small intestine is mediated by two families of phosphate transporters: type II and type III phosphate transporters (reviewed in [12,13]). Although the expression of the transcellular phosphate transporters changes in response to high or low dietary phosphate content [17,19], there is still a debate as to the overall contribution of the transcellular phosphate transport pathway in comparison to the paracellular pathway. Paracellular or passive phosphate transport is thought to involve the diffusion of phosphate across intestinal tight junctions. In contrast to the extensively studied transcellular phosphate absorption pathway, the paucity of information on the regulation of the paracellular pathway makes the small

intestine an area of intense focus in the search for management therapies for phosphate imbalance.

There is a body of evidence supporting the interaction between the systems involved in phosphate homeostasis [20,21]. In addition to the role of the small intestine in the absorption of phosphate, it has been speculated that the small intestine interacts with the kidneys by releasing an unknown phosphaturic factor [22]. However, due to the lack of evidence to support this hypothesis, it is now believed that this interaction between the small intestine and the kidneys may be as a result of changes in the levels of the systemic regulators of phosphate in response to postprandial phosphate levels [23,24]. More importantly, the accepted osteo-renal interaction involving the action of the bone-derived phosphaturic factor fibroblast growth factor-23 (FGF-23), on the renal phosphate transporters is responsible for the maintenance of phosphate homeostasis [25]. The release of FGF-23 in response to elevated extracellular phosphate levels following dietary phosphate intake links the small intestine to the osteo-renal mechanism of phosphate metabolism, and these interactions maintain phosphate balance.

### 1.2. $Na^+$-dependent phosphate cotransporters

Three families of $Na^+$-dependent phosphate cotransporters have been identified: type I, type II, and type III transporters [26–28]. These transporters are integral membrane proteins, which are involved in the active transport of phosphate across epithelial cells. The mechanism driving this active transport process involves the action of the $Na^+/K^+$ ATPase in the basolateral membrane of the epithelia cells. The $Na^+/K^+$ ATPase generates the $Na^+$ gradient required for the downhill transport of $Na^+$ coupled to phosphate. A large body of evidence suggests that the type II phosphate transporters are the most important

transporter family involved in the maintenance of phosphate homeostasis (reviewed in [20]), while there is no significant evidence for the contribution of the type I and type III transporters.

### 1.2.1. $Na^+$-dependent phosphate cotransporter type II

The $Na^+$-dependent phosphate cotransporter type II (NaPi-II) have been shown to be vital for the reabsorption of phosphate in the renal proximal tubules [29,30] and the small intestine [31]. The SLC34 genes encode this family of transporters, and the transport proteins derived from these genes are inserted on the brush border membrane (BBM) of the cell to mediate phosphate transport. The members of the SLC34 gene family of phosphate transporters are SLC34A1 (NaPi-IIa), SLC34A2 (NaPi-IIb) and SLC34A3 (NaPi-IIc) [32]. Although these transporters belong to the same family and share similar structural homology, their tissue distribution (Table 1.1.) and transport kinetics show transporter-specific features (Table 1.2).

**Table 1.1. Tissue distribution of the $Na^+$-dependent phosphate cotransporter type II**

| Transporter | Tissue distribution | References |
|---|---|---|
| NaPi-IIa | Kidney, Brain and osteoclasts. | 33–37 |
| NaPi-IIb | Small intestine, salivary gland, mammary gland, Lungs, liver, thyroid gland, uterus, ovary, prostate gland and testes. | 37–41 |
| NaPi-IIc | Kidney, spleen, testes, brain, colon, skin and ovary. | 33,34,37 |

#### 1.2.1.1. Localisation of the type II $Na^+$-dependent phosphate transporters

Under normal dietary conditions, NaPi-IIa is localised in all segments (S1-S3) of the proximal tubule, while NaPi-IIc is localised only in the S1 segment (Figure

1.2) [33,34]. In rodents, the expression and localisation of NaPi-IIa and -IIc proteins changes with age [42,43]. Compared to weaned rats, preweaned rats show higher levels of the renal NaPi-II proteins, with similar levels in both superficial and juxtaglomerular nephron [42]. However, in weaned and adult rats, renal NaPi-II proteins are higher in the juxtaglomerular nephron [42]. Studies have shown that the relative distribution of NaPi-IIa and -IIc in the different segments of the superficial and juxtaglomerular nephrons is affected by dietary phosphate levels [44]. During dietary phosphate restriction, there are higher levels of these transporters in superficial nephrons compared to the juxtaglomerular nephrons [44]. In addition to the kidney, NaPi-IIa protein has also been identified in the brain [35] and bone cells [36], while only NaPi-IIc mRNA has been found in the spleen, testes, brain, colon, skin and ovary [37] (Table 1.1).

NaPi-IIb protein is expressed in the BBM of intestinal epithelial cells in rodents and humans (Figure 1.3). The distribution of this transporter throughout the whole length of the small intestine varies in different species [38,39]. In the mouse small intestine, NaPi-IIb is highly expressed in the ileum, with low expression levels detected in the duodenum and jejunum, unlike in rat where the jejunum shows the highest levels of NaPi-IIb [17,39]. The mouse ileum and rat jejunum have been demonstrated to have the highest expression of NaPi-IIb, and this protein is correlated with the highest rate of $Na^+$-dependent phosphate absorption in these intestinal segments [38,39,45]. Because of this correlation of intestinal NaPi-IIb with phosphate transport in these species, a higher rate of $Na^+$-dependent phosphate absorption in the human jejunum compared to the ileum [46] suggests that the expression levels of NaPi-IIb protein in rats and humans are similar. There is evidence for an age-dependent variation in the expression of NaPi-IIb in the small

intestine of rodents, with the highest expression observed in preweanling animals compared to adults [47,48]. The expression of NaPi-IIb protein has also been detected in the lungs, liver, salivary gland, thyroid gland, mammary gland, testes, ovary and the uterus [37,40,41].

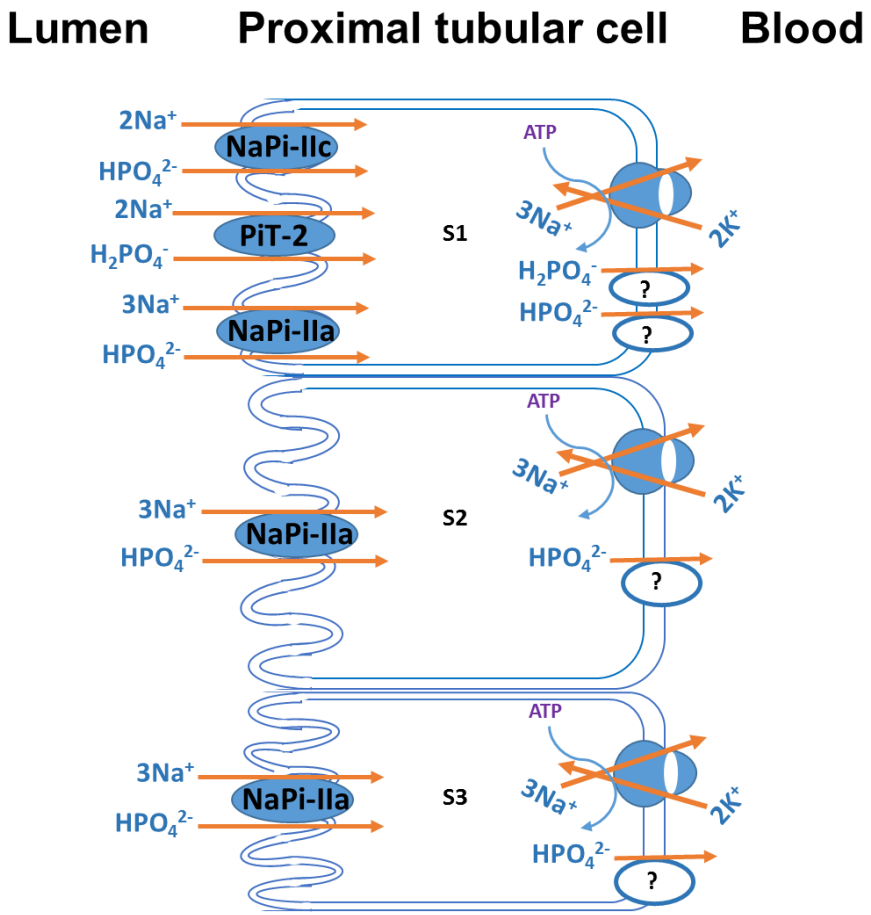


**Figure 1.2. Phosphate transport in the renal proximal tubule**. The type II (NaPi-IIa and NaPi-IIc) and type III (PiT-2) transporters mediate the transport of phosphate across the BBM of the proximal tubule (S1-S3 segments). These transporters are activated by the energy generated by the downhill transport of $Na^+$ across the BBM, with the concentration gradient of $Na^+$ maintained by the $Na^+/K^+$ ATPase pump at the basolateral membrane. The mechanism underlying the transport of phosphate across the basolateral membrane is currently unknown (?).

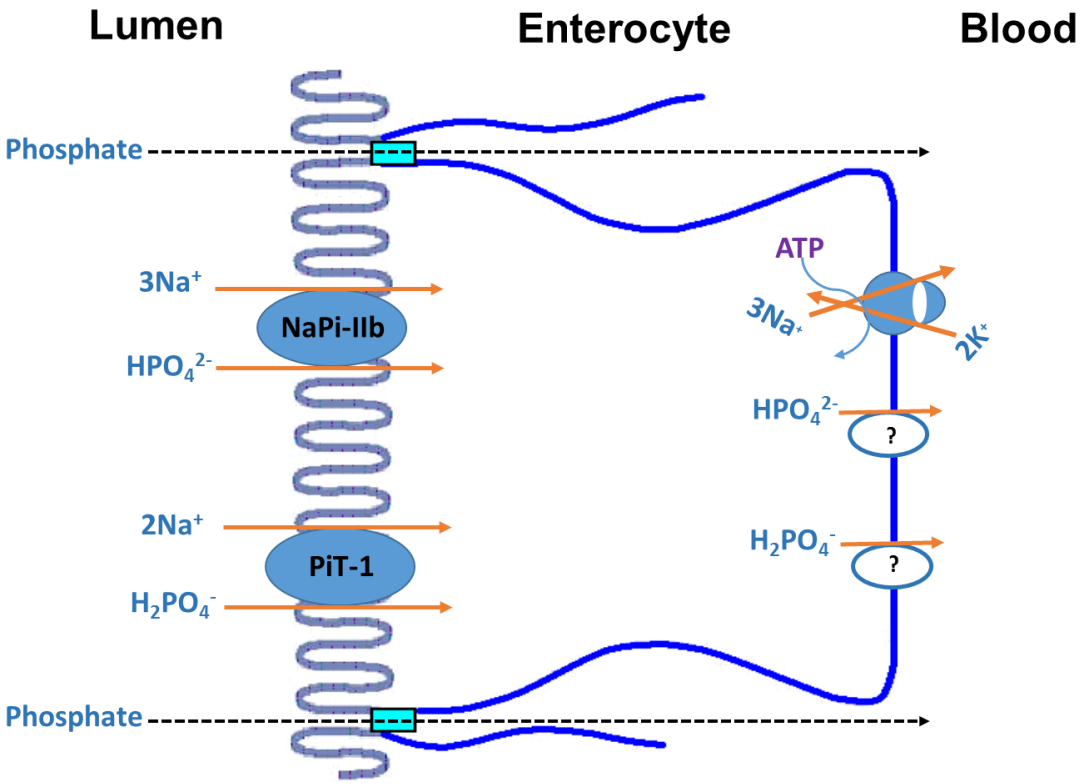


**Figure 1.3. Phosphate transport in the small intestine**. NaPi-IIb and PiT-1 mediate the active transport of phosphate across the BBM of the small intestine. These transporters are activated by the energy generated by the downhill transport of $Na^+$ across the BBM, with the concentration gradient of $Na^+$ maintained by the $Na^+/K^+$ ATPase pump at the basolateral membrane. The mechanism underlying the transport of phosphate across the basolateral membrane is currently unknown (?). Phosphate also diffuses passively through tight junctions, indicated by the dotted arrows.

### 1.2.1.2. Molecular structure of the type II $Na^+$-dependent phosphate transporters

The NaPi-II proteins are integral membrane proteins with 8 – 12 transmembrane domains (TMDs), with both the C- and N-terminal regions situated in the intracellular compartment [13,27,29,49]. Human NaPi-IIa is a protein with 639 amino acid residues [32] and has a molecular weight of approximately 70 kDa [50]. In comparison, the rat NaPi-IIa has been predicted to have a molecular weight of approximately 90 kDa, with 637 amino acid residues [51]. Human NaPi-IIb protein is made up of 689 amino acids, and its molecular weight varies between 77 – 108 kDa based on the degree of glycosylation [52], with the fully glycosylated protein known to have a molecular weight of 108 kDa [27,40]. Human NaPi-IIc is formed by 599 amino acid residues [32], with a molecular weight of approximately 75 kDa [27]. The structural topology of NaPi-IIa has been studied extensively in the last two decades. Using an *in vitro* translation approach, NaPi-IIa protein has been shown to have a large hydrophobic extracellular loop, situated between the 5$^{th}$ and 6$^{th}$ TMDs [53]. Two regulatory sites have been identified in the NaPi-IIa protein; the K-R motif, which interacts with PTH and a triglyceride-rich lipoprotein motif, which interacts with the PDZ proteins (discussed in more detail in section 1.2.1.5.2): NHERF1, NHERF2, NHERF3, NHERF4 and SHANK2E [54–56]. NaPi-IIc has been shown to interact with two PDZ proteins; NHERF1 and NHERF3 [57], with no convincing evidence for its interaction with the other PDZ proteins. Although NaPi-IIb has also been shown to interact with NHERF1, unlike NaPi-IIa and -IIc, evidence suggests that NaPi-IIb does not interact with NHERF3 [58]. The detailed structure of NaPi-IIb and NaPi-IIc is still under investigation; however, bioinformatics analysis suggests that the NaPi-IIb protein has at least 8 TMDs, 4 extracellular loops and 5 intracellular domains, with the N- and C-terminal regions

situated in the intracellular compartment [59], while NaPi-IIc has been predicted to have 8 TMDs [29].

Genetic mutation studies involving specific modifications in selected TMDs have revealed the relationship between the structural components of the transporters and their function. Mutation at Ser-460 (by replacing with Cysteine), a site at the top of the 9$^{th}$ TMD of NaPi-IIa, has shown that this site is critical for its cotransport function (reviewed in [13]). Similar sites in NaPi-IIb (Ser-448) and NaPi-IIc (Ser-437) have also been shown to play a role in the $Na^+$-phosphate cotransport function of these proteins [60,61]. The linker regions between TMD1 and 2, and TMD7 and 8 have been implicated in the voltage-activated structural changes necessary for their cotransport function [62]. The structural position of the N- and C-terminal regions of the NaPi-II proteins make both regions suited for interacting with regulatory molecules, both intracellular regulatory proteins and systemic regulators [13,27,49,63].

#### 1.2.1.3. Transport Kinetics of the type II $Na^+$-dependent phosphate transporters

NaPi-II proteins transport divalent phosphate ion ($HPO_4^{2-}$) via an active transport process that involves the downhill movement of $Na^+$ [64]. NaPi-IIa and NaPi-IIb transport phosphate with a $Na^+$: phosphate stoichiometry of 3:1 [61], while NaPi-IIc transports phosphate with a 2:1 stoichiometry (Table 1.2) [65]. The transport of phosphate by NaPi-IIa and NaPi-IIb results in the influx of a net positive charge into the cell, making both transporters electrogenic. However, no net positive charge is deposited in the intracellular compartment by NaPi-IIc-mediated phosphate transport, making this transporter an electroneutral phosphate carrier. Unlike NaPi-IIa and NaPi-IIb, the presence of charged aspartate as a member of

a conserved trio of amino acids at the bottom of the 4th TMD in NaPi-IIc confers the electroneutrality of this transporter [64,66]. Heterologous expression studies in *Xenopus oocytes* have shown that the process of activation of NaPi-IIa and -IIb involves the binding of $2Na^+$, which exposes the phosphate binding site, after which another $Na^+$ binds to cause a conformational change that results in the transport of phosphate into the cell [61]. In contrast, for NaPi-IIc, the binding of $1Na^+$ to an allosteric or immobile site on the extracellular region of the transporter catalytically exposes the phosphate and $Na^+$ binding sites, thus, allowing the binding of $2Na^+$ and divalent phosphate ion [60]. The binding of these ions causes a conformational change resulting in the transport of the bound divalent phosphate ion and $2Na^+$ [60]. The affinity for $Na^+$ and phosphate is similar in all NaPi-II proteins, with an affinity constant ($K_m$) of approximately 40 mM for $Na^+$ and < 100 µM for phosphate [32]. However, there is slight variations between the transporters (Table 1.2). These affinities are representative for the NaPi-II proteins at pH 7.4, which is the pH at which the transporters function optimally [67]. The kinetic properties of the NaPi-II proteins are significantly affected by changes in proton ($H^+$) concentration or pH [68]. Early findings suggested that changes in pH alter the interaction of the NaPi-II proteins with $Na^+$ due to an increase in the $K_m$ for $Na^+$ [69]. Additionally, their transport function may also be affected by the reduction of $HPO_4^{2-}$ to $H_2PO_4^-$ by a decrease in pH, thus, reducing the concentration of $HPO_4^{2-}$ available for binding with the NaPi-II proteins [68]. It is now believed that the overall effect of $H^+$ on the function of the NaPi-II proteins is the sum of the effects due to changes in the $K_m$ for $Na^+$ and the divalent-monovalent phosphate ion shuttling [70].

**Table 1.2. Kinetic features of the $Na^+$-dependent phosphate cotransporter type II**

| **Properties** | **NaPi-IIa** | **NaPi-IIb** | **NaPi-IIc** |
|---|---|---|---|
| Stoichiometry ($Na^+$: $HPO_4^{2-}$) | 3:1 | 3:1 | 2:1 |
| $K_m$ for $Na^+$ (mM) | ~ 45 | ~ 30 | ~ 45 |
| $K_m$ for $HPO_4^{2-}$ (µM) | ~ 50 | ~ 50 | ~ 70 |
| Electrogenicity | Electrogenic (+1) | Electrogenic (+1) | Electroneutral (0) |
| Effect of pH on activity | Reduces in low pH | Increases in low pH | Reduces in low pH |
| Transport capacity | High | High | Low |

### 1.2.1.4. Inhibitors of the type II $Na^+$-dependent phosphate transporters

To understand the role of the renal and intestinal NaPi-II proteins, studies into generating experimental inhibitors of the activities of these proteins have been carried out extensively. Among the inhibitors examined, phosphonoformic acid (PFA), which is a competitive inhibitor, remains the most potent, readily available and widely accepted inhibitor of the function of these transporters [71]. Like PFA, nicotinamide has been shown to inhibit the function of both intestinal and renal type II transporters [72,73]. In addition, arsenate has been reported to act as a competitive inhibitor of NaPi-IIb, with high affinity of NaPi-IIb for arsenate due to the structural similarity of arsenate to $HPO_4^{2-}$ [74]. Both arsenate and nicotinamide are known to negatively affect cellular metabolism and are therefore not commonly used as experimental inhibitors of NaPi-II proteins. Azaindole analogues, especially PF-06869206, have been recently shown to be a new group of orally bioavailable NaPi-IIa specific inhibitors [75]. In addition, there is

evidence in rodents showing that two new compounds ASP3325 [76] and NTX9066 [77] potently inhibit NaPi-IIb.

#### 1.2.1.5. Regulation of the type II $Na^+$-dependent phosphate transporters

The regulation of the levels of NaPi-II proteins at the BBM of renal and intestinal cells involves both systemic and cellular regulators. The cellular regulators include protein kinases such as protein kinase A (PKA), protein kinase C (PKC) and protein kinase G (PKG); and the scaffolding proteins (e.g. NHERF1 and NHERF3) associated with the C-terminal of the NaPi-II proteins. These scaffolding proteins are widely known to mediate the effects of the systemic regulators on the levels of the NaPi-II proteins at the BBM.

##### 1.2.1.5.1. Systemic regulators of the type II $Na^+$-dependent phosphate transporters

A large body of evidence supports the role of parathyroid hormone (PTH), FGF-23, α-klotho, 1,25-dihydroxycholecalciferol ($1,25(OH)_2D_3$), and dietary phosphate in the regulation of the expression of the NaPi-ll proteins. In addition, dopamine, atrial natriuretic peptide (ANP), Insulin-like growth factor 1 (IGF-1), matrix extracellular phosphoglycoprotein (MEPE), secreted frizzled-related protein-4 (sFRP-4), fibroblast growth factor-7 (FGF-7), estrogen, glucocorticoids and metabolic acidosis affect the expression or activity of these transporters (reviewed in [20]).

###### 1.2.1.5.1.1. PTH

PTH is an 84 amino acid polypeptide hormone, which is synthesised and released from the parathyroid gland in response to changes in circulating calcium ($Ca^{2+}$), phosphate, $1,25(OH)_2D_3$ and FGF-23 levels [78,79]. This hormone has been shown to downregulate the expression of NaPi-IIa within minutes after binding to its

receptor in the renal proximal tubule [79–81]. The mechanisms underlying this role of PTH in the downregulation of NaPi-lla has been reported to involve post-translational shuttling of the protein from the BBM to intracellular sites where the protein is degraded [80]. It has been hypothesised that the regulation of the transcription of NaPi-IIa by acute exposure of renal proximal tubular epithelial cells to PTH does not contribute to its role in the reduction of the abundance of this transporter at the BBM [54], however, it is possible that persistently elevated PTH levels may inhibit the transcription of NaPi-IIa mRNA. PTH acts by binding to the PTH-type 1 receptor (PTHR1) [82], which is a G-protein coupled receptor localised at both the BBM and basolateral membrane of the renal proximal tubular cell [83]. The binding of PTH to PTHR1 activates both phospholipase C (PLC)-$Ca^{2+}$ and adenylate cyclase-cyclic adenosine monophosphate (cAMP) second messenger pathways. PTH binds to the basolateral membrane PTH-receptors to activate the cAMP-PKA pathway leading to an increase in the cellular levels of active PKA [37]. PKA has been shown to phosphorylate NHERF1 at Ser-77 [84] and ezrin [85], and this phosphorylation destabilises the NHERF1-ezrin network resulting in the internalisation of NaPi-IIa. In contrast, PTH binding to PTHR1 at the BBM preferentially activates the PLC-PKC signalling pathway, resulting in an increase in the cellular levels of active PKC [86,87]. PKC phosphorylates NHERF1 at Ser-77 resulting in reduced interaction between NHERF1 and NaPi-IIa at the BBM [84]. In addition to the downregulation of NaPi-lla by PTH, there is evidence that PTH reduces the activity of the NHE3 [88], and this may contribute to the PTH-induced loss of NaPi-lla function in the renal proximal tubules. It is plausible that the activity of NHE3 is directly linked to the cellular activity of NHERF1, such that when NHE3 activity is reduced the activity of NHERF1 is also affected, and this may result in the internalisation of NaPi-IIa. Internalised NaPi-IIa is rapidly

degraded in the lysosomes [80,89], and the recovery of apical NaPi-IIa levels following the removal of PTH signalling requires the biosynthesis of new NaPi-IIa protein [89]. The mechanism underlying the role of PTH on NaPi-llc internalisation is still under investigation, however, studies by Segawa and colleagues suggest that like NaPi-IIa, PKA and PKC signalling pathways may be responsible [90]. Unlike the rapid internalisation of NaPi-lla by PTH, NaPi-llc internalisation is a slow process, which occurs within several hours [91], and the internalised protein is left undegraded and may recycle back to the apical membrane in the absence of PTH [90].

In addition to its role in regulating renal phosphate transporters, the role of PTH in the maintenance of phosphate homeostasis involves its actions on bone resorption, and interaction with other hormones of phosphate homeostasis, notably FGF-23 and $1,25(OH)_2D_3$. In bone, specifically osteoblasts, PTH-mediated resorption increases extracellular $Ca^{2+}$ and phosphate levels by increasing the expression of the receptor activator of nuclear factor kB ligand (RANKL) via PKA, PKC and extracellular signal-regulated kinase (ERK) mechanisms [92]. PTH has been shown to increase FGF-23 synthesis by enhancing FGF-23 gene expression in osteocytes [11]. In addition, PTH binds to its receptors in the kidney to activate the renal 25-hydroxyvitamin D-1-α hydroxylase enzyme, which mediates the conversion of $25(OH)D_3$ to $1,25(OH)_2D_3$ [93–95], a steroid hormone that upregulates NaPi-IIb expression. These actions of PTH, including the FGF-23 permissive effects, suggest that PTH decreases the total body phosphate levels in the short-term while activating the synthesis of $1,25(OH)_2D_3$ to replenish the body's phosphate levels in the long-term.

#### 1.2.1.5.1.2. FGF-23 and α-Klotho

FGF-23 is a member of the fibroblast growth factor family, which is made up of 251 amino acid residues [96]. It is synthesised in osteocytes and transported in the blood to its target organs, mainly the kidney. Two forms of FGF-23 have been detected in the circulation: full length or intact FGF-23 and c-terminal FGF-23 fragments (cFGF-23), which is known to be the inactive form of intact FGF-23 [97,98]. FGF-23 is released in response to increased extracellular phosphate levels and it acts mainly in the kidney where it downregulates the proximal tubular expression of NaPi-lla and -llc, and inhibits the synthesis of $1,25(OH)_2D_3$ [99]. A large body of evidence suggests that FGF-23 is the major regulator of phosphate homeostasis [100]. Overexpression of FGF-23 in mouse models results in hypophosphatemia and low circulating levels of $1,25(OH)_2D_3$ [101]. In contrast, persistently high extracellular phosphate and $1,25(OH)_2D_3$ levels as well as suppressed PTH levels were observed in mice following FGF-23 ablation [8,98,102]. Genetic disorders characterised by excessive levels of FGF-23 in humans such as autosomal dominant hypophosphataemic rickets, autosomal recessive hypophosphataemic rickets and X-linked hypophosphataemia are associated with persistently low circulating phosphate levels [103–105], thus, indicating the essential role of FGF-23 in phosphate homeostasis in humans.

Recent studies have shown that in the renal proximal tubule, FGF-23 predominantly binds to FGF-23 receptor (FGFR) type 1, in the presence of its membrane co-receptor α-klotho, to cause the downregulation of NaPi-IIa and -IIc [106,107]. Evidence from α-klotho-deficient mice demonstrates a critical role of this protein in FGF-23 function as these mice have been shown to exhibit a phenotype identical to FGF-23 knock-out mice [108]. Specifically, α-klotho knock-out mice have

increased NaPi-IIa levels at the proximal tubular BBM and are unable to regulate circulating phosphate levels following phosphate loading, thus, developing hyperphosphataemia under this condition [108]. There is evidence that FGF-23-mediated internalisation of NaPi-lla involves the phosphorylation of NHERF1 by the ERK1/2 pathway and serum glucocorticoid-regulated kinase-1 (SGK1) mechanism [109]. The role of FGF-23 in regulating the synthesis of $1,25(OH)_2D_3$ involves the interaction of FGF-23 with FGFR3 and FGFR4 in the kidney [110]. Even though it is known that the actions of FGF-23 on renal phosphate transporters and $1,25(OH)_2D_3$ involve different receptors, it is still unknown whether the FGF-23-mediated NaPi-lla internalisation and inhibition of $1,25(OH)_2D_3$ secretion have different cellular mechanisms. However, emerging evidence in Janus kinase 3 (JAK3) knock-out mice suggests that an FGF-23 related-JAK3 regulation of renal 25-hydroxyvitamin D-1-α hydroxylase activity is a key mechanism involved in the regulation of $1,25(OH)_2D_3$ synthesis by FGF-23 [111].

Unlike α-klotho, which is known to play a vital role in increasing the affinity of FGFR for FGF-23 and the potency of bound FGF-23 [112,113], studies in *Xenopus oocytes* have shown that circulating klotho may directly downregulate the apical expression of renal NaPi-IIa and intestinal NaPi-IIb [114]. Circulating or soluble klotho is synthesised from the cell surface of the extracellular domain of membrane α-klotho by membrane-bound proteolytic enzymes and released into the extracellular fluid [115]. This form of klotho has been shown to stimulate the synthesis of FGF-23 in osteocytes [116] and this may be the mechanism by which circulating klotho downregulates NaPi-IIa. Whether circulating klotho interacts with specific receptors to activate cellular signalling pathways in its target organs remains to be seen. Moreover, it has been reported that circulating klotho

downregulates NaPi-IIa due to its glucuronidase activity in the renal proximal tubule [117].

Interestingly, a putative link between FGF-23 and PTH secretion has been suggested [118–120]. However, the underlying mechanism is still unclear. The identification of abundant membrane α-klotho expression in the parathyroid gland suggests that FGF-23 may affect PTH secretion by a klotho-dependent mechanism [121]. There is evidence that FGF-23 inhibits the secretion of PTH [120], and because PTH increases the release of FGF-23 from osteocytes, the interaction of these hormones creates a negative feedback loop for the regulation of phosphate balance (Figure 1.4). In addition, the direct link between FGF-23-α-klotho complex and circulating PTH and $1,25(OH)_2D_3$ levels (Figure 1.4), suggest that FGF-23 can directly or indirectly impact phosphate balance by regulating the expression of both renal and intestinal NaPi-ll proteins.

#### 1.2.1.5.1.3. $1,25(OH)_2D_3$

$1,25(OH)_2D_3$ is a steroid hormone predominantly synthesised from a precursor steroid on the skin. Its synthesis involves a series of physiological processes in the liver and kidney resulting in the release of the active $1,25(OH)_2D_3$, which is a hormone primarily involved in bone mineralization. Active $1,25(OH)_2D_3$ is released into the circulation from the kidney by the action of 25-hydroxyvitamin D-1-α hydroxylase (encoded by Cyp27b1 gene) on $25(OH)D_3$ [122]. In the early 1970s, the release of $1,25(OH)_2D_3$ was reported to be stimulated by PTH in response to low extracellular $Ca^{2+}$ levels [123]. Soon after, evidence that rats maintained on a low phosphate diet had significantly elevated $1,25(OH)_2D_3$ levels despite high levels of extracellular $Ca^{2+}$, indicated that circulating phosphate and consequently, renal tubular cell phosphate, affects $1,25(OH)_2D_3$ secretion [124].

Treatment of rats with $1,25(OH)_2D_3$ has been demonstrated to directly stimulate the upregulation of intestinal NaPi-IIb [39,48]. Previous findings that jejunal $Na^+$-dependent phosphate absorption was significantly upregulated following $1,25(OH)_2D_3$ administration to $1,25(OH)_2D_3$-deficient rodents [125,126] provide additional evidence for the stimulatory role of $1,25(OH)_2D_3$ on NaPi-IIb.

As a steroid hormone, $1,25(OH)_2D_3$ acts by interacting with its intracellular receptor, VDR, to activate NaPi-IIb gene promoter activity and modulate NaPi-IIb gene expression [48]. The effect of $1,25(OH)_2D_3$ on NaPi-IIb expression and the underlying mechanism in rodents has been reported to be age-dependent [48]. In preweaning rats, the effect of $1,25(OH)_2D_3$ on NaP-llb has been shown to be mediated partly by an alteration in NaPi-llb gene expression and partly by posttranslational modification of the protein [48]. However, reports from 8-week old VDR knock-out mice suggest that VDR-mediated effects of $1,25(OH)_2D_3$ on NaPi-llb levels occur by posttranscriptional mechanisms [127]. While NaPi-llb mRNA expression levels are unaffected in adult VDR knock-out mice, its protein levels and transport activity were significantly suppressed in the knock-outs compared with wild-type mice [127]. Taken together, this suggests that in young animals with high circulating levels of $1,25(OH)_2D_3$, this hormone interacts with its receptor to increase the expression of NaPi-IIb by both transcriptional and posttranslational mechanisms, hence, this is why there are relatively higher levels of NaPi-IIb in young animals compared to adults. To understand the mechanism underlying the posttranslational effect of $1,25(OH)_2D_3$ on NaPi-IIb levels, evidence from cell culture studies suggests the presence of caveolae-associated VDRs, which when activated by $1,25(OH)_2D_3$ binding, initiate multiple G-protein dependent-intracellular second messenger systems, leading to the generation of PKC and

MAP/RAS kinases [128–131]. These mechanisms may be responsible for the posttranslational modification of NaPi-IIb protein in response to $1,25(OH)_2D_3$. However, there is a paucity of information to support this mechanism *in vivo*, thus, its physiological role is still in doubt.

Furthermore, there is evidence for the presence of a $1,25(OH)_2D_3$ response element in rodent NaPi-IIa [132] and human NaPi-IIc [133] gene, suggesting that this regulator may have a direct effect on the mRNA expression levels of these transporters. However, unlike the action of PTH on the renal phosphate transporters, there is lack of convincing evidence to support a direct effect of $1,25(OH)_2D_3$ on NaPi-IIa and -IIc protein levels [134]. Moreover, increased circulating FGF-23 levels in response to high levels of $1,25(OH)_2D_3$ [135] suggests that the later indirectly downregulates renal NaPi-IIa and -IIc proteins. Interestingly, mice lacking VDR have been shown to be associated with low levels of renal NaPi-IIa and NaPi-IIc protein in the renal proximal tubular BBM, suggesting that the loss of $1,25(OH)_2D_3$ signalling or low levels of this hormone may negatively impact the levels of these transporters [136]. Since PTH is known to cause NaPi-IIa and -IIc downregulation, the low protein levels of these transporters in VDR knock-out mice may be due to the feedback stimulation of PTH release by the lack of $1,25(OH)_2D_3$ signalling [136]. Although the exact effect of $1,25(OH)_2D_3$ on NaPi-IIa and -IIc has not yet been determined, the fact that high or low levels of $1,25(OH)_2D_3$ results in the feedback release of FGF-23 or PTH suggests that $1,25(OH)_2D_3$ indirectly causes the downregulation of renal NaPi-IIa and -IIc protein levels.

#### 1.2.1.5.1.4. Dietary phosphate

The intake of a high phosphate diet has been shown to induce renal BBM NaPi-lla and -llc downregulation in a manner similar to PTH [137,138]. The effect of high phosphate diet on NaPi-IIa and -IIc levels appears to be relatively rapid compared to that of FGF-23 [138]. It was previously proposed that this effect of dietary phosphate on the renal NaPi-ll proteins was independent of PTH, $1,25(OH)_2D_3$ and FGF-23 [139,140] and that the release of a gut-derived factor may be a key driver [22]. However, recent evidence indicates that changes in the levels of renal NaPi-II proteins following an oral phosphate load require changes in circulating PTH levels, and there is still no evidence for a gut-derived phosphaturic factor suggested to be involved in regulating renal NaPi-II proteins following an oral phosphate load [23,24]. In contrast to the effect of a high phosphate diet, low dietary phosphate significantly upregulates the expression of the NaPi-ll proteins [16,44]. The upregulation of NaPi-IIa and -IIc does not require *de novo* synthesis of the proteins but has been demonstrated to involve posttranslational mechanisms, which is likely to be as a result of shuttling of the proteins from intracellular stores to the renal BBM [141,142]. Taken together, these findings suggest that high dietary phosphate increases circulating phosphate levels leading to an increase in PTH and a consequent downregulation of renal NaPi-IIa and -IIc (Figure 1.4), while a low phosphate diet causes the activation of mechanisms within the renal epithelial cells involved in the shuttling and anchoring of the renal NaPi-II transporters on to the BBM. There is evidence that the adaptation of renal NaPi-IIa and -IIc to changes in dietary phosphate levels requires the interaction of the transporters with the PDZ proteins, NHERF1 and NHERF3, which are associated with the C-terminal of the transporters [16,141,142]. Specifically, NHERF1 is known to be mainly responsible for the upregulation of NaPi-IIa in response to low dietary phosphate

levels [16,141,142], while NHERF3 has been shown to be the PDZ protein involved in the adaptation of NaPi-IIc to a low phosphate diet [141]. Therefore, these PDZ proteins are the key players involved in the intracellular mechanisms underlying the anchoring of NaPi-IIa and NaPi-IIc to the BBM in response to a low phosphate diet.

Dietary phosphate concentration is considered the major regulator of NaPi-IIb expression in the small intestine [17,19,38,127,143,144]. Like $1,25(OH)_2D_3$, dietary phosphate restriction has been shown to upregulate NaPi-IIb levels, while a high phosphate diet is known to cause NaPi-IIb downregulation at the BBM of enterocytes [17,19,38,58,127,143–146]. Because a low phosphate diet stimulates the synthesis of $1,25(OH)_2D_3$ [147,148], it was previously thought that this hormone was responsible for the adaptation of intestinal NaPi-IIb to changes in dietary phosphate levels [149]. However, it is now known that the upregulation of NaPi-IIb in response to a low phosphate diet is independent of $1,25(OH)_2D_3$ and VDR signalling [19,127]. In these studies, the authors demonstrated that the adaptation of NaPi-IIb under this dietary condition was unaffected in VDR and 25-hydroxyvitamin D-1-α hydroxylase knock-out mice. There are conflicting reports on the mechanisms underlying the upregulation of intestinal NaPi-IIb by low dietary phosphate levels. While an early report indicated that the upregulation of NaPi-IIb in response to a low phosphate diet had no effects on NaPi-IIb mRNA [143], more recent reports have shown that changes in both NaPi-IIb mRNA and protein are observed under this dietary phosphate condition [19,38,127].

It is still unclear if the regulation of NaPi-IIb by a low dietary phosphate is manifested at transcriptional level or mediated solely by posttranslational mechanisms. Evidence from the adaptation of NaPi-llb to acute and chronic

administration of a low or a high phosphate diet suggests the possibility of the involvement of both mechanisms, but with intestinal-segment specificity in rats [17]. Giral and Colleagues [17] showed that chronic administration of a low phosphate diet resulted in the upregulation of rat jejunal NaPi-IIb protein and mRNA, with no effect observed in the duodenum. However, when the rats that had been chronically adapted to the low phosphate diet were acutely switched to a high phosphate diet, there was a significant upregulation of duodenal NaPi-IIb protein only, with no change observed in the jejunum. Taken together, these findings suggest that the adaptation of jejunal NaPi-IIb to dietary phosphate involves the de novo synthesis of NaPi-IIb, while posttranslational modification of already synthesised NaPi-IIb may be responsible for NaPi-IIb upregulation in the duodenum.

Furthermore, there are speculations that a low phosphate diet activates intracellular mechanisms, which involves the PDZ proteins that play important roles in NaP-IIb trafficking to and from the enterocyte BBM [32,58,150]. Studies have shown that the regulation of NaPi-IIb by a low phosphate diet requires the expression of NHERF1 [58]. Giral and colleagues demonstrated that the upregulation of NaPi-IIb in response to dietary phosphate restriction is impaired in NHERF1 knock-out mice [58]. Myosin VI protein has also been implicated in the regulation of NaPi-IIb expression by low phosphate intake [150]. Changes in NaPi-IIb in response to high or low phosphate intake is significantly blunted in myosin VI knock-out mice compared to the wild-type mice [150]. Taken together, these reports suggest that NHERF1 and myosin VI are key targets in the regulation of NaPi-IIb by dietary phosphate levels (See section 1.2.1.5.2 for more detail)

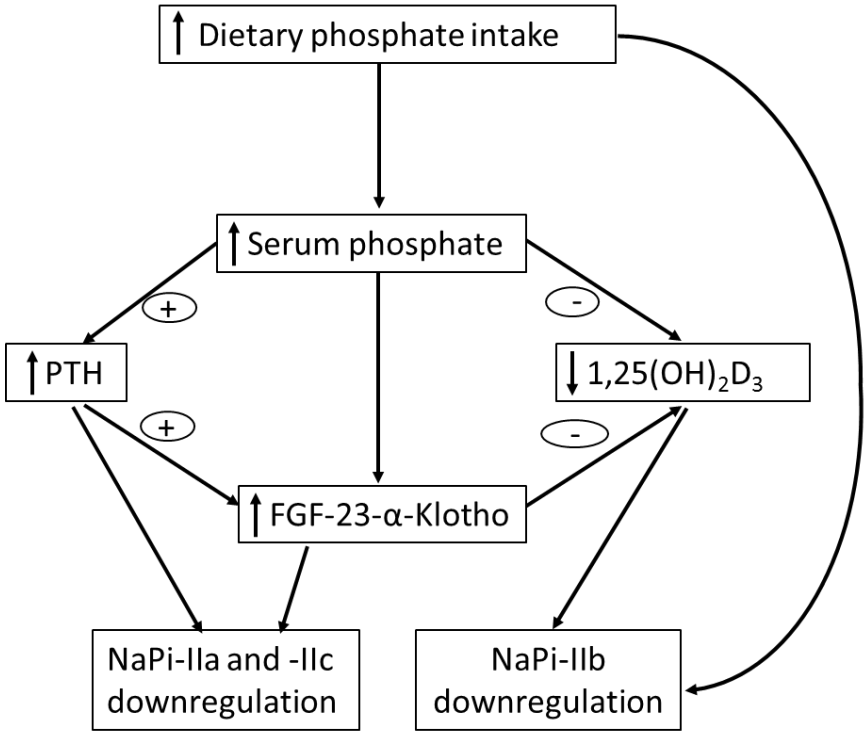


**Figure 1.4. Systemic regulation of renal NaPi-IIa and -IIc, and intestinal NaPi-IIb by dietary phosphate, FGF-23-α-klotho axis, PTH and vitamin D**. High dietary phosphate intake stimulates (+) increased PTH and FGF-23 release. PTH and the activation of FGF-23-α-klotho axis cause the downregulation of NaPi-IIa and -IIc levels. High dietary phosphate intake inhibits (-) the release of $1,25(OH)_2D_3$ and this cause the downregulation of intestinal NaPi-IIb. Dietary phosphate also directly downregulates intestinal NaPi-IIb levels.

#### 1.2.1.5.1.5. Acid-base status

The phosphate buffer system is known to be one of the major renal tubular mechanism for the secretion of excess $H^+$, and as a result of this, there is increased urinary excretion of phosphate in metabolic acidosis [151]. To cause this response, it is expected that the expression of the proximal tubular phosphate transporters, NaPi-IIa and -IIc will be altered during acid-base imbalance. There are conflicting reports on the effect of metabolic acidosis on NaPi-lla and -llc. There is evidence to suggest that the mRNA and protein levels of NaPi-lla are downregulated during metabolic acidosis [152], while other studies have failed to demonstrate this effect despite a significant increase in urinary phosphate excretion [151,153]. Since NaPi-lla and -llc are known to preferentially transport divalent phosphate, which is readily reduced to monovalent phosphate at low luminal pH, it has been hypothesised that the transport activity of these proteins is significantly reduced during metabolic acidosis [68]. Moreover, there is evidence that the $K_m$ of the NaPi-II proteins is increased at low pH, and this affects the interaction of the transporter with $Na^+$ and phosphate, thus, causing a significant reduction in renal phosphate reabsorption [68,69].

As a compensatory mechanism to increased renal excretion of phosphate in acidosis, intestinal NaPi-IIb and phosphate absorption have been shown to be upregulated [151] and the mobilization of phosphate from bone increases to buffer serum phosphate levels [154]. The mechanism underlying this upregulation of intestinal phosphate absorption in metabolic acidosis has been attributed to an increase in NaPi-llb protein, with no change in its mRNA expression [151].

#### 1.2.1.5.1.6. IGF-1

In humans and weanling rats, insulin-like growth factor-1 (IGF-1) has been reported to reduce renal phosphate excretion by increasing proximal tubular $Na^+$-dependent phosphate transport [155]. IGF-1 has been reported to increase renal proximal tubular phosphate reabsorption leading to increased circulating phosphate, known to be necessary for the growth and development of the skeletal system in young animals [155]. IGF-1 has been implicated in the regulation of the expression or activity of renal NaPi-II proteins [156]. Activation of the tyrosine kinase receptor by IGF-1 upregulates the protein levels and increases the membrane stability of the type II $Na^+$-dependent transporter in OK cells [157].

#### 1.2.1.5.1.7. Dopamine

Dopamine has been implicated in the renal adaptation to a high phosphate diet, with increased levels of dopamine shown to be associated with an increase in urinary phosphate excretion [158]. Reports by Bacic and colleagues have demonstrated that acute dopamine administration causes NaPi-IIa internalisation by activating the dopamine type 1 receptor [159]. Interaction of dopamine with this receptor in the proximal tubule activates the cAMP-PKA and PLC-PKC signalling pathways, leading to increased intracellular levels of PKA and PKC, which both initiate NaPi-IIa internalisation [159,160].

#### 1.2.1.5.1.8. ANP

ANP has been shown to increase the fractional excretion of phosphate by inhibiting $Na^+$-dependent phosphate transport in the renal proximal tubule [161]. ANP has been demonstrated to downregulate NaPi-IIa protein levels at the BBM of the renal proximal tubular cell via the activation of the guanylate cyclase-cGMP-PKG signalling cascade [162].

#### 1.2.1.5.1.9. Estrogen

Recent evidence demonstrates that estrogen downregulates the mRNA and protein levels of NaPi-IIa in a dose-dependent manner in ovariectomised rats, but had no effect on NaPi-IIc levels in the renal proximal tubules [163]. This effect of estrogen has been shown to be mediated by the activation of two estrogen receptor subtypes (ERα and ERβ) [163]. In parathyroidomised rats, estrogen has also been shown to downregulate NaPi-IIa levels indicating that the effect of estrogen is independent of PTH [164]. This effect of estrogen causes significant phosphate wasting and hypophosphataemia [163,164]. In contrast, there is evidence that estrogen upregulates the expression of NaPi-IIb protein at the BBM of the small intestine by increasing NaPi-IIb gene transcription [165]. In cell culture experiments, estrogen has been reported to increase the activity of the NaPi-IIb gene promoter [165], indicating that estrogen has a direct effect on the de novo synthesis of NaPi-IIb protein. In addition, estrogen has also been demonstrated to stimulate the production of $1,25(OH)_2D_3$ [166]. Thus, the effect of estrogen on $1,25(OH)_2D_3$ synthesis is an additional mechanism through which estrogen upregulates NaPi-IIb protein levels.

#### 1.2.1.5.1.10. Glucocorticoids

Elevated levels of circulating glucocorticoids, for example, following glucocorticoid administration or in Cushing's disease, are associated with hypophosphataemia and phosphaturia [167]. Chronic treatment with glucocorticoids has been shown to downregulate NaPi-lla mRNA and protein levels in the renal proximal tubule [168]. It is speculated that glucocorticoids interact with SGK-1 receptor to cause the phosphorylation of NHERF1 and this initiates NaPi-IIa endocytosis and the resultant downregulation of NaPi-IIa at the BBM [37]. Studies

in preweaning animals have shown that glucocorticoids affect the expression of intestinal NaPi-IIb, as glucocorticoid injection in these animals has been shown to downregulate the mRNA expression and protein levels of NaPi-IIb in the small intestine [47].

#### 1.2.1.5.1.11. Thyroid hormones

There are indications that thyroid hormones affect NaPi-lla expression and its transport activity [169,170]. Euzet and colleagues demonstrated that acute administration of 3,5,3'-triiodothyronine, a form of thyroid hormone, in rats, increases the expression of NaPi-lla mRNA and protein, while also increasing the affinity and capacity of the transporter [169].

#### 1.2.1.5.1.12. Phosphatonins

Phosphatonins were first suggested when the $Na^+$-dependent transport of phosphate was significantly affected in opossum-kidney cells that were cultured in a conditioned medium obtained from the tumour of a patient with oncogenic osteomalacia, a disorder characterised by renal phosphate wasting and low serum phosphate levels [171]. Although FGF-23 (discussed in detail in section 1.2.1.5.1.2) was later identified as the major phosphatonin responsible for maintaining phosphate homeostasis [103–105,172,173], other phosphatonins such as MEPE, sFRP and FGF-7 have also been demonstrated to play a role in the maintenance of phosphate balance by regulating the expression and functions of the NaPi-II proteins (reviewed in [139]).

##### 1.2.1.5.1.12.1. MEPE

MEPE was first cloned and characterised from an oncogenic hypophosphataemic osteomalacia tumour [174] and has been demonstrated to inhibit renal and intestinal $Na^+$-dependent phosphate transport in a dose-dependent manner resulting in an

increase in fractional phosphate excretion in rats [175,176]. Studies by Marks and colleagues have shown that MEPE significantly downregulates renal NaPi-IIa protein levels, but has no effect on NaPi-IIc levels [176]. Although the effects of MEPE on intestinal NaPi-IIb levels has not been reported, the role of MEPE in the reduction of phosphate absorption in the rat jejunum, a region with high NaPi-IIb expression [176], suggests that this phosphatonin may downregulate NaPi-IIb protein levels. Even though a link between FGF-23 and MEPE has been reported [177], and clinical data has also established a positive correlation between serum MEPE and PTH levels [178], the acute effect of MEPE on renal NaPi-IIa levels and intestinal phosphate absorption was shown to be independent of PTH and FGF-23, suggesting a direct effect of MEPE on the levels of the NaPi-II proteins [176].

#### 1.2.1.5.1.12.2. sFRP-4

sFRP-4 has been shown to increase renal phosphate excretion in rats by a PTH independent mechanism [179]. This effect of sFRP-4 on renal phosphate excretion occurs due to its role in NaPi-IIa internalisation and the consequent downregulation of NaPi-IIa protein levels in the renal proximal tubule [180]. There is limited information on the effect of sFRP-4 on intestinal NaPi-IIb expression, however, sFRP-4 is known to reduce circulating $1,25(OH)_2D_3$ levels [181] and via this mechanism, sFRP-4 may inhibit intestinal NaPi-IIb levels.

#### 1.2.1.5.1.12.3. FGF-7

Like MEPE, reports from oncogenic hypophosphataemic osteomalacia, a phosphate-wasting syndrome, have identified FGF-7 as a potent phosphatonin [182]. High levels of FGF-7 in conditioned medium obtained from cell cultures of tumours associated with oncogenic osteomalacia has been shown to be responsible for the inhibition of phosphate uptake by renal epithelial cells [182]. This

effect was reversed by an FGF-7-neutralising antibody, suggesting that FGF-7 may inhibit the activity of the renal NaPi-ll proteins.

#### 1.2.1.5.2. Cellular regulators of the type II $Na^+$-dependent phosphate transporters

Common intracellular protein kinases, PKA, PKC and PKG, have been reported to play key roles in mediating the shuttling of NaPi-II proteins to and from the BBM of epithelial cells in response to changes in dietary phosphate levels and some of the systemic regulators, like PTH (discussed in section 1.2.1.5.1.1) [37,87,90,160,162,183]. These cellular enzymes are also known to mediate the effect of the PDZ proteins on the expression of NaPi-II proteins at the BBM of epithelial cells [160,184,185]. Structurally, the C-terminal region of the NaPi-II proteins bears a PDZ-recognition sequence, which interacts with cytoplasmic regulatory proteins such as the NHERF family and Shank 2E, to alter the stability and expression of the proteins on the BBM [186–188]. Among the NHERF family involved in the local regulation of NaPi-II proteins, NHERF1 and NHERF3 have been identified in the PDZ domain; however, while NHERF1 has been demonstrated as a key regulator of NaPi-IIa expression [37,189], NHERF3 is known to be involved in NaPi-IIc regulation [141]. The loss of NHERF1 function in NHERF1 knock-out mice results in the internalisation of NaPi-IIa from the renal proximal tubular BBM [189]. Evidence in NHERF1 knock-out mice and NHERF1 mutations in humans have shown that the mutation or deletion of the NHERF1 gene results in hypophosphataemia, a consequence of the lack of NaPi-IIa expression in the renal proximal tubule [189,190]. Another protein, ezrin, has been implicated in the function of NHERF1 and the overall expression of NaPi-IIa [191–193]. It has been hypothesised that ezrin interacts with NHERF1 to form a complex, which anchors NaPi-IIa to the apical membrane

[32,185]. Furthermore, the actions of the systemic regulators of NaPi-IIa protein, for example, PTH, increases the intracellular levels of kinases such as PKA and PKC, and these enzymes interfere with the interaction of NHERF1 and ezrin, thus, causing the internalisation of NaPi-IIa [184]. PKA has been shown to phosphorylate ezrin, while both PKA and PKC are known to phosphorylate NHERF1, and this phosphorylation destabilises the NHERF1-ezrin network, leading to the loss of NaPi-IIa expression at the apical membrane [85,160,184,185]. Moreover, the cGMP-PKG signalling pathway has also been suggested to induce the internalisation of NaPi-IIa by unknown mechanisms [162]. It remains to be seen if PKG phosphorylates ezrin or NHERF1 like the other protein kinases.

Shank 2E is highly concentrated on the BBM and closely localised with high levels of NaPi-IIa under low dietary phosphate conditions [188,194]. Under a high dietary phosphate condition, the degradation of shank 2E has been speculated to be associated with the well known downregulation of NaPi-IIa [188,194]. Although the mechanism underlying the role of Shank 2E on NaPi-IIa stability on the BBM is still under investigation, the interaction of Shank 2E with NHE3 and the consequent regulation of NHE3 trafficking by this regulatory protein [195] may impact NHERF1 activity, thus, affecting BBM NaPi-IIa stability. In addition, a GTPase enzyme, dynamin II, which is known to be involved in the internalisation of clathrin-coated vesicles has been shown to interact with Shank 2E [196]. Furthermore, mounting evidence suggests that a PDZ-independent protein, Gamma-aminobutyric acid (GABA) receptor-associated protein (GABARAP) is also involved in the intracellular signalling pathways regulating the expression of NHERF1 and NaPi-IIa protein [197]. The deletion of GABARAP gene in GABARAP knock-out mice has been shown to be associated with reduced NaPi-IIa

expression and a consequent increase in urinary phosphate excretion, indicating that GABARAP causes the upregulation of NaPi-IIa protein [197].

Recent evidence demonstrates that like NaPi-IIa, NaPi-IIb also interacts with NHERF1, and this interaction regulates the expression of NaPi-IIb at the BBM [58]. Studies in NHERF1 knock-out mice have shown that the adaptation of NaPi-IIb to changes in dietary phosphate is impaired in the absence of NHERF1 protein, suggesting a key role for NHERF1 in the anchoring of NaPi-IIb to the BBM of enterocytes [32,58]. In addition, myosin VI has also been implicated in the regulation of NaPi-IIb by dietary phosphate [150]. Unlike NaPi-IIa, GABARAP downregulates the expression of NaPi-IIb [198]. The mechanism underlying the role of GABARAP in the downregulation of NaPi-IIb is still unknown. However, it is plausible that this effect of GABARAP on NaPi-IIb is not a direct effect, but only secondary to its action on renal NaPi-IIa, thus, compensating for the increased retention of phosphate by the kidneys to maintain systemic phosphate balance.

Emerging evidence suggests that SPS1-related proline/alanine-rich kinase (SPAK) and oxidative stress-responsive kinase 1 (OSR1) are also regulators of NaPi-IIa and NaPi-IIb expression and activity in the renal proximal tubular cell and enterocyte BBM [199–201]. In *Xenopus oocyte* expressing NaPi-IIa, OSR1 co-expression has been demonstrated to increase NaPi-IIa-mediated phosphate transport activity [199]. Under normal dietary phosphate condition, reduced circulating phosphate levels as a result of the downregulation of NaPi-IIa protein abundance and activity has been shown in OSR1-knock-in mice, heterozygously carrying a with-no-lysine protein kinase (WNK)-insensitive mutation [199]. The adaptation of these mice to a low phosphate diet was also reported to be significantly impaired, suggesting a key role for this kinase in NaPi-IIa function

[199]. In addition, Xiao and colleagues have demonstrated the presence of SPAK and OSR1 expression in the intestine of mice [202], and that the co-expression of these kinases in *Xenopus oocytes* causes the upregulation of NaPi-IIb, resulting in an increase in NaPi-IIb-mediated phosphate current [200]. The increased NaPi-IIb-mediated phosphate current was speculated to be due to SPAK and OSR1 induced phosphorylation of NaPi-IIb-regulating signalling proteins such as AMP-activated kinase, serine/threonine-protein kinase B-Raf and SGK1 [200].

### 1.2.2. $Na^+$-dependent phosphate cotransporter type I

The type I $Na^+$-dependent phosphate cotransporter (NPT) is encoded by the SLC17 gene and has been shown to be expressed in a number of tissues including the small intestine, colon, liver, pancreas, kidney, brain, bone and lung [203–205]. Among the different homologues of NPT identified previously, only the type A1 to A4 (NPT1, $Na^+/HPO_4^{2-}$ homologue, NPT3 and NPT4) have been shown to be involved in transcellular phosphate transport [205]. NPT1 (encoded by SLC17A1) is mainly expressed in the renal proximal tubular brush border membrane [206,207] and to a lesser extent in the sinusoidal membrane of liver cells [208]. Northern blot analysis has shown that NTP3 (encoded by SLC17A2) is highly expressed in the heart and muscle cells and found at relatively low levels in the lungs, placenta, liver and brain [205]. RT-PCR and northern blot analysis have shown that NPT4 (encoded by SLC17A3) expression is localised in the small intestine, kidney, testes and liver, while the $Na^+/HPO_4^{2-}$ transporter homologue (encoded by SLC17A4) have been shown to be expressed in the liver, pancreas, small intestine and colon [205]. Other members of the NPT family (type A5 to A8, encoded by the SLC17A5-8) have been reported to mediate the transport of other anions such as glutamate and sialin in different organs [205].

The NPT transporter is a 465 amino acid protein, which is predicted to have 6-12 TMDs [205]. Early findings suggest that the members of the NPT family share approximately 20% structural homology with the type II and type III $Na^+$-dependent phosphate cotransporters [33]. Further studies are required to understand the detailed topology of these transporters. In addition, there is limited information available on how the structure of these transporters is adapted to the transport of phosphate across the membrane of cells. Although the kinetic properties and ionic coupling of $Na^+$ and phosphate by the NPTs have not been extensively studied, studies of human NPT1 have shown that the transport of phosphate and organic anions is electrogenic and not significantly affected by pH [208,209].

Inorganic phosphate transport in bone has been suggested to be mediated by a $Na^+$-dependent cotransport mechanism in mammals [203]. During bone resorption, released phosphate may be transported into the osteoclast via all the identified $Na^+$-dependent phosphate cotransporters, including the type I cotransporter. Even though this class of phosphate transporters has been identified in bone cells, kidney and intestine, its contribution to systemic phosphate homeostasis is poorly understood. Concerning the regulation of the NPT transporters in various tissues, studies by Soumounou and colleagues [210] suggest that the expression of NPT1 is regulated by hepatocyte nuclear factor (HNF)–1α and HNF-3β, with HNF-1α reported to upregulate NPT1 and NPT4 expression [211]. This regulation of the NPT1 by the HNFs is suggested to be at the transcriptional level [210]. At least in the brain, high phosphate diet increases the expression of the NPTs [212], but whether dietary phosphate affects the expression of NPTs in different tissues remains to be seen.

### 1.2.3. $Na^+$-dependent phosphate cotransporter type III

The type III phosphate transporters (PiTs) have been identified to be involved in the BBM transport of phosphate in epithelial cells [17,213,214]. Two members of the PiT family, which are encoded by the SLC20 genes have been characterized in mammals; PiT-1 (encoded by SLC20A1) and PiT-2 (encoded by the SLC20A2) [12]. The molecular structure of PiT-1 and PiT-2 is similar to the NaPi-II proteins in that they are proposed to have 12 TMDs, but unlike the NaPi-II proteins, both the N- and C- terminal tails are in the extracellular region [215,216]. Bai and colleagues [217] predicted that PiT-2 has 653 amino acid residues, while the amino acid sequence of PiT-1 has been suggested to be 59% identical to PiT-2 [218]. Cell culture and human PiT expression studies in *Xenopus oocytes* have identified the presence of a histidine residue ($H_{502}$) in the C-terminal, which is shown to confer the phosphate transport function of these proteins [215]. This phosphate transport function was shown to be unaffected following the removal of the large intracellular domain and its associated TMD [215], suggesting that the intracellular region and TMDs may not contribute to the transport properties of PiT proteins.

#### 1.2.3.1. Transport kinetics of the type III $Na^+$-dependent phosphate cotransporters

Studies into the kinetic properties of PiT proteins using *Xenopus oocyte* have revealed their electrogenic nature [218]; they transport monovalent phosphate ($H_2PO_4^-$) coupled with $Na^+$ in a 2:1 $Na^+$: phosphate stoichiometry [219]. To activate the PiT proteins, one $Na^+$ molecule binds to the transporter followed by a conformational change that allows the random binding of phosphate and another $Na^+$ [219]. This substrate interaction with the transporter results in a net influx of a positive charge, which confers the electrogenicity of this transporter. In the

absence of $Na^+$, $Li^+$ can drive the transport of phosphate, but with markedly slower transport rate [49]. Like NaPi-II proteins, the affinity of PiT proteins for phosphate and $Na^+$ is approximately 100 µM and 50 mM respectively [140]. The sensitivity of this transporter has been shown to be stable between pH 3 to 6, and unlike NaPi-II proteins, their transport function is not drastically affected by pH changes [140]. In a $Na^+$ free medium, lowering the pH from alkaline to acidic state did not abolish PiT-2 mediated phosphate uptake in *Xenopus oocyte* suggesting that $H^+$ may also drive PiT transport activity [140]. Presently, other than PFA, which is a very poor inhibitor of the activity of PiT proteins, no specific inhibitors have been identified for this class of transporters [71].

#### 1.2.3.2. Localization of the type III $Na^+$-dependent phosphate cotransporters

Although PiT-1 and PiT-2 mRNA have been reported to be ubiquitously expressed in several tissues in humans and rodents (reviewed in [12]), evidence for the role of PiT proteins in phosphate transport has been shown in the small intestine, kidney and brain [14,17,146,213,214,220,221]. Immunohistochemistry and Western blot analysis have shown that PiT proteins are localised in the kidney and small intestine of both rats and mice [17,146,198,213,214]. Even though both PiT-1 and PiT-2 mRNA have been detected in the kidney (reviewed in [20]) and small intestine [17], only PiT-2 protein has been shown to be present at the BBM of the proximal tubule of the kidney, mainly in the S1 segment (Figure 1.2) [91,198,213], while PiT-1 protein is mainly present in the rat small intestine [17]. In the small intestine, PiT-1 mRNA has been reported to be highest in the ileum of rats, however, like the intestinal localisation of NaPi-IIb, PiT-1 protein expression is mainly detected in the duodenum and jejunum [17]. Surprisingly, PiT-2 protein has recently been reported to be present in all three segments of the rat small

intestine [146]. There is limited information on the regional expression of PiT-1 in the small intestine of mice and humans. Even though PiT proteins have been detected in the kidney and small intestine, their overall contribution to phosphate transport in these organs is negligible. In contrast, recent evidence suggests that PiT-1 and PiT-2 mRNA and protein are highly detected in the brain and have been speculated to be the major phosphate transporters in the brain of humans and rodents [220,221].

#### 1.2.3.3. Regulation of the type III $Na^+$-dependent phosphate transporters

There are conflicting reports on the regulation of intestinal PiT-1 by dietary phosphate levels. While PiT-1 protein and mRNA levels have previously been shown to be unaffected by dietary phosphate manipulations [17], recent evidence has demonstrated that PiT-1 protein in the duodenum and jejunum is chronically regulated by dietary phosphate content, as its levels were upregulated in these segments following a 5-10 day administration of a phosphate-deficient diet [146]. However, there is still a lack of convincing evidence for a significant role of PiT-1 in intestinal phosphate absorption. Importantly, in NaPi-IIb knock-out mice, the observation that more than 90% of $Na^+$-dependent phosphate transport is abolished [31,222], supports the claim that PiT-1 plays little or no role in intestinal phosphate absorption. In the kidney, the abundance of PiT-2 protein has been demonstrated to be regulated by dietary phosphate [214]. In the renal proximal tubule, even though PiT-2 is normally localised in the S1 segment, its expression spreads throughout the S1 – S3 segments in rat fed a phosphate-deficient diet [213]. In addition, PiT-2 at the BBM of the proximal tubular epithelial cell is upregulated in rats fed with a phosphate-deficient diet over time [214]. While NaPi-IIa downregulation in rats switched from a chronically low phosphate to a high

phosphate diet is seen within 2 hours, PiT-2 is downregulated only after 24 hours [214]. It is interesting to note that dietary $K^+$ restriction also affects the expression of PiT-2 in the BBM of the renal proximal tubule, with significantly low levels of PiT-2 protein observed during dietary $K^+$ restriction in rats [213]. This suggests a significant link between renal phosphate transport and $K^+$ homeostasis since $K^+$ restriction has been shown to cause phosphaturia as a result of NaP-IIc and PiT-2 downregulation [213]. Like NaPi-lla and NaPi-llc, PTH and FGF-23 downregulate PiT-2 expression in the proximal tubule [30,91]. Metabolic acidosis and pH have also been reported to regulate PiT-2 expression and activity, with acidosis demonstrated to upregulate renal PiT-2 expression and increased PiT-2 activity was shown at low pH [14]. Even though there was residual phosphate uptake in renal BBM vesicles prepared from NaPi-IIa and -IIc double knock-out mice, severe hypophosphataemia and bone abnormalities were shown in these mice, suggesting that the role of PiT-2 in renal phosphate reabsorption is minimal [223]. However, further studies are required to clarify the precise contribution of the described changes in renal PiT-2 to phosphate homeostasis under various conditions.

### 1.3. Renal phosphate handling

The kidney controls the excretion of phosphate in the circulation by selectively reabsorbing phosphate from the glomerular filtrate as it travels down the different segments of the nephron. Although a small amount of plasma phosphate is bound to plasma proteins, more than 90% of total plasma phosphate is filtered into the proximal tubule [224]. With a normal glomerular filtration rate of approximately 125 ml/min in humans, the kidney under physiological conditions filters 4500-8000 mg of phosphate daily. In the proximal tubules, approximately 70% of the filtered

phosphate is reabsorbed [225], while a small but significant proportion is reabsorbed in the distal nephron [225,226]. In total, 80% - 90% of phosphate in the glomerular filtrate is reabsorbed in the nephron and only 10% - 20% is excreted in urine [227]. In addition, the rate of phosphate reabsorption in the renal proximal tubule has been shown to be higher in deep nephrons compared to superficial nephrons [228]. The reabsorption of phosphate in the proximal tubule is a transcellular process, mediated by the previously discussed $Na^+$-dependent phosphate cotransporters: NaPi-IIa, NaPi-IIc and PiT-2. The control of phosphate reabsorption is determined by the expression levels of NaPi-lla, NaPi-llc and potentially PiT-2 [227]. Studies in NaPi-IIa knock-out mice have shown that NaPi-IIa plays a key role in the renal regulation of phosphate homeostasis as these mice were characterised by hypophosphataemia and significant renal phosphate wasting, while NaPi-IIc knock-out mice showed normal plasma phosphate levels with no phosphate wasting [223]. NaPi-IIc levels have been shown to be upregulated in NaPi-IIa knock-out mice to compensate for the excessive loss of phosphate [223]. Additionally, NaPi-IIa and -IIc have been reported to play synergistic roles in mediating renal phosphate reabsorption as NaPi-IIa and IIc double knock-out mice have been demonstrated to display a more severe hypophosphataemia and renal phosphate wasting [223]. Nevertheless, NaPi-IIa is known to contribute approximately 70% to proximal tubular phosphate transport, while NaPi-IIc accounts for less than 30% [30,223,229]. Taken together, this suggests that NaPi-IIc plays a contributory role in renal phosphate reabsorption, but mainly becomes important when NaPi-IIa function is impaired in rodents. As described previously, NaPi-IIa is expressed in all three segments of the proximal tubule (S1-S3), with relatively higher expression in the S1 and S2 segments of the proximal tubule [230]. This suggests

that a large proportion of phosphate in the glomerular filtrate is reabsorbed in the S1 and S2 segments compared to the S3 segment of the proximal tubule [227].

There is a large body of evidence suggesting the existence of differential phosphate handling in humans and rodents [231]. Unlike in mice, clinical reports from phosphate-related genetic disorders have suggested that NaPi-IIc, encoded by the SLC34A3, is the major proximal tubular phosphate transporter in humans [29,232–234]. Specific point mutations in human SLC34A3 gene, but not SLC34A1 are associated with severe phosphate wasting and hypophosphataemia [29,234]. However, the recent identification of an autosomal-recessive mutation in the NaPi-IIa gene, SLC34A1, and its associated defect in $Ca^{2+}$ and phosphate metabolism, suggest a significant role for NaPi-IIa in phosphate homeostasis, at least in human infants [235]. In addition, a loss-of-function mutation in human NaPi-IIa with Falconi syndrome has also been reported to cause hypophosphataemia, suggesting that NaPi-IIa and NaPi-IIc may be playing a synergistic role in renal phosphate reabsorption in humans [236] and that NaPi-IIc likely plays a more significant role (reviewed in [20]). Immunohistochemistry data have shown that while the BBM of the renal proximal tubules of rodents stains strongly for NaPi-IIa and faintly for NaPi-IIc, the opposite pattern was observed in humans [231]. Unlike in rodents, NaPi-IIc has also been detected in the renal distal tubules of humans [231]. Taken together, these findings suggest that in addition to its high expression and key role in the renal proximal tubular phosphate transport, human NaPi-IIc mediates distal tubular phosphate reabsorption and is therefore considered the major renal phosphate transporter in healthy humans.

As previously described, the regulation of proximal tubular reabsorption of phosphate involves hormonal and dietary factors that affect the expression of the

phosphate transporters at the BBM. Among the factors regulating renal phosphate handling, FGF-23, dietary phosphate, α-klotho and PTH are the key players (reviewed in [237]). There is evidence that the signalling pathway for α-klotho-mediated FGF-23 action on the renal phosphate transporters occurs in the distal tubule, which is spatially separated from proximal tubular NaPi-IIa and -IIc [238]. Thus, since the FGF-23-klotho axis is regarded as a key mechanism in the regulation of phosphate homeostasis, further studies are required to examine the exact role of this distal tubular FGF-23-klotho signalling in the regulation of overall renal phosphate transport.

### 1.4. Intestinal phosphate handling

Early studies investigating the site of phosphate absorption in the gastrointestinal tract revealed that phosphate is absorbed in all three segments of the small intestine and the colon of rodents and humans [239–242]. Chyme containing inorganic phosphate and other nutrients travel along the different segments of the small intestine spending two-thirds of the total transit time in the jejunum and ileum while lasting only a few minutes in the duodenum [243]. The relatively longer transit time of chyme and the features of villi in the jejunum and ileum support the widely accepted dogma that these segments are the major sites of intestinal phosphate absorption. Although phosphate absorption in the colon has not yet been reported to play a significant role under normal conditions, during excessive phosphate intake, the absorption of phosphate in the colon can significantly affect serum phosphate levels [239]. Moreover, there is evidence that the administration of phosphate-containing enemas results in hyperphosphataemia in humans [242]. Taken together, these findings suggest that under certain conditions, the

absorption of phosphate across the colonic epithelia significantly affects systemic phosphate levels.

At least two mechanisms account for the absorption of phosphate in the small intestine; paracellular and transcellular phosphate transport [18]. Early studies aimed at understanding the mechanisms underlying intestinal phosphate absorption reported an active transcellular component, which is known to be $Na^+$-dependent and a passive paracellular process, mediated by the simple diffusion of phosphate [244]. This passive paracellular component of intestinal phosphate absorption was shown to be a linear process that is driven by the electrochemical gradient of phosphate across the intestinal epithelial membrane [46,240,245]. It is generally accepted that the passive paracellular phosphate transport process is $Na^+$-independent [45,245,246], but a very early report in the rat small intestine indicated that this passive phosphate transport process is significantly dependent on $Na^+$ [240]. Interestingly, recent studies suggest that $Na^+$ absorption via NHE3 regulates paracellular phosphate transport in the small intestine [77,247], and this may account for an important component of paracellular phosphate absorption. Furthermore, It is widely known that NaPi-llb and PiT-1 are the active $Na^+$-dependent phosphate transporters at the BBM of the small intestine of mice, rat and humans, however, NaPi-llb is thought to be the major transporter responsible for transcellular phosphate absorption in the small intestine of these species [17,18,31,39,248–250]. Studies on the kinetics of NaPi-IIb have shown that NaPi-IIb is a high affinity and a low capacity transporter, with a $K_m$ of approximately 50 µM [40,70]. Even though it has been predicted to have a higher concentrating capacity compared to the PiT proteins [49], its overall contribution to intestinal phosphate transport is still being debated.

Using NaPi-IIb knock-out mice, two very recent studies reported conflicting data concerning the contribution of NaPi-IIb to intestinal phosphate absorption in the mouse small intestine [77,251]. In the ileum of NaPi-IIb knock-out mice, while NaPi-IIb was shown to contribute more than 90% to phosphate uptake using *in situ* intestinal loop techniques and 10 mM phosphate solution [77], Ikuta *et al* [251], employed the everted sac technique and 4 mM phosphate solution to show that NaPi-IIb contributed approximately 30% to phosphate uptake. In a previous study in NaPi-IIb knock-out mice chronically maintained on a low phosphate diet, phosphate absorption following a 500 mM oral phosphate gavage was shown to consist of approximately 50% NaPi-IIb-mediated component, with the remaining 50% mediated by a NaPi-IIb-independent mechanism, suggested to be the passive paracellular transport pathway [31]. The differences in the findings obtained in these studies may be due to the lack of consistency in the techniques employed. Additionally, there is evidence that NaPi-IIb knock-out mice maintained on a normal or a high phosphate diet exhibited normal serum phosphate levels, and NaPi-IIb was reported to be important for intestinal phosphate transport only in mice chronically fed a low phosphate diet [145,222,251]. In rats, most of the early studies investigating the relative contribution of the $Na^+$-dependent and $Na^+$-independent mechanisms of phosphate absorption showed that the saturable $Na^+$-dependent component, now known to be NaPi-IIb mediated, is regulated by $1,25(OH)_2D_3$ is [39,126,149,252]. As discussed previously, NaPi-IIb protein is highest in the rat jejunum, where it has been suggested to contribute approximately 30-35% of total transepithelial phosphate transport in rats maintained on a normal phosphate diet, suggesting a dominant role for the $Na^+$-independent component of phosphate transport [45].

Studies on the levels of postprandial luminal phosphate in the gastrointestinal tract of rats and mice have shown that the physiological concentration of free phosphate in the lumen of the small intestine is in the millimolar range, considerably higher than the $K_m$ of NaPi-IIb [45,251]. Thus, this high phosphate levels in the intestinal lumen following a normal phosphate diet appears to be unfavourable for NaPi-IIb as the transporter will likely become saturated, suggesting that the passive $Na^+$-independent component may be the dominant pathway for phosphate absorption in the small intestine of rats and mice [45,251]. Considering the low $K_m$ of NaPi-IIb and the report that it mediates a saturable phosphate transport process, it has been speculated that under physiological conditions, when intestinal phosphate levels are expected to be in the millimolar range, passive $Na^+$-independent phosphate transport mechanism is the predominant pathway for phosphate absorption in rats and mice [45,145].

In comparison to rodents, there is limited information on the regional expression and functions of the $Na^+$-dependent transporters, NaPi-IIb and PiT protein in the human small intestine, thus, the contribution of the $Na^+$-dependent and $Na^+$-independent transport pathways to total transepithelial phosphate absorption in humans is unclear. However, NaPi-IIb mRNA has been shown to be highest in the human duodenum, with low expression levels in the ileum, while the jejunum showed the lowest expression [253]. Functional studies in humans have shown that the jejunum is the major segment responsible for phosphate absorption and that in this segment phosphate transport is mainly $Na^+$-dependent, while passive concentration-dependent phosphate transport has been reported in the ileum [46]. Interestingly, a significant component of this passive concentration-dependent phosphate transport in the human ileum has been shown to be dependent on

transepithelial water movement [46]. The human small intestine is known to be highly permeable to water, permitting rapid movement of water through paracellular pores due to osmotic gradient [254]. Because of this, the transport of water-soluble phosphate by solvent drag would be expected to contribute to this passive mechanism of phosphate absorption. However, based on the evidence that the passive transport mechanism in the human small intestine is independent of intestinal transepithelial $Na^+$ gradient [245], the major osmotically active solute in intestinal luminal content, solvent drag is, therefore, an unlikely driver for passive phosphate transport.

Furthermore, a recent cell culture study investigating the mechanism underlying passive phosphate transport using Caco-2 brush border epithelial (BBE) cell line revealed that the rate of phosphate influx through the BBE membrane was unaffected by the $Na^+$ gradient across the membrane [246]. Another potential mechanism responsible for the passive $Na^+$-independent component of phosphate absorption is phosphate transport via a passive transcellular transporter (carrier protein). There is evidence that the changes in the $Na^+$-independent passive phosphate transport in Caco-2 BBE cells in response to increasing phosphate concentration in the uptake solution requires *de novo* protein synthesis [246]. Whether a passive transcellular carrier protein is involved in this adaptive response remains to be seen. Although pH has been reported to affect the passive phosphate transport process in rodents [126] and in Caco-2 BBE cell lines [246], there is no evidence suggesting that this effect involves a passive carrier protein or a facilitated transporter. Thus, the mechanism underlying passive phosphate transport remains unresolved. Using electrophysiological techniques, the paracellular pathway has been shown to mediate the passive

$Na^+$-independent transport of phosphate in the small intestine [255], and because intestinal claudins are known to be involved in paracellular ion permeability, it is possible that these claudins may play a role in controlling the passive paracellular phosphate absorption process.

### 1.5. Intestinal claudins

Enterocytes are attached to one and other by the aggregation of tight junction proteins, of which claudins have been shown to be a key component. These claudins have been shown to play important roles in the paracellular transport of electrolytes and water [256–259]. Other components of intestinal tight junctions are occludin, tricellulin and junctional adhesion molecules [260]. Studies in occludin knock-out mice [261] and genetic mutations in the tricellulin gene [262] suggest that these proteins play minor roles in intestinal barrier function. Moreover, the junctional adhesion molecules have been shown to be activated during immune response [260,263] and thus, may play a less significant role in maintaining tight junction integrity under normal conditions.

Claudins are transmembrane proteins encoded by the claudin (*CLDN*) genes. In humans, 23 *CLDN* genes have been identified, while a total of 24 *CLDN* genes have been reported for rats and mice [264]. Most claudins are made up of at least 120 amino acid residues, with molecular weight between 20 – 27kDa [264,265]. Structurally, claudins span the membrane 4 times, with 2 extracellular loops and the N and C terminals facing the cytoplasm [265]. Functionally, intestinal claudins can be classified into those that mediate the barrier functions of the intestine (tightening or pore-sealing claudins) and those that mediate channel formation (pore-forming claudins) for electrolytes and water transport [266]. Among the claudins that have been detected in the intestine of mice, rats and humans,

claudins 2, 12, and 15 have been shown to play vital roles as paracellular pores or channels for electrolytes (pore-forming claudins), while claudins 1, 3, 4, 5 and 8 are known to strengthen tight junction integrity, thus, classified as pore-sealing claudins [267]. There is still some controversy concerning the classification of claudin 7 as either a pore-sealing or a pore-forming claudin [267,268]. There is evidence that claudin 7 can function as both a pore-sealing and a pore-forming claudin since this protein has been shown to play a significant role as a $Na^+$ pore as well as a barrier for anions, mainly $Cl^-$ [269]. The pore-forming claudins are known to be predominantly distributed in leaky epithelia like the renal proximal tubule and small intestine, while the large intestine is characterised by the presence of pore-sealing claudins [270]. A better understanding of the localisation and distribution of the intestinal claudins, their functions, charge selectivity and regulatory mechanisms will be essential in identifying a potential role for any of the claudins in mediating intestinal phosphate absorption.

### 1.5.1. Localisation and distribution of intestinal claudins

Intestinal Claudins are generally localised at the junction between the BBM and lateral membranes of enterocytes. Immunohistochemistry and immunofluorescent analysis have shown that most of these claudins exist in gradients along the intestinal crypt-villus axis [271,272]. The pore-forming claudins are more concentrated in the crypts and their expression levels diminish towards the villus [271–273]. However, the most highly expressed pore-sealing claudin in the small intestine, claudin 3, shows no crypt-villus gradient, while claudin 4 has been reported to be highest on the epithelial cells on the villus surface [271]. As summarised in Table 1.3, the highest expression of claudin 1 in the intestine of rodents and humans has been shown in colonic epithelia [268,273,274]. Claudin 2,

which is localised in the BBM, has been shown to be highest in the ileum of all three species, while low levels are observed in the duodenum of rat and humans, and the jejunum of mice [268,275,276]. In the rat intestine, claudin 3 is localised on the BBM, and has its highest levels in the duodenum and colon [268], while in mice and humans, the ileum shows the highest levels of claudin 3 [272,275,276]. In addition to their localisation in the apical membrane, claudin 4 and 7 have also been shown to be localised in the lateral and basolateral membranes [273]. In mice, claudin 4 levels appear to be similar in all the segments of the small intestine and colon, while its levels in rats and humans are highest in the colon [268,273,275,276]. In rats and mice, claudin 7 has been reported to be highest in the ileum [268,276], while in humans, claudin 7 is highest in the colon [275]. Claudin 8 levels in mice and humans increase down the intestine [272,276], with the lowest levels seen in the duodenum [275,276], while claudin 8 in the rat intestine is highest in the colon, with moderately high levels in the duodenum [268]. Claudins 12 and 15 have been shown to be localised in the apical-most surface of the lateral membrane [272]. In humans, the levels of claudin 12 are similar in all the segments tested, while claudin 15 is highest in the duodenum [275]. The levels of these claudins in the human jejunum have not been reported. In mice, claudin 12 is most highly expressed in the ileum, while relatively higher levels of claudin 15 have been reported in the proximal segments of the intestine; duodenum and jejunum [272,276]. In the rats, the jejunum shows the highest levels of claudin 12 [268], while the regional expression of claudin 15 in this species has not yet been documented.

**Table 1.3. Expression profile of intestinal claudins in rats, mice and humans**

| Claudins | Species | Duodenum | Jejunum | Ileum | Colon | References |
|---|---|---|---|---|---|---|
| Claudin 1 | Mice | + | + | + | ++ | 276 |
| | Rats | + | ++ | + | +++ | 268 |
| | Humans | + | nd | - | ++ | 273,275 |
| Claudin 2 | Mice | ++ | + | +++ | ++ | 276 |
| | Rats | + | ++ | +++ | - | 268,271,273 |
| | Humans | + | nd | +++ | - | 273,275 |
| Claudin 3 | Mice | + | ++ | +++ | +++ | 276 |
| | Rats | +++ | + | + | +++ | 268,271 |
| | Humans | + | nd | + | +++ | 275 |
| Claudin 4 | Mice | + | + | + | + | 276 |
| | Rats | ++ | + | + | +++ | 268,273 |
| | Humans | + | nd | + | +++ | 275 |

| | | | | | | |
|---|---|---|---|---|---|---|
| Claudin 7 | Mice | + | ++ | +++ | + | 272,276 |
| | Rats | + | + | +++ | ++ | 268 |
| | Humans | ++ | nd | + | +++ | 275 |
| Claudin 8 | Mice | + | + | ++ | +++ | 276 |
| | Rats | ++ | - | + | +++ | 268 |
| | Humans | - | nd | + | +++ | 275 |
| Claudin 12 | Mice | + | + | ++ | + | 272,276 |
| | Rats | + | +++ | ++ | + | 268 |
| | Humans | + | nd | + | + | 275 |
| Claudin 15 | Mice | +++ | +++ | ++ | + | 272,276 |
| | Rats | nd | nd | nd | nd | |
| | Humans | +++ | nd | ++ | + | 275 |

Expression levels are represented as very low or not detected (-), mild (+), moderate (++), high (+++) and not determined (nd)

### 1.5.2. Physiological functions and regulation of intestinal claudins

As the names imply, the pore-sealing claudins 1, 3, 4, 5 and 8 are known to inhibit the diffusion of electrolytes and water molecules through the paracellular pathways [274,277–280], while the pore-forming claudins play important roles in the selective transport of cations, anions and water [256,257,259,281]. Amongst the pore-sealing claudins, claudin 3 is known to be the most highly expressed claudin in the small intestine and colon [273,276,282,283] and has been shown to be significantly downregulated by prolactin and vitamin D [284,285]. Zinc ($Zn^{2+}$) has recently been reported as an important intracellular regulator of claudin 3, with low levels of $Zn^{2+}$ in the enterocytes demonstrated to cause the downregulation of claudin 3 mRNA expression and protein levels [286]. Claudin 4, another highly expressed pore-sealing claudin, has been shown to act as a selective barrier to the diffusion of $Na^{+}$ [280]. Quercetin, the most abundant flavonoid, has been shown to strengthen tight junction barrier properties by upregulating claudin 4 levels in Caco-2 cells [287]. Moreover, claudin 8, has also been reported to act as a barrier for both monovalent and divalent cations, and its levels are regulated by aldosterone [279,288]. Although claudin 1 and claudin 5 expression have been detected in the intestine, their physiological roles have not been studied in detail in this tissue. However, claudin 1 is known to be the major tight junction protein in the epidermis of the skin as mice lacking claudin 1 die of dehydration few hours after birth [289], while claudin 5 has been shown to be a major component of the blood brain barrier [278].

Pore-forming claudins 2 and 12 have been shown to be primarily involved in $1,25(OH)_2D_3$-dependent paracellular $Ca^{2+}$ absorption [257]. Additionally, claudin 2 in leaky epithelia like the jejunum, has also been reported to act as a channel for

monovalent cations like $Na^+$ and $K^+$; and water, driven by the osmotic gradient generated by $Na^+$ transport through the channel [270]. Studies in claudin 7 knock-out mice have shown that claudin 7 selectively acts as a barrier for $Cl^-$ and organic solutes [290], while also mediating paracellular $Na^+$ transport [269]. There is a paucity of information on the hormonal regulation of intestinal claudin 7, however estrogen has been shown to significantly upregulate claudin 7 levels in the luminal epithelial cells of the uterus in rats [291]. A large body of evidence supports the role of claudins 2 and 15 as the major pore-forming claudins in the small intestine (reviewed in [292]). Studies in claudin 2 and 15 double knock-out mice have shown that these claudins are the major pathway for the paracellular transport of $Na^+$ [293]. Interestingly, the transport of $Na^+$ via these claudins significantly impacts the transcellular transport of glucose, amino acids and lipids [293]. Additionally, studies have demonstrated that the loss of $Na^+$ and glucose absorption in the small intestine of the claudin 2 and 15 double knock-out mice was mainly due to the absence of claudin 15 [256]. It is worth noting that mice lacking NHE3 are characterised by reduced claudin 2 and 15 levels compared to wild-type mice [294], suggesting a role for NHE3 in the regulation of claudin 2 and 15 expressions.

Furthermore, intestinal claudins have been shown to change with age [273,276]. While the levels of claudin 3, 4, 7 and 15 have been shown to increase with age, claudin 8 is unaffected [276]. Claudin 2 levels have been shown to be significantly higher in newborn and suckling animals, and its levels decrease with increasing age [276]. The high levels of claudin 2 in young animals may be because of the significant need for $Ca^{2+}$ during bone development since claudin 2 is primarily involved in paracellular $Ca^{2+}$ absorption. Intestinal claudins have been reported

to be regulated acutely by posttranslational modifications, including phosphorylation, glycosylation and palmitoylation of the proteins [295]. Because most claudins have been shown to have a PDZ-binding motif at their intracellular C-terminal [260], phosphorylation of these proteins appears to be the most common posttranslational regulatory pathway. Notably, PKA and PKC have both been reported to control paracellular permeability by phosphorylating pore-sealing claudins within the enterocyte [265]. PKA–mediated phosphorylation of claudin 3 has been shown to affect its anchoring to tight junctions [296], while PKC-δ-induced phosphorylation of claudin 4 has been demonstrated to facilitate the assembly of this pore-sealing claudin into intestinal epithelial tight junctions [297]. Other enzymes that have been reported to phosphorylate claudins in order to alter tight junction properties are: WNK4, tyrosine kinase, mitogen-activated protein kinase (MAPK) and c-Jun N-terminal kinase (JNK) [260]. For instance, JNK has been shown to upregulate claudin 2 expression [298], while MAPK has been demonstrated to play a role in the downregulation of claudin 2 expression [299].

### 1.5.3. Charge and size selectivity of pore-forming claudins

Based on the electrical charge and the molecular size of the solutes in luminal content, the pore-forming claudins in the small intestine are designed to selectively permit the diffusion of both organic and inorganic solutes. Increasing evidence suggests that a charged amino acid side chain in the first extracellular loop of the protein structure of claudins is responsible for the charge selectivity of pore-forming claudins [300]. Claudins are hypothesised to be lined by charged amino acid residues, which create a charge selective filter such that electrolytes with the same electrical charge as the amino acid side-chain are repelled and are unable to diffuse through the claudin channel, hence, why most pore-forming

claudins are cation selective [295]. Genetic studies involving the introduction of a single positive charge at position M2 of the first extracellular loop of claudin 15 reverses the preference of this claudin from being a $Na^+$ pore to a $Cl^-$ channel [301]. There is limited information on the respective pore sizes of all the intestinal pore-forming claudins. However, a recent study investigating the permeability of claudin 15 to organic and inorganic solutes of different sizes have revealed some size-dependent differences in the permeability of positively charged solutes through this claudin in Madin-Darby canine kidney (MDCK) cells [302]. Tanaka and colleagues [302] showed that the pore size of claudin 15 is approximately 5.6 Å in diameter and that the permeability of large organic cations like methylammonium, ethylammonium tetramethylammonium, tetraethylammonium, arginine, and N-methyl-D-glucamine through this claudin is significantly less than that of $Na^+$. In addition, the pore size of claudin 2 has been reported to be approximately 6.5–7.5 Å in diameter [303], thus, only cations that are less than this pore diameter are likely to diffuse freely through this claudin. It is worth noting that in addition to the presence of pore-forming claudins mediating paracellular transport of cations in the small intestine, there are also leak pores between enterocytes that are up to 50-60 Å in radius in the crypts, and less than 6 Å in the upper portion of the villus [304]. These pores have been shown to be relatively permeable to all solutes, with no charge-selectivity [304]. Evidence from cell culture studies suggests that increased expression of the pore-sealing claudins, for instance, claudin 3, may significantly seal these leak pores between enterocytes and thus, reduce the paracellular transport of both charged and uncharged solutes [277].

### 1.6. Iron and the regulators of phosphate homeostasis

Increasing evidence from both clinical and animal studies suggests a link between iron deficiency and phosphate homeostasis [305–308]. In autosomal dominant hypophosphataemic rickets (ADHR), the mutation within the FGF-23 pro-protein convertase site affects the physiological cleavage of the intact FGF-23 within the osteocytes [307]. This results in elevated levels of intact FGF-23 in the circulation, responsible for the hypophosphataemia seen in ADHR. The observation that low serum iron levels are associated with high intact FGF-23 concentrations during the active phase of this disease [309] suggests a link between iron homeostasis and intact FGF-23.

In addition, there is evidence that iron deficiency affects the transcription of FGF-23 in osteocytes [310]. Unlike in ADHR, FGF-23 is continuously cleaved within osteocytes in iron deficient humans with normal renal function, resulting in the presence of excess cFGF-23 in the circulation, while intact FGF-23 levels are unaffected [305]. In the same study, treatment of the iron deficiency significantly reduced the transcription of FGF-23, resulting in lowered levels of cFGF-23 and unchanged phosphate levels in the circulation. Additionally, intravenous iron injection in healthy subjects with normal serum iron levels had no impact on intact FGF-23 [311]. In rodents, neonatal iron deficiency has been shown to increase intact FGF-23 levels in both normal and ADHR mice [307], but not in adult mice [310]. Moreover, iron deficiency has also been linked to $1,25(OH)_2D_3$ deficiency in neonatal mice, which was reported to be as a result of significantly increased levels of intact FGF-23 associated with iron deficiency [307]. Clinical evidence in iron deficient children suggests that an association between iron deficiency and $1,25(OH)_2D_3$ deficiency exists [312]. The exact impact of iron deficiency on the

functions of the hormones of phosphate homeostasis, particularly how iron deficiency affect intestinal phosphate absorption and renal phosphate reabsorption remains to be determined.

### 1.7. Aims of study

Rats and mice are widely used as experimental models to study the mechanisms of intestinal phosphate absorption. Although the transporters mediating phosphate absorption in rats and mice are known to show significant variations in different segments of the small intestine [17,39], there is limited information on the segmental profile of these transporters in the human small intestine. Therefore, the aim of the experiments described in chapter 3 was to understand the regional differences in the expression of the transcellular phosphate transporters, NaPi-IIb and PiT-1 and the mediator of paracellular phosphate absorption, NHE3, in mice, rats and humans. Since previous evidence suggests that there may be some variations between the mechanisms underlying phosphate absorption in different segments of the small intestine in rodents [17,38,39,45], the contribution of NaPi-IIb and NHE3 to phosphate absorption in the proximal and distal small intestine of mice, and the duodenum and jejunum of rats, was investigated. Furthermore, the aim of the experiments in subsequent chapters was to investigate the link between diet-induced iron deficiency and phosphate homeostasis, with a particular focus on how iron deficiency impacts the mechanisms of phosphate absorption in the rat duodenum and jejunum. The inhibition of intestinal phosphate absorption by phosphate binders is a major treatment strategy for managing hyperphosphatemia in CKD patients [313,314]. Therefore, understanding the mechanisms of intestinal phosphate absorption and the differences that exist in different intestinal segments will provide more insights

into the generation of a segment-specific method for inhibiting intestinal phosphate absorption.

# Chapter Two

## 2.0. General Methods

## 2.1. Animals

Male animals, C57BL/6 mice and Sprague-Dawley rats, both 6 – 8 weeks' old and intestinal specific NaPi-IIb homozygous knock-out and wild-type mice of 8 – 10 weeks of age were used for the study. The Sprague-Dawley rats were obtained from Charles River Laboratories (Harlow, UK), and the NaPi-IIb knock-out and wild-type mice were generated in Professor Carsten Wagner's laboratory, Institute of Physiology, University of Zurich, Switzerland. These animals were transferred to the Comparative Biology Service Unit at UCL Medical School, Royal Free Hospital, London. All animals were allowed free access to drinking water and standard rodent diet (RM1, SDS Ltd, Witham, UK) or custom iron diets (Harlan Laboratories, Inc. Madison, WI, USA). A maximum of three rats or six mice were housed in a single cage, maintained on a 12-hour light/dark cycle. All procedures were conducted in accordance with the UK legislation (Animal Scientific Procedures Act, 1986, Amendment regulations 2012).

## 2.2. Intestinal tissue collection

Rat and mouse intestinal mucosa scrapes were obtained from the duodenum (between the pylorus and ligament of Treitz), jejunum (from the ligament of Treitz to the halfway point through the small intestine) and ileum (between the halfway points to the ileocecal junction). All tissues were immediately frozen in liquid nitrogen and stored at -80 °C until required. Human tissue biopsies were taken from the small intestine of healthy adult volunteers that arrived at the endoscopy unit of Sahlgrenska University Hospital, Gothenburg, Sweden in the morning after an overnight fast. Following conscious sedation with midazolam and alfentanil, an endoscope was introduced into the gastrointestinal tract and the biopsies were harvested from the duodenum, proximal jejunum and ileum, and the tissue was

put in RNA STAT-60 (Amsbio, Abingdon, U.K) after which they were immediately frozen in liquid nitrogen and transferred to a -80 °C freezer. All human tissue samples were packaged in Professor Lars Fandriks Laboratory at the University of Gothenburg, Sweden, and shipped on dry ice to me in London, where they were used for the current study. All volunteers gave written consent, and the Regional Ethical Review Board of Gothenburg, Sweden, approved the study.

### 2.3. Measurement of mRNA levels

#### 2.3.1. RNA extraction and Quantification

All materials used for RNA extraction were sterilised using an autoclave. Total RNA was isolated from intestinal and kidney tissues using TRIzol (Life Technologies, Paisley, UK). Whole tissue samples or intestinal tissue scrapes were ground in liquid nitrogen using a mortar and pestle. Approximately 50-100 mg of the ground tissue sample was then mixed with 1 mL TRIzol, shaken vigorously and incubated at room temperature for 5 minutes. Phase separation was done by adding 0.2 mL of chloroform to the tissue – TRIzol mixture and shaken vigorously by hand for 15 seconds. The mixture was incubated for 3 minutes at room temperature, following which it was centrifuged at 12000 g for 15 minutes at 4 ˚C. The aqueous phase of the sample was transferred to a fresh tube. RNA was isolated by adding 0.5 mL of 100 % isopropanol to the aqueous phase and the mixture was incubated at room temperature for 10 minutes. To obtain the RNA pellet, the mixture was centrifuged at 12000 g for 10 minutes at 4 ˚C, after which the supernatant was removed. The RNA pellet was washed using 1 ml of 75 % ethanol and centrifuged at 7500 g for 5 minutes at 4 ˚C. The supernatant was removed and the RNA pellet was dried briefly at room temperature. The dried RNA pellet was resuspended using an appropriate

volume of DEPC-treated water. The concentration and purity of the extracted RNA sample were measured using the NanoDrop spectrophotometer (LabTech international). To further assess the purity of the RNA, electrophoresis of the RNA was carried out on a 2% agarose-TAE gel, which was stained with ethidium bromide and run at 50 V for 1 hour. The bands of the RNA were visualised under UV light using a transilluminator (Peqlab Biotechnologie GmbH, Germany). The RNA samples were stored at -80 °C until required.

### 2.3.2. cDNA Synthesis

The RNA sample was treated with deoxyribonuclease I (Life Technologies, Paisley, UK) according to the manufacturer's instructions. 1 µL each of 10X DNase I reaction buffer and DNase I, Amp Grade (1 U/µL) was added to 1 µg of the RNA sample. DEPC-treated water was added to the sample mixture to obtain a total volume of 10 µL. The mixture was vortexed and incubated at room temperature for 15 minutes. To inactivate the DNase I enzyme, 1 µL of EDTA was added to the reaction mixture and heated at 65 °C for 10 minutes. Complementary DNA (cDNA) was then synthesised by the reverse transcription of the pretreated RNA using a cDNA synthesis kit (PCR Biosystems Ltd, London, UK) following manufacturer's instructions. 4 µL of 5x cDNA synthesis mix, 1 µL of 20x RTase and 4 µL of PCR-grade $dH_2O$ was added to the pretreated RNA sample. The reaction mixture was incubated in a heat block at 42 °C for 30 minutes (step 1) and 85 °C for 10 minutes (step 2) to synthesise the cDNA and denature the RTase enzyme respectively. As a negative control, a non-reverse transcriptase sample was prepared using the pretreated RNA, mixed with 4 µL of 5x cDNA synthesis mix and 5 µL of PCR-grade $H_2O$ and then incubated in the

heat block using the same protocol as stated above. The cDNA and the non-reverse transcriptase samples were stored at -20 °C.

### 2.3.3. Real-time polymerase chain reaction

The mRNA expression levels of the genes of interest were analysed by real-time polymerase chain reaction (RT-PCR) using 2xqPCR BIO SyGreen kit (PCR Biosystems Ltd, London, UK) and primers (Table 2.1). Primers were obtained from Qiagen, UK or predesigned primer sequences were sent to Sigma-Aldrich where they were manufactured (Table 2.1). cDNA, 1.0 µL, was added to a reaction mix (containing 0.5 µL of PCR primer, 5.0 µL of SybraGreen and 3.5 µL of PCR-grade $dH_2O$) in a 96-well plate. The non-reverse transcriptase negative control and the reaction mix alone were run on the same plate to confirm the absence of DNA contamination in the samples the reaction mix respectively. The PCR reaction set up was prepared according to the manufacturer's instructions. The reaction was performed on a Light Cycler 96 instrument (Roche Diagnostics, East Sussex, UK) as follows: preincubation at 95 °C for 10 min, 3-step amplification consisting of: 95 °C for 10 s (step 1), 60 °C for 10 s (step 2) and 72 °C for 10 s (step 3). A total of 35 or 45 cycles for the 3-step amplification were carried out followed by a melting stage consisting of 95 °C for 10 s, 60 °C for 60 s and 97 °C for 1 s. The final condition of the melting stage was continuous, with five readings recorded per unit temperature. The data was analysed using the Light Cycler 96 analysis software and the relative quantification (Rel Quant) of the mRNA for each gene of interest to β-actin was taken as the mRNA expression levels.

**Table 2.1. RT-PCR primers**

| Primer name | Cat. Number | Forward Sequence | Reverse Sequence |
|---|---|---|---|
| Rat claudin 3 | QT01169406 | - | - |
| Rat claudin 4 | QT00376726 | - | - |
| Rat claudin 7 | QT00400267 | - | - |
| Rat claudin 8 | QT00428617 | - | - |
| Rat claudin 12 | QT01607319 | - | - |
| Rat claudin 15 | QT01584604 | - | - |
| Rat SGLT1 | QT00001246 | - | - |
| Rat GLUT2 | - | ACTCCGATTAGAAACGTCA | CGTAAGGCCCGAGGAA |
| Rat NaPi-IIb | QT00188594 | - | - |
| Mouse NaPi-IIb | - | ATCCACTCACGTTGGG | CTGCGAACCAGCGATA |
| Human NaPi-IIb | QT00071883 | - | - |
| Rat NHE3 | QT00180985 | - | - |

| | | | |
|---|---|---|---|
| Mouse NHE3 | QT01039829 | - | - |
| Human NHE3 | QT00095914 | - | - |
| Rat/mouse PiT-1 | - | GGTGGGATGTGCAGTTTTCT | CAAGAGAGGAGGTGGTGTCG |
| Human PiT-1 | QT00028763 | - | - |
| Rat Cyp27b1 | QT00386953 | - | - |
| Rat VDR | - | AGGCTACAAAGGTTTCTTCA | TAGCTTGGGCCTCAGACTGT |
| Rat α-Klotho | QT00185822 | - | - |
| Rat DMT1 | QT00182623 | - | - |
| Mouse DMT1 | QT01047368 | - | - |
| Rat NaPi-IIa | - | AQTCTCATTCGGATTTGGT | CACTTGTGCCTTGACG |
| Rat NaPi-IIc | QT00185633 | - | - |
| Rat β-actin | QT00193473 | - | - |
| Mouse β-actin | QT00095242 | - | - |
| Human β-Actin | - | AACAAGATGAGATTGGCATGG | AGTGGGGTGGCTTTTAGGAT |

## 2.4. Measurement of protein levels

### 2.4.1. Intestinal brush border membrane vesicle preparation

Intestinal BBM vesicles were prepared from snap frozen and stored duodenum and jejunum (at -80 °C) using the $MgCl_2$ precipitation method [39]. Mucosa tissue lining these segments was scraped off using glass slides and suspended in a buffer containing 50 mM mannitol, 2 mM HEPES (pH 7.1) and an EDTA free protease inhibitor cocktail tablet (Sigma-Aldrich, UK). The mucosa tissue was homogenised three times for 20 seconds with a 5-second interval after each homogenisation step, using an Ultra Turax homogeniser (Janke & Kunkel, FRG, UK) set at half speed. Following homogenisation, samples were collected for the assessment of whole cell protein concentration and alkaline phosphatase activity in the protein suspension or homogenate mixture, and $MgCl_2.6H_2O$ was then added to a final concentration of 10 mM in the homogenate. The homogenate was stirred on ice for 20 minutes after which it was centrifuged at 4600 g for 10 min to obtain a supernatant. The supernatant was centrifuged at 41600 g for 30 min to obtain a pellet. The pellet was suspended in a buffer containing 300 mM mannitol, 20 mM HEPES and 0.1 mM $MgSO_4$ (pH 7.2) and an EDTA free protease inhibitor cocktail tablet (Sigma-Aldrich, UK), by passing six times through a 21-gauge needle. The suspension was centrifuged at 9300 g for 15 min, and the supernatant obtained was centrifuged for a further 30 minutes at 41600 g to obtain the BBM pellet. The BBM pellet was resuspended in the latter buffer by passing six times through a 21-gauge needle.

### 2.4.2. Kidney brush border membrane vesicle preparation

Kidney BBM vesicles were prepared from snap frozen and stored kidneys (at -80°C) using the double $MgCl_2$ precipitation method [315]. Kidney cortical slices were

homogenised in 30 ml buffer containing 300 mM mannitol, 5 mM EGTA and 12 mM Tris-HCl (pH 7.4) for 2 min using an Ultra Turax homogeniser (Janke & Kunkel, FRG, UK) set at half speed. Cold deionized water, 42 ml, was added and briefly mixed. Samples were collected for the assessment of whole cell protein concentration and alkaline phosphatase activity, following which $MgCl_2.6H_2O$ was added to make a final concentration of 12 mM. The solution was stirred on ice for 15 minutes and then centrifuged at 2000 g for 15 minutes. The supernatant was re-centrifuged at 33000 g for 30 minutes to obtain a pellet, which was suspended in 20 ml buffer containing 150 mM mannitol, 2.5mM EGTA and 6mM Tris-HCl (pH 7.4) and then homogenised using a hand operated Glass-Teflon homogeniser. A second precipitation using $MgCl_2.6H_2O$, low- and high-speed centrifugations as described above were repeated to obtain a pellet. The pellet was then re-suspended in 20 ml buffer containing 300 mM mannitol, 2.5 mM EGTA and 12 mM Tris-HCl (pH 7.4), homogenised and centrifuged at 33000 g for 30 minutes to obtain the purified BBM pellet. The appropriate volume of the latter buffer was added to re-suspend the BBM pellet using a 1 ml syringe and a 21-gauge needle, and the protein concentration of both renal and intestinal BBM was determined using a Bradford assay [316]. To validate the purity of the BBM, alkaline phosphatase levels in the initial homogenate and the BBM were measured using the method of Forstner *et al*. [317] and the BBM vesicles were approximately 10-fold enriched. All buffers used in the kidney BBM vesicle preparation contained 0.25 mM PMSF and aprotinin (protease inhibitor). All the steps in the isolation of intestinal and kidney BBM vesicle were carried out at 4 °C.

### 2.4.3. Western blotting

Intestinal and kidney BBM vesicles were mixed with Laemmli sample buffer, after which electrophoresis of the samples was carried out on a 10% SDS – polyacrylamide gel at 20 mA and the proteins transferred on to polyvinylidene difluoride (PVDF) membrane by electroblotting, run at 15V for 75 min. Following protein transfer, the PVDF membranes containing the separated proteins were incubated in PBS containing 0.1% Tween 20 (PBS-T) and 6% fat-free milk for 1 hour at room temperature. The membranes were then incubated with antibodies (raised in rabbit or goat) to the protein of interest (Table 2.2) for 16 h at 4 °C. The membranes were washed with PBS-T four times (1 x for 15 min and 3 x for 5 min each), after which they were incubated with either an anti-rabbit antibody (1:2000 dilution, GE Healthcare, Buckinghamshire, UK) or anti-goat antibody (1:1000 dilution, Santa Cruz Biotechnology, Heidelberg, Germany) conjugated to horseradish peroxidase for 1 hour at room temperature. The membranes were washed with PBS-T as described above and the bound antibodies were visualized using a Flour-S Multi-Imager System (Biorad, Hemmel Hempstead, UK), governed by the chemiluminescent method of detection.

The membranes were stripped of the antibodies using a blot restore buffer (Thermo Scientific, Hemmel Hempstead, UK) and non-specific protein binding was blocked with PBS-T containing 6% fat-free milk as described above. The membranes were then incubated with a mouse monoclonal antibody raised against *Xenopus laevis* β-actin (Table 2.2) for 1 hour at room temperature. The membranes were then washed and incubated with the anti-mouse antibody (1:5000 dilution, Sigma Ltd, Amersham, UK) for 1 hour at room temperature and

then visualized. The ratio of the protein of interest to β-actin band volumes was calculated for each sample and presented as arbitrary units (a.u).

**Table 2.2. Western blot antibodies**

| Protein of interest | Species | Source | Catalogue number | Dilutions |
|---|---|---|---|---|
| NaPi-IIa | Rabbit polyclonal | Institute of Physiology-UZH | - | 1:2000 |
| NaPi-IIb | Rabbit polyclonal | LSBio, Inc. | LS-C37453 | 1:500 |
| NaPi-IIc | Rabbit polyclonal | Abcam | ab155986 | 1:1000 |
| NHE3 | Rabbit polyclonal | StressMarq Biociences | SPC-400 | 1:1000 |
| PiT-1 | Rabbit polyclonal | David's Biotechnologie | Custom antibody | 1:100 |
| DMT1 | Rabbit polyclonal | Alpha Diagnostic Int. | NRAMP24-A | 1:500 |
| Claudin 3 | Rabbit polyclonal | Abcam | ab199635 | 1:500 |
| SGLT1 | Goat polyclonal | Santa Cruz Biotechnology | Sc-20584 | 1:1000 |
| GLUT2 | Rabbit polyclonal | Bio-rad | 4670-1659 | 1:1000 |
| β-actin | Mouse monoclonal | Santa Cruz Biotechnology | Sc-69879 | 1:500 |

## 2.5. *In vivo* phosphate uptake experiments

Measurement of transepithelial phosphate absorption *in vivo* was determined using the *in situ* intestinal loop technique [39,176]. Animals were weighed and anaesthetized by an intraperitoneal injection of 45 mg/Kg pentobarbitone sodium (Pentoject; Animal care Ltd, Kent, UK), and maintained at 37 °C on a regulated heating blanket (Harvard Apparatus Ltd, Kent, UK). Following cannulation of the femoral artery in rats, a longitudinal abdominal incision was made and a 5-cm long segment of the duodenum (2 cm distal to the pylorus) or jejunum (5 cm distal to the ligament of Treitz) or ileum (5 cm proximal to the ileocecal junction) was cannulated, flushed with warm 0.9% saline and then flushed with air. Uptake solution (500 µl for rats or 200 µl for mice) containing 16 mM $Na^+$-HEPES, 140 mM NaCl, 3.5 mM KCl and 10 mM $KH_2PO_4$ (pH 7.4) and 0.37 MBq $^{33}P$ (PerkinElmer, Bucks, UK) was instilled into the lumen of the cannulated segment and immediately tied off. For rats, blood (500 µl) was collected from the cannulated femoral artery at 10, 20 and 30 minutes after instilling the uptake solution. However, in mice, a single blood collection was done via cardiac puncture approximately 10 minutes after instilling the uptake buffer into the cannulated intestinal segment. Collected blood samples were centrifuged at 1500 g for 15 min at 4 °C to obtain plasma. After 30 minutes, the cannulated intestinal segment was removed, blotted and the length was measured and recorded. The amount of phosphate transferred from the intestinal segment into 1 ml of plasma was calculated using the data obtained from the scintillation counting (Tri-Carb 2900TR; Perkin Elmer) of $^{33}P$ in plasma and the initial uptake solution.

### 2.6. *In vitro* phosphate uptake experiments

Phosphate transport across the BBM was measured *in vitro* using the everted sleeve technique [45]. Rats were weighed and anaesthetized as described above. Following a longitudinal abdominal incision, segments of the duodenum and jejunum (2-4 cm long) were removed, flushed with warm HEPES buffer containing 16 mM $Na^+$-HEPES, 3.5 mM KCl, 10 mM $MgCl_2$, 1 mM $CaCl_2$ and 125 mM NaCl (pH 7.4) and everted on a glass rod using a thread to hold the tissue in place. The everted tissue was incubated for 5 minutes in the HEPES buffer containing 10 mM glucose, bubbled with 100% $O_2$ and continuously stirred, with the temperature maintained at 37 °C. Following the 5-minute incubation, the tissue was transferred into a chamber containing the uptake solution, which was composed of the HEPES buffer, 10 mM $KH_2PO_4$ and 0.37 MBq $^{33}P$ (PerkinElmer, Bucks, UK) for 2 minutes, with the solution gently stirred and bubbled with 100% $O_2$. The tissue was then washed in a solution containing 150 mM NaCl and 100 mM $KH_2PO_4$ (a 10-fold excess of non-radioactive phosphate in the uptake buffer) for 10 minutes, followed by another 5-minutes wash in PBS. The tissue (approximately 100 mg) was weighed and digested in 2 ml SOLVABLE™ (PerkinElmer, Bucks, UK). Aliquots (100 µl) of the digested sample and initial uptake solution were counted as previously described, and the amount of phosphate transferred into the tissue was calculated and expressed as nmoles of phosphate/100 mg of intestinal tissue.

### 2.7. Urine and Blood biochemistry

Animals were put in metabolic cages overnight (16 hours) to collect urine samples before the *in vivo* or *in vitro* experiments. Blood samples were collected at the end of the experiment by either cardiac puncture or via femoral artery

cannulation. For plasma samples, blood was put in heparinised tubes, while for serum collection, blood was put in anticoagulant free containers to allow the formation of blood clots. Blood samples were then centrifuged at 7500 g for 10 minutes at 4 °C to obtain serum and plasma.

### 2.7.1. Measurement of iron levels - haematocrit levels and iron Assays

Non-haemolysed blood samples were collected via the femoral artery cannulation into heparinised capillary tubes and spun using a micro-haematocrit centrifuge (Hawksley, England) for 5 minutes. The haematocrit levels were read using a micro-haematocrit reader.

Serum samples were sent to the Chemical Pathology Department, at the Royal Free Hospital for measurement of iron levels. Samples were analysed using Randox reagents (Randox Laboratories, UK) using an RX series analyser, RX Daytona plus.

Unsaturated iron-binding capacity (UIBC) and total iron-binding capacity (TIBC) were measured using a commercially available assay kit (Pointe Scientific Inc. Canton, MI, USA) following manufacturer's instruction. For UIBC measurement, a known amount of ferrous ion was added to the serum sample in alkaline pH in order to bind to the transferrin binding sites. The unbound ferrous ions were measured by their reaction with ferrozine in the iron-colour reagent (Ferrozine reaction). The difference between the number of ferrous ions added and the unbound ions gives the UIBC. TIBC was obtained by the summation of the UIBC and the serum iron levels. For consistency, serum iron levels used for estimating the TIBC was measured using the ferrozine reaction. The iron buffer reagent releases ferrous ions from transferrin-bound ferric iron in acidic pH, and the ferrous ions react with ferrozine in the iron colour reagent to give a violet colour.

The absorbance of the reaction product was measured at 560 nm using a spectrophotometer.

### 2.7.2. Measurement of phosphate levels

Serum and urine phosphate levels were measured using a Phosphate Colorimetric Assay Kit (BioVision Inc, Milpitas, CA, USA) following manufacturer's instruction. The assay utilises the reaction between phosphate ions with malachite green and ammonium molybdate. This reaction forms a chromogenic complex (green colour) and the absorbance of this complex is measured at a wavelength of 620 – 650 nm.

### 2.7.3. Hormone assays

All assays were carried out on serum or plasma samples following the manufacturer's instructions. Serum intact FGF-23 concentrations were analysed using a commercially available enzyme-linked immunosorbent assay (ELISA) (Kainos Laboratories Inc., Tokyo, Japan), plasma c-term FGF-23 concentrations were assessed using a rodent-specific c-term FGF-23 ELISA (Immutopics, Inc., San Clemente, CA, USA), serum 1,25 $(OH)_2D_3$ ELISA kit (LSBio Inc., Seattle, WA, USA) was used to measure 1,25 $(OH)_2D_3$ levels, and plasma PTH concentrations were assayed using rat bioactive intact PTH ELISA kit (Immutopics, Inc., San Clemente, CA, USA).

#### 2.7.3.1. Serum intact FGF-23 assay test principle

The intact FGF-23 ELISA is governed by a two-step reaction principle. First, intact FGF-23 in the test sample binds to the immobilised antibody in the microtiter well to form an FGF-23/antibody complex. The second reaction step involves the binding of the FGF-23/antibody complex with horseradish peroxidase (HRP)-labelled antibody to form a sandwich-like complex. The catalytic activity of the

peroxidase enzyme depends on the levels of intact FGF-23 in the sandwich-like complex. Activated peroxidase catalyses the reaction between 3,3',5,5'-Tetramethylbenzidine (TMBZ) and hydrogen peroxide (both in the substrate) to give a chromogenic product, whose absorbance at a wavelength of 450 nm reflects the level of intact FGF-23 in the sample.

#### 2.7.3.2. Plasma c-term FGF-23 assay test principle

The wells in the c-term FGF-23 ELISA plate contain two affinity purified goat polyclonal antibodies that detect epitopes within the C-terminal region of mouse or rat FGF-23. One of the antibodies is conjugated with HRP, while the other is biotinylated for capturing FGF-23 in the sample. The c-term FGF-23 in the sample is bound to both antibodies in a streptavidin-coated microtiter well to form a sandwich-like complex. Like intact FGF-23, the activity of the peroxidase is directly proportional to the amount of c-term FGF-23 in the sample, and the absorbance of the chromogenic product, formed from the reaction between TMBZ and hydrogen peroxide in the substrate, gives the level of c-term FGF-23 in the sample.

#### 2.7.3.3. Serum $1,25(OH)_2D_3$ assay test principle

Unlike the sandwich-ELISA assays described above, this assay is based on a competitive binding principle. Samples or standards were added to each well together with an HRP-conjugated target antigen. The free antigen in the sample competes with the HRP-conjugated antigen for binding to a capture antibody in each well of the microtiter assay plate. The antigen in the sample is able to displace the HRP-conjugated target antigen from binding with the capture antibody, thus reducing the activity of the peroxidase enzyme. Hydrogen peroxide and TMBZ in the substrate reacts to produce a chromogenic product whose

absorbance at 450 nm is inversely correlated with the concentration of $1,25(OH)_2D_3$ in the sample. Therefore, the higher the antigen ($1,25(OH)_2D_3$) in the sample, the lower the intensity of the colour generated or optical density from the experiment.

#### 2.7.3.4. Plasma intact PTH assay test principle

Two affinity purified goat polyclonal antibodies present in the streptavidin-coated microtiter well detect full-length or intact PTH. One of the antibodies, which captures the antigen (PTH) is biotinylated and it recognises epitopes within the C-terminal portion of the peptide, while the other antibody recognises the N-terminal epitope, and it is conjugated with the enzyme HRP for detection. Intact PTH in the sample binds to both antibodies to form a sandwich-like complex. Like other sandwich ELISA described above, the concentration of PTH in the samples is directly proportional to the absorbance of the chromogenic product of the HRP-catalysed reaction.

### 2.8. Statistical analysis

Data are presented as mean ± SEM. Where possible, statistical analysis was performed using unpaired Student's t-test, one-way ANOVA with Tukey's post-test or a two-way ANOVA with Bonferroni's post-test to determine any statistical differences between groups. All analyses were performed using GraphPad Prism 5.0 software, and statistical significance were depicted as follows: $*P < 0.05$, $**P < 0.01$ or $***P < 0.001$.

# Chapter Three

## 3.0. Comparison of the mechanisms of intestinal phosphate absorption in mice, rats and humans

### 3.1. Introduction

The quest for a safe and reliable management therapy for hyperphosphataemia in CKD patients is ongoing. Phosphate absorption in the small intestine is known to be the major target for controlling serum phosphate levels in patients with end-stage renal disease (ESRD), and rodents are widely used as experimental models for the study of potential therapies for the control of intestinal phosphate absorption. As described in section 1.4, it is recognised that there are species differences in the major small intestinal segments responsible for phosphate absorption in rodents, and there is an ongoing debate concerning the relative contribution of the $Na^+$-dependent and $Na^+$-independent phosphate transport pathways. Using a physiological phosphate concentration, a previous report demonstrated that total transepithelial phosphate absorption *in vivo* was solely mediated by the $Na^+$-independent pathway in the rat duodenum, while only 70% of jejunal phosphate transport was mediated by this pathway, with the remaining 30% mediated by the $Na^+$-dependent pathway [45]. Interestingly, even though the $Na^+$-independent pathway for phosphate absorption appears to be the predominant pathway under physiological conditions in rats, the administration of a novel NaPi-IIb inhibitor, ASP 3325, was shown to be beneficial in reducing plasma phosphate levels in normal rats and those with ESRD [76]. In contrast, clinical studies in humans demonstrated that this inhibitor was ineffective in the treatment of hyperphosphataemia in ESRD patients [318]. Whether these contradictory observations are as a result of differences in experimental conditions or highlight that NaPi-IIb plays no role in intestinal phosphate absorption in humans remains to be confirmed.

Emerging evidence suggests that NHE3 significantly contributes to small intestinal phosphate absorption. This is attributed to the findings that the administration of tenapanor, a competitive inhibitor of NHE3, significantly reduced intestinal phosphate absorption and serum phosphate levels in rats and humans with CKD, but plays an insignificant role in mice [77,247]. It is therefore becoming apparent that the differences in intestinal phosphate transport mechanisms in various species may explain the discrepancies in the efficacy of both NaPi-IIb and NHE3 inhibitors on phosphate absorption in rats, mice and humans. Importantly, even though there is evidence suggesting that the proximal small intestine is the major segment for phosphate absorption in rats and humans [319], there is still a lack of information on the pattern of expression of the transcellular phosphate transporters, NaPi-IIb and PiT-1, and the mediator of paracellular phosphate absorption, NHE3, in humans. The aim of this chapter was to first compare the expression levels of NaPi-IIb, PiT-1 and NHE3 in the different segments of the small intestine of rat, mice and humans, and secondly, to confirm the contribution of NaPi-IIb, NHE3 and the $Na^+$-independent pathway to overall phosphate absorption in rats and mice using physiological phosphate concentrations.

## 3.2. Methods

### 3.2.1. Animals and intestinal tissue collection

Male Sprague Dawley rats and C57BL/6J mice, aged 6-8 weeks and intestinal specific NaPi-IIb knock-out and wild-type mice, aged 8-12 weeks, were used for this study. Animals were fed with RM1 diet, which contains 0.52% phosphate as described in section 2.1. For tissue collection, animals were anaesthetised by intraperitoneal injection with pentobarbitone sodium (40-50 mg/kg body weight,

Pentoject; Animalcare Ltd, York, UK) and mucosa scrapes were obtained from defined regions of the small intestine as described in section 2.2. The mucosa scrapes from the mouse duodenum and jejunum were pooled together to ensure that the tissues were enough for RNA and protein preparations, and were referred to as the proximal small intestine, while the ileum was taken as the distal small intestine. After tissue collection, cervical dislocation in mice and exsanguination (by cutting the heart) in rats were carried out to ensure animals were dead. The tissues were snap frozen in liquid nitrogen and stored at -80 °C until required.

### 3.2.2. Human tissue collection

As described in section 2.2, human intestinal tissue biopsies were obtained from healthy adult volunteers apparently consuming a normal phosphate diet. Tissue biopsies were collected from the duodenum (20 cm distal to the pylorus), jejunum (50 cm distal to the ligament of Treitz) and the ileum (50 cm proximal to the ileocecal junction). Tissues were snap frozen in liquid nitrogen and stored at -80 °C until required.

### 3.2.3. RT-PCR

As described in section 2.3.1, RNA was extracted from thawed human tissue biopsies and the mucosa scrapes collected from rats and mice, using the Trizol method. cDNA was synthesised from 1 µg of RNA by reverse transcription reaction as described in section 2.3.2 and RT-PCR experiments were carried out as described in section 2.3.3 to test the levels of NaPi-IIb, PiT-1 and NHE3, using rat, mouse and human specific primers (Table 2.1).

### 3.2.4. Western blot

BBM proteins were prepared from thawed intestinal mucosa scrapes obtained from rats and mice using the $MgCl_2$ precipitation method as described in section

2.4.1. Intestinal BBM protein (20-50 µg) were used for Western blotting to establish the protein levels of NaPi-IIb, PiT-1 and NHE3 as described in section 2.4.3, using specific primary antibodies (Table 2.2) and their corresponding secondary antibodies. The ratio of NaPi-IIb, PiT-1 and NHE3 to *β*-actin was expressed as a.u.

### 3.2.5. *In vivo* uptake

*In vivo* phosphate uptake experiments were carried out in the jejunum and ileum of mice, using 8-10 mM phosphate solution in the uptake buffer as described in section 2.5. To test the relative contribution of the jejunum and ileum to overall phosphate absorption, the amount of phosphate transferred into blood after 10 minutes per 5 cm of the cannulated jejunum or ileum was determined. In addition, the relative contribution of NaPi-IIb and NHE3 to phosphate absorption was investigated using a potent NaPi-IIb inhibitor, NTX9066, and an NHE3 inhibitor, tenapanor [77], both obtained from Ardelyx Inc. (Fremont, CA, USA).

### 3.2.6. *In vitro* uptake

*In vitro* phosphate uptake experiments were carried out using rat duodenal and jejunal segments to test the contribution of NaPi-IIb, NHE3 and $Na^+$-independent mechanism to phosphate absorption in these intestinal segments as described in section 2.6. To test the contribution of NaPi-IIb to phosphate absorption, 10 mM PFA, a competitive inhibitor of NaPi-IIb was added to the uptake buffer. To investigate the contribution of NHE3, 10 µM tenapanor was added to the uptake buffer, while uptake buffer prepared using $Na^+$ free HEPES and choline chloride, an iso-osmotic replacement for $Na^+$, was used to test the contribution of the $Na^+$-independent pathway to phosphate absorption in these segments. The uptake buffer in all experiments contained physiological concentration of luminal

phosphate, 10 mM. The amount of phosphate transferred from the uptake buffer into the intestinal tissue (phosphate uptake) was expressed in nmoles/100mg of the intestinal segment. Phosphate uptake in the presence of PFA or tenapanor or the $Na^+$-free uptake solution was expressed as a percentage of the total phosphate uptake using a normal physiological luminal solution containing $Na^+$.

### 3.2.7. Statistical analysis

Data are presented as mean ± SEM using bar graphs. Statistical analysis was carried out as described in section 2.8, and statistical significance was depicted as follows: *$P$<0.05, **$P$<0.01 or ***$P$<0.001.

## 3.3. Results

### 3.3.1. Regional expression of the transcellular phosphate transporters in the small intestine of mice, rats and humans

As previously described [38,39], in the mouse small intestine, NaP-IIb mRNA levels were significantly higher in the distal small intestine compared to the proximal small intestine (Figure 3.1A). In contrast, although NaPi-IIb mRNA has been reported in rat duodenum [39], its levels were very low compared to the jejunum, which is the segment that showed the highest expression of NaPi-IIb mRNA (Figure 3.1B). In contrast to rat and mouse NaPi-IIb profile, human NaPi-IIb mRNA was highest in the duodenum, followed by the jejunum, with very low levels in the ileum (Figure 3.1C).

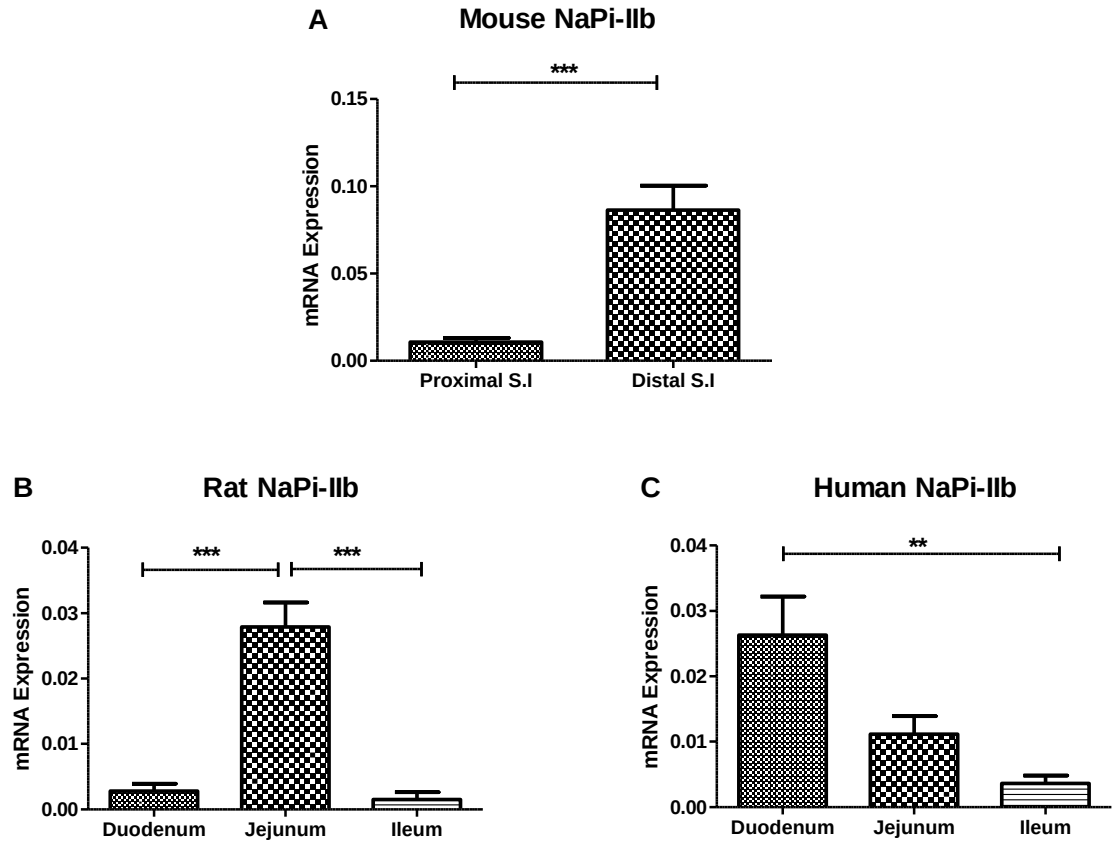


**Figure 3.1. RT-PCR quantification of NaPi-IIb in distinct regions of mouse, rat and human small intestine**. Duplicate PCR reactions were performed for each sample and the mRNA expression of NaPi-IIb is given as the ratio of NaPi-IIb to *β*-actin. An unpaired t-test (A) and a one-way ANOVA with Tukey's multiple comparisons post-tests (B and C) were used to compare results between groups (n=5-9). ***P*<0.01, ****P*<0.001

Interestingly, intestinal PiT-1 mRNA also showed some variations in the regional expression profile between species. In mice, PiT-1 mRNA was significantly higher in the proximal small intestine compared to the distal small intestine (Figure 3.2A). However, in rats, PiT-1 mRNA was significantly higher in the jejunum compared to the duodenum (Figure 3.2B). Although PiT-1 mRNA expression was similar in the duodenum, jejunum and ileum of humans (Figure 3.2C), its contribution to phosphate absorption in this species is unclear.

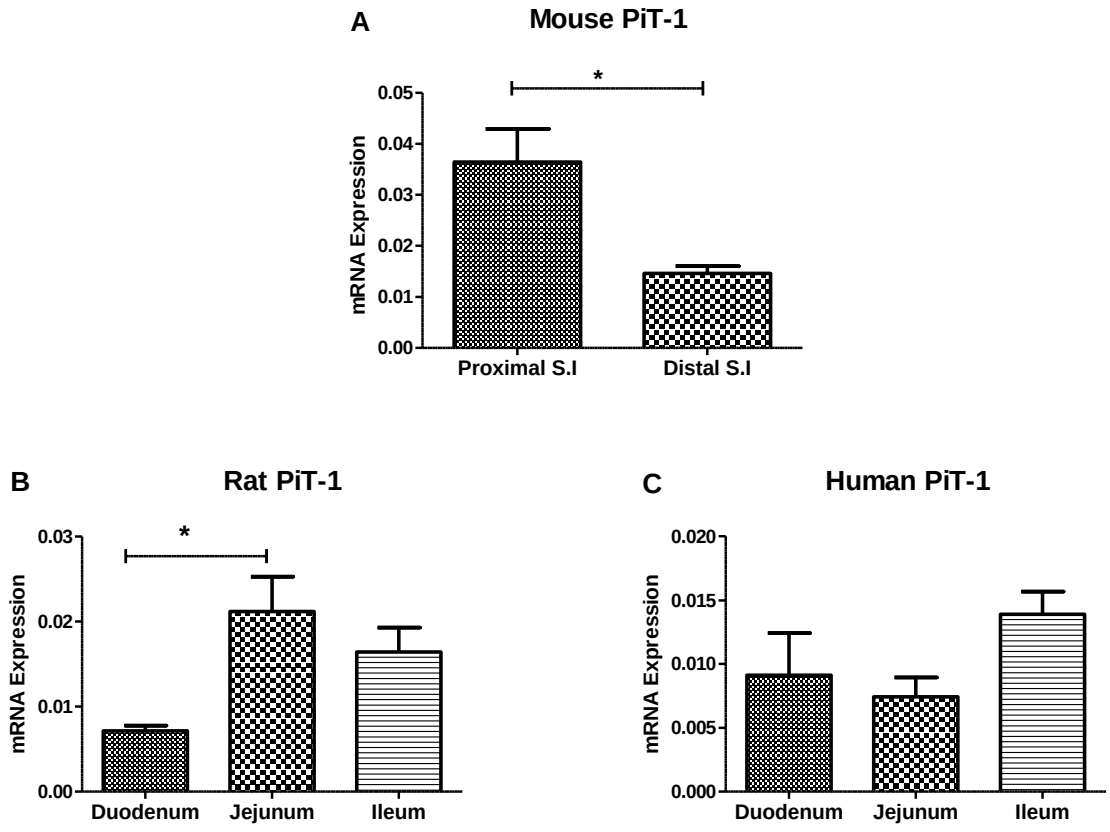


**Figure 3.2. RT-PCR quantification of PiT-1 in distinct regions of mouse, rat and human small intestine**. Duplicate PCR reactions were performed for each sample and the mRNA expression of PiT-1 is given as the ratio of PiT-1 to *β*-actin. An unpaired t-test (A) and a one-way ANOVA with Tukey's multiple comparisons post-tests (B and C) were used to compare results between groups (n=5-10). **P*<0.05.

The detection of NaPi-IIb in the rat small intestine using a commercially available antibody against this protein has been a major challenge in phosphate research for many years. However, I have validated a commercially available antibody against NaPi-IIb (Source Bioscience, Cat. No.: LS-C37453) by carrying out Western blotting experiment using intestinal BBM protein prepared from NaPi-IIb knock-out and wild-type mice, and have used this antibody for the detection of NaPi-IIb protein in the current study. The presence of very weak bands in NaPi-IIb knock-out mice at the predicted size for this protein, 100-105 kD (Figure 3.3), confirms that this antibody is specific for NaPi-IIb.

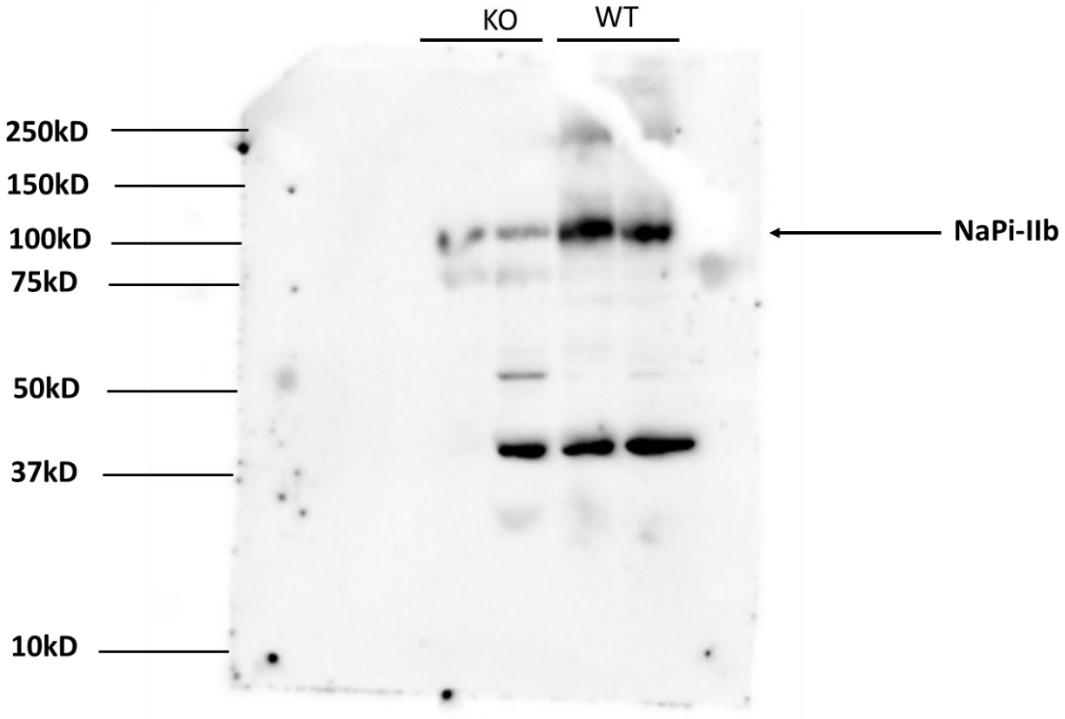


**Figure 3.3. Validation of NaPi-IIb antibody**. Western blot image showing the protein levels of NaPi-IIb in wild-type and NaPi-IIb knock-out mice (n=2).

As previously reported [17,38,39] and like NaPi-IIb mRNA profile, its protein levels were significantly higher in the mouse distal small intestine compared to the proximal small intestine (Figure 3.4A), while rat NaPi-IIb protein was significantly higher in the jejunum compared to very low levels detected in the duodenum (Figure 3.4B). Since NaPi-IIb protein has been reported to be undetectable in the ileum of rats [17], its levels in this segment of rats were not investigated in this study. Moreover, it is interesting to note that NaPi-IIb protein was highly detected in the mouse small intestine and its levels were generally higher and more consistent in the mouse (detected in 20 µg BBM protein) compared to what was seen in the rat small intestine (detected only in 50 µg BBM protein) (Figure 3.4A and B).

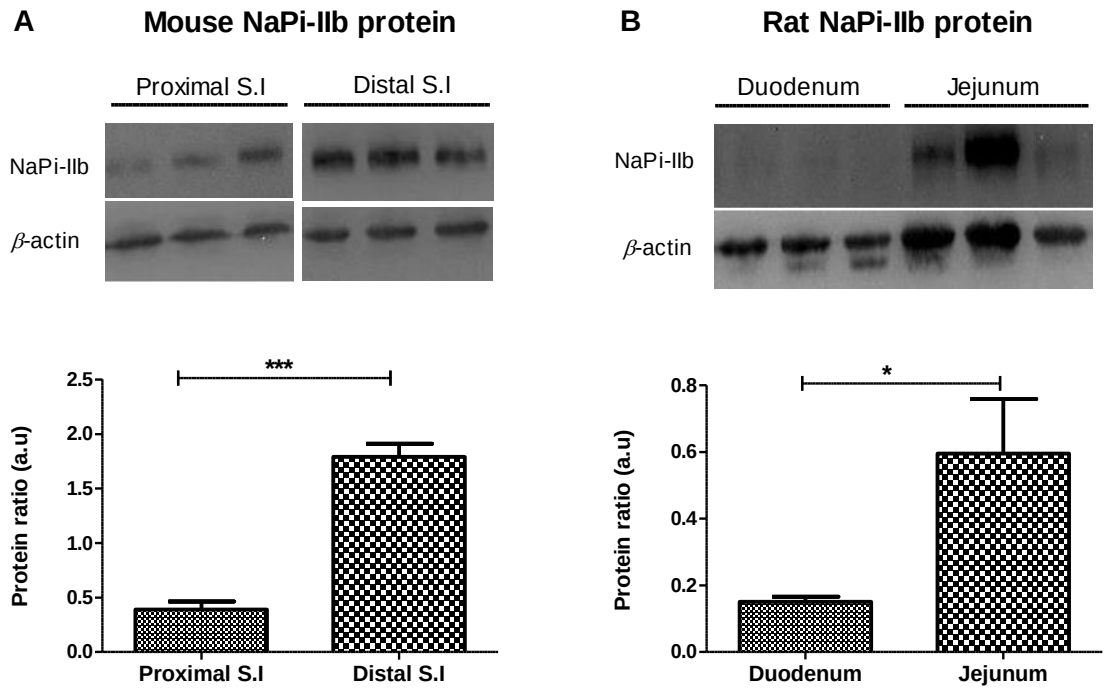


**Figure 3.4. Western blot analysis of NaPi-IIb protein in distinct regions of mouse and rat small intestine**. Representative Western blot image and quantification of NaPi-IIb protein relative to *β*-actin in the small intestine. The abundance of NaPi-IIb protein is given as the ratio of NaPi-IIb to *β*-actin, expressed in arbitrary units (a.u). An unpaired t-test was used to compare results between groups (n= 4-6). **P*<0.05, ****P*<0.001.

The regional profile for PiT-1 protein in the mouse small intestine appears to be different from its mRNA levels. Unlike the mRNA profile, PiT-1 protein was similar in both proximal and distal small intestinal segments of mice (Figure 3.5A). In contrast, rat PiT-1 protein was significantly higher in the jejunum compared to the duodenum (Figure 3.5B), which is in agreement with the findings of Giral and colleagues [17]. PiT-1 protein has been reported to be undetectable in the ileum of rats [17,146], thus, this protein was not investigated in the rat ileum in this study.

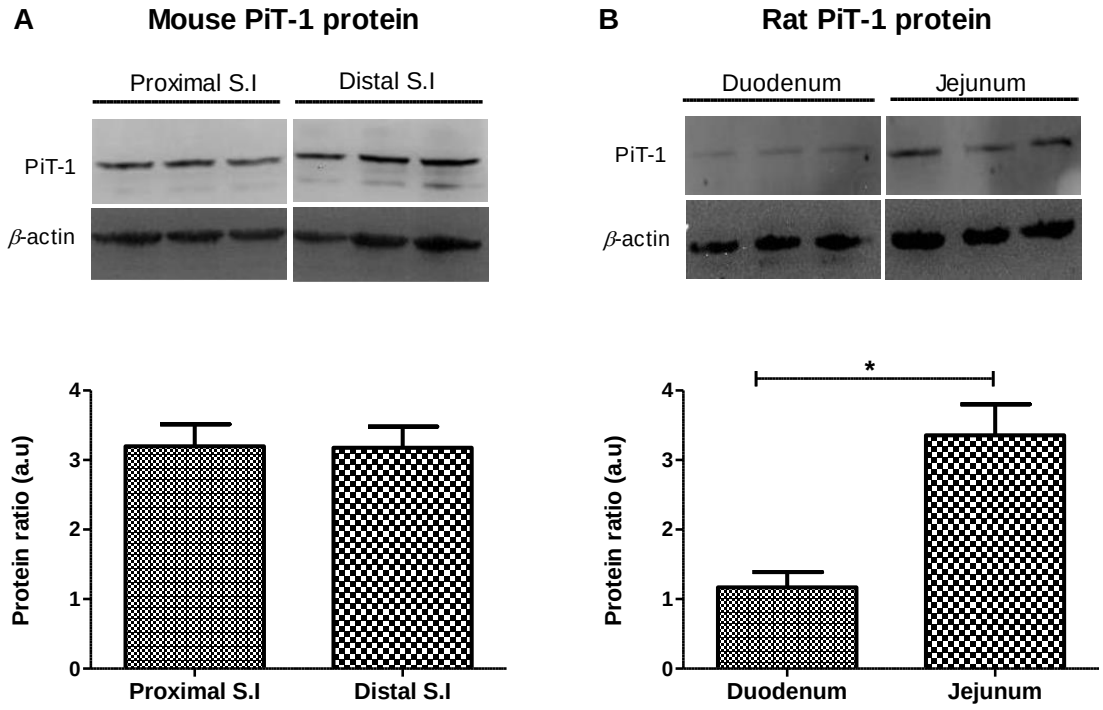


**Figure 3.5. Western blot analysis of PiT-1 protein in distinct regions of mouse and rat small intestine**. Representative Western blot image and quantification of PiT-1 protein relative to *β*-actin in the small intestine. The abundance of PiT-1 protein is given as the ratio of PiT-1 to *β*-actin, expressed in arbitrary units (a.u). An unpaired t-test was used to compare results between groups (n=3-5). **P*<0.05.

### 3.3.2. Regional expression of NHE3 in the small intestine of mice, rats and humans

To gain more insight into the potential role of the recently reported NHE3-regulated paracellular phosphate absorption in the small intestinal of mice, rats and humans [77], the mRNA levels of NHE3 were mapped using RT-PCR and its protein levels were tested using Western blotting. In mice, compared to the distal small intestine, NHE3 mRNA and protein levels were significantly higher in the proximal small intestine (Figure 3.6A and 3.7A), a segment known to contribute only a small proportion to intestinal phosphate absorption in this species. Although not statistically significant, the mRNA expression of NHE3 in the rat and human small intestine showed a similar trend, with the highest levels observed in the jejunum (Figure 3.6B and C), the major segment suggested to be responsible for intestinal phosphate absorption in these species. This suggests that the rat is a better animal model for studying the NHE3-regulated paracellular mechanism of phosphate absorption in the human small intestine. Surprisingly, in contrast to the RT-PCR data, NHE3 protein levels were significantly higher in the duodenum compared to the jejunum of rats (Figure 3.7B). Consistent with NHE3 protein profile in mice, this finding indicates that NHE3 protein is higher in the proximal segments compared to the distal segments of the small intestine of rodents.

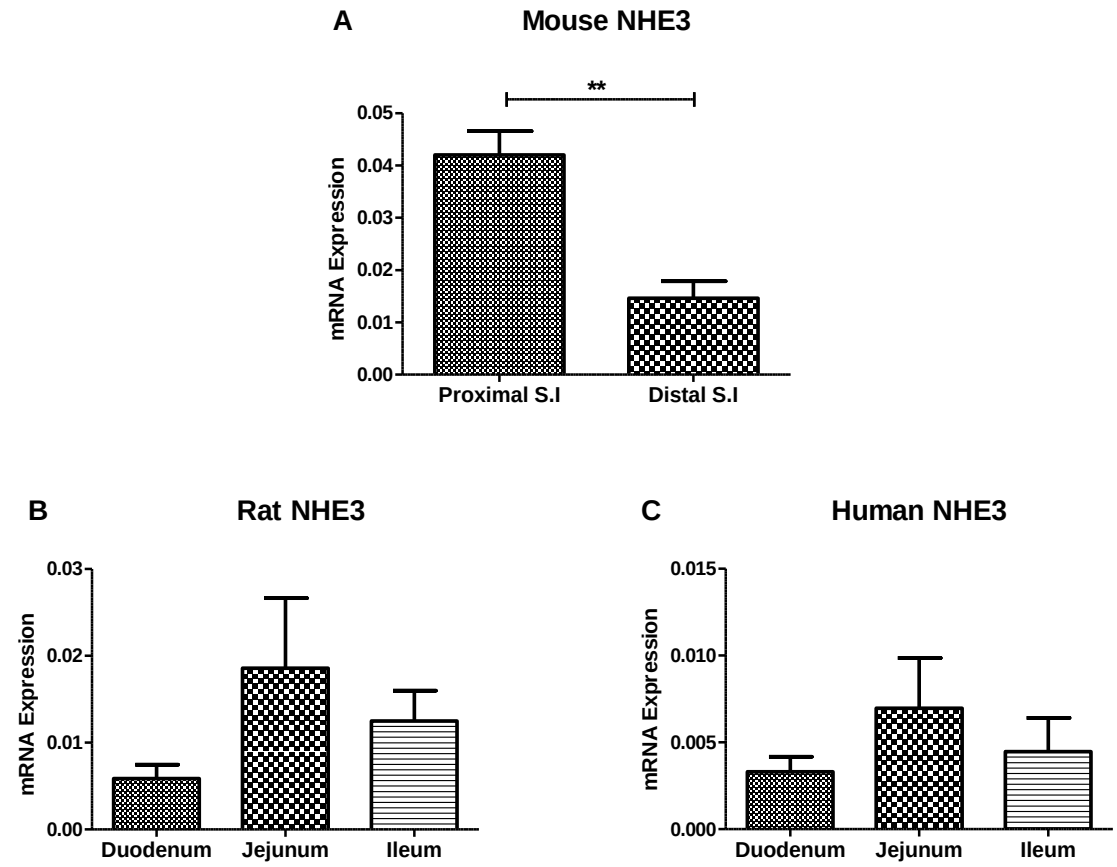


**Figure 3.6. RT-PCR quantification of NHE3 in distinct regions of mouse, rat and human small intestine**. Duplicate PCR reactions were performed for each sample and the mRNA expression of NHE3 is given as the ratio of NHE3 to *β*-actin. An unpaired t-test (A) and a one-way ANOVA with Tukey's multiple comparisons post-tests (B and C) were used to compare results between groups (n=5-10). ***P*<0.01.

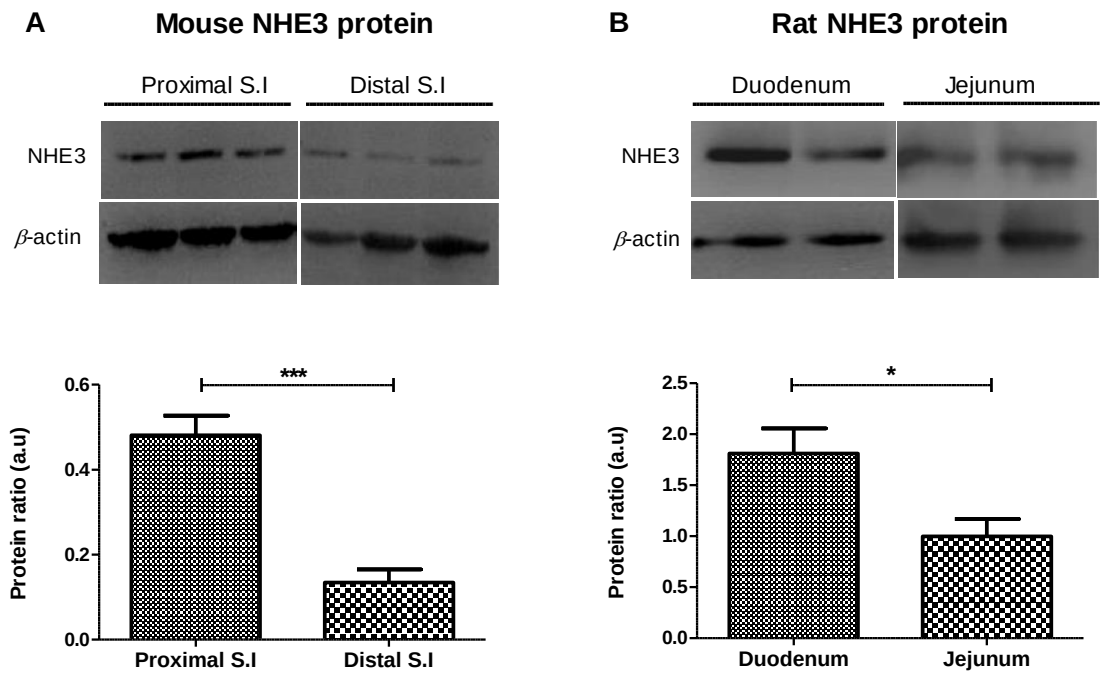


**Figure 3.7. Western blot analysis of NHE3 protein in distinct regions of mouse and rat small intestine**. Representative Western blot image and quantification of NHE3 protein relative to *β*-actin in the small intestine. The abundance of NHE3 protein is given as the ratio of NHE3 to *β*-actin, expressed in arbitrary units (a.u). An unpaired t-test was used to compare results between groups (n= 5-6). **P*<0.05, ****P*<0.001.

### 3.3.3. Mechanism of phosphate absorption in the mouse small intestine

The ileum is known to be the major segment responsible for the absorption of phosphate in the mouse small intestine. To confirm the previously suggested relative contribution of the jejunum and ileum to intestinal phosphate absorption in mice, *in vivo* intestinal loop experiments were carried out in these segments, and the total transepithelial phosphate absorption in each segment was determined. The result showed that total transepithelial phosphate absorption was significantly higher in the ileum (Figure 3.8), which is the segment with the highest levels of NaPi-IIb, compared to the jejunum. This confirms the widely accepted dogma that the ileum is the major segment for phosphate absorption in mouse small intestine.

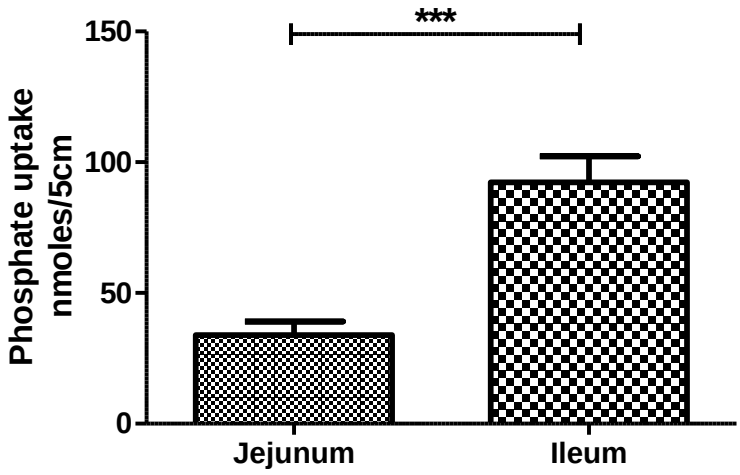


**Figure 3.8. Total transepithelial phosphate absorption in distinct regions of the mouse small intestine**. Values presented are the amount of phosphate transferred by 5 cm of the small intestine into 1 ml of blood after 10 minutes of phosphate instillation into the intestine, using a normal buffer containing $Na^+$. An unpaired t-test was used to compare results between the jejunum and ileum (n=6). *** $P<0.001$.

To test the contribution of mouse NaPi-IIb to total transepithelial phosphate absorption under normal intestinal phosphate condition, uptake buffer containing a physiological phosphate concentration of 10 mM, and increasing concentrations of a potent NaPi-IIb inhibitor, NTX9066, were used for *in vivo* uptake experiments. The result showed a concentration-dependent inhibition of transepithelial phosphate absorption in the mouse ileum in the presence of NTX9066, with approximately 88% inhibition observed at 100 μM (Figure 3.9). The inhibition of total transepithelial phosphate absorption by 100 μM of NTX9066 was approximately the same as what was observed in NaPi-IIb knock-out mice [77], suggesting that NaPi-IIb is the major phosphate transporter in the mouse small intestine under normal intestinal phosphate concentration.

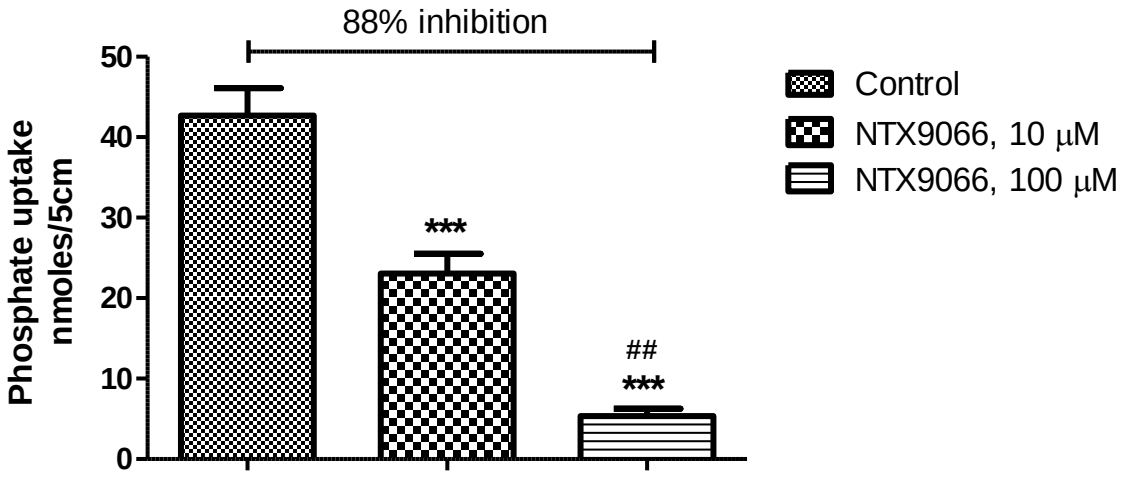


**Figure 3.9. Effect of NaPi-IIb inhibitor, NTX9066, on phosphate transport in the mouse ileum measured *in vivo***. Values presented are the amount of phosphate transferred by 5 cm of the small intestine into 1 ml of blood after 10 minutes of phosphate instillation into the intestine, using a normal buffer containing $Na^+$ (control) and buffer containing $Na^+$ + 10 or 100 μM of NTX9066. A one-way ANOVA with Tukey's multiple comparisons post-tests was used to compare results between groups (n=5-10). *** $P<0.001$ compared to the control group and $^{\#\#}P<0.01$ compared to NTX9066, 10 μM group.

Tenapanor, a potent NHE3 inhibitor, was also used to test whether there is any role for NHE3-regulated paracellular phosphate transport pathway in the jejunum and ileum of mice. Total transepithelial phosphate absorption in the mouse small intestine was investigated using buffers containing 8 mM phosphate, with or without 10 µM tenapanor. The results showed similar transepithelial phosphate absorption between normal (control) buffer and buffer containing tenapanor in both the jejunum and ileum (Figure 3.10A and B). This suggests that there is no significant role for the NHE3-dependent paracellular phosphate transport pathway in the mouse small intestine.

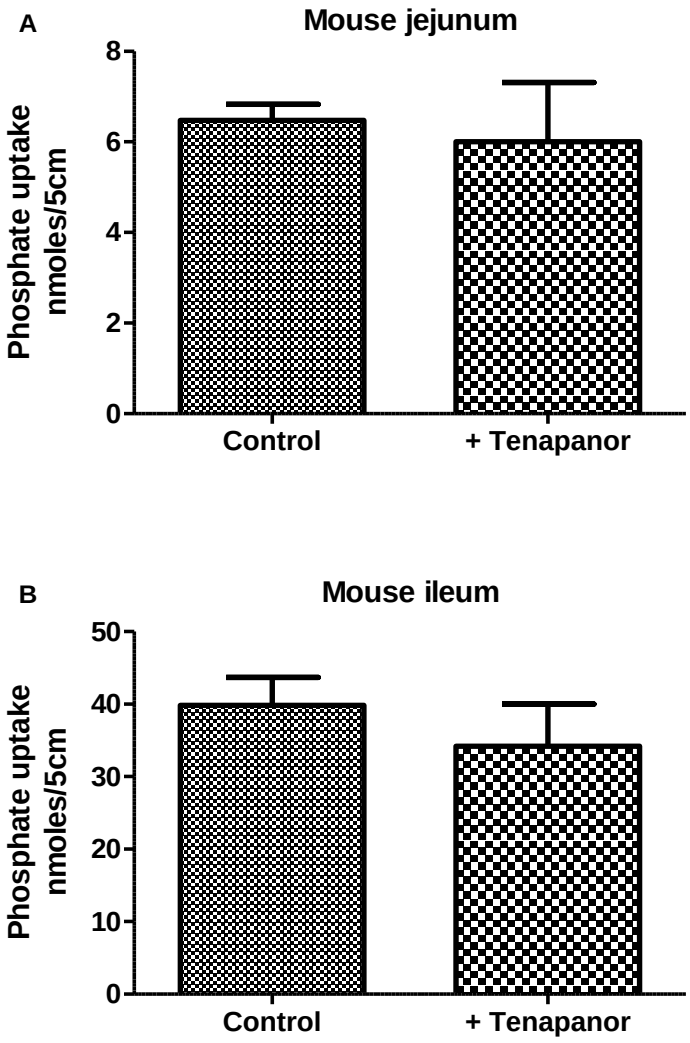


**Figure 3.10. Effect of the NHE3 inhibitor, tenapanor, on phosphate transport in the mouse small intestine measured *in vivo***. Values presented are the amount of phosphate transferred by 5 cm of the intestinal segment into 1 ml of blood after 10 minutes of phosphate instillation into the intestine, using a normal buffer containing $Na^+$ (control) and buffer containing $Na^+$ + 10 µM tenapanor. An unpaired t-test was used to compare results between groups (n=3-9).

### 3.3.4. Mechanism of phosphate absorption in the rat duodenum and jejunum

To evaluate the relative contribution of the rat duodenum and jejunum to intestinal phosphate absorption, the capacity of phosphate absorption via these segments was assessed using the *in vitro* everted sleeve technique. The result showed that the jejunum has a significantly higher capacity to absorb phosphate compared to the duodenum (Figure 3.11A). Additionally, to compare the mechanisms of phosphate absorption in the duodenum and jejunum of rats, the contribution of the $Na^+$-dependent and $Na^+$-independent phosphate transport pathways in these segments were investigated using a physiological uptake buffer containing 10 mM phosphate, in the presence or absence of $Na^+$. As previously reported [45], phosphate absorption via the $Na^+$-dependent pathway was higher in the jejunum, which is the intestinal segment with the highest levels of NaPi-IIb in the rat, compared to the duodenum (Figure 3.11B). In contrast, phosphate absorption via the $Na^+$-independent pathway was higher in the duodenum compared to the jejunum (Figure 3.11C). It is worth noting that the $Na^+$-independent mechanism mediated approximately 75% of duodenal phosphate transport (Figure 3.11C). These findings confirm that in the rat proximal small intestine, the jejunum is the major segment responsible for $Na^+$-dependent phosphate absorption, while phosphate transport in the duodenum predominantly occurs via the $Na^+$-independent pathway.

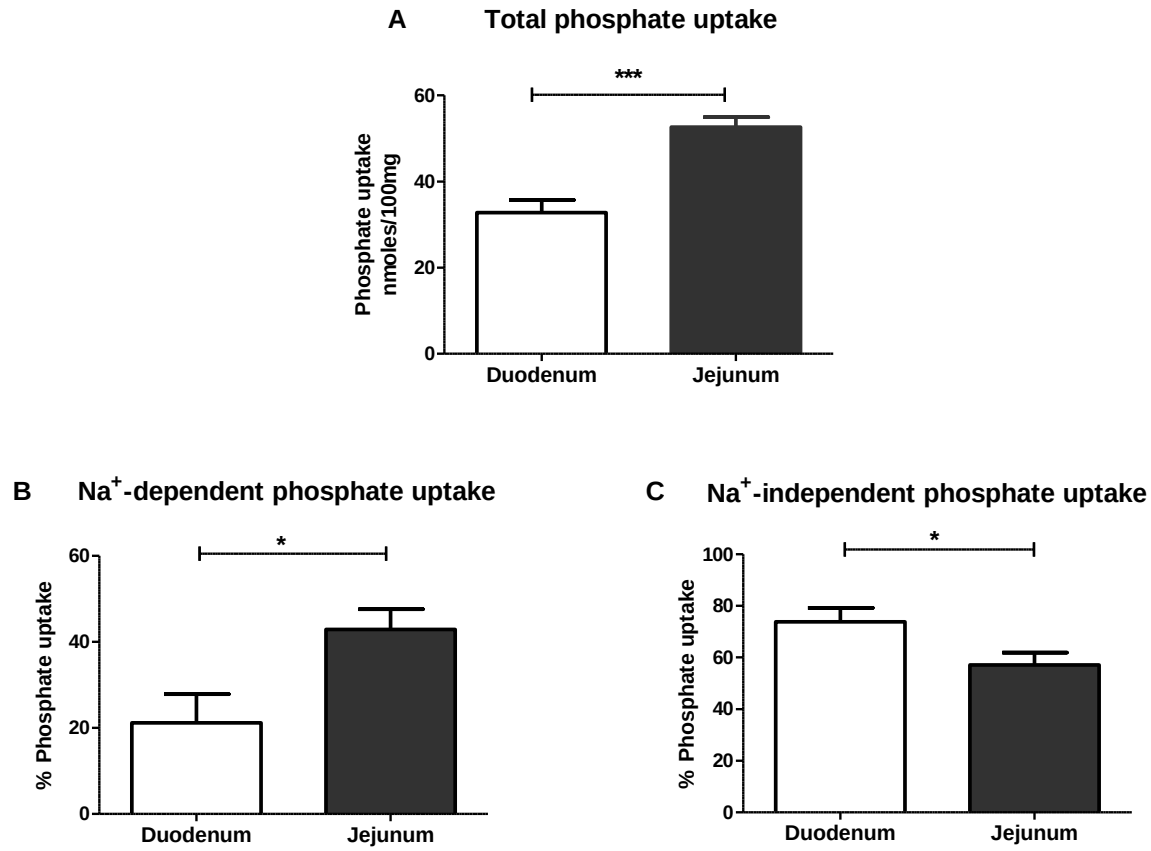


**Figure 3.11. Phosphate transport measured *in vitro*: a comparison between the duodenum and jejunum of rats**. Total phosphate uptake is presented in nmoles transferred into 100 mg of intestinal tissue in 2 minutes (A). The proportion of $Na^+$-dependent phosphate uptake (B) and $Na^+$-independent phosphate uptake (C) are presented as a percentage of the total phosphate uptake using normal uptake buffer containing $Na^+$. The $Na^+$-dependent phosphate uptake was determined by subtracting the $Na^+$-independent phosphate uptake from the total phosphate uptake, while the $Na^+$-independent uptake was obtained from experiments carried out using a buffer in which $Na^+$ has been replaced by iso-osmotic choline chloride. An unpaired t-test was used to compare results between groups (n=5-6). *$P$<0.05, ***$P$<0.001.

### 3.3.5. Role of NaPi-IIb and NHE3 as components of the $Na^+$-dependent pathway of intestinal phosphate absorption in rats

Using the *in vitro* everted sleeve technique, the proportion of the $Na^+$-dependent phosphate transport pathway that is mediated by NaPi-IIb and NHE3 in the duodenum and jejunum of the rat was investigated. PFA, a well-known competitive inhibitor of NaPi-IIb and tenapanor were used to test the contribution of these transporters to phosphate absorption in the duodenum and jejunum of normal rats. In the duodenum, phosphate uptake was unaffected by PFA or tenapanor, suggesting that the PFA-sensitive NaPi-IIb and tenapanor-sensitive NHE3 have no significant contribution to the $Na^+$-dependent component of phosphate absorption (approximately 25%) in this segment. In contrast, there was a significant contribution of NHE3, approximately 25%, to phosphate absorption in the jejunum (Figure 3.12B), with the PFA-sensitive NaPi-IIb pathway having a smaller contribution, approximately 13% (Figure 3.12B). In addition, the sum of the PFA-sensitive NaPi-IIb-mediated pathway and tenapanor-sensitive NHE3-regulated paracellular pathway in the jejunum was almost equal to the proportion of phosphate uptake via the $Na^+$-dependent pathway, approximately 40% (Figure 3.11B and 3.12B). Interestingly, phosphate uptake in the presence of tenapanor was not significantly different from uptake via the $Na^+$-independent pathway in the jejunum (Figure 3.12B), suggesting that NHE3-regulated paracellular phosphate transport may be the major $Na^+$-dependent phosphate absorption pathway that is detectable in the jejunum.

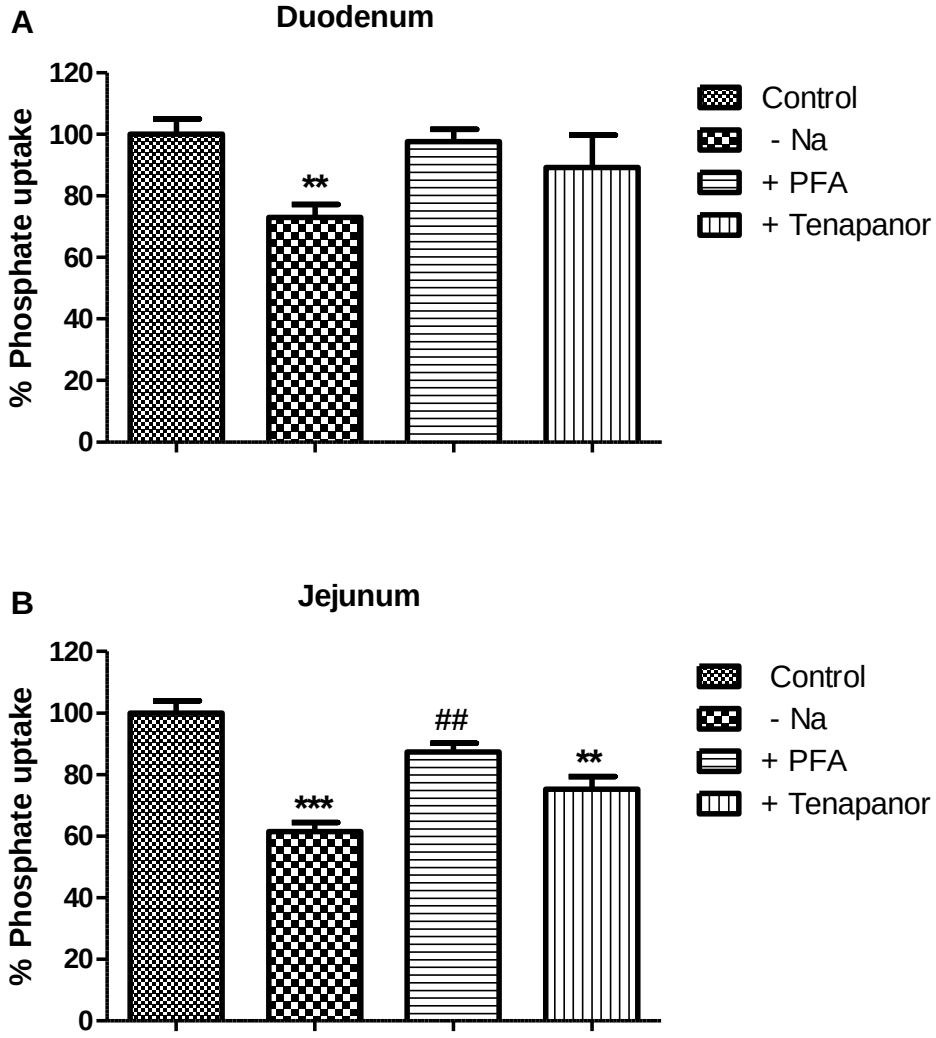


**Figure 3.12. The contribution of the Na+-independent, NaPi-IIb and NHE3-dependent mechanisms of phosphate transport in the rat proximal small intestine measured *in vitro***. Values presented are a percentage of the total phosphate transport in the presence of $Na^+$ (control) using duodenal tissue (A) and jejunal tissue (B). $Na^+$-independent uptake ($-Na^+$) was determined using a buffer in which $Na^+$ has been replaced with iso-osmotic choline chloride; NaPi-IIb dependent uptake was determined using a buffer containing $Na^+$ + 10 mM PFA, and NHE3 dependent uptake was determined using a buffer containing $Na^+$ + 10 µM tenapanor. A one-way ANOVA with Tukey's multiple comparisons post-tests were used to compare results between groups (n=6-26). $^{**}P<0.01$, $^{***}P<0.001$ compared to the control group and $^{\#\#}P<0.01$ compared to -Na group.

## 3.4. Discussion

### 3.4.1. Comparison of the mechanism of intestinal phosphate absorption in mice, rats and humans

Previous functional studies investigating the regional profile of phosphate absorption in the human small intestine [46,320] and findings from the comparison of the regional profile of NaPi-IIb have led to the assumption that the rat is a more appropriate animal model than the mouse to study new compounds for targeting intestinal phosphate absorption in CKD patients [39]. However, recent clinical data in humans concerning the negative outcome of a novel NaPi-IIb inhibitor [318], which has been demonstrated to be effective in reducing intestinal phosphate absorption in rats [76] questions this assumption. Based on this finding, it is likely that the rat is not a good model to study NaPi-IIb-mediated phosphate absorption in humans. In addition, an inhibitor of NHE3, tenapanor, has recently been reported to be effective in reducing intestinal phosphate absorption in the small intestine of rats and humans, but not in mice [77,247]. Thus, the mechanisms of intestinal phosphate absorption in different species seem to be more complex than previously thought.

There is limited information on the segmental profile of the transcellular phosphate transporters and NHE3 in the human small intestine, therefore, one of the aims of the current study was to compare the regional profile of these transporters in rats, mice and humans. In addition, the contribution of NaPi-IIb- and NHE3-dependent phosphate transport mechanisms in the small intestine of rodents was investigated. The results showed that unlike in rats and mice, NaPi-IIb mRNA was highest in the human duodenum, while the segmental profile of NHE3 in the human small intestine mirrored that of rats. Based on the similar

profile of NHE3 mRNA in the small intestine of rat and humans, the rat appears to be a more appropriate model than the mouse to study the NHE3-regulated paracellular mechanism of phosphate absorption in humans. A limitation of this study is that there was a lack of human tissue biopsies for BBM protein preparation in order to investigate the protein levels of the transcellular phosphate transporters and the NHE3 using Western blotting. However, I attempted to investigate this using immunohistochemistry on paraffin-embedded human intestinal tissues, but the studies were unsuccessful because the antibodies were unable to detect NaPi-IIb, PiT-1 or NHE3 in the human tissues. Nevertheless, the profile of NaPi-IIb mRNA is consistent with previous findings that the human duodenum exhibits the highest levels of NaPi-IIb mRNA transcripts [253]. Compared with the other small intestinal segments, the duodenum is known to have a shorter length, and therefore, the sojourn time of chyme in this region is short. For example, the duodenum of adult rat is approximately 8 cm in length, with a transit time of chyme along this segment of 3 minutes [243]. In comparison, the jejunum is approximately 36 cm in length, with a transit time of 43 minutes, while the ileum is also approximately 36 cm in length, with a transit time of 141 minutes [243]. Therefore, the short length and transit time of chyme in the duodenum, where NaPi-IIb is most highly expressed, may be responsible for the recently reported lack of therapeutic effect of NaPi-IIb inhibitors for the treatment of hyperphosphataemia in humans [318]. Based on these findings, the importance of duodenal NaPi-IIb in phosphate absorption in humans remains uncertain.

### 3.4.2. Mechanism of phosphate absorption in the mouse small intestine

In this study, the regional profile of mouse intestinal NaPi-IIb and NHE3 was investigated and the contribution of these proteins to phosphate absorption

examined. Consistent with previous studies [31,39], the evidence from the current study showed a positive relationship between NaPi-IIb levels and the capacity of phosphate absorption in specific intestinal segments. In this regard, low mRNA and protein levels of NaPi-IIb in the proximal segments of the mouse small intestine were associated with a low capacity of phosphate absorption in these segments, while high NaPi-IIb levels were associated with a high capacity of phosphate absorption in the mouse ileum. In contrast, high levels of NHE3 were detected in the proximal small intestine, a segment associated with relatively lower phosphate absorption compared to the distal small intestine. While these findings suggest a role for NaPi-IIb in intestinal phosphate absorption in mice, it looks as though NHE3 may not be playing any role. Previous studies investigating the role of NaPi-IIb in intestinal phosphate absorption in mice have carried out uptake experiments *in vitro*, using BBM proteins or everted gut sacs, and have employed uptake buffers with low phosphate concentrations (≤ 1.2 mM), a condition that favours NaPi-IIb transport [31,222]. Even though these studies demonstrated that NaPi-IIb accounts for approximately 90-95% of $Na^+$-dependent phosphate transport across the BBM of the mouse ileum [31,222], it has been speculated that NaPi-IIb is only important in mice maintained on a low phosphate diet (≤ 0.1% phosphate) [145,319,321]. These authors hypothesised that at physiological phosphate concentration, NaPi-IIb would have a minor contribution to transepithelial phosphate absorption and that paracellular phosphate transport would predominate. Based on the findings that the physiological concentration of phosphate in the gastrointestinal tract of mice fed a normal phosphate diet is at least 4 mM and may be as high as 35 mM [251,319], 8-10 mM of phosphate was used in the current study. Using a physiological technique that measures transepithelial phosphate absorption *in vivo*, the result of this study showed that

NaPi-IIb contributes approximately 90% of total transepithelial phosphate absorption in the ileum of mice maintained on a normal diet. Interestingly, the NaPi-IIb inhibitor, NTX9066 caused a dose-dependent inhibition of transepithelial phosphate absorption in the ileum, and at 100 µM, the inhibition of phosphate absorption by this inhibitor was the same as what was recently reported in NaPi-IIb knock-out mice [77]. Additionally, recent findings from uptake experiments using tenapanor in NaPi-IIb knock-out mice [77] and the finding of this study, demonstrated that the inhibition of NHE3 had no effect on transepithelial phosphate absorption in the jejunum and ileum of mice. This suggests that under physiological phosphate concentration, NHE3-regulated paracellular phosphate transport has little or no contribution to intestinal phosphate absorption in mice. Taken together, these findings support the claim that NaPi-IIb is the major phosphate transporter responsible for transepithelial phosphate absorption in the mouse small intestine under normal dietary phosphate condition.

Contrary to this hypothesis is the study by Sabbagh *et al* in NaPi-IIb knock-out mice [31], suggesting that NaPi-IIb only accounts for 50% of total transepithelial phosphate absorption *in vivo*. It is worth noting that the authors gavaged a solution containing superphysiological phosphate concentration (500 mM) and measured serum phosphate levels at 30 minutes and 60 minutes following phosphate gavage. The discrepancy between the findings of Sabbagh *et al* [31] and the findings of the current study may be because of the differences between the phosphate concentration in the uptake buffers and techniques employed in these studies. In contrast to the 10 mM of phosphate used in the current study, a phosphate load of 500 Mm used by Sabbagh *et al* [31] will generate a tremendous concentration gradient and may be sufficient to completely saturate the high

levels of NaPi-IIb in the mouse small intestine. Therefore, this would favour paracellular phosphate diffusion that may not be attainable under a physiological condition. Alternatively, using the above experimental set up of Sabbagh *et al* [31], there is no evidence that the changes in serum phosphate in both NaPi-IIb knock-out and wild-type mice were solely due to intestinal phosphate absorption. Phosphate exchange between serum and bone minerals may have contributed to the levels of phosphate detected in the serum of NaPi-IIb knock-out mice gavaged 500 mM of phosphate. To rule out the contribution of bone phosphate, this experiment could be repeated using radioactive phosphorus ($^{32}P$ or $^{33}P$) to accurately measure the amount of phosphate absorbed across the intestinal epithelium. Using this method, the potential contribution of bone phosphate in the current study was ruled out as $^{33}P$ transferred from the uptake buffer into the circulation is taken as a direct measure of only the phosphate absorbed by the small intestine.

Other studies speculating that intestinal NaPi-IIb plays a minor role under normal or high dietary phosphate condition have employed the investigation of faecal phosphate levels [31,145,222,251], an approach that is crude and only measures apparent phosphate absorption. These studies showed that NaPi-IIb knock-out mice maintained on either a normal or high phosphate diet exhibited only a moderate increase or no significant increase in faecal phosphate excretion compared to wild-type mice [31,222,251]. However, the importance of NaPi-IIb was demonstrated by the observation that there was approximately 45% increase in faecal phosphate excretion when NaPi-IIb knock-out mice were chronically fed a phosphate-deficient diet [145]. Although these findings suggest that NaPi-IIb plays a lesser role in intestinal phosphate absorption under normal or high dietary

phosphate conditions, the potential contribution of secreted phosphate, for example, salivary and intestinal phosphate secretion [322–326], to faecal phosphate levels were not considered. Early studies investigating phosphate absorption in the small and large intestines revealed that faecal phosphate levels represent the summation of both absorption and secretion of phosphate [326]. Approximately 7 mmol of phosphate is secreted into the gastrointestinal tract per day, and some of this phosphate is reabsorbed in addition to the absorption of dietary phosphate [327]. Based on these reports, the contribution of NaPi-IIb cannot be ascertained from the fact that faecal phosphate excretion was unchanged or showed only a moderate increase in NaPi-IIb knock-out mice maintained on a normal or a high phosphate diet. The *in situ* intestinal loop technique and buffers containing 8-10 mM of phosphate used by King *et al* [77] and in the current study, remain the most direct physiological approach to investigate the transport mechanisms underlying transepithelial phosphate absorption in the small intestine. Therefore, based on the evidence of this study and the findings of King *et al*. in NaPi-IIb knock-out mice [77], NaPi-IIb is the major transporter responsible for intestinal phosphate absorption in mice. Interestingly, the importance of mouse NaPi-IIb in intestinal phosphate absorption is confirmed by the fact that renal phosphate excretion is significantly adjusted to maintain serum phosphate levels in NaPi-IIb knock-out mice maintained on a normal phosphate diet [31,251,328].

### 3.4.3. Mechanism of phosphate absorption in the rat small intestine

In rats, the high levels of jejunal NaPi-IIb mRNA and protein are consistent with the widely accepted dogma that the jejunum is the major segment responsible for NaPi-IIb-mediated $Na^+$-dependent transcellular phosphate transport. Conversely, even though low levels of duodenal NaPi-IIb mRNA and protein were observed

in the current study, a considerable amount of phosphate absorption was observed in this segment. These findings suggest the presence of multiple phosphate transport pathways in the rat proximal small intestine. Moreover, in the rat ileum, even though NaPi-IIb and PiT-1 protein have not been detected [17], a significant contribution of the $Na^+$-dependent phosphate transport mechanism to total transepithelial transport has been reported in this segment [45]. Whether an unknown $Na^+$-dependent transporter is responsible for this phosphate transport mechanism or there is a $Na^+$-dependent passive phosphate transport pathway in the ileum as speculated by McHardy and Parsons [240], remains to be confirmed.

#### 3.4.3.1. Duodenum

In the rat duodenum, the fact that very low levels of NaPi-IIb were detected, and the lack of effect of PFA on phosphate uptake *in vitro*, suggest that there is no NaPi-IIb-mediated transcellular phosphate transport pathway in this segment. In agreement with this, duodenal phosphate uptake using a physiological phosphate concentration of 10 mM *in vivo* has been shown to have no $Na^+$-dependent component [45], suggesting no role for NaPi-IIb in duodenal phosphate absorption in the rat. To support the finding that NaPi-IIb has no significant role in the duodenum, previous findings in rats treated with $1,25(OH)_2D_3$, a major regulator of NaPi-IIb function, have shown that this hormone has no effect on duodenal phosphate absorption [39,329]. However, contrary to the findings that NaPi-IIb plays no role in duodenal phosphate absorption is the *in vitro* data by Giral *et al*., which demonstrated that the duodenum exhibited the highest $Na^+$-dependent phosphate transport activity compared to other segments of the small intestine [17]. They showed that increased phosphate uptake in duodenal BBM vesicles of rats switched from a chronic low phosphate diet to an acute high phosphate diet

was associated with increased NaPi-IIb levels [17]. Although these findings suggest a role for duodenal NaPi-IIb, it is important to note that these experiments were carried out using 0.1 mM phosphate in the uptake buffer, a concentration that favours active NaPi-IIb-mediated transport activity. Based on the kinetics of NaPi-IIb, it is currently known that this transporter functions optimally at a $K_m$ of 0.05–0.1 mM and that at higher phosphate concentrations its transport function does not increase accordingly [20,70]. Importantly, the concentration of free phosphate in the rat intestine after a standard phosphate diet has been reported to be much higher than the $K_m$ of NaPi-IIb, ranging from approximately 6–12 mM [45]. Evidence from the current study using a phosphate concentration within this range indicates that NaPi-IIb has no contribution to total transepithelial phosphate absorption in the duodenum.

Although recent evidence indicated that the NHE3-regulated paracellular phosphate transport pathway significantly contributes to total transepithelial phosphate absorption in the jejunum of rats [77], there is no evidence suggesting the presence of this pathway in the rat duodenum. Therefore, the contribution of NHE3 in duodenal phosphate absorption was investigated in this study. Even though high levels of NHE3 protein was detected in the duodenum, the finding that tenapanor had no effect on duodenal phosphate transport indicates that this transporter plays no significant role in mediating phosphate absorption in this segment. The reason for this lack of effect of NHE3 inhibition on duodenal phosphate transport is not known. However, it is possible that NHE3 is already partially inhibited by the acidic environment of the duodenal enterocyte, and further inhibition by tenapanor may result in only a moderate change in phosphate transport in this segment as seen in this study. Surprisingly, based on the

evidence that NaPi-IIb and NHE3 have no significant contribution to duodenal phosphate transport, and because low levels of PiT-1 were detected in this segment, the contribution of the $Na^+$-dependent phosphate transport pathway observed *in vitro* (approximately 25%), cannot be completely explained by these transporters. Thus, further studies are required to identify the transporter(s) responsible for the $Na^+$-dependent component of phosphate absorption in the duodenum of rats.

The finding from this study that the $Na^+$-independent mechanism of phosphate transport is the predominant pathway for phosphate absorption in the duodenum is in agreement with previous data [45,246]. Interestingly, the previously reported increase in phosphate uptake *in vitro* in the duodenum of rats switched from a chronically low phosphate diet to an acutely high phosphate diet was preserved when the experiment was conducted using a $Na^+$-free buffer [246]. This indicates that rather than duodenal NaPi-IIb that was suggested by Giral *et al*. [17], the $Na^+$-independent phosphate transport pathway appears to be responsible for this effect [246]. Candeal and colleagues [246] showed a significantly higher $Na^+$-independent phosphate uptake in BBM vesicles prepared from the duodenum of rats acutely switched to a high phosphate diet for 4 hours compared to those maintained on a low phosphate diet [246]. Therefore, it is possible that dietary phosphate levels, particularly high phosphate diet, regulate the $Na^+$-independent phosphate transport pathway. In addition, studies in Caco-2 BBE cells have shown that the $Na^+$-independent phosphate transport pathway is also regulated by pH, with reduced phosphate transport via this pathway observed at low pH and vice versa [246]. In contrast, recent findings suggest that the $Na^+$-dependent mechanism of phosphate absorption in the proximal small intestine increases

with decreasing pH [146]. These differential effects of pH on the $Na^+$-dependent and $Na^+$-independent phosphate transport pathways could be explored to unravel the nature of the $Na^+$-independent phosphate transport pathway.

Reports from early studies on the mechanism of intestinal phosphate absorption in rodents and mammals (reviewed in [252]) showed that the $Na^+$-independent phosphate transport pathway is characterised by a non-saturable concentration-dependent phosphate transport process. Although Candeal and colleagues observed a similar $Na^+$-independent phosphate transport mechanism in Caco-2 BBE cells [246], the identity of the transporters involved in this pathway was not determined and it is still unknown. Whether this $Na^+$-independent mechanism involves an unknown passive transcellular phosphate carrier protein or is mediated via the paracellular pathway remains to be seen. Interestingly, cell culture studies have shown that the concentration-dependent increase in phosphate transport via the $Na^+$-independent pathway requires gene transcription and synthesis of new proteins [246]. The identity of these genes or proteins is yet to be reported.

#### 3.4.3.2. Jejunum

In this study, unlike the duodenum where NaPi-IIb and NHE3 were demonstrated to have no significant contribution to phosphate absorption, these transporters were responsible for the $Na^+$-dependent phosphate transport pathway observed in the jejunum, contributing approximately 40% of total phosphate absorption in this segment. Since the discovery of NaPi-IIb [40], most of the studies investigating phosphate absorption in the rat small intestine have focused on this protein, which mediates a saturable $Na^+$-dependent phosphate transport mechanism [45,126,245,320]. Based on the relatively higher expression of jejunal NaPi-IIb

compared to other intestinal segments, this protein was later suggested to be the major transporter responsible for $Na^+$-dependent phosphate absorption in the rat jejunum [17,39,144,248], with $1,25(OH)_2D_3$ known to be a key regulator [39,48,126]. Interestingly, evidence from the current study indicates that in the presence of a physiological phosphate concentration of 10 mM in the jejunum, NaPi-IIb only contributes approximately 13% to total phosphate absorption, with the bulk of the $Na^+$-dependent phosphate transport occurring via the recently reported NHE3-regulated paracellular pathway. Previous uptake studies in rats that have demonstrated evidence to support a key role for NaPi-IIb in jejunal phosphate absorption have carried out uptake experiments using uptake solution containing phosphate concentrations close to the Km of NaPi-IIb [17,255]. However, a phosphate concentration of 10 mM, which would likely saturate the relatively low levels of rat NaPi-IIb compared to that of the mouse, was used in the current study, and at this concentration, NaPi-IIb was shown to play a minor role in mediating $Na^+$-dependent phosphate transport in the rat jejunum. Nevertheless, *in vivo* studies in normal rats and those with CKD have shown that the inhibition of NaPi-IIb by nicotinamide or ASP3325 resulted in a significant inhibition of jejunal NaPi-IIb-mediated phosphate absorption and consequently reduced serum phosphate levels [76,248]. The discrepancy between these studies [76,248] and the current study in the contribution of NaPi-IIb to jejunal phosphate absorption in rats requires further clarification.

It has recently been shown that NHE3-regulated paracellular phosphate transport significantly contributes to total transepithelial phosphate absorption in both rat and human small intestine and that the inhibition of this pathway significantly impacts systemic phosphate levels in uremic rats and CKD patients [77,247]. In

agreement with the findings of King *et al* [77], the result of this study indicates that NHE3-regulated paracellular phosphate transport pathway is the major $Na^+$-dependent phosphate mechanism in the rat jejunum. Surprisingly, in comparison to the duodenum (where NHE3 protein was high, but no NHE3-regulated phosphate transport was observed), significantly lower levels of NHE3 protein were observed in the jejunum of rats, yet inhibition occurred. This expression profile could be because NHE3 protein is required in the duodenum to physiologically secrete $H^+$ to protect the duodenal enterocytes from gastric acid and the potential intracellular $H^+$ toxicity. The discrepancy in the relative inhibition of NHE3-regulated phosphate transport by tenapanor may be as a result of the fact that duodenal transepithelial electrical resistance (TEER) is significantly higher than that of the jejunum [77], thus inhibiting NHE3 may not be as effective in reducing paracellular phosphate absorption in the duodenum in comparison to the jejunum.

Moreover, like the duodenum, the $Na^+$-independent pathway appears to be the predominant pathway in the jejunum, accounting for approximately 60% of total phosphate absorption *in vitro*. This finding is consistent with previous *in vivo* data showing that at physiological phosphate concentration, the $Na^+$-independent phosphate transport pathway contributes more than 60% of total transepithelial phosphate absorption [45]. The $Na^+$-independent phosphate transport pathway in the jejunum shares similar concentration-dependent passive transport features with the duodenum. Findings from early studies have ruled out the contribution of solvent drag as a mediator of this pathway since it appears to be unaffected by water movement in response to the movement of solutes with varying tonicities like mannitol, urea and glucose [240]. Like the duodenum, the molecular candidate

responsible for the $Na^+$-independent phosphate transport pathway is still unclear. However, it is currently speculated that this transport pathway involves the diffusion of phosphate through paracellular pores [45,145,319,330]. Since claudins are known to be the major determinants of the permeability of the paracellular pathway to various electrolytes, these proteins may play significant roles in mediating $Na^+$-independent phosphate transport in the duodenum and jejunum. It is also possible that an unknown transcellular $Na^+$-independent phosphate transporter is responsible for this transport pathway [45,330]. Further studies are required to clarify the transporters or tight junction proteins involved in mediating the $Na^+$-independent transcellular or paracellular phosphate transport process in the jejunum.

### 3.5. Conclusion

There are significant variations in the regional expression profile of the transcellular phosphate transporters in the small intestine of mice, rats and humans. The finding that NaPi-IIb expression is highest in the human duodenum, a segment that is short and has a rapid transit time for chyme, may explain the lack of therapeutic efficacy of NaPi-IIb inhibitors in treating hyperphosphatemia in CKD patients. In contrast, the efficacy of tenapanor in inhibiting intestinal phosphate absorption in both rats and humans is consistent with the similar expression profile of NHE3 in these species. Using a physiological phosphate concentration of 10 mM, the results of this study suggest that while NaPi-IIb is the major phosphate transporter in mice, it plays little or no significant role in mediating phosphate absorption in the rat duodenum and jejunum. Interestingly, NHE3-regulated phosphate transport is likely responsible for the majority of the $Na^+$-dependent component of phosphate absorption in the rat jejunum. The

findings of this study confirm that the $Na^+$-independent component of phosphate absorption is the predominant pathway for phosphate absorption in the rat duodenum and jejunum under physiological phosphate concentration in the lumen.

# Chapter Four

## 4.0. Effect of diet-induced iron deficiency on phosphate homeostasis in rats

## 4.1. Introduction

Systemic iron homeostasis is controlled by the peptide hormone hepcidin, which inhibits intestinal iron absorption in the duodenum via the downregulation of the basolateral iron transporter, ferroportin [331,332] and the BBM divalent metal transporter type 1 (DMT1) [333]. Iron deficiency, characterised by low systemic iron levels and depleted iron stores, is known as the most common nutrient deficiency globally, affecting more than 25% of the world population [334–336]. In addition to reports associating iron deficiency with decreased bone mineralisation and osteoporosis [337–341], increasing evidence suggests a link between iron deficiency and phosphate homeostasis (discussed in section 1.6). In normal individuals, iron deficiency has been shown to increase the transcription of the major phosphate regulator, FGF-23, in osteocytes, an observation that is in contrast to reduced FGF-23 transcription following intravenous iron administration [305]. Moreover, iron deficiency anaemia and hyperphosphataemia are commonly seen in CKD patients, and the treatment of iron deficiency anaemia by iron supplementation in these patients has been shown to affect the levels of FGF-23 [342].

Furthermore, there is evidence that other regulators of phosphate homoeostasis, PTH and $1,25(OH)_2D_3$, also interact with the regulator of iron balance [306,343,344]. Notably, an interaction between $1,25(OH)_2D_3$ and hepcidin has recently been reported [344,345]. In patients with CKD, $1,25(OH)_2D_3$ insufficiency is inversely associated with serum hepcidin concentrations [345] and in healthy individuals, high dose $1,25(OH)_2D_3$ administration significantly decreases plasma hepcidin levels [344]. Therefore, in keeping with these novel interactions between hepcidin and the regulators of phosphate homeostasis, the aim of this chapter was to determine whether diet-induced iron deficiency affects the mechanisms of phosphate

homeostasis, with a particular focus on how intestinal and renal phosphate transport are impacted. Changes in serum levels of the recognised regulators of phosphate homeostasis were also investigated to test if diet-induced iron deficiency alters intestinal or renal phosphate transport via any of these regulators.

## 4.2. Methods

### 4.2.1. Animals and diet

Male Sprague-Dawley rats, aged 6 – 8 weeks, were either fed a control iron diet (TD. 80394) containing 48 ppm of iron or an iron deficient group diet (TD. 80396) containing 2-6 ppm of iron for 2 weeks. Other than the iron content, both diets had the same composition and contained 0.6% phosphate. All diets were purchased from Harlan Laboratories, Inc. Madison, WI, USA. For urine collection, following the 2-week period of diet administration, animals were individually housed in metabolic cages overnight (16 hours).

### 4.2.2. *In vitro* uptake experiments

Rats were weighed and anaesthetized as described in section 2.5. *In vitro* phosphate uptake experiments were carried out using 2-4 cm long duodenal or jejunal segments as described in section 2.6. To determine the effect of diet-induced iron deficiency on total phosphate uptake across the BBM, uptake buffer containing $Na^+$ and a physiological phosphate concentration of 10 mM was used. The amount of phosphate transferred from the uptake buffer into the intestinal tissue (phosphate uptake) after 2 minutes was expressed in nmoles/100mg of the intestinal segment.

### 4.2.3. *In vivo* uptake experiments

Phosphate uptake experiments in the duodenum or jejunum were carried out as described in section 2.5. To test the effect of diet-induced iron deficiency on total transepithelial phosphate absorption, uptake buffer containing $Na^+$ and a physiological phosphate concentration of 10 mM was instilled into the intestinal segments. The amount of phosphate transferred into blood per 5 cm of the cannulated duodenum or jejunum after 10, 20 and 30 minutes of instilling phosphate into the segment was determined and expressed in nmoles/5 cm.

### 4.2.4. Blood and urine biochemistry

Blood samples were collected at the end of the experiment by cardiac puncture and haematocrit measured using a micro-haematocrit reader. Serum and plasma were obtained from whole blood as described in section 2.7. Serum iron and other markers of iron deficiency were measured using commercially available assay kits as described in section 2.7.1. Serum and urine phosphate levels were measured using a colorimetric phosphate assay kit (Biovision Inc., Milpitas, CA, USA) as described in section 2.7.2. Urine volume was measured using a graduated cylinder, and the urine flow rate ($\dot{V}$) was estimated by: urine volume (mL)/ time (minutes).

Urinary phosphate excretion ($U_{Pi}$) was calculated using the equation below:

$U_{Pi}$ (µmol/min) = urinary phosphate concentration x $\dot{V}$

Serum intact FGF-23 (Kainos Laboratories Inc., Tokyo, Japan), c-term FGF-23 (Immutopics, Inc., San Clemente, CA, USA), $1,25(OH)_2D_3$ (LSBio Inc., Seattle, WA, USA) and plasma intact PTH (Immutopics, Inc., San Clemente, CA, USA) were measured by ELISA as described in section 2.7.3.1 - 2.7.3.4.

### 4.2.5. RT-PCR experiment

Total RNA was isolated from the whole kidney and from intestinal mucosa scrapes obtained from the duodenum and jejunum as described in section 2.3.1. cDNA was synthesised from the extracted RNA as described in section 2.3.2. RT-PCR experiment was carried out as described in section 2.3.3 to test the relative mRNA expression of renal NaPi-IIa, NaPi-IIc, α-Klotho, 25-Hydroxyvitamin D3 1-alpha-hydroxylase (Cyp27b1), and duodenal and jejunal VDR, with reference to *β*-actin. Rat specific primers (Table 2.1) were used for RT-PCR experiments.

### 4.2.6. Western blotting experiment

Kidney BBM vesicles were prepared as described in section 2.4.2. Kidney BBM protein (20µg) was used for Western blotting experiments to establish the protein levels of NaPi-IIa and NaPi-IIc as described in section 2.4.3, using specific antibodies (Table 2.2). The ratio of these proteins to *β*-actin was expressed as a.u.

### 4.2.7. Statistical analysis

Data are presented as mean ± SEM, statistical analysis was carried out as described in section 2.8, and statistical significance was depicted as follows: *$P$<0.05, **$P$<0.01 or ***$P$<0.001.

## 4.3. Results

### 4.3.1. Validation of iron deficient rat models

To confirm that 2-week administration of an iron deficient diet induces iron deficiency, the markers of iron deficiency: haematocrit, serum iron, UIBC and TIBC were measured. Rats administered an iron deficient diet had significantly decreased serum iron and haematocrit, and significantly increased UIBC and

TIBC, compared with rats fed a control iron diet (Table 4.1). This indicates that the administration of an iron deficient diet for 2 weeks significantly induced iron deficiency in the animals used for this study. Weight gain during the 2-week dietary regime was similar in both groups (Table 4.1).

**Table 4.1. Effect of diet-induced iron deficiency on markers of iron status and animal weight**. Data are presented as mean ± SEM (n = 5-13) and analysed using an unpaired t-test. ****P*<0.001 compared with control.

| | Control | Iron deficient |
|---|---|---|
| Haematocrit (%) | 42.38 ± 0.45 | 37.08 ± 0.75 *** |
| Serum iron (µmol/l) | 36.50 ± 2.82 | 9.22 ± 1.15 *** |
| Serum UIBC (µg/dl) | 353.30 ± 19.86 | 473.30 ± 12.91 *** |
| Serum TIBC (µg/dl) | 412.60 ± 20.03 | 530.20 ± 17.12 *** |
| Animal weight (g) | 345.00 ± 13.41 | 333.60 ± 13.85 |

### 4.3.2. Effect of diet-induced iron deficiency on intestinal phosphate absorption

Using the *in vitro* phosphate uptake technique and a physiological concentration of luminal phosphate in the uptake buffer, the effect of diet-induced iron deficiency on phosphate absorption across the BBM of the duodenum and jejunum was investigated. The result demonstrated that diet-induced iron deficiency significantly inhibited phosphate uptake across duodenal and jejunal BBM *in vitro* (Figure 4.1A and B). In the duodenum, iron deficiency resulted in approximately 70% inhibition of phosphate uptake across the BBM (Figure 4.1A), while approximately 50% of phosphate uptake was inhibited in the jejunum (Figure 4.1B), measured after 2 minutes. To test if this effect occurs *in vivo*, *in situ* intestinal loop technique was employed, using the same phosphate concentration

in the uptake buffer as in the *in vitro* uptake experiment. Consistent with the phosphate uptake results *in vitro*, diet-induced iron deficiency significantly inhibited total transepithelial phosphate absorption in the duodenum (approximately 65% inhibition) and jejunum (approximately 40% inhibition), measured *in vivo* after 10 minutes of instilling phosphate into the segment (Figure 4.1C and D). However, this inhibition of phosphate absorption was more prominent in the duodenum and was still present when measured after 30 minutes (Figure 4.1C), in contrast to the jejunum, where the inhibition of phosphate absorption decreased with time and at 30 minutes, phosphate absorption was similar in both groups (Figure 4.1D). This finding suggests that unlike the duodenum, there may be a potential compensation for the iron deficiency-induced inhibition of phosphate absorption in the jejunum. Other phosphate transport pathways that are not affected by iron deficiency may be responsible for this potential compensatory mechanism.

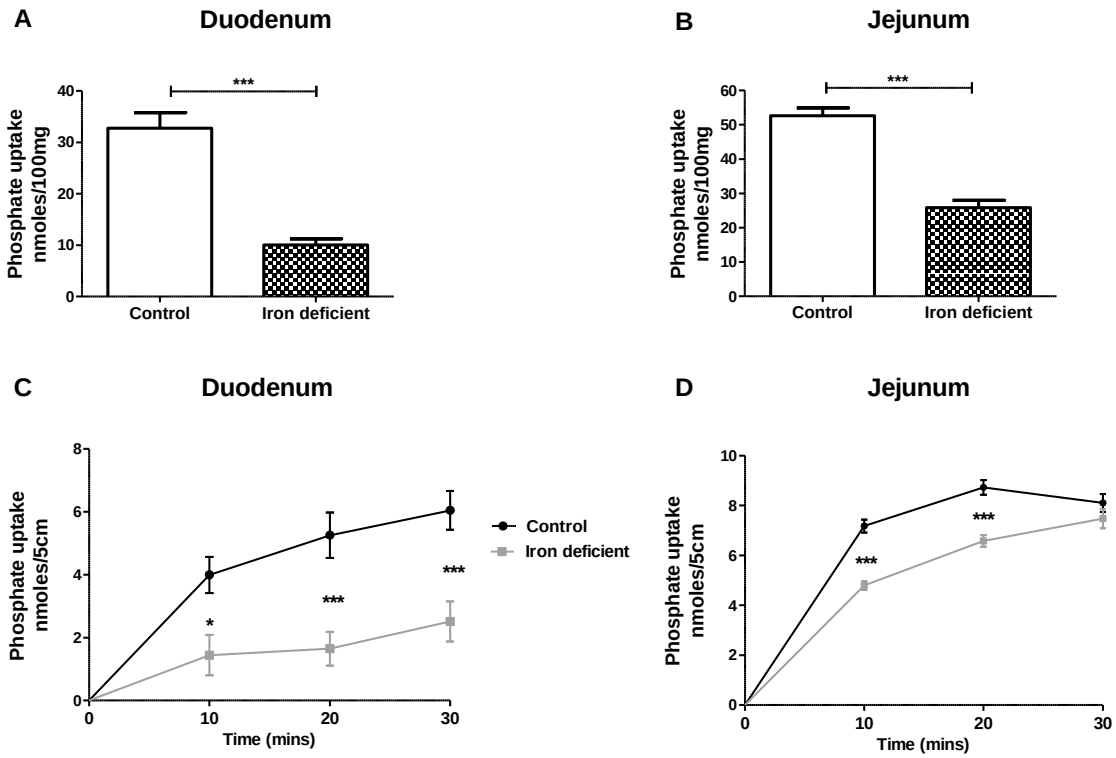


**Figure 4.1. Diet-induced iron deficiency inhibits intestinal phosphate absorption**. Phosphate uptake was determined *in vitro* (A and B) in control and iron deficient rats, using a buffer containing 10mM phosphate and $Na^+$. An unpaired t-test was used to compare results between groups (n=6). ****P*<0.001. Phosphate uptake at different time points was determined *in vivo* (C and D), in control and iron deficient rats, using a buffer containing 10mM phosphate and $Na^+$. A two-way ANOVA with Bonferroni's multiple comparisons post-test was used to compare differences between groups (n=7-8). **P*<0.05, ****P*<0.001.

### 4.3.3. Effect of diet-induced iron deficiency on serum phosphate levels and renal phosphate excretion

To examine whether the inhibition of phosphate absorption in the duodenum and jejunum significantly impacts serum phosphate levels, phosphate assay experiment was carried out to measure the levels of phosphate in the animals. Similar serum phosphate levels were observed in control and iron deficient animals (Figure 4.2A). This indicates that even though diet-induced iron deficiency significantly inhibited intestinal phosphate absorption, this effect had no impact on systemic phosphate levels. To understand the physiological mechanism responsible for the lack of change in serum phosphate levels observed in the iron deficient animals, the effect of diet-induced iron deficiency on renal phosphate excretion was investigated. Although not significant, the result showed a trend for a decrease in urinary phosphate excretion ($P$=0.1; Figure 4.2B). Additionally, the effect of diet-induced iron deficiency on the mRNA and protein levels of the renal phosphate transporters; NaPi-IIa and NaPi-IIc were tested using RT-PCR and Western blotting. The result showed a trend for upregulation of NaPi-IIa protein in the iron deficient group ($P$=0.07; Figure 4.3C), while NaPi-IIa and NaPi-IIc mRNA, as well as NaPi-IIc protein, were unchanged (Figure 4.3A, B and D). Taken together, these findings suggest that there may be a renal compensation for the reduced intestinal phosphate absorption seen in the iron deficient rats and this likely accounts for the unchanged serum phosphate levels.

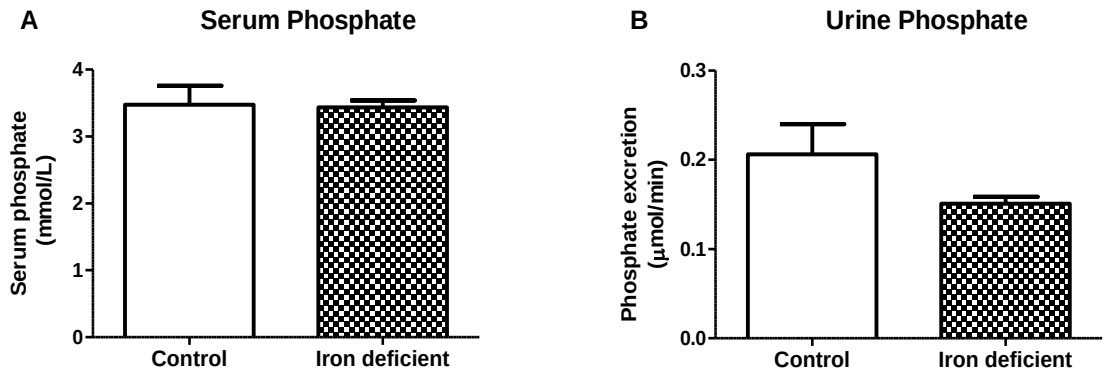


**Figure 4.2. Effect of diet-induced iron deficiency on serum phosphate and urinary phosphate excretion**. Changes in serum phosphate levels (A) and urinary phosphate excretion (B) in control and iron deficient rats were analysed using an unpaired t-test (n=4-6).

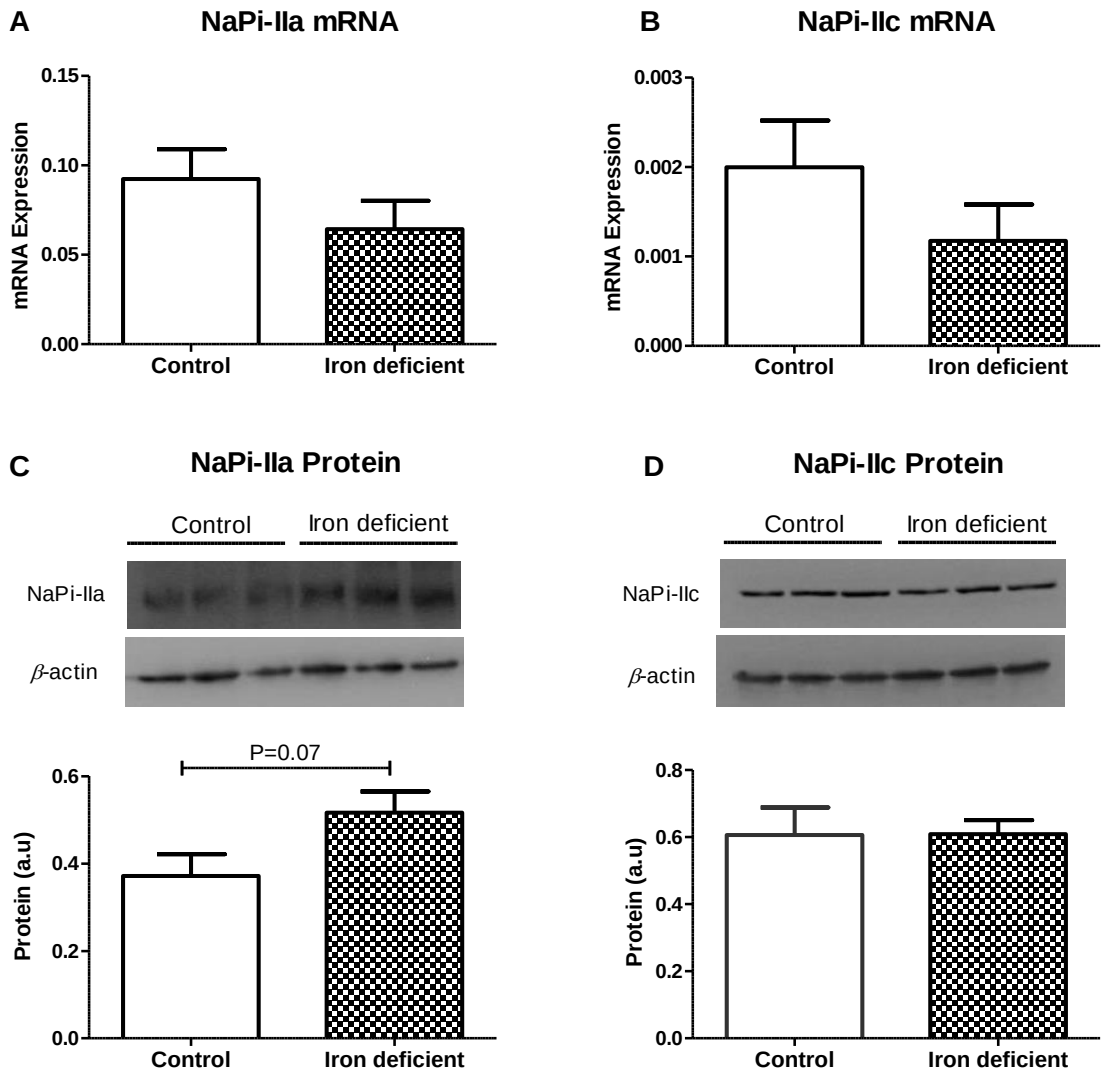


**Figure 4.3. Effect of diet-induced iron deficiency on renal NaPi-IIa and NaPi-IIc**. RT-PCR quantification of mRNA levels of NaPi-IIa and NaPi-IIc (A and B). Duplicate PCR reactions were performed for each sample and the mRNA expression of NaPi-IIa and NaPi-IIc is given as their ratio to *β*-actin. Representative Western blot image and quantification of NaPi-IIa and NaPi-IIc protein (C and D) in control and iron deficient rats. The abundance of NaPi-IIa and NaPi-IIc protein is given as the ratio of their band density to *β*-actin, expressed in arbitrary units (a.u). An unpaired t-test was used to compare results between groups (n=5-6).

### 4.3.4. Effect of diet-induced iron deficiency on regulators of phosphate homeostasis

To gain more insight into the underlying mechanisms responsible for the inhibition of intestinal phosphate absorption by diet-induced iron deficiency and the potential renal compensation, the levels of the systemic regulators of phosphate homeostasis, FGF-23, PTH and $1,25(OH)_2D_3$ were examined. The results showed that these regulators were unchanged in the iron deficient group compared to control (Figure 4.4A-D). Using RT-PCR, the mRNA levels of Cyp27b1, the gene encoding the enzyme that catalyses the rate limiting-step for $1,25(OH)_2D_3$ synthesis and FGF-23 co-receptor, α-klotho, were also shown to be unchanged in response to diet-induced iron deficiency (Figure 4.5A and B). These findings suggest that the systemic regulators of phosphate homeostasis are unaffected by diet-induced iron deficiency, and thus, play no role in the inhibition of intestinal phosphate absorption seen in the iron deficient animals. To further rule out any potential contribution of $1,25(OH)_2D_3$ signalling to the mechanism underlying the inhibition of intestinal phosphate absorption by diet-induced iron deficiency, RT-PCR experiment was used to test the mRNA expression of VDR in the duodenum and jejunum. Surprisingly, VDR mRNA expression was significantly increased in the duodenum (Figure 4.5C), where the inhibition of phosphate absorption by diet-induced iron deficiency was more prominent, while jejunal VDR was unaffected (Figure 4.5D). Since $1,25(OH)_2D_3$ signalling is known to increase intestinal phosphate and $Ca^{2+}$ absorption, the exact significance of this upregulated duodenal VDR is unclear.

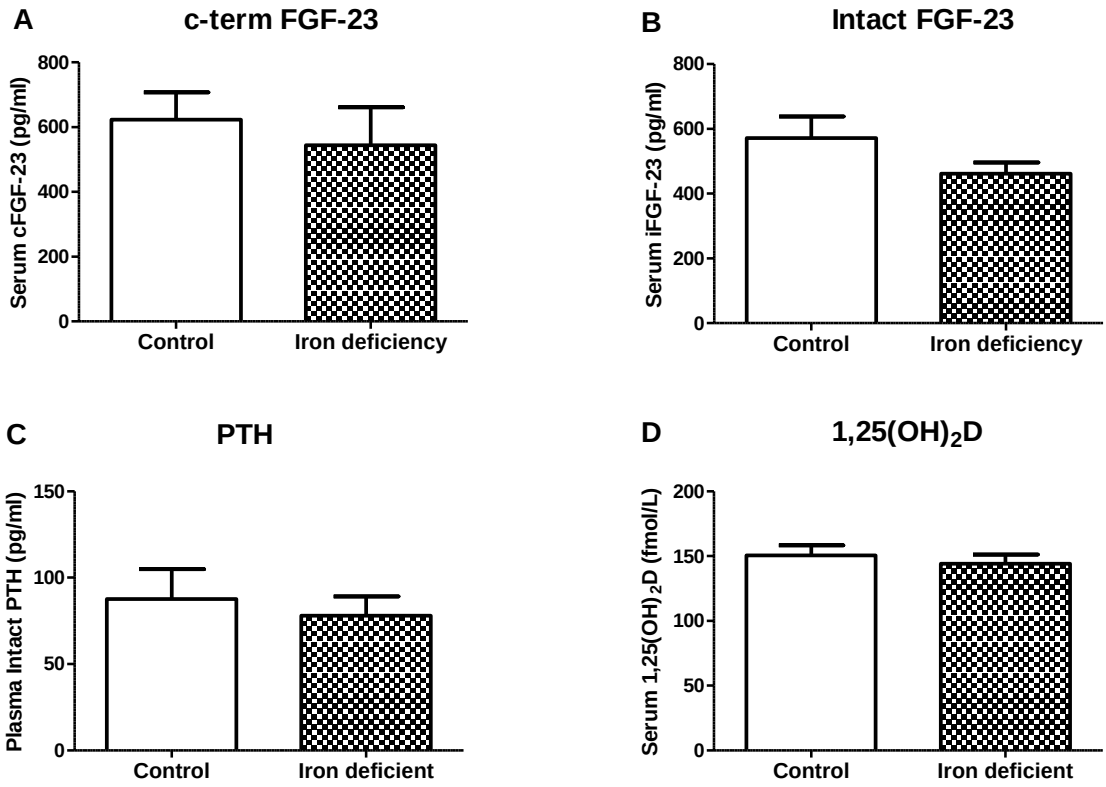


**Figure 4.4. Effect of diet-induced iron deficiency on systemic regulators of phosphate homeostasis**. Serum levels of c-term FGF-23, Intact FGF-23, $1,25(OH)_2D_3$ and plasma levels of intact PTH were determined in control and iron deficient animals using ELISA. An unpaired t-test was used to compare differences between groups (n=6-11).

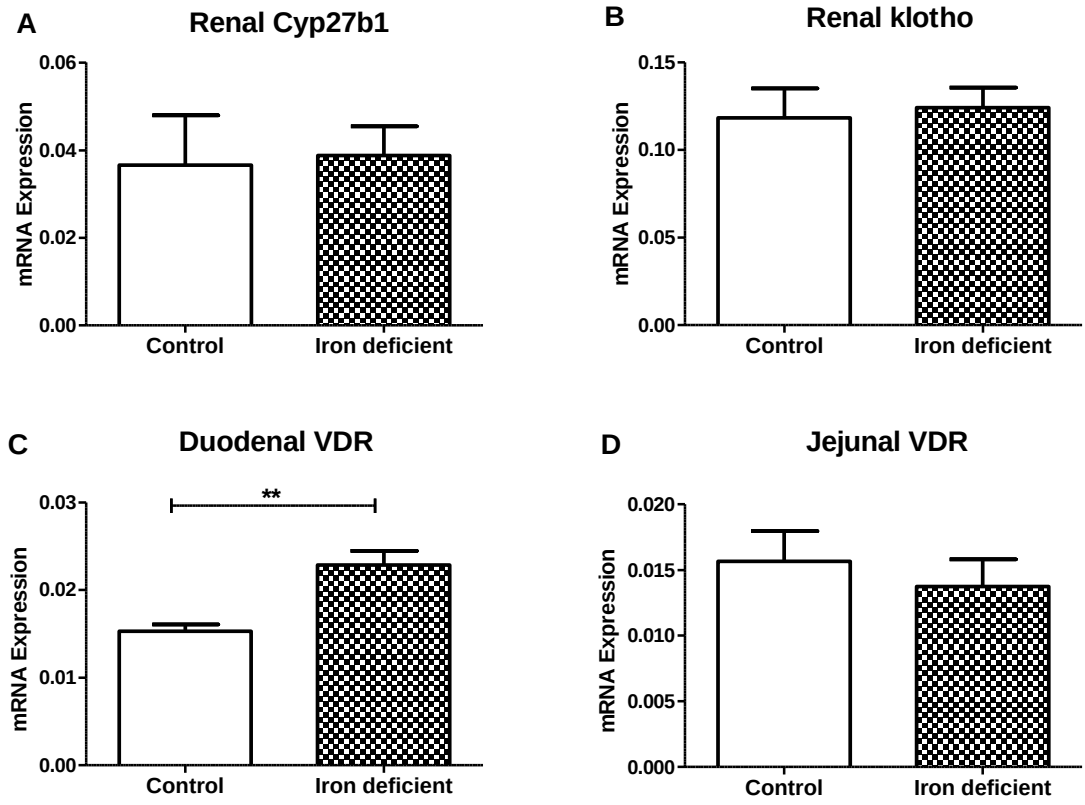


**Figure 4.5. Effect of diet-induced iron deficiency on renal Cyp27b1 and Klotho, and intestinal VDR**. RT-PCR quantification of the mRNA levels of Cyp27b1, klotho, duodenal VDR and jejunal VDR (A-D). Duplicate PCR reactions were performed for each sample and the mRNA expression of Cyp27b1, klotho, duodenal VDR and jejunal VDR is given as their respective ratio to *β*-actin. An unpaired t-test was used to compare results between groups (n=6). ***P*<0.01

## 4.4. Discussion

Based on the evidence linking iron deficiency with phosphate imbalance (reviewed in section 1.6) and bone disease [337–341], the effect of diet-induced iron deficiency on the intestinal and renal mechanisms of phosphate homeostasis was examined. Using *in vitro* and *in vivo* techniques, diet-induced iron deficiency was shown to significantly inhibit intestinal phosphate absorption in normal rats, but this effect had no impact on serum phosphate levels. A trend for increased renal NaPi-IIa protein levels in iron deficient rats and a consequent reduction in renal phosphate excretion, although not significant, may be responsible for the normal phosphate balance observed in iron deficient animals. In addition, the bone phosphate buffering mechanism, which was not investigated in the current study, may also contribute to the maintenance of phosphate homeostasis in iron deficient rats. Evidence from the current study indicated that the effect of diet-induced iron deficiency on the intestinal and renal mechanisms of phosphate transport were not dependent on the recognised systemic phosphate regulators, FGF-23, PTH and $1,25(OH)_2D_3$.

Intestinal absorption of phosphate via the transcellular pathway is widely considered to be mediated by NaPi-IIb. Previous findings using gene chip analysis and quantitative PCR techniques have shown that in response to diet-induced iron deficiency in rats, the NaPi-IIb gene, SLC34A2, is significantly downregulated in the duodenum and jejunum, with a more prominent decrease observed in the duodenum compared to the jejunum [346,347]. In keeping with these findings, the observation that the inhibition of phosphate absorption by diet-induced iron deficiency was stronger in the duodenum compared to the jejunum in the current study suggests that the effect of iron deficiency on intestinal

phosphate absorption may have been due to changes in NaPi-IIb levels. However, the evidence presented in chapter 3 and previous reports in rats [45,246] indicate that NaPi-IIb plays no significant role in duodenal phosphate absorption while contributing only a small proportion to jejunal phosphate absorption at physiological phosphate concentration. These findings make it unlikely that the downregulation of duodenal NaPi-IIb mRNA by iron deficiency (presented in chapter 5, Figure 5.3A) is responsible for the robust inhibition of phosphate absorption observed in this study. Based on the *in vitro* phosphate uptake data (Figure 3.11), it is interesting to note that the $Na^+$-independent pathway appears to be the predominant phosphate transport mechanism, mediating approximately 75% and 60% of total phosphate transport in the duodenum and jejunum respectively. These overall proportions of $Na^+$-independent phosphate transport are comparable to the proportion of phosphate transport inhibition in the duodenum and jejunum in response to iron deficiency. Since the $Na^+$-independent phosphate transport pathway contributes a higher proportion of phosphate transport in the duodenum compared to the jejunum *in vivo* [45], it is possible that this phosphate transport pathway is affected by iron deficiency and this may be the reason for the stronger and long-lasting phosphate inhibition observed in the duodenum. Taken together, these findings indicate that instead of NaPi-IIb, the $Na^+$-independent pathway is the phosphate transport mechanism that is likely affected in iron deficiency. Additional experiments to test this hypothesis are discussed in chapter 5.

There is however data from the investigation of the $1,25(OH)_2D_3$ – VDR signalling in the current chapter that supports the hypothesis that NaPi-IIb is not involved in the inhibitory effect of diet-induced iron deficiency on intestinal phosphate

absorption. NaPi-IIb-mediated phosphate absorption in the rat small intestine is known to be regulated by the $1,25(OH)_2D_3$ – VDR signalling pathway, with the effect of this hormonal pathway occurring only in the jejunum [39,126,329,348]. However, in the current study, iron deficiency inhibited phosphate absorption in the duodenum and jejunum, with a more striking effect in the duodenum, a segment where $1,25(OH)_2D_3$ has been reported to have no effect on phosphate absorption [39,329]. The iron deficiency-induced inhibition of jejunal phosphate absorption does not correlate with the fact that iron deficiency had no effect on circulating $1,25(OH)_2D_3$ levels and VDR mRNA expression in this segment. Based on this finding and since $1,25(OH)_2D_3$ has been demonstrated to increase NaPi-IIb-mediated phosphate absorption in the jejunum [39,48], it is therefore apparent that the effect of iron deficiency on phosphate absorption may not be dependent on changes in NaPi-IIb function. Moreover, even though $1,25(OH)_2D_3$ has not been reported to affect NaPi-IIb-mediated phosphate absorption in the duodenum of rats [39,329], the significantly upregulated mRNA levels of duodenal VDR in iron deficiency would have been expected to increase phosphate absorption in this segment. In contrast to this expected increase in phosphate absorption, was the finding that phosphate absorption was inhibited in the duodenum of iron deficient rats in the current study. This further supports the hypothesis that the downregulation of NaPi-IIb mRNA (Figure 5.3A) [346,347] in iron deficient animals is not responsible for the inhibition of intestinal phosphate absorption. Interestingly, the upregulated VDR in the duodenum in response to iron deficiency may be associated with duodenal $Ca^{2+}$ absorption. Iron deficiency has been reported to inhibit intestinal $Ca^{2+}$ absorption [338,349], with emerging evidence in our laboratory suggesting that this effect may be due to the reduction in calbindin D9K-mediated transcellular $Ca^{2+}$ transport (unpublished data). Because the duodenum is known

to be involved in 1,25$(OH)_2D_3$-sensitive $Ca^{2+}$ absorption, the upregulated VDR may be a component of a possible compensatory mechanism in response to a potential inhibition of transcellular $Ca^{2+}$ absorption in this segment. In line with this hypothesised compensatory mechanism for $Ca^{2+}$ absorption, the upregulation of a 1,25$(OH)_2D_3$-sensitive $Ca^{2+}$ pore, claudin 2, has previously been reported in the duodenum in response to diet-induced iron deficiency [347]. To understand the exact significance of the iron deficiency-induced upregulation of VDR in the duodenum, further studies are required to examine the effect of iron deficiency on the mechanisms of intestinal $Ca^{2+}$ absorption.

Interestingly, in the jejunum, the observation that the magnitude of iron deficiency-induced inhibition of phosphate absorption *in vivo* decreased over a period of 30 minutes suggests the activation of a potential compensatory mechanism for this inhibition of phosphate absorption. Since my findings suggest that iron deficiency inhibits the $Na^+$-independent phosphate absorption pathway in the rat small intestine, there may be a potential increase in the activity of the transcellular $Na^+$-dependent phosphate transporters in the jejunum, NaPi-IIb and PiT-1, both known to be most highly expressed in this segment (discussed in chapter 3). It is worth noting that like the duodenum that is known to be responsible for transcellular 1,25$(OH)_2D_3$-VDR-dependent $Ca^{2+}$ transport, the jejunum is the segment involved in transcellular phosphate absorption, mediated by the 1,25$(OH)_2D_3$-VDR signalling pathway. Surprisingly, the unchanged levels of 1,25$(OH)_2D_3$ or jejunal VDR in response to iron deficiency, suggests that the potential compensatory mechanism for the inhibited phosphate absorption over time in the jejunum may not be dependent on the function of this hormonal pathway.

In animals with normal renal function, the kidney is known to be the major regulator of phosphate homeostasis, therefore, the effect of iron deficiency on phosphate balance and renal phosphate handling was investigated. In diet-induced iron deficiency, even though there was a significant inhibition of intestinal phosphate absorption, serum phosphate levels were unchanged. This may have been due to the trend for upregulation of renal NaPi-IIa and a moderate decrease in urinary phosphate excretion observed in this study. In agreement with this suggestion, the inhibition of intestinal phosphate absorption in NaPi-IIb knock-out mice maintained on a normal phosphate diet has been shown to be associated with reduced urinary phosphate excretion. Interestingly, changes in renal phosphate excretion in NaPi-IIb knock-out mice are not always associated with changes in FGF-23 and NaPi-IIa levels [31,222,251,328]. For example, when NaPi-IIb knock-out mice are maintained on 0.63% phosphate diet, the decreased urinary phosphate excretion is associated with reduced intact FGF-23 levels and increased renal NaPi-IIa protein expression [31]. However, when these mice were maintained on a 0.9% phosphate diet, the reduced urinary phosphate excretion was not associated with changes in NaPi-IIa and intact FGF-23 [251]. In addition, studies have shown that intestinal phosphate absorption following gastric phosphate loading or instillation of a phosphate bolus into the small intestine of rats is associated with significant renal phosphate wasting, which was demonstrated to be a consequence of increased circulating levels of phosphate and PTH [23,24]. Therefore, in the current study, the lack of change in FGF-23, the trend for NaPi-IIa upregulation and the moderate reduction in urinary phosphate excretion in response to iron deficiency may be due to the magnitude of inhibition of intestinal phosphate absorption. The relatively smaller inhibition of phosphate absorption observed in the jejunum (the major segment for phosphate absorption

in rats) in response to iron deficiency, may explain the lack of significant change in urinary phosphate excretion and renal NaPi-IIa levels.

Age and sex have been identified to be among the causes of the inconsistent renal adaptation to reduced intestinal phosphate absorption in rodents [222,328]. For example, to maintain phosphate balance during a period of low intestinal phosphate absorption in NaPi-IIb knock-out mice, reduced urinary phosphate excretion has been reported in both 4-week and 20-week old mice [328]. However, while this renal phosphate adaptation occurs as a result of reduced circulating levels of FGF-23 and NaPi-IIa upregulation in 4-week old NaPi-IIb knock-out mice, no change in both NaPi-IIa and FGF-23 was seen in the 20-week old mice [328]. Hernando and colleagues reported that changes in the circulating levels of phosphate regulators in response to the inhibition of intestinal phosphate absorption by the loss of NaPi-IIb was less apparent in adult males compared to females, where NaPi-IIa upregulation and reduced intact FGF-23 levels were seen [222]. Based on these reports, the age and sex of the animals used in the current study may have affected the renal adaptation to the reduced intestinal phosphate absorption seen in the iron deficient animals.

Importantly, the degree of renal adaptation in response to intestinal phosphate absorption seems to vary with the amount of phosphate absorbed in the small intestine, which is determined by the levels of phosphate in the diet. For example, intact FGF-23, PTH and urinary phosphate levels in both NaPi-IIb knock-out and wild-type mice have been shown to be lowest in mice maintained on a 0.1% phosphate diet, compared to those maintained on a 0.8% or 1.2% phosphate diet [145]. These findings, in addition to those discussed in the previous two paragraphs, suggest that diet-induced iron deficiency does not have a direct effect on NaPi-

IIa function or renal phosphate excretion and that the adaptation of the renal system to maintain phosphate balance in iron deficiency occurs in response to the reduced intestinal phosphate absorption.

Previous reports in mice and humans have shown that iron deficiency affects FGF-23 transcription and processing in osteocytes, leading to increased circulating c-term FGF-23 and unchanged intact FGF-23 levels under normal physiological conditions [305,309,310]. However, in the current study, the levels of c-term FGF-23 were unchanged in response to diet-induced iron deficiency. The discrepancy between the current study and previous findings on the levels of c-term FGF-23 in response to iron deficiency may be as a result of the previously reported blood collection time-dependent variation in the levels of c-term FGF-23 in normal rats [311]. A study involving repeated blood collection from normal anaesthetised or non-anaesthetised rats at 3 different time points has shown that c-term FGF-23 is an unstable hormone [311]. In the current study, the time of blood collection from animals was different as blood was collected after phosphate uptake experiment from each animal. In contrast to the unstable levels of c-term FGF-23, the levels of intact FGF-23 have been reported to be stable over a similar period of time [311]. Importantly, in the current study, diet-induced iron deficiency had no effects on the levels of biologically active intact FGF-23, which is consistent with previous findings [305,309,310]. Reports on the biology of FGF-23 have shown that the levels of intact FGF-23 are regulated by FGF-23 gene transcription and intracellular cleavage of newly synthesised intact FGF-23 to c-term FGF-23 within osteocytes, with both forms released into the circulation [350]. Only the intact FGF-23 is thought to be involved in phosphate homeostasis, with the role of the c-term FGF-23 currently unknown. It has been hypothesised that

continuous FGF-23 production and cleavage to c-term FGF-23 fragments provide osteocytes with the innate ability to increase or decrease the secretion of intact FGF-23 more rapidly by adjusting the rate of cleavage [306]. In phosphate homeostasis, one of the roles of intact FGF-23 is to decrease the levels of a major regulator of intestinal phosphate absorption, $1,25(OH)_2D_3$, by inhibiting the mRNA expression of Cyp27b1 enzyme and increasing that of Cyp24a1 [306,351]. The mRNA expression of Cyp27b1 and the levels of $1,25(OH)_2D_3$ in response to diet-induced iron deficiency were tested in this study. Consistent with the unchanged levels of intact FGF-23, the results showed that both Cyp27b1 mRNA and $1,25(OH)_2D_3$ levels were unaffected in the iron deficient animals. Interestingly, it is noteworthy that age interferes with the impact of iron deficiency on FGF-23 and $1,25(OH)_2D_3$. In normal mice that are less than 6 weeks old and healthy children, previous studies have reported changes in intact FGF-23 and $1,25(OH)_2D_3$ levels in response to iron deficiency [306,307,312]. Thus, the fact that adult rats were used for the current study may explain the discrepancy between my findings and these reports.

PTH and α-klotho are also considered important regulators of phosphate balance, as both have been shown to affect the levels or actions of FGF-23 and $1,25(OH)_2D_3$ [10,95,116]. Recent clinical data in 6-10-year old children with beta-thalassemia have shown that iron overload in this condition is associated with low PTH levels, and these children were shown to have higher phosphate levels compared to healthy children [352]. In the current study, the investigation into whether changes in PTH and α-klotho were associated with the inhibition of phosphate absorption in iron deficiency revealed that these regulators were unchanged in adult animals. This finding, therefore, suggests that in normal adult

animals, like intact FGF-23 and $1,25(OH)_2D_3$, PTH and α-klotho levels are not linked to the inhibition of intestinal phosphate absorption or the moderate changes in renal phosphate excretion in diet-induced iron deficiency.

### 4.5. Conclusion

In summary, the findings of this chapter demonstrate that diet-induced iron deficiency inhibits phosphate absorption in the duodenum and jejunum of rats, with a more prominent effect in the duodenum. The results indicate that the inhibition of intestinal phosphate absorption by diet-induced iron deficiency is not dependent on the circulating levels of recognised phosphate regulators, suggesting that this impact on phosphate absorption may be mediated via mechanisms within the enterocytes. The mechanisms underlying the inhibition of intestinal phosphate absorption by iron deficiency is reported in the next chapter. Importantly, based on the evidence discussed in this chapter in relation to previous findings (described in section 1.6), it is now known that abnormal iron metabolism interferes with the mechanisms of phosphate homeostasis, and a complete understanding of this link may improve clinical outcomes in patients with impaired iron and phosphate metabolism. In addition, since iron deficiency is highly prevalent globally, a proper understanding of the link between iron, FGF-23 and other regulators of phosphate homeostasis will be essential in preventing the development of bone disease in iron deficient individuals.

# Chapter Five

## 5.0. Effect of diet-induced iron deficiency on the mechanisms of intestinal phosphate absorption

## 5.1. Introduction

As demonstrated in chapter 3, intestinal phosphate absorption in the rat proximal small intestine occurs mainly via a $Na^+$-dependent NHE3-regulated paracellular pathway and a $Na^+$-independent pathway. While the findings of chapter 4 indicate that diet-induced iron deficiency significantly inhibited intestinal phosphate absorption, it is not known whether one or both these mechanisms of phosphate absorption are affected. The results do however suggest that the underlying mechanisms are independent of the systemic regulators of phosphate homeostasis, and of particular interest, do not involve $1,25(OH)_2D_3$, which is known to regulate NaPi-IIb levels. Until recently, NaPi-IIb has been considered to be the rate-limiting step for intestinal phosphate absorption [353], however, as discussed in chapter 3, it is now known that under normal physiological phosphate concentration, NaPi-IIb becomes saturated and that the $Na^+$-independent phosphate transport mechanism, thought to be mediated via the paracellular pathway is predominantly responsible for phosphate absorption in rats [45,145].

Paracellular absorption of solutes and ions from the intestinal lumen into the circulation is influenced by the composition and architectural organisation of tight junction complexes. Numerous integral membrane proteins and scaffolding proteins combine to form tight junctions, but it is recognised that the claudin protein family plays a key role in the function of these complexes (reviewed in [354]). Claudins have been shown to form either epithelial barriers (pore-sealing claudins) or paracellular channels (pore-forming claudins), and like NaPi-IIb (described in chapter 3), these claudins also have a distinct regional profile in the intestine [268]. The most highly expressed pore-sealing claudins, claudin 3 and 4,

have been demonstrated to be higher in the rat duodenum compared to the jejunum, and the pore-forming claudins 2 and 12 are higher in the jejunum (described in section 1.5.1). While numerous studies have reported a role for claudins in the paracellular transport of $Na^+$, $K^+$, $Ca^{2+}$ and $Cl^-$ [257,258,267,269], there is as yet no evidence linking claudins to paracellular phosphate transport.

Recently, NHE3 has been demonstrated to regulate paracellular phosphate absorption in the small intestine of rats and humans [77,247]. Inhibition of NHE3 by tenapanor has been shown to reduce paracellular phosphate absorption [77]. In intestinal stem cell-derived monolayers, NHE3 inhibition results in a reduction in intracellular pH, which causes an increase in TEER, and this mechanism has been suggested to be responsible for the inhibition of paracellular phosphate absorption following tenapanor treatment [77]. Interestingly, there is evidence that the TEER increases in iron deficient Caco-2 cells, a response shown to involve changes in the localisation of claudin 4 [355]. Whether this increase in the TEER in iron deficient Caco-2 cells occurs in intact enterocytes and whether this results in changes in paracellular phosphate absorption is yet to be determined. Therefore, the aim of this chapter was to investigate the cellular mechanisms underlying the inhibition of phosphate absorption in iron deficient rat model. Firstly, the effect of diet-induced iron deficiency on the $Na^+$-dependent (NaPi-IIb- and NHE3-regulated phosphate transport pathways) and the $Na^+$-independent mechanisms of phosphate absorption were investigated, and the levels of intestinal claudins in response to diet-induced iron deficiency were examined.

## 5.2. Methods

### 5.2.1. Animals

Male Sprague Dawley rats and C57BL/6J mice, aged 6-8 weeks, were used for this study. As described in section 4.2.1, animals were either fed a control iron diet (TD. 80394) containing 48 ppm added iron or an iron deficient group diet (TD. 80396) containing approximately 2-6 ppm added iron for 2 weeks. Following the dietary regime, animals were weighed and anaesthetised as described in section 2.5. For haematocrit and serum phosphate measurement, blood was collected via femoral artery cannulation or via cardiac puncture, and haematocrit and phosphate levels were measured as described in section 2.7.1 and 2.7.2 respectively. Mucosa scrapes were then obtained from defined regions of the small intestine of the animals as described in section 2.2, snap frozen in liquid nitrogen and stored at -80 °C until required.

### 5.2.2. *In vitro* phosphate uptake

As described in section 2.6, *in vitro* phosphate uptake experiments were carried out using rat duodenal and jejunal segments to test the contribution of NaPi-IIb, NHE3 and the $Na^+$-independent pathway to the inhibition of phosphate absorption in rats fed an iron deficient diet. To test the role of NaPi-IIb in response to iron deficiency, 10 mM PFA was added to the uptake buffer. Similarly, to test the role of NHE3, 10 µM tenapanor was added to the uptake buffer, while uptake buffer prepared using $Na^+$ free HEPES and choline chloride was used to test whether the $Na^+$-independent mechanism was responsible for the iron deficiency-induced inhibition of phosphate absorption. The uptake buffer in all experiments contained a physiological phosphate concentration of 10 mM. Phosphate uptake in the presence of PFA or tenapanor or the $Na^+$-free uptake solution was expressed as

a percentage of the total phosphate uptake using normal physiological uptake solution containing $Na^+$.

### 5.2.3. *In vivo* phosphate uptake

As described in section 2.5, *in vivo* phosphate uptake experiments were carried out in the jejunum and ileum of mice to test the effect of diet-induced iron deficiency on intestinal phosphate absorption using an uptake buffer containing $Na^+$ and 10 mM phosphate. The amount of phosphate transferred into the blood in 10 minutes per 5 cm of the cannulated jejunum or ileum was determined and expressed in nmoles/5 cm.

### 5.2.4. RT-PCR

As described in section 2.3.1, RNA was extracted from thawed intestinal mucosa scrapes collected from rats, using the Trizol method. cDNA was synthesised from 1 µg of RNA by reverse transcription reaction as described in section 2.3.2. and RT-PCR experiments were carried out to test the mRNA expression of NaPi-IIb, NHE3, DMT1, claudins 3,4,7,8,12 and 15, SGLT1 and GLUT2 using rat-specific primers (Table 2.1).

### 5.2.5. Western blotting

Intestinal BBM vesicles were prepared as described in section 2.4.1. Intestinal BBM protein (20-50 µg) was used for Western blotting experiments to establish the protein levels of NaPi-IIb in rats and mice, and the protein levels of NHE3, DMT1, claudin 3, SGLT1 and GLUT2 in rats, as described in section 2.4.3. using specific antibodies (Table 2.2). The ratio of the band densities of these proteins to *β*-actin was expressed as a.u.

### 5.2.6. Statistical analysis

Data are presented as mean ± SEM. Statistical analysis was carried out as described in section 2.8, and statistical significance was depicted as follows: *$P$<0.05, **$P$<0.01 or ***$P$<0.001.

## 5.3. Results

### 5.3.1. Validation of iron deficient animal models

As described in section 4.3.1, the significantly reduced haematocrit and serum iron levels confirm that the rat used for the experiments described in this chapter were iron deficient. In mice, the 2-week administration of an iron deficient diet significantly reduced the haematocrit levels compared to control (Table 5.1). The dietary regime had no impact on the weight of either the rats or mice (Table 4.1 and 5.1). In addition, as observed in rats (Figure 4.3), serum phosphate levels in control and iron deficient mice were similar (Table 5.1).

**Table 5.1. Effect of diet-induced iron deficiency on haematocrit, serum phosphate and the weight of mice**. Data are presented as mean ± SEM (n = 5-11) and analysed using an unpaired t-test. *$P$<0.05 compared with control.

| | Control | Iron deficient |
|---|---|---|
| Haematocrit (%) | 44.56 ± 0.96 | 40.55 ± 1.09 * |
| Serum phosphate (mmol/l) | 3.64 ± 0.15 | 3.41 ± 0.13 |
| Animal weight (g) | 25.04 ± 0.48 | 24.35 ± 0.53 |

### 5.3.2. Effect of diet-induced iron deficiency on the mechanisms of phosphate absorption in rats

Using the *in vitro* everted sleeve technique, the contribution of NaPi-IIb, NHE3 and the $Na^+$-independent pathway to the inhibitory effect of diet-induced iron

deficiency on intestinal phosphate absorption were tested. As described in chapter 3, using 10 mM phosphate in the uptake buffer, this technique has previously been used to show the presence of a significant $Na^+$-dependent component of phosphate absorption in the duodenum and jejunum of rats [45]. While the data presented in chapter 3 showed that NaPi-IIb- and NHE3-regulated phosphate transport pathways accounted for the $Na^+$-dependent component of phosphate absorption in the jejunum, these transporters had no contribution in the duodenum. In this chapter, the uptake experiments using PFA are difficult to interpret given the relatively low contribution of PFA-sensitive NaPi-IIb pathway to overall phosphate transport in control animals (Figure 5.1A and B). In contrast, in the jejunum where there is a significant contribution of NHE3 to phosphate absorption in control animals, this component was not inhibited by tenapanor in the iron deficient animals, suggesting that iron deficiency impacts NHE3 activity in this segment (Figure 5.2B). In addition, the fact that the proportion of jejunal phosphate absorption inhibited by iron deficiency was significantly more than the proportion of phosphate absorption mediated by NHE3 (Figure 5.2B), suggests that iron deficiency may be impacting another phosphate transport pathway in this segment. In the duodenum, tenapanor has no significant effect on transport in control animals, therefore, ruling out any impact of iron deficiency on this pathway of phosphate absorption in this segment (Figure 5.2A). Western blotting and RT-PCR experiments were performed to test if there were any changes in the protein and mRNA levels of NaPi-IIb and NHE3 in response to diet-induced iron deficiency. In the duodenum, while NaPi-IIb mRNA levels were significantly downregulated (Figure 5.3A), NaPi-IIb protein was not detected (Figure 3.4B, chapter 3), which could be because duodenal NaPi-IIb mRNA is 10-fold lower than jejunal NaPi-IIb mRNA levels. The very low levels or lack of NaPi-IIb protein

in the duodenum raises the question of whether there is any physiological relevance of the downregulation of NaPi-IIb mRNA by iron deficiency in this segment. In contrast, NaPi-IIb mRNA and protein levels were unchanged in the jejunum in response to iron deficiency (Figure 5.3B and C). Similarly, NHE3 mRNA and protein levels were unchanged in the duodenum and jejunum in response to iron deficiency (Figure 5.4A-D). Taken together, these findings suggest that while NaPi-IIb function and NHE3-regulated paracellular phosphate transport pathway were unaffected by diet-induced iron deficiency in the duodenum, NHE3-regulated phosphate transport appears to be affected in the jejunum, but this is not associated with altered transporter levels. Additionally, in comparison to the jejunum, the duodenum was shown to exhibit a more striking effect of iron deficiency on phosphate absorption. The observation that the duodenum has low levels of NaPi-IIb and PiT-1, and that phosphate transport is unaffected by PFA or tenapanor in this segment highlight that the $Na^+$-independent pathway is likely to be most affected by iron deficiency.

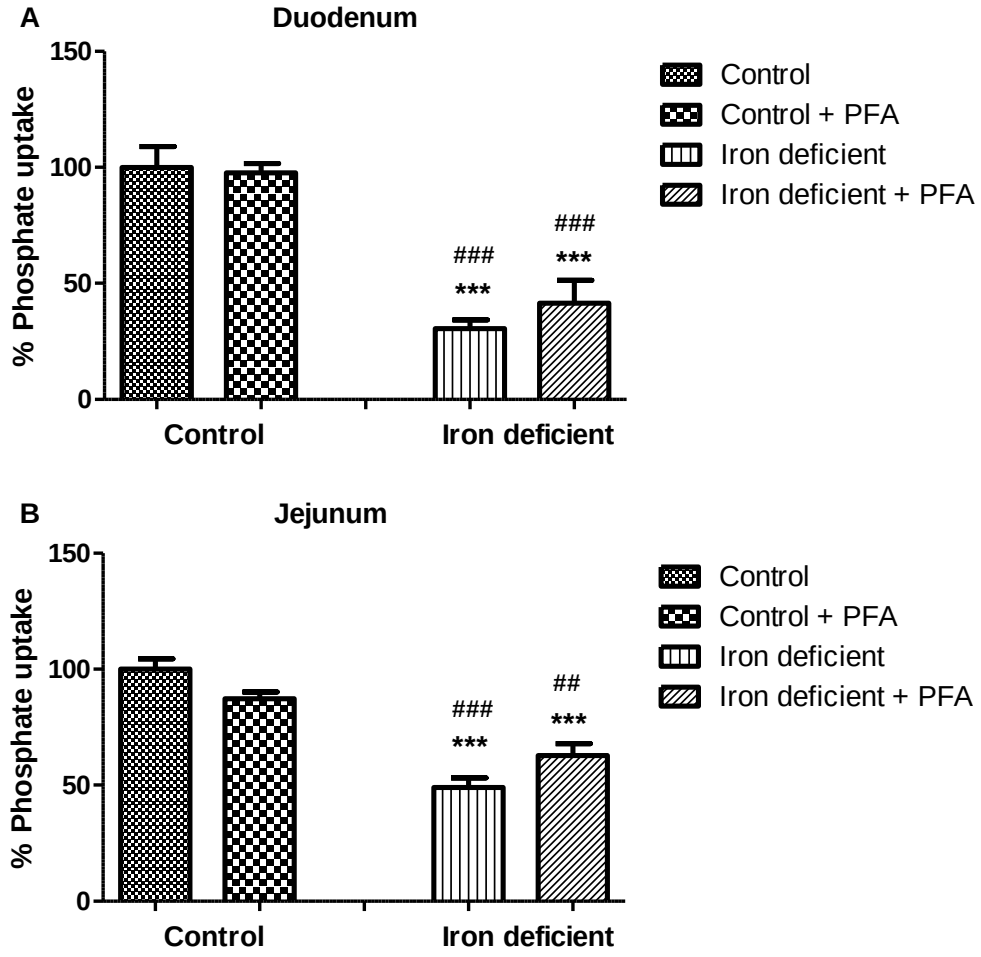


**Figure 5.1. Effect of iron deficiency on NaPi-IIb-mediated phosphate transport in the rat proximal small intestine measured *in vitro***. Phosphate uptake in the duodenum (A) and jejunum (B). Values presented are a percentage of the total phosphate transport using a buffer containing $Na^+$ in the control group (control). NaPi-IIb-dependent uptake was determined using a buffer containing $Na^+$ + 10 mM PFA. A one-way ANOVA with Tukey's multiple comparisons post-tests was used to compare differences between the control and iron deficient groups (n=6). ***$P$<0.001 compared with control, $^{\#\#}P$<0.01 and $^{\#\#\#}P$<0.001 compared with control + PFA.

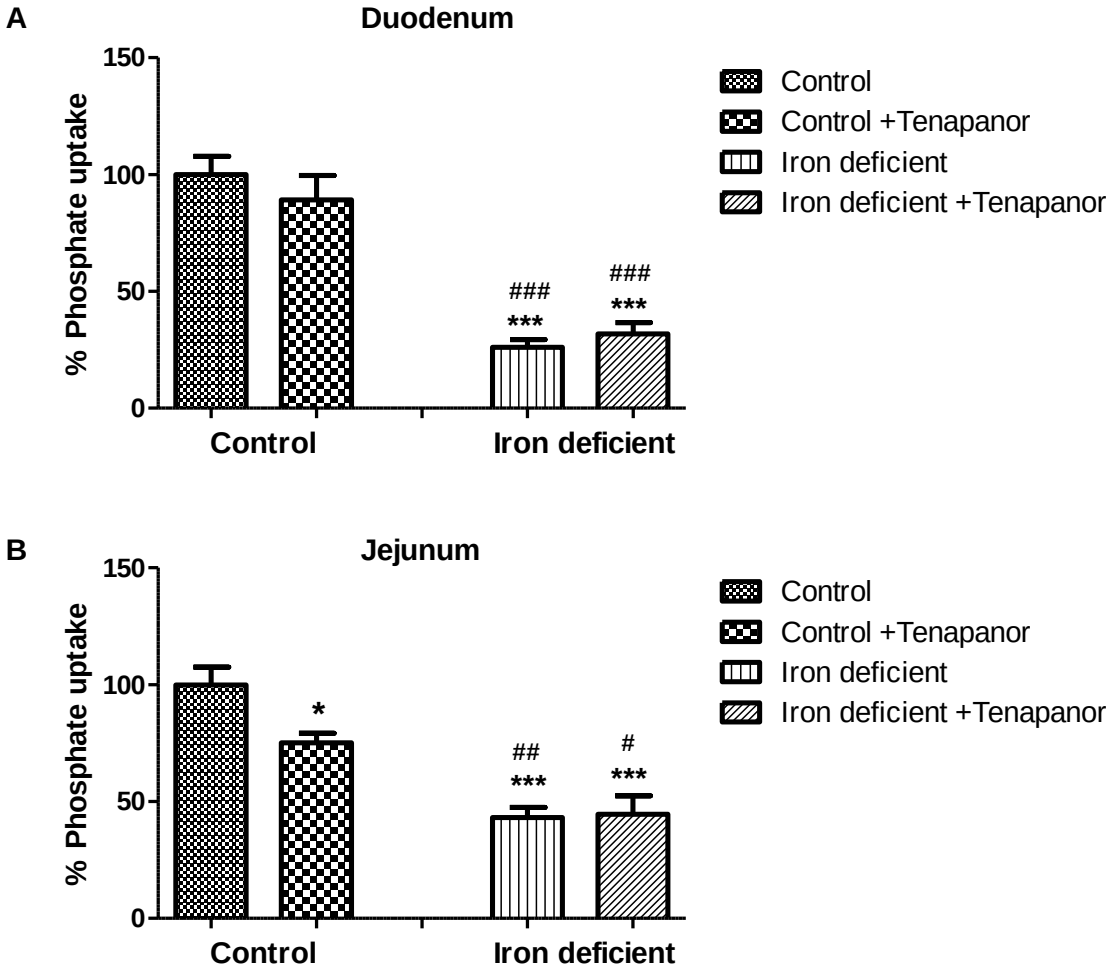


**Figure 5.2. Effect of iron deficiency on NHE3-regulated paracellular phosphate transport in the rat proximal small intestine measured *in vitro***. Phosphate uptake in the duodenum (A) and jejunum (B). Values presented are a percentage of the total phosphate transport using a buffer containing $Na^+$ in the control group (control). NHE3-regulated phosphate uptake was determined using a buffer containing $Na^+$ + 10 µM tenapanor. A one-way ANOVA with Tukey's multiple comparisons post-tests was used to compare differences between the control and iron deficient groups (n=5-6). ***$P$<0.001 compared with control; and $^{\#}P$<0.05, $^{\#\#}P$<0.01 and $^{\#\#\#}P$<0.001 compared with control + tenapanor.

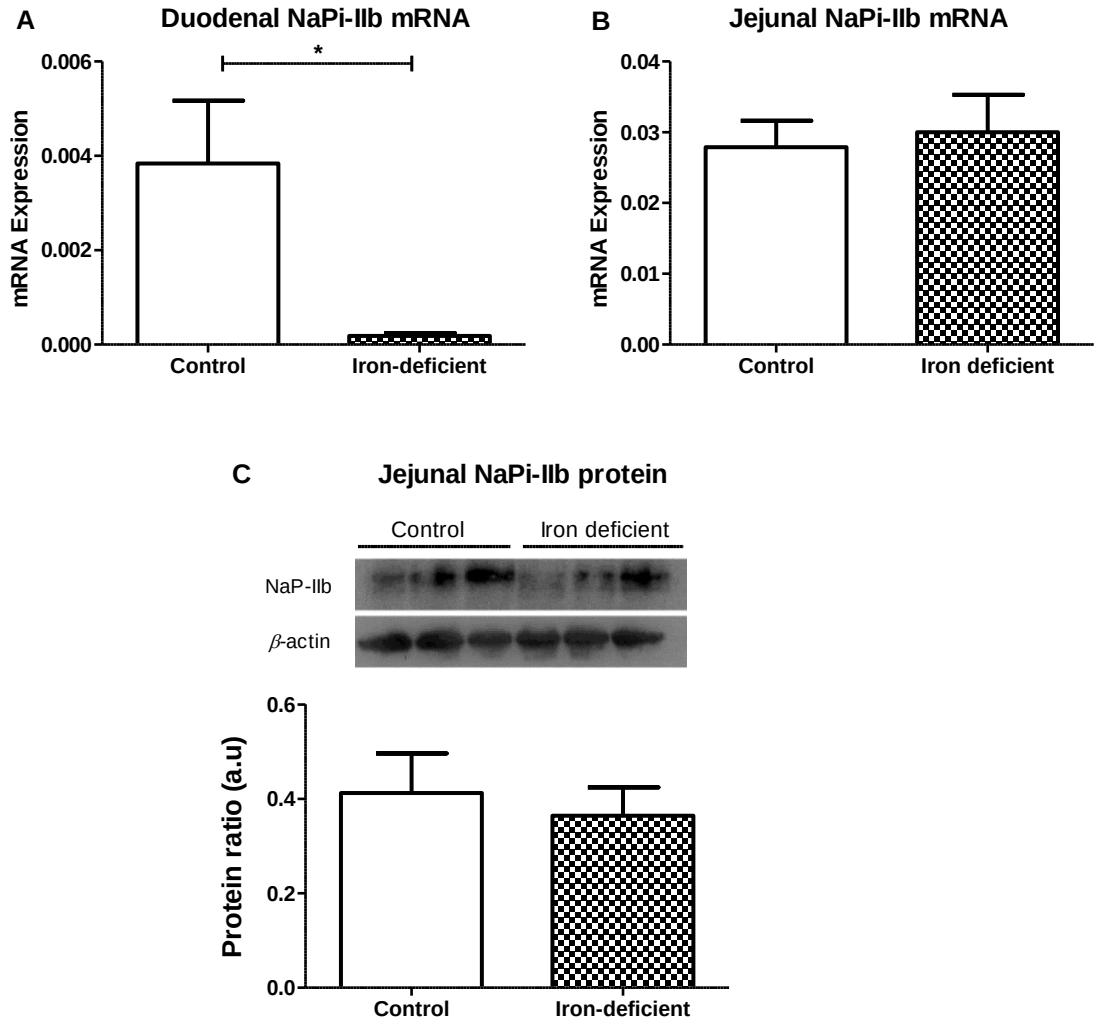


**Figure 5.3. Effect of iron deficiency on NaPi-IIb mRNA and protein in the proximal small intestine of the rat**. RT-PCR was used to determine NaPi-IIb mRNA in the duodenum (A) and jejunum (B) in response to iron deficiency. Duplicate PCR reactions were performed for each sample and the mRNA expression of NaPi-IIb is given as the ratio of NaPi-IIb to *β*-actin. Representative Western blot image and quantification of NaPi-IIb protein levels in the jejunum (C) in control and iron deficient animals. The abundance of NaPi-IIb protein is given as the ratio of NaPi-IIb band density to *β*-actin, expressed in arbitrary units (a.u). An unpaired t-test was used to compare results between groups (n= 5-6). **P*<0.05.

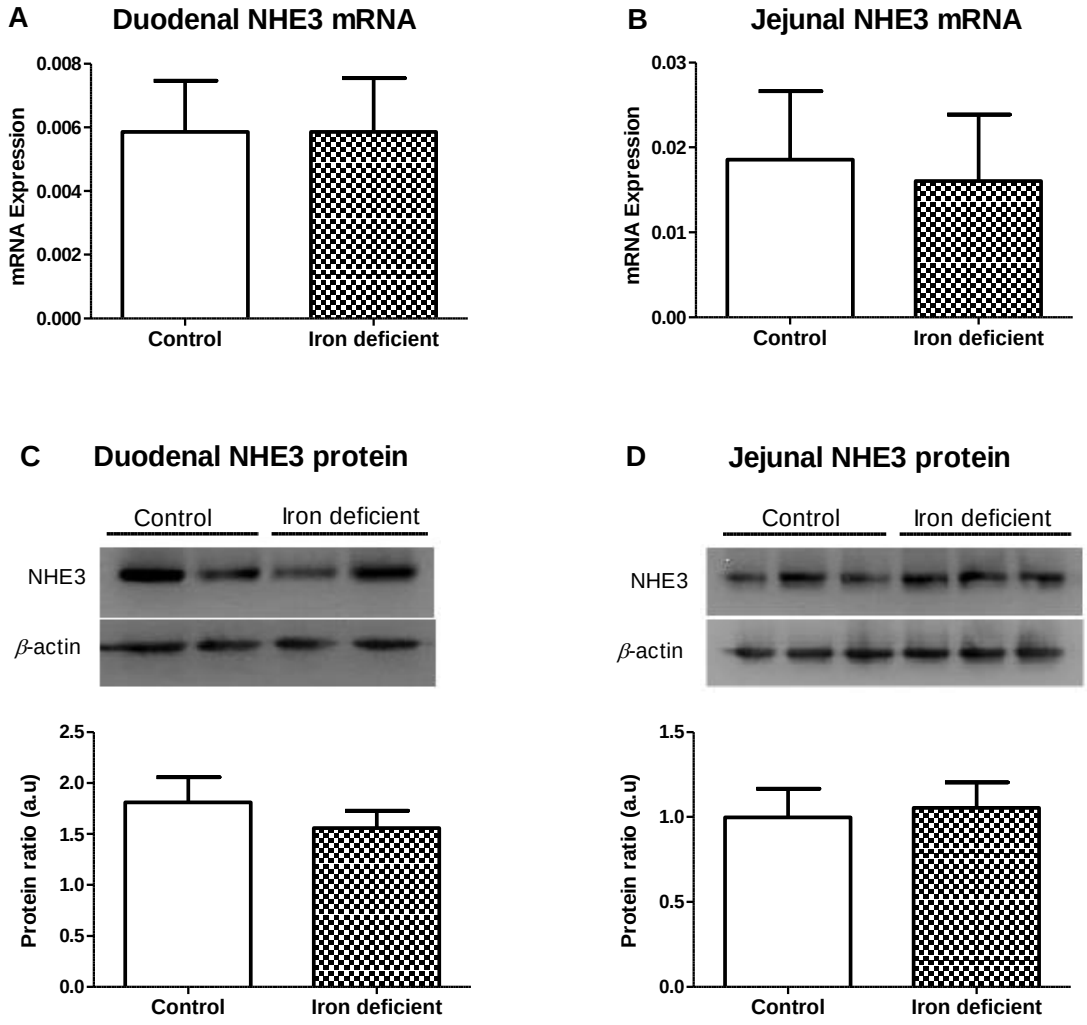


**Figure 5.4. Effect of iron deficiency on NHE3 mRNA and protein in the proximal small intestine of the rat**. RT-PCR was used to determine NHE3 mRNA in the duodenum (A) and jejunum (B) in response to iron deficiency. Duplicate PCR reactions were performed for each sample and the mRNA expression of NHE3 is given as the ratio of NHE3 to *β*-actin. Representative Western blot image and quantification of NHE3 protein levels in the duodenum (C) and jejunum (D) in control and iron deficient animals. The abundance of NHE3 protein is given as the ratio of NHE3 band density to *β*-actin, expressed in arbitrary units (a.u). An unpaired t-test was used to compare results between groups (n= 4-6)

Furthermore, phosphate uptake experiments using a $Na^+$-free buffer was used to examine the role of the $Na^+$-independent mechanism in the inhibition of phosphate absorption by iron deficiency. Interestingly, in the duodenum where the $Na^+$-independent component of phosphate transport is most predominant in the rat small intestine [45] (Figure 3.11 and 3.12, chapter 3), iron deficiency significantly inhibited phosphate uptake via this pathway (Figure 5.5A). This result indicates that the $Na^+$-independent mechanism of intestinal phosphate absorption is the pathway affected by diet-induced iron deficiency in the duodenum. Surprisingly, phosphate uptake via the $Na^+$-independent pathway in the jejunum was not significantly different between the control and iron deficient animals, but approximately 14% inhibition of phosphate transport via this pathway was observed in response to iron deficiency (% phosphate uptake; control - Na, 57.1 ± 4.7% *Vs* iron deficient - Na, 43.1 ± 5.3%, Figure 5.5B). In addition, the significant $Na^+$-dependent component of phosphate absorption seen in the jejunum of control animals was not present in the iron deficient animals (Figure 5.5B). Taken together, these findings suggest that the effect of diet-induced iron deficiency on jejunal phosphate absorption have both $Na^+$-dependent and $Na^+$-dependent component, with a more significant effect on the $Na^+$-dependent component.

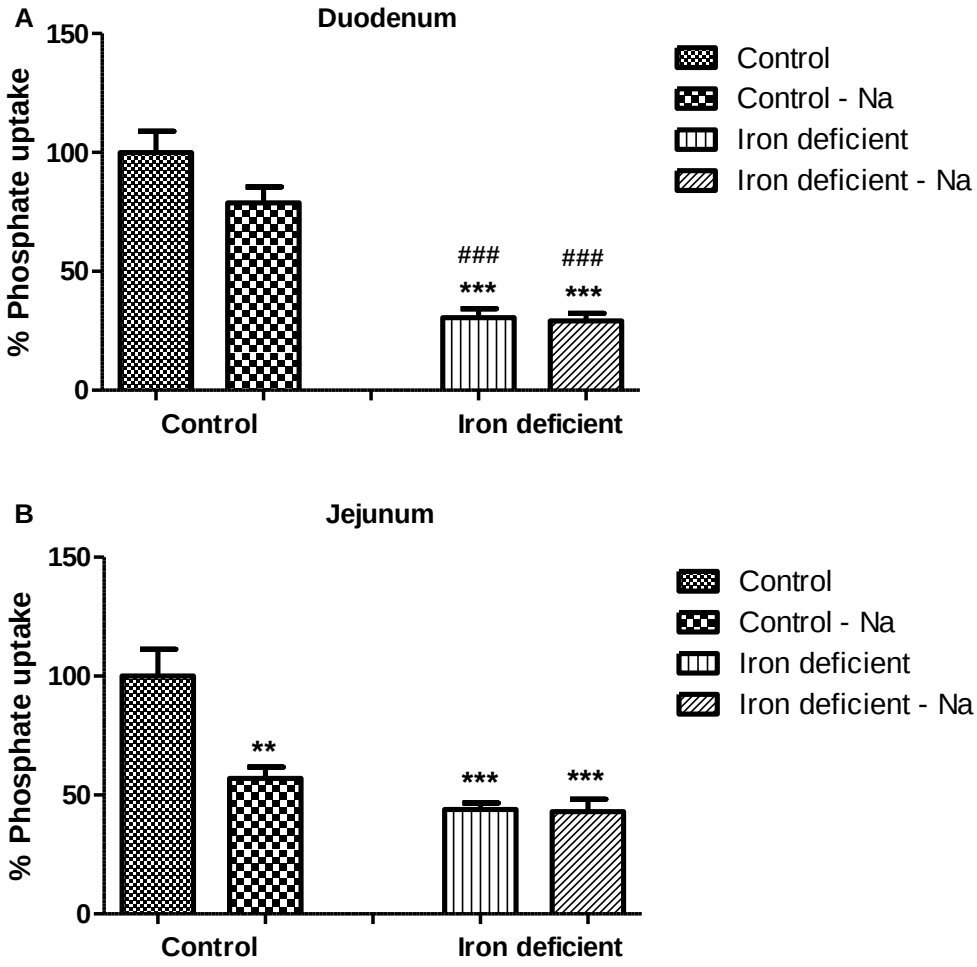


**Figure 5.5. Effect of iron deficiency on the Na+-independent phosphate transport in the rat proximal small intestine measured *in vitro***. Phosphate uptake in the duodenum (A) and jejunum (B). Values presented are a percentage of the total phosphate transport using a buffer containing $Na^+$ in the control group (control). $Na^+$-independent uptake (-$Na^+$) was determined using buffer in which $Na^+$ has been replaced with iso-osmotic choline chloride. A one-way ANOVA with Tukey's multiple comparisons post-tests was used to compare differences between the control and iron deficient groups (n=5-6). ***P*<0.01 and ****P*<0.001 compared with control, and $^{###}P$<0.001 compared with control - $Na^+$.

### 5.3.3. Effect of diet-induced iron deficiency on phosphate absorption in mice

To confirm that NaPi-IIb function does not contribute to the iron deficiency-induced inhibition of phosphate absorption in the rat small intestine, *in vivo* phosphate uptake experiments were conducted in the mouse jejunum and ileum. Like the experiments in rats, uptake experiments were carried out using a buffer containing 10 mM phosphate to test if intestinal phosphate absorption is affected in iron deficient mice, and whether any changes in phosphate absorption is associated with NaPi-IIb protein levels. In the jejunum of mice, iron deficiency significantly downregulated NaPi-IIb protein levels (Figure 5.7A) but had no effect on transepithelial phosphate absorption (Figure 5.6A). As shown in chapter 3 (Figure 3.1A and 3.4A), the mouse jejunum is known to exhibit low levels of NaPi-IIb [38,39] and because iron deficiency had no impact on phosphate uptake in this segment, the downregulation of NaPi-IIb protein in response to iron deficiency may be physiologically irrelevant. Interestingly, in the ileum where NaPi-IIb has been demonstrated to be highest in mice [38,39] (Figure 3.1A and 3.4A), iron deficiency had no effect on phosphate uptake (Figure 5.6B) and NaPi-IIb protein levels (Figure 5.7B), thus, confirming that NaPi-IIb function is unaffected by diet-induced iron deficiency.

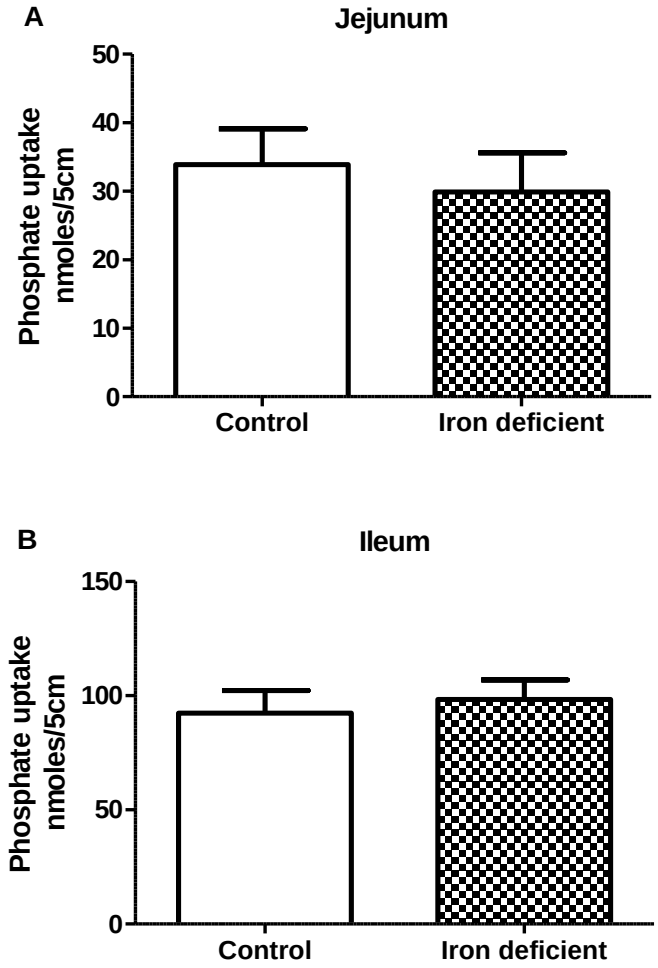


**Figure 5.6. Effect of iron deficiency on phosphate transport in the small intestine of mice measured *in vivo***. Values presented are the amount of phosphate transferred by 5 cm of the jejunum (A) and ileum (B) into 1 ml of blood after 10 minutes of phosphate instillation into the intestine, using a normal buffer containing $Na^+$. An unpaired t-test was used to compare results between groups (n=6).

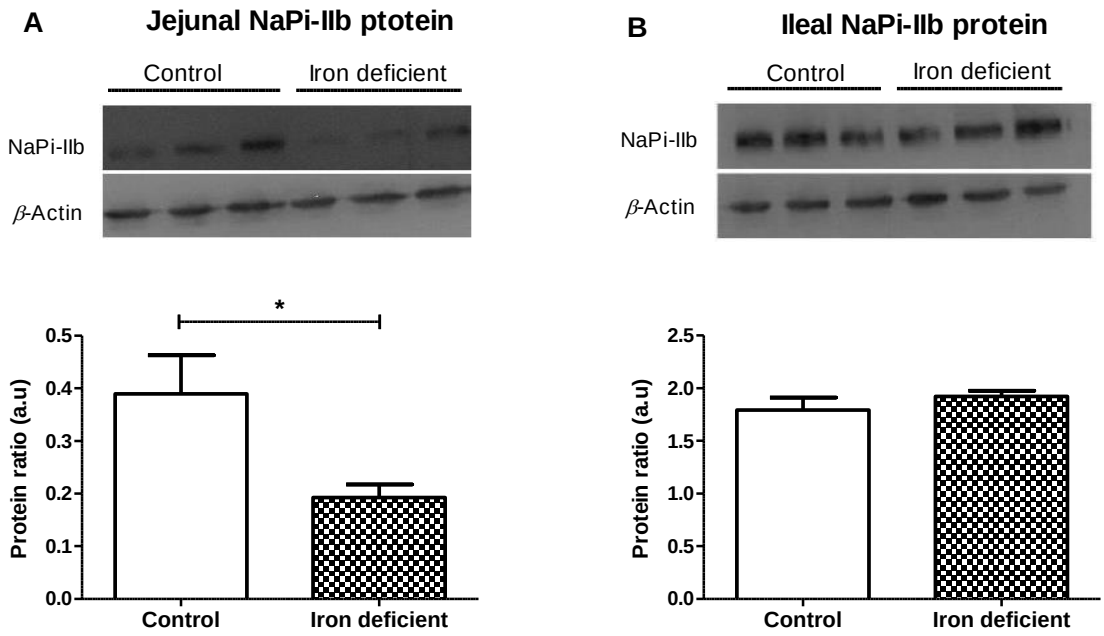


**Figure 5.7. Effect of iron deficiency on NaPi-IIb protein levels in the small intestine of mice**. Representative Western blot image and quantification of NaPi-IIb protein levels in the jejunum (A) and ileum (B) in control and iron deficient animals. The abundance of NaPi-IIb protein is given as the ratio of NaPi-IIb band density to *β*-actin, expressed in arbitrary units (a.u). An unpaired t-test was used to compare results between groups (n=6). **P*<0.05.

### 5.3.4. Diet-induced iron deficiency inhibits duodenal phosphate absorption in rats by a mechanism involving DMT1 and claudin 3

To gain more insight into the underlying cellular mechanisms responsible for the inhibition of intestinal phosphate absorption by diet-induced iron deficiency in rats, the expression of the pore-forming and pore-sealing claudins, known to control paracellular ion transport, was examined using RT-PCR. The results demonstrated that claudin 3 was the most abundant pore-sealing claudin transcript in the proximal small intestine of rats (Figure 5.8A and 5.8B), particularly in the duodenum, and that diet-induced iron deficiency significantly upregulated its expression in this segment (Figure 5.8A). In contrast, mRNA levels of the other duodenal pore-sealing claudins 4 and 8, duodenal pore-forming claudins 7, 12 and 15, and all jejunal claudins investigated in this study were unchanged (Figure 5.8B, 5.9A and B). Western blotting revealed that duodenal claudin 3 protein levels were significantly upregulated by diet-induced iron deficiency, confirming that increased mRNA levels translated to elevated claudin 3 protein levels in the rat model (Figure 5.10A). Surprisingly, even though jejunal phosphate absorption was also significantly inhibited by diet-induced iron deficiency, there were no changes in the mRNA or protein levels of claudin 3 in this segment (Figure 5.8B and 5.10B).

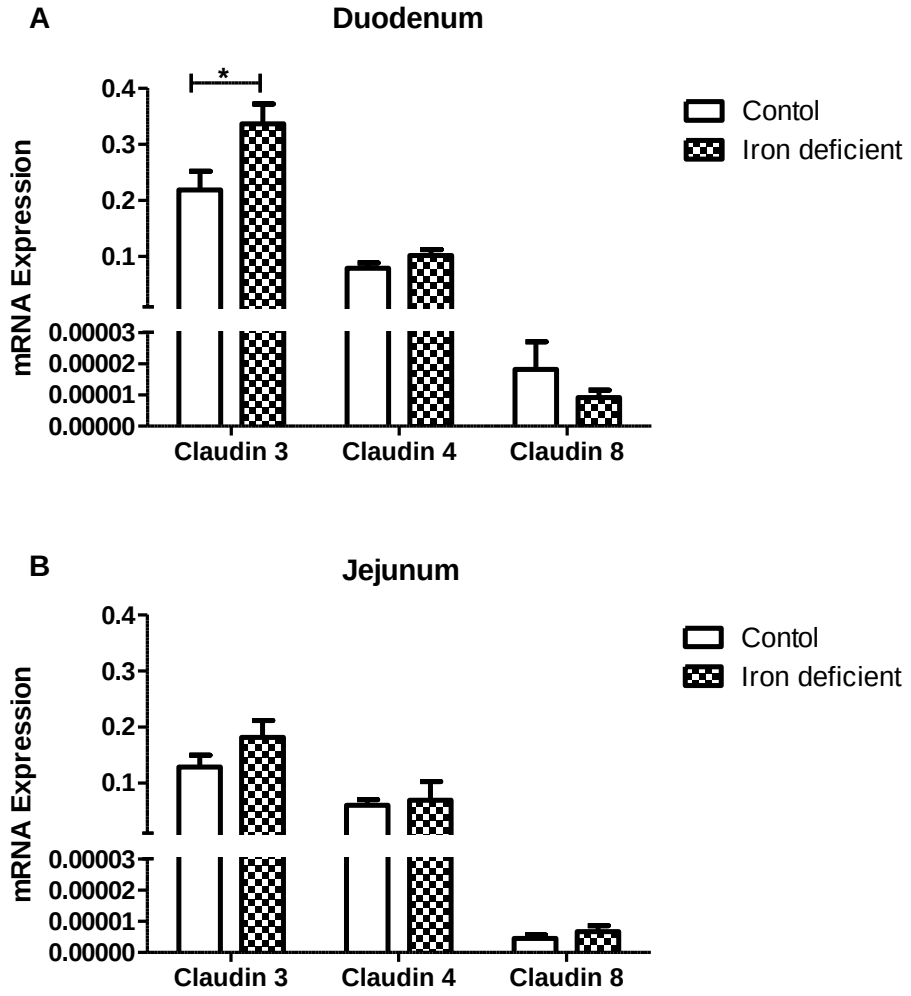


**Figure 5.8. RT-PCR quantification of pore-sealing claudins in the proximal small intestine of rats**. The effect of iron deficiency on each claudin was determined in the duodenum (A) and jejunum (B). Duplicate PCR reactions were performed for each sample and the mRNA expression of each claudin is given as the ratio of the claudin to *β*-actin. An unpaired t-test was used to compare results between the control and iron deficient group for each claudin (n=6). **P*<0.05.

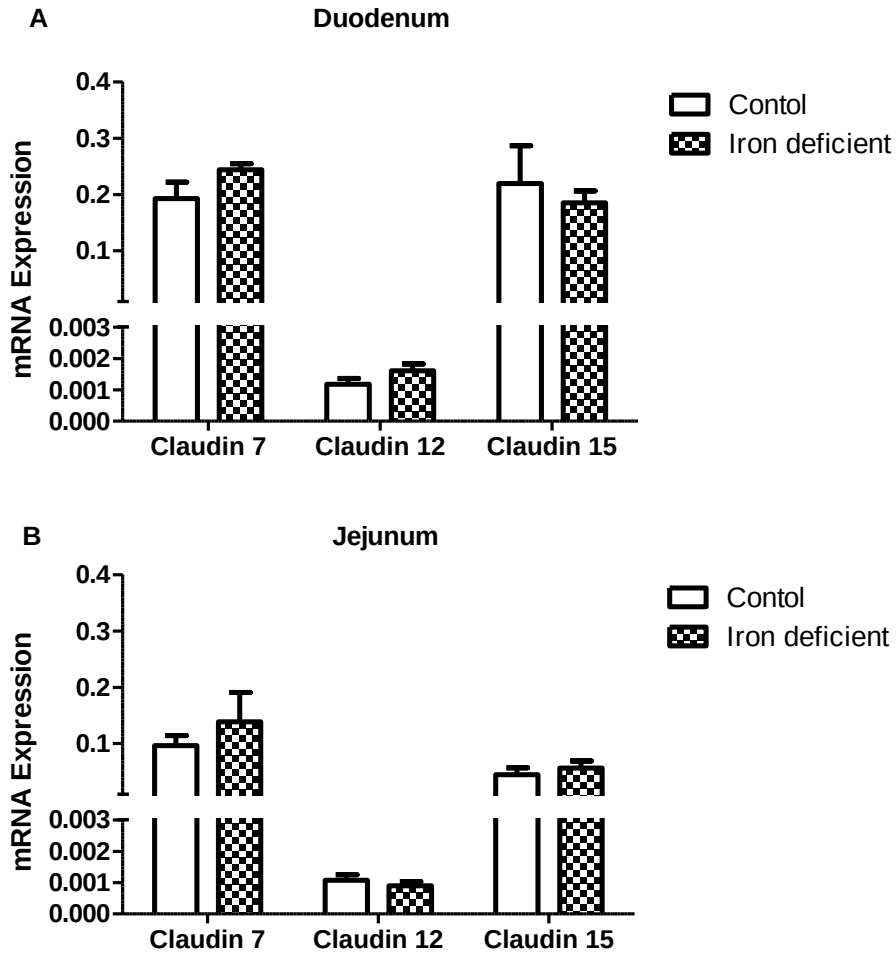


**Figure 5.9. RT-PCR quantification of pore-forming claudins in the proximal small intestine of rats**. The effect of iron deficiency on each claudin was determined in the duodenum (A) and jejunum (B). Duplicate PCR reactions were performed for each sample and the mRNA expression of each claudin is given as the ratio of the claudin to *β*-actin. An unpaired t-test was used to compare results between the control and iron deficient group for each claudin (n=6).

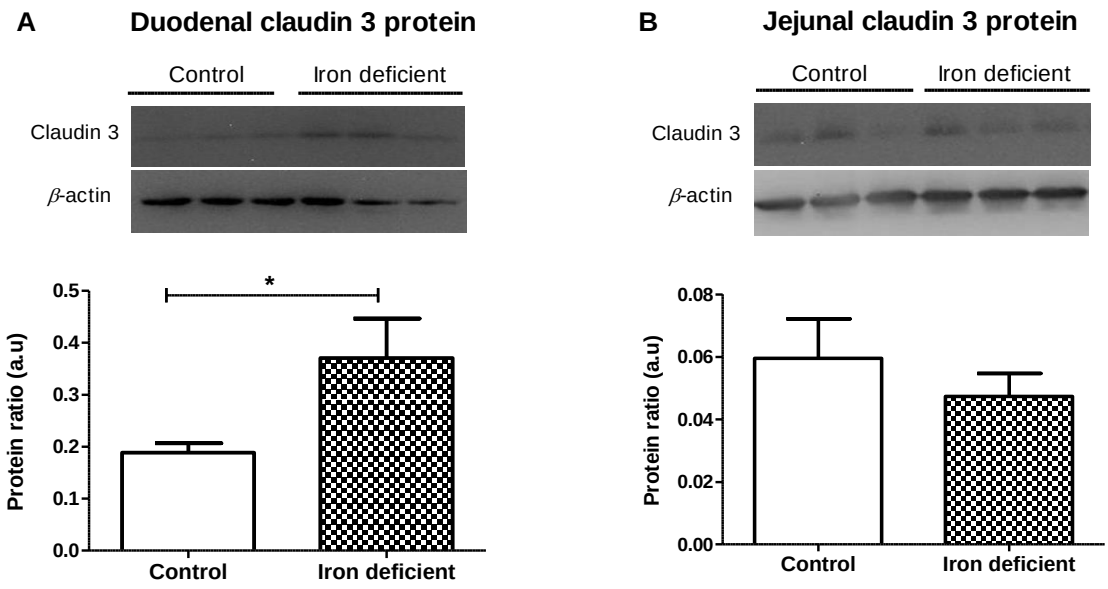


**Figure 5.10. Claudin 3 protein levels are increased in the duodenum, but not jejunum, by iron deficiency**. Representative Western blot image and quantification of claudin 3 protein levels in the duodenum (A) and jejunum (B) of control and iron deficient animals. The abundance of claudin 3 protein is given as the ratio of claudin 3 band density to *β*-actin, expressed in arbitrary units (a.u). An unpaired t-test was used to compare results between groups (n=6). **P*<0.05.

Iron is primarily absorbed in the duodenum, the first step of which utilises the BBM ferrous iron transporter DMT1. As expected in rats, there was a significant upregulation of duodenal DMT1 mRNA and protein levels in the iron deficient group compared to control (Figure 5.11A and 5.11C). Iron deficiency had no significant effect on jejunal DMT1 mRNA expression (Figure 5.11B), although very low levels were detected in this segment. However, like the duodenum, iron deficiency significantly upregulated jejunal DMT1 protein levels (Figure 5.11D). Consistent with the widely accepted dogma that iron is mainly absorbed in the duodenum, it is noteworthy that in iron deficient rats, the levels of DMT1 protein in the duodenum (a.u. 0.3825 ± 0.05895, n=6; Figure 5.11C) was approximately three times more than that in the jejunum (a.u. 0.1399 ± 0.01861, n=5; Figure 5.11D). In keeping with the finding that the inhibition of phosphate absorption is more prominent in the duodenum compared to the jejunum, it is speculated that changes in DMT1 function may contribute to the underlying mechanisms responsible for this inhibition of phosphate absorption. DMT1 is known to be an $H^+$-dependent cotransporter of ferrous iron. Therefore, in addition to increased iron absorption, upregulation of this transporter also results in an increase in $H^+$ uptake and intracellular acidification of the enterocyte [356–358]. There is also evidence that DMT1 functions as a uniporter for $H^+$ in the absence of iron when the extracellular pH is acidic [357,358]. This function of DMT1 as an $H^+$ uniporter may be more predominant in the duodenum since pH in this segment has been previously reported to be 6.6 compared to the jejunum with pH greater than 6.6 [243]. Based on this variation in luminal pH and the relatively higher expression of DMT1 in the duodenum, the possibility of DMT1-induced $H^+$ accumulation occurring in response to diet-induced iron deficiency may be higher in the duodenum compared to the jejunum.

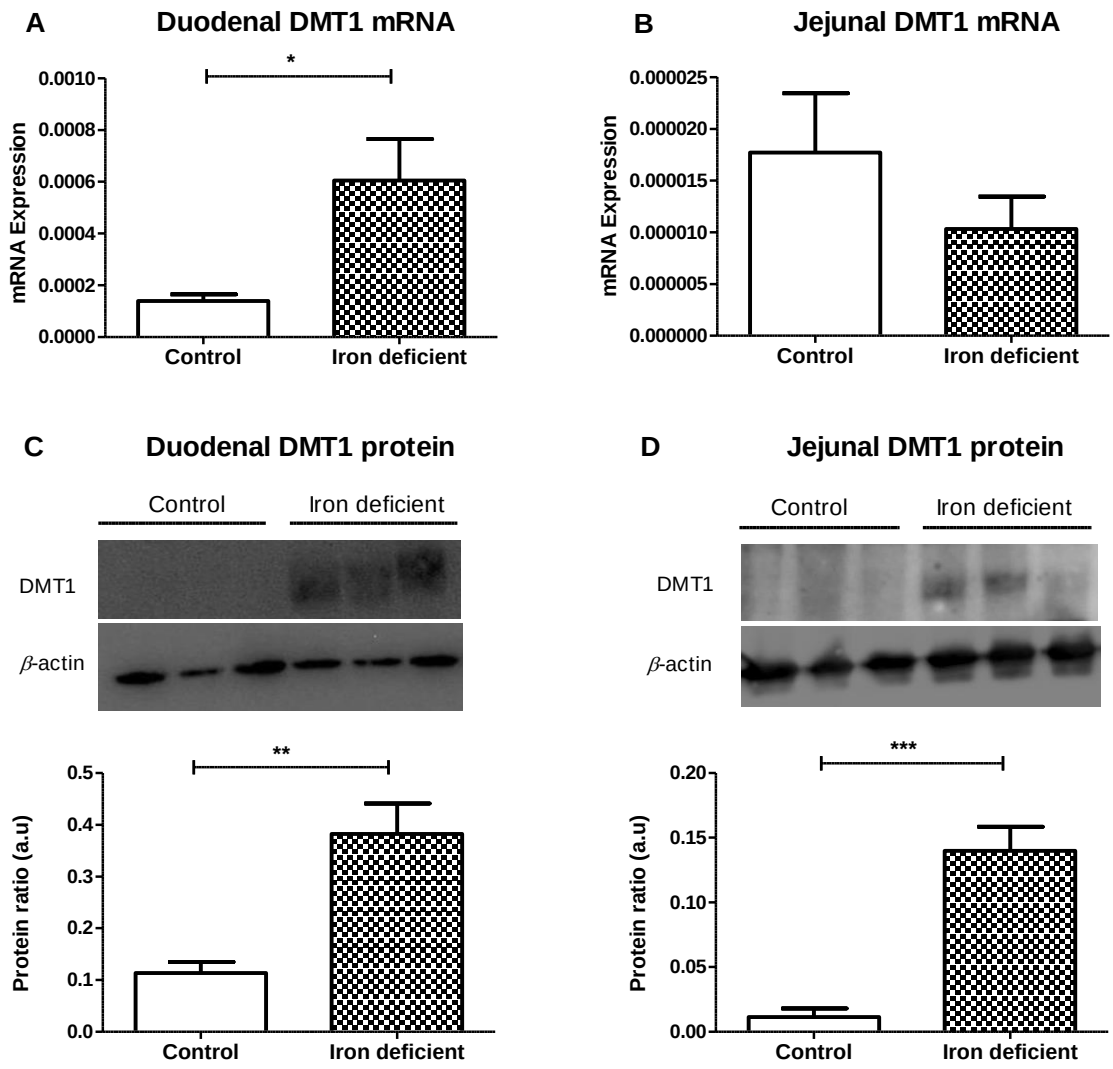


**Figure 5.11. DMT1 levels are increased in the proximal small intestine of rat by iron deficiency**. RT-PCR quantification of mRNA levels of DMT1 (A and B). Duplicate PCR reactions were performed for each sample and the mRNA expression of DMT1 is given as the ratio of DMT1 to *β*-actin. Representative Western blot image and quantification of DMT1 protein levels in the duodenum (C) and jejunum (D) of control and iron deficient animals. The abundance of DMT1 protein is given as the ratio of DMT1 band density to *β*-actin, expressed in arbitrary units (a.u). An unpaired t-test was used to compare results between groups (n= 4-6). ***P*<0.01, ****P*<0.001.

Finally, to test if diet-induced iron deficiency impacts other nutrient absorption pathways in the duodenum and jejunum, mRNA and protein levels of the $Na^+$-dependent glucose cotransporter, SGLT1, and the facilitative glucose transporter, GLUT2, were investigated. The results showed that diet-induced iron deficiency had no effect on the mRNA (Figure 5.12) and protein levels (Figure 5.13) of these glucose transporters.

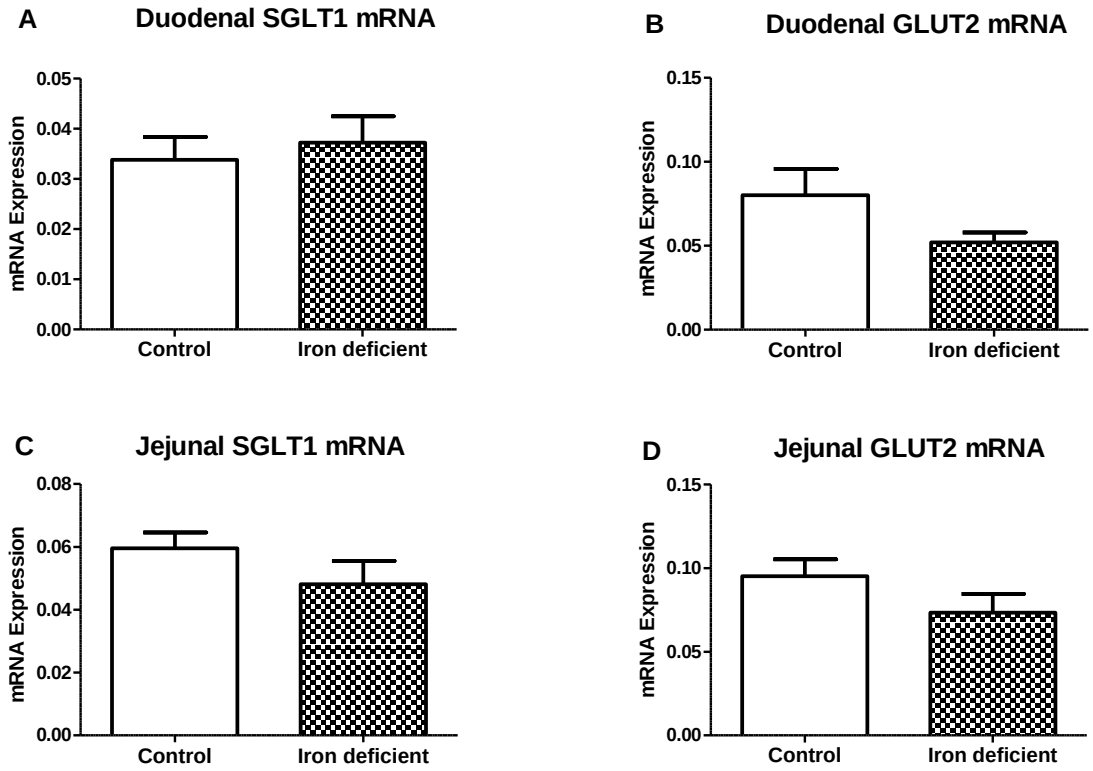


**Figure 5.12. Intestinal glucose transporter mRNA levels are unaffected by iron deficiency**. RT-PCR quantification of mRNA levels of SGLT1 and GLUT2 was assessed by RT-PCR in the duodenum (A and B) and jejunum (C and D) of control and iron deficient animals. Duplicate PCR reactions were performed for each sample and the mRNA expression of SGLT1 and GLUT2 is given as the ratio of these transporters to *β*-actin. An unpaired t-test was used to compare the differences between groups (n=5-6).

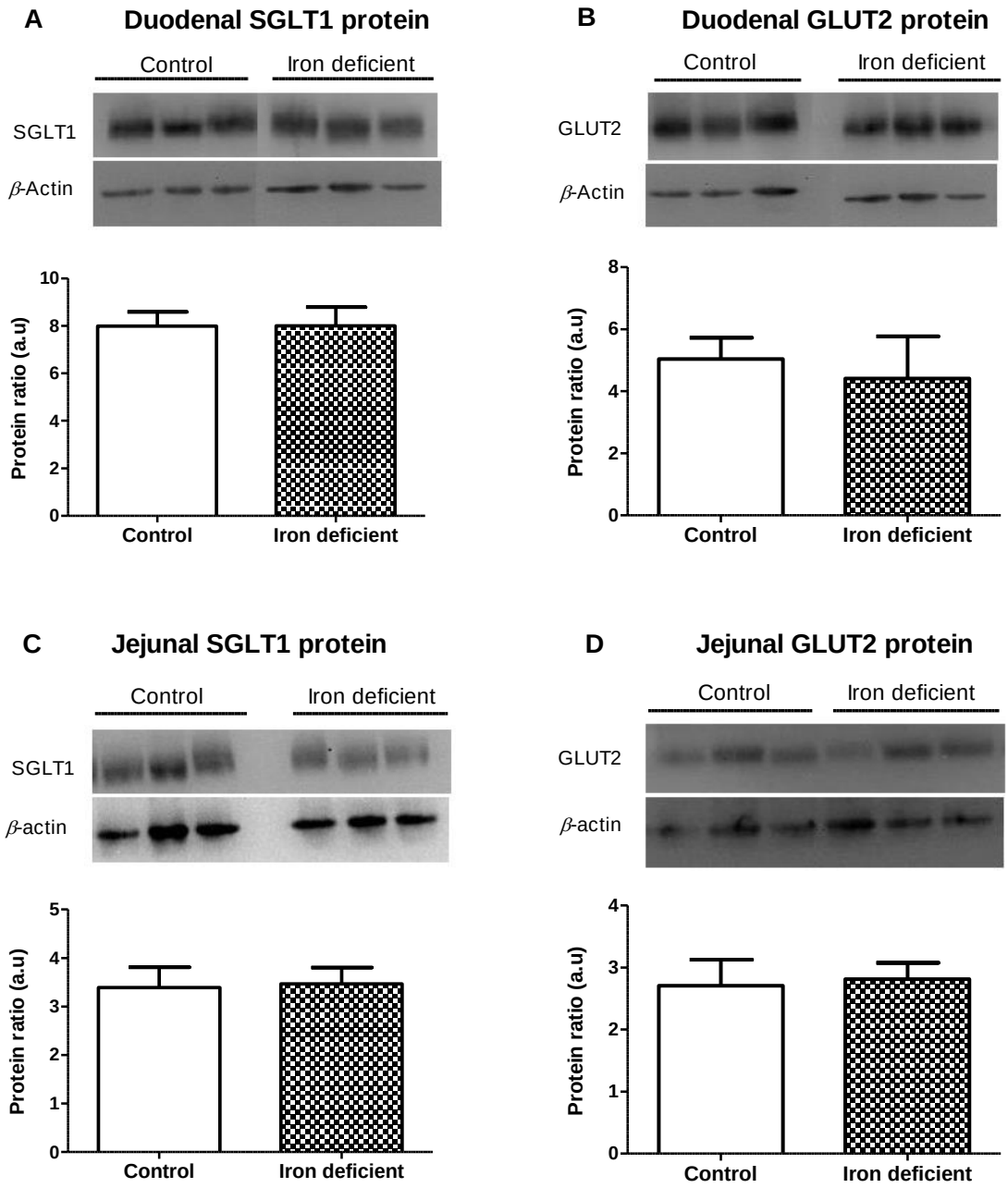


**Figure 5.13. Intestinal glucose transporter protein levels are unaffected by iron deficiency**. Representative Western blot image and quantification of SGLT1 and GLUT2 protein levels in the duodenum (A and B) and jejunum (C and D) of control and iron deficient animals. The abundance of SGLT1 and GLUT2 protein is given as the ratio of the band density of each protein to *β*-actin, expressed in arbitrary units (a.u). An unpaired t-test was used to compare the differences between groups (n=5-6).

## 5.4. Discussion

In this study, the effect of diet-induced iron deficiency on the mechanisms of phosphate transport in the rat duodenum and jejunum was investigated, and phosphate uptake experiments in iron deficient mice were used to determine the role of NaPi-IIb. Interestingly, while NaPi-IIb function was unaffected by diet-induced iron deficiency, the results demonstrated that the mechanisms underlying the inhibition of phosphate absorption in response to iron deficiency are different in the duodenum and jejunum of rats. In iron deficiency, the $Na^+$-independent phosphate transport pathway was inhibited in the duodenum by a mechanism likely involving DMT1 and claudin 3, while the NHE3-regulated paracellular pathway for phosphate transport appears to be the mechanism mainly affected in the jejunum.

In agreement with the evidence from early studies investigating intestinal phosphate absorption [46,126,240] and more recent findings [45,246,318], it is now recognised that in the rat and human small intestine, NaPi-IIb likely plays a minor role in intestinal phosphate absorption when physiological phosphate concentrations are present in the intestinal lumen. Even though diet-induced iron deficiency has previously been reported to downregulate the expression of the NaPi-IIb gene in the duodenum [346,347], evidence that very low levels of NaPi-IIb are present in this segment (discussed in chapter 3) suggests that this transporter may not be responsible for the significantly inhibited intestinal phosphate absorption caused by iron deficiency in rats. Consistent with this suggestion, the inhibition of phosphate absorption by iron deficiency in the rat duodenum and jejunum was unaffected by PFA. In addition, in the mouse ileum where NaPi-IIb is most highly expressed and plays a major role in phosphate transport in the

presence of 10 mM luminal phosphate (discussed in chapter 3), transepithelial phosphate transport or NaPi-IIb protein levels was not affected by iron deficiency. Like the rat duodenum, the jejunum of mice is known to have low levels of NaPi-IIb, and in this segment of mice, diet-induced iron deficiency was demonstrated to downregulate NaPi-IIb in the current study. Interestingly, the downregulation of NaPi-IIb in the proximal small intestine of mice in response to iron deficiency had no impact on transepithelial phosphate transport. Taken together, these findings suggest that iron deficiency-induced downregulation of NaPi-IIb has no physiological relevance in intestinal segments where this protein is undetected or lowly expressed (e.g. duodenum of rat and the proximal small intestine of mice). These findings confirm that the inhibition of phosphate absorption by diet-induced iron deficiency does not involve NaPi-IIb. However, the significantly downregulated NaPi-IIb mRNA levels in the duodenum of rats in response to iron deficiency may prevent any potential compensation by the NaPi-IIb-mediated transcellular phosphate absorption pathway in this segment.

Recent reports indicate that NHE3 plays a key role in mediating intestinal phosphate absorption in rats [77,247], and this role of NHE3 has been demonstrated to involve changes in intracellular pH and TEER, both affecting paracellular phosphate transport [77]. In the current study, the contribution of the NHE3-regulated paracellular phosphate transport mechanism in response to iron deficiency was investigated. The finding that the NHE3-regulated paracellular pathway for phosphate transport has no contribution to phosphate absorption in the duodenum (discussed in chapter 3), suggests that the effect of iron deficiency on phosphate absorption in this segment is unlikely to involve NHE3. Consistent with this hypothesis, the inhibition of phosphate absorption by iron deficiency was

unaffected by tenapanor in the duodenum. In contrast, using tenapanor, the finding that iron deficiency abolished the significant NHE3-regulated paracellular phosphate transport pathway in the jejunum, suggests that this phosphate transport mechanism is inhibited at least in part by iron deficiency in this segment. Based on this finding, the fact that iron deficiency had no effect on either the mRNA or protein levels of NHE3 suggests that rather than expression levels, iron deficiency impacts the activity of this transporter in the jejunum. Taken together, while the NHE3-regulated paracellular pathway for phosphate transport appears to be inhibited by iron deficiency in the jejunum, the inhibition of phosphate absorption in the duodenum does not involve this transport pathway.

The $Na^+$-independent phosphate transport pathway is now known to be the predominant pathway in the duodenum (discussed in chapter 3), and this pathway is suggested to involve a non-saturable concentration-dependent phosphate transport process, which is a key feature of simple diffusion [252]. Given that the proximal small intestine is known to be a leaky epithelium, with high permeability to ions and water [252,359,360], it is likely that the $Na^+$-independent phosphate absorption is mediated by paracellular diffusion. In the current study, to investigate if iron deficiency affects this $Na^+$-independent mechanism, phosphate uptake was conducted using a $Na^+$-free buffer containing a phosphate concentration of 10 mM to favour passive diffusion. As described in section 4.3.2, in the duodenum, approximately 70% of phosphate transport was inhibited by iron deficiency *in vitro*, this being similar to the proportion of phosphate transport mediated by the $Na^+$-independent pathway. To support the speculation in the previous chapter, the findings of the current chapter indicated that iron deficiency inhibits the $Na^+$-independent phosphate transport pathway in the duodenum.

However, the result of the $Na^+$-free uptake experiment in the jejunum did not show the same effect as observed in the duodenum. The fact that phosphate uptake in the jejunum of control and iron deficient animals were not statistically different when $Na^+$ was removed from the uptake buffer supports the hypothesis that iron deficiency may be affecting a $Na^+$-dependent phosphate transport mechanism, suggested to be the NHE3-regulated paracellular pathway. Nevertheless, evidence from this study suggests that the inhibition of jejunal phosphate absorption by iron deficiency is not entirely due to changes in NHE3-regulated paracellular phosphate transport. A small proportion of the $Na^+$-independent phosphate transport pathway appears to be inhibited by iron deficiency in the jejunum. Taken together, these findings suggest that iron deficiency inhibits paracellular phosphate transport through the $Na^+$-independent pathway in the duodenum, and via both NHE3-regulated and $Na^+$-independent pathways in the jejunum.

Previous studies have shown that similar to phosphate absorption, intestinal $Ca^{2+}$ absorption in the duodenum and jejunum is mediated by multiple transport mechanisms [361,362]. Thus, to understand phosphate absorption clues can be taken from the cellular mechanisms underlying intestinal $Ca^{2+}$ absorption. While transcellular $Ca^{2+}$ absorption has been studied extensively, paracellular $Ca^{2+}$ transport mechanisms are now gaining prominence. Transcellular and paracellular $Ca^{2+}$ transport mechanisms are known to occur in both the duodenum and jejunum, however, the relative contribution of these pathways in each segment varies depending on dietary $Ca^{2+}$ content [363]. In the duodenum, during dietary $Ca^{2+}$ restriction, the transcellular pathway contributes approximately 80%, while under high dietary $Ca^{2+}$ conditions, paracellular $Ca^{2+}$

transport accounts for more than 90% of total transepithelial $Ca^{2+}$ absorption [363]. Similarly, in the jejunum, paracellular $Ca^{2+}$ absorption accounts for more than 80% of total $Ca^{2+}$ absorption under normal or high dietary $Ca^{2+}$ conditions [363]. Therefore, analogous to $Ca^{2+}$ absorption, a drive towards understanding the relative contribution of these pathways to intestinal phosphate absorption under different dietary conditions, and the mechanism(s) involved in paracellular phosphate absorption, is underway. It is now recognised that pore-sealing claudins are involved in the control of intestinal membrane permeability by virtue of their role in maintaining tight junction integrity, and therefore, affect the paracellular diffusion of ions [277]. Consequently, differences in the regional expression pattern, together with alterations in the levels of these claudins may have an impact on paracellular phosphate transport in defined segments of the intestine. In keeping with previous reports [267], the results of this study demonstrated that pore-sealing claudins, in particular, claudin 3, were higher in the duodenum than jejunum and that this in combination with an absence of NaPi-IIb, may explain the lower levels of transepithelial phosphate absorption seen in this region. In addition, the inhibitory effect of diet-induced iron deficiency on duodenal phosphate absorption may be a consequence of increased claudin 3 protein levels sealing the paracellular pathway. Interestingly, $1,25(OH)_2D_3$, the main systemic regulator of intestinal phosphate absorption has been reported to reduce claudin 3 expression levels [285], although the functional consequence of this on paracellular phosphate transport has not been investigated. It is also of interest that in addition to the well-known effect of $1,25(OH)_2D_3$ on the transcellular $Ca^{2+}$ transport pathway [364], the hormone also affects the expression of the pore-forming claudins, 2, 12 and 15 [257,294], which mediate paracellular $Ca^{2+}$ transport. However, although there is evidence for the role of $1,25(OH)_2D_3$ in the

regulation of paracellular $Ca^{2+}$ and phosphate transport processes [257,364], the results of this study indicate that the upregulation of duodenal claudin 3 in response to diet-induced iron deficiency is not associated with changes in $1,25(OH)_2D_3$ or its regulators, PTH and FGF-23.

Ideas as to the possible cellular mechanism that may be involved in the inhibition of paracellular phosphate absorption by diet-induced iron deficiency can be taken from evidence linking NHE3 and hepcidin-enhanced duodenal $Ca^{2+}$ absorption [365]. In β-thalassemic mice, iron hyperabsorption via DMT1 was hypothesised to increase the $H^+$ concentration within the enterocyte, resulting in reduced transcellular $Ca^{2+}$ absorption [365]. Hepcidin administration in these mice decreased iron hyperabsorption and subsequently enhanced transcellular $Ca^{2+}$ transport [365]. The authors reported that although paracellular $Ca^{2+}$ absorption *per se* was unaffected, the effect of iron hyperabsorption on mineral transport was not restricted to the transcellular $Ca^{2+}$ pathway since paracellular absorption of $Zn^{2+}$ was also inhibited in β-thalassemic mice [365,366]. In addition, tenapanor was shown to abolish the hepcidin enhanced transcellular $Ca^{2+}$ transport in these mice, further confirming that changes in $H^+$ concentration within the enterocyte affect mineral absorption [365]. Importantly, tenapanor administration has recently been demonstrated to inhibit intestinal phosphate absorption in rats fed a normal phosphate diet via a pH-mediated inhibition of the paracellular pathway [77]. The current study, and previous studies in both rodents and Caco-2 cells, consistently show that duodenal DMT1 mRNA and protein levels are upregulated under iron deficient conditions [356,367]. Since DMT1 is an $H^+$-coupled iron cotransporter, its upregulation by iron deficiency may result in intracellular accumulation of $H^+$ within the enterocyte and subsequent intracellular acidification [356–358]. Based on

these findings, it is hypothesised that in iron deficiency, this DMT1-mediated increase in intracellular acidification stimulates the upregulation of claudin 3 protein levels within the duodenal enterocyte tight junctions, leading to the sealing of the paracellular pathways and the subsequent inhibition of paracellular phosphate absorption in this segment.

The potential intracellular signalling mechanisms underlying this hypothesised effect of intracellular acidification on claudin 3 are unknown but may involve the regulatory role of intracellular protein kinases on tight junctions. PKA and PKC have both been reported to control paracellular permeability by phosphorylating pore-sealing claudins within the tight junctions of enterocytes [265]. PKA–mediated phosphorylation of claudin 3 has been shown to affect its anchoring to tight junctions [296], while PKC-δ-induced phosphorylation of claudin 4 has been demonstrated to facilitate the assembly of this pore-sealing claudin into intestinal epithelial tight junctions [297]. However, to date, there is no evidence reporting that iron deficiency or intracellular acidification of the enterocyte affects PKA or PKC levels or activity. Interestingly, the previously reported finding that metabolic acidosis upregulates claudin 3 mRNA expression [368] suggests that increased intracellular $H^+$ may directly alter claudin 3 gene transcription.

Although it is speculated in the current study that DMT1-induced changes in intracellular pH result in claudin 3 upregulation in the duodenum, this mechanism is unlikely to explain the inhibition of transepithelial phosphate absorption in the jejunum of iron deficient rats. Even though a significant upregulation of DMT1 protein in jejunum was observed in response to iron deficiency in the current study, relatively low levels of DMT1 mRNA and protein were detected in this segment compared to the duodenum. Therefore, it is unlikely that DMT1 will have

any significant impact on intracellular pH in the jejunum. Recent findings in the jejunum have shown that tenapanor-induced increase in intracellular $H^+$ did not affect the protein levels or trafficking of claudin 3 and that the inhibition of phosphate absorption may instead be due to a pH-sensitive conformational change in the tight junction [77]. Thus, the inhibition of phosphate absorption that was observed in the jejunum in iron deficiency may be a result of dynamic remodelling or enhanced stability of claudin 3 protein already present within the tight junction (reviewed in [283]), rather than the increase in expression levels seen in the duodenum. Additionally, recent findings have shown that the $H^+$-coupled peptide cotransporter 1 (PEPT1), which is localised on the apical membrane throughout the rat small intestine [369], is also involved in intestinal iron absorption [370]. Therefore, it is possible that this transporter is also upregulated during diet-induced iron deficiency, and that this leads to intracellular $H^+$ accumulation as documented for DMT1 and therefore, potentially affects the expression or dynamic remodelling of claudin 3. While changes in claudin 3 mRNA and protein levels in the duodenum are responsible for the inhibition of paracellular phosphate absorption in this segment, this was not seen in the jejunum and thus, may explain why there was a less striking effect of diet-induced iron deficiency in the jejunum.

Alternatively, the inhibition of phosphate absorption in the duodenum and jejunum may be independent of changes in intracellular pH. Recent evidence indicates that intracellular $Zn^{2+}$ depletion decreases claudin 3 gene transcription and protein levels [286]. Therefore, because DMT1 has also been demonstrated to mediate BBM $Zn^{2+}$ transport [358], it is plausible that DMT1-induced increase in intracellular $Zn^{2+}$ levels in enterocytes may cause the upregulation of claudin 3

expression in the duodenum or changes in tight junction permeability in the jejunum. In addition, increased intracellular iron levels have also been linked to reduced TEER and a consequent increase in tight junction permeability, an effect reported to be a result of claudin 4 internalisation due to apoptosis and necrosis [355]. Therefore, it is possible that intracellular iron levels of duodenal and jejunal enterocytes may directly affect the localisation of pore-sealing tight junction proteins, leading to changes in the paracellular permeability of these intestinal segments to phosphate.

### 5.5. Conclusion

In summary, this is the first study to show that diet-induced iron deficiency inhibits transepithelial phosphate absorption in the duodenum and jejunum of rats via mechanisms that likely involve the paracellular pathway. The findings of this study suggest that in the duodenum, a DMT1-induced increase in intracellular $H^+$ concentration enhances claudin 3 levels in the tight junction and that this mechanism may be responsible for the inhibition of paracellular phosphate absorption. In the jejunum, the inhibition of NHE3 activity by iron deficiency may result in a pH-sensitive conformational change in the tight junction, leading to the inhibition of paracellular phosphate transport. A detailed understanding of the intracellular signalling pathways involved in regulating the conformation and protein levels of claudin 3 may be beneficial in the identification of novel therapeutic targets for the management of hyperphosphataemia in CKD and patients with dysfunctional mineral metabolism.

# Chapter Six

## 6.0. General discussion

### 6.1. Aims of the experiments described in this thesis

Early studies investigating the mechanisms of intestinal phosphate absorption identified two transport mechanisms; a passive paracellular process, mediated by the simple diffusion of phosphate and an active transcellular mechanism, known to be $Na^+$-dependent and regulated by $1,25(OH)_2D_3$ [46,126,239–241,244,371–373]. Following the discovery and characterisation of NaPi-IIb in 1998 [40], this protein was thought to be the rate-limiting step in intestinal phosphate absorption [353] and using nicotinamide, it was subsequently targeted to reduce intestinal phosphate absorption in CKD patients [249]. However, emerging clinical data using a potent NaPi-IIb inhibitor, which was effective in rats [76], but not in humans [318], indicated that NaPi-IIb might not be the major phosphate transporter in humans. Interestingly, recent findings using tenapanor demonstrated a vital role for NHE3 in mediating intestinal phosphate absorption in rats and humans, but not in mice [77]. Because of these discrepancies in the efficacy of both NaPi-IIb and NHE3 inhibitors on intestinal phosphate absorption in mice, rats and humans, the suitability of rodents as experimental models to study intestinal phosphate absorption needed further clarification. Therefore, one of the aims of the experiments described in this thesis was to understand the mechanisms of intestinal phosphate absorption in mice, rats and humans.

Secondly, recent reports have shown that alterations in serum iron levels affect bone mineral metabolism in rodents, healthy individuals and in patients with genetic phosphate disorders like ADHR [337–341,374–376]. Although changes in $Ca^{2+}$ absorption in iron deficiency have been reported in the small intestine of rats [338,349], there are conflicting reports concerning intestinal phosphate absorption [349,377]. Therefore, the other aim of the experiments described in this thesis was to

investigate the effect of diet-induced iron deficiency on phosphate homeostasis, with a particular focus on the effect of iron deficiency on intestinal phosphate absorption and the underlying mechanisms.

### 6.2. Mechanism of intestinal phosphate absorption in mice, rats and humans

In mice, the phosphate uptake data confirmed previously reported findings [38,39] that the ileum is the major segment responsible for NaPi-IIb-mediated phosphate absorption, and the higher capacity of phosphate absorption in this segment in comparison to the jejunum was consistent with the expression levels of NaPi-IIb. Additionally, complete inhibition of NaPi-IIb by 100 µM NTX9066 or loss of NaPi-IIb in knock-out animals [77] resulted in 85-90% inhibition of transepithelial phosphate absorption in the ileum, with NHE3-regulated paracellular phosphate absorption mediating the remaining 10-15%. Unlike the mouse ileum, the proximal small intestine is characterised by lower levels of NaPi-IIb and higher levels of NHE3. Even with the high levels of NHE3 in the proximal small intestine of mice, its contribution to transepithelial phosphate absorption in this segment was less than 10% of total phosphate absorption. Based on this finding, it appears that phosphate absorption in the proximal small intestine of mice is mainly mediated by NaPi-IIb as its low levels are consistent with low phosphate transport in this segment. Although the contribution of PiT-1 protein to phosphate absorption in mice was not investigated, the similar expression profile of this protein in the proximal and distal small intestinal segments is not consistent with the different transport capacities between these segments. These findings suggest that PiT-1 plays a minor role in intestinal phosphate absorption in mice. Based on these findings, phosphate absorption in the mouse small intestine is

mainly mediated by NaPi-IIb, with PiT-1 and NHE3-regulated paracellular transport playing only a minor role (Figure 6.1).

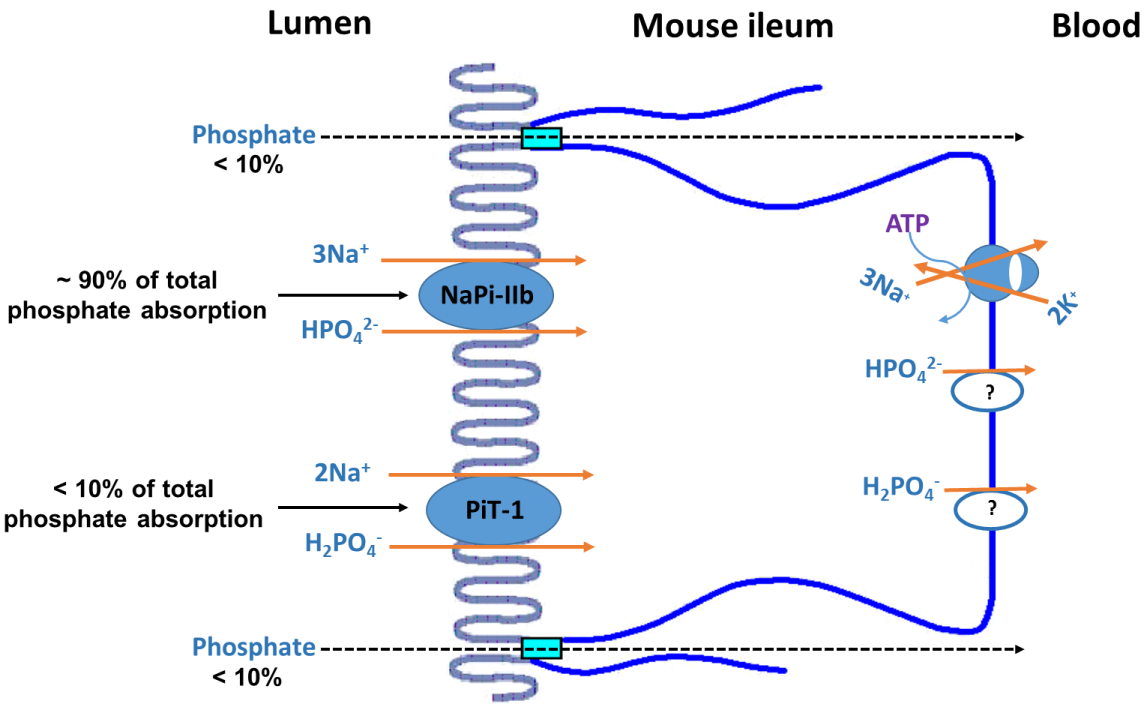


**Figure 6.1. Mechanism of phosphate absorption in the mouse ileum**. Under normal dietary phosphate condition, phosphate absorption is mainly mediated by NaPi-IIb, while PiT-1 and the paracellular pathway play a small role.

Interestingly, even though the findings of this study indicate that NaPi-IIb is the major phosphate transporter in the mouse small intestine, there is evidence suggesting that NaPi-IIb is not the predominant phosphate transport pathway under physiological conditions [31,145,251,321]. Most of the studies speculating that NaPi-IIb-mediated phosphate transport pathway in mice is not the major pathway put this hypothesis forward following the analysis of the levels of faecal phosphate in NaPi-IIb knock-out mice without considering the potential contribution of phosphate secretory pathways in the gastrointestinal tracts [322–326] and phosphate absorption in the colon [239]. It is possible that phosphate transport in the large intestine is mediated by passive paracellular diffusion, and this may potentially compensate for the loss of NaPi-IIb-mediated phosphate transport in the small intestine of NaPi-IIb knock-out mice. Therefore, the speculation against a predominant role for NaPi-IIb in the small intestine requires further clarification. Future studies are required to investigate the contribution of gastrointestinal phosphate secretion to faecal phosphate levels. This will provide more insights into the validity of the analysis of faecal phosphate levels as a measure of intestinal phosphate absorption. To investigate the rate of gastrointestinal phosphate secretion, $^{33}$P-labelled phosphate solution could be injected intravenously into NaPi-IIb knock-out and wild-type mice, and the levels of $^{33}$P should be measured in intestinal content or faeces obtained from these mice. Additionally, the contribution of passive paracellular phosphate transport in the large intestine of NaPi-IIb knock-out mice should also be investigated to determine the contribution of the large intestine to overall phosphate absorption. This could be done by oral gavage of a phosphate load labelled with $^{33}$P, followed by measuring the amount of $^{33}$P transferred into the circulation at different time points. Using the documented duration of chyme in different intestinal segments

[243], the rate of absorption of phosphate in the large intestine can be identified and its contribution to total phosphate absorption could be determined.

In rats, the expression of the transcellular phosphate transporters, NaPi-IIb and PiT-1, was highest in the second part of the proximal small intestine, the jejunum, as previously reported by Giral and colleagues [17]. In addition to previous findings in our laboratory [45], the results of this study showed that the jejunum has the highest capacity for phosphate transport and therefore, it is the major segment responsible for intestinal phosphate absorption in rats. Unlike in mice, phosphate absorption in the rat proximal small intestine is known to be mediated by both $Na^+$-dependent and $Na^+$-independent phosphate transport mechanisms. Evidence from the regional profiling of rat NaPi-IIb and PiT-1 in this study indicated that in comparison to the jejunum, the duodenum is characterised by very low levels of these $Na^+$-dependent phosphate transporters. The fact that duodenal NaPi-IIb and PiT-1 are very low indicates that these transporters play no role in duodenal phosphate absorption in rat. In contrast, higher levels of another $Na^+$-dependent BBM transporter involved in paracellular phosphate absorption, NHE3, was detected in the duodenum.

The uptake data of this study showed that the $Na^+$-dependent phosphate transport pathway in the duodenum mediates approximately 25% of total phosphate transport, with phosphate uptake via the NHE3-regulated pathway accounting for approximately 10% of this 25% of total phosphate transport. Since NaPi-IIb and PiT-1 play no role in this segment, an unknown $Na^+$-dependent phosphate transporter is likely responsible for the remaining 15% of phosphate absorption via the $Na^+$-dependent pathway. Using uptake buffer containing 50 µM phosphate, Candeal and colleagues recently characterised an unknown PFA-

sensitive $Na^+$-dependent phosphate transporter in the proximal small intestine that preferentially mediates the transport of monovalent phosphate and its transport activity was shown to be higher at low luminal pH [146]. Since PFA inhibited less than 5% of duodenal phosphate uptake in the current study (using 10 mM phosphate), it is unlikely that this recently characterised and yet unknown $Na^+$-dependent phosphate transporter is responsible for the remaining 15% of phosphate absorption via the $Na^+$-dependent pathway. Moreover, previous findings in our laboratory [45] and the results of the current study indicated that the $Na^+$-independent phosphate transport pathway is the major pathway responsible for duodenal phosphate absorption, accounting for approximately 75% of overall phosphate transport (Figure 6.2A)

In comparison to the duodenum, the $Na^+$-independent pathway mediated approximately 60% of the total phosphate transport in the jejunum, with the remaining 40% mediated by the $Na^+$-dependent pathway (Figure 6.2B). NHE3 and NaPi-IIb are the transporters responsible for $Na^+$-dependent phosphate transport in the jejunum, with NHE3 mediating more than 25% of total phosphate absorption, while NaPi-IIb mediates less than 15% (Figure 6.2B). While the mechanism underlying the $Na^+$-dependent phosphate absorption in the jejunum involves NaPi-IIb and NHE3, the physiological mechanism or the transporter responsible for the predominant $Na^+$-independent pathway in both the duodenum and jejunum is yet to be identified.

Early studies investigating intestinal phosphate absorption demonstrated a significant concentration-dependent passive transport process in the duodenum and jejunum (reviewed in [252]). There are however conflicting reports as to whether this passive phosphate transport process is $Na^+$-dependent [46,240] or $Na^+$-

independent [126,245]. While a $Na^+$-dependent NHE3-regulated passive paracellular phosphate transport mechanism has been reported in the jejunum [77], previous *in vivo* data in the duodenum showing similar amounts of transepithelial phosphate transport in the presence or absence of $Na^+$ [45] suggests that the passive phosphate transport process in the duodenum is $Na^+$-independent. In keeping with this suggestion, it is worth noting that no significant NHE3-regulated passive paracellular phosphate transport was seen in the duodenum in the current study, while both the NHE3-regulated and the $Na^+$-independent passive phosphate transport pathways were observed in the jejunum.

The passive $Na^+$-independent phosphate transport pathway has been speculated to be mediated by paracellular diffusion [45,319]. The finding of this study supports the hypothesis that diet-induced iron deficiency results in the inhibition of $Na^+$-independent phosphate transport in the duodenum of rats, likely due to claudin 3 upregulation. Increased levels of this claudin have been reported to reduce the paracellular permeability of the small intestine to all ions [277]. However, it is also possible that a $Na^+$-independent transcellular phosphate transporter exists in the small intestine [45,319,330]. Future studies are required to clarify the exact mechanism underlying the $Na^+$-independent phosphate transport pathway in the duodenum and jejunum of rats under physiological luminal phosphate concentration. In summary, the mechanism of duodenal phosphate absorption is predominantly mediated by a $Na^+$-independent paracellular phosphate transport process, with a smaller role for a $Na^+$-dependent phosphate transport process that is not entirely mediated by NaPi-IIb, PiT-1 and NHE3. However, in the jejunum, phosphate absorption is mediated by a NaPi-IIb pathway, an NHE3-regulated paracellular pathway, and a $Na^+$-independent paracellular pathway,

with the latter demonstrated in the current study to have the highest contribution (Figure 6.2B).

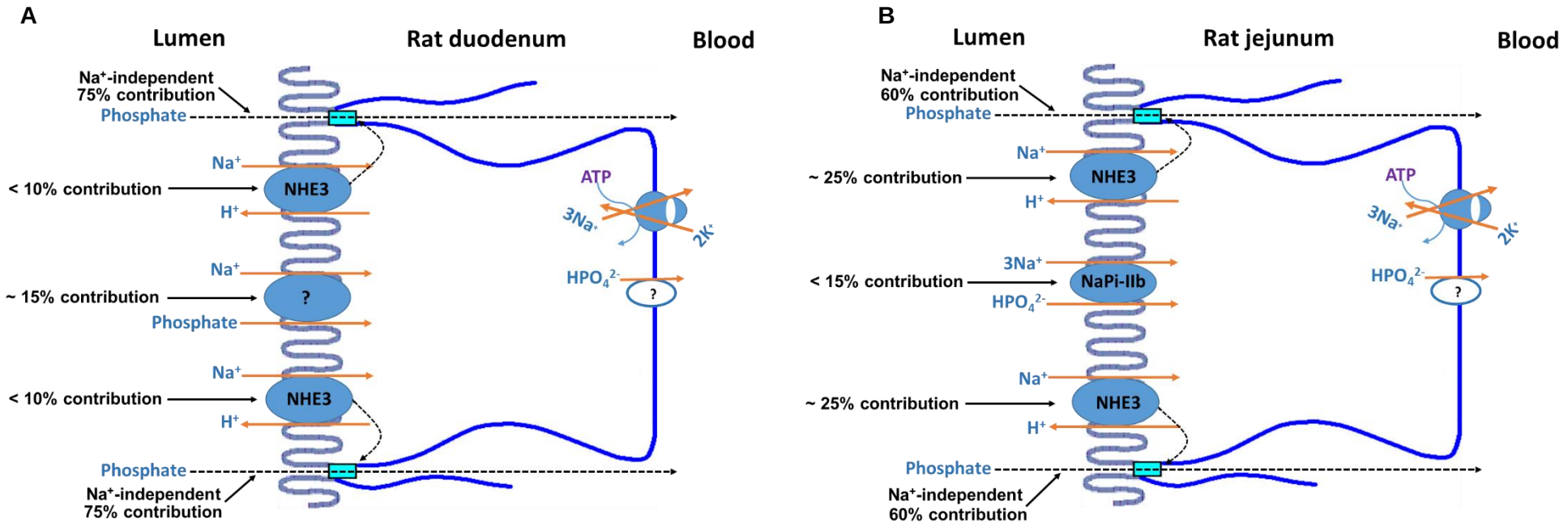


**Figure 6.2. Mechanism of phosphate absorption in the proximal small intestine of rats**. (A) Phosphate absorption in the duodenum is predominantly mediated by the $Na^+$-independent paracellular pathway (~ 75%), with less than 10% of phosphate absorption mediated by NHE3 and a yet to be identified (?) $Na^+$-dependent phosphate transporter mediating ~ 15%. (B) Phosphate absorption in the jejunum is predominantly mediated by a $Na^+$-independent (~ 60%) and an NHE3-regulated (~ 25%) paracellular pathway, with NaPi-IIb playing a minor role.

Unlike rodents, the segmental profile of NaPi-IIb in the human small intestine showed that the duodenum exhibits the highest levels of this active phosphate transporter. Interestingly, the similar segmental expression of NHE3 in rats and humans suggests that the rat is a better model than the mouse to study NHE3-regulated paracellular phosphate transport, which has been shown to be a key phosphate transport pathway in humans [77,247]. Like rodents, intestinal phosphate absorption in humans is thought to be mediated by both NaPi-IIb-mediated active transport and concentration-dependent passive phosphate transport. The functional profile of phosphate absorption in humans has been reported to be similar to that of rats, mainly occurring in the duodenum and jejunum, with little absorption seen in the ileum [39,45]. Although previous studies in humans have not directly compared the capacity of phosphate absorption between the duodenum and jejunum, there is evidence that the capacity of phosphate transport in the jejunum is high [46,320,378]. Based on this evidence, in addition to its relatively long length, the jejunum has been speculated to absorb the majority of dietary phosphate [379]. Interestingly, the segmental profile of NaPi-IIb observed in this study showing that NaPi-IIb levels are highest in the duodenum could explain the lack of effect of NaPi-IIb inhibitors in inhibiting overall phosphate absorption in humans [318]. This may be because of the relatively shorter length of the duodenum and consequently shorter transit time of chyme along this segment [243]. In addition, it may also be because of the fact that normal phosphate concentration in the diet is considerably higher than the $K_m$ of NaPi-IIb. In keeping with this suggestion, studies investigating the mechanism of phosphate absorption in patients with CKD have revealed that this process is mediated by an active transcellular pathway that becomes saturated when luminal phosphate concentration exceeds 2 mM, and a passive phosphate transport pathway that increases linearly with

luminal phosphate concentration [371]. Because the concentration of phosphate in the lumen of the small intestine of these patients ranges from 3.0-12.2 mM [371], it is very likely that passive phosphate transport pathway is mainly responsible for phosphate absorption in the human small intestine.

There is evidence that this passive phosphate transport process in humans is dependent on intestinal luminal $Na^+$ concentration [46,77]. Consistent with this evidence, recent cell culture studies and clinical data have shown that NHE3 inhibition leads to a reduction in passive paracellular phosphate transport [77,247]. This transport pathway is speculated to be particularly present in the jejunum of humans, a segment demonstrated in this study to have the highest levels of NHE3. Although NaPi-IIb-mediated active transport and NHE3-regulated paracellular pathway for phosphate transport have previously been studied in humans, there is limited information concerning the role of the $Na^+$-independent pathway. *In vitro* phosphate uptake studies using human Caco-2 BBE cells [246] suggest that the $Na^+$-independent transport pathway exhibits similar concentration-dependent passive phosphate transport characteristics like the $Na^+$-independent passive transport mechanism reported in the human small intestine *in vivo* [245]. The exact contribution of the $Na^+$-independent phosphate transport pathway in humans remains to be determined. In summary, NaPi-IIb plays a small role in phosphate absorption in the human small intestine under normal luminal phosphate concentration, with both the NHE3-regulated and $Na^+$-independent passive paracellular transport pathway likely playing a major role (Figure 6.3).

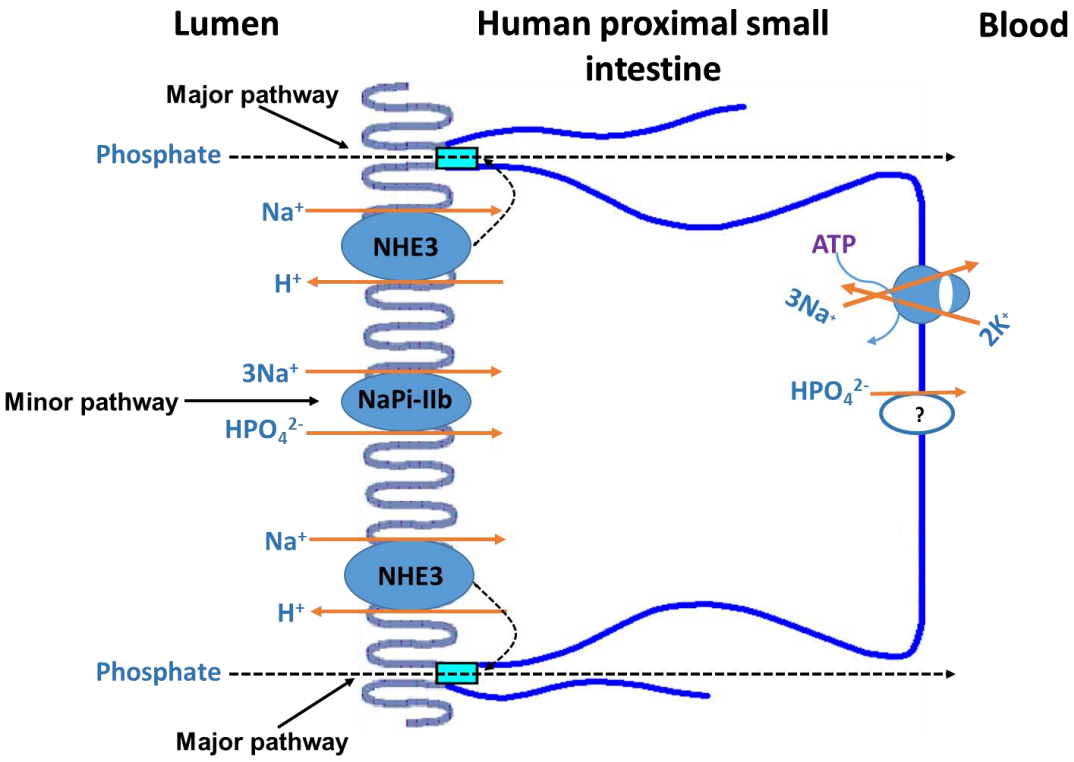


**Figure 6.3. Mechanism of phosphate absorption in the human small intestine**. The $Na^+$-independent and NHE3-regulated paracellular pathway for phosphate transport is the major pathway in humans, with NaPi-IIb playing a minor role.

### 6.3. Effect of diet-induced iron deficiency on phosphate homeostasis

The most striking finding of this study was that diet-induced iron deficiency inhibits phosphate absorption in the duodenum and jejunum of normal rats, with a more prominent effect in the duodenum. The known systemic regulators of phosphate homeostasis played no role in the inhibition of phosphate absorption by iron deficiency caused by a 2-week administration of an iron deficient diet. Although this is the first study showing that diet-induced iron deficiency significantly inhibits intestinal phosphate absorption, there was no impact on phosphate balance. This may be because the kidney, which is known to be the major regulator of phosphate homeostasis under physiological conditions, could adjust phosphate excretion to match the amount of phosphate absorbed from the diet. In line with this suggestion, a moderate decrease in renal phosphate excretion was observed, which was consistent with a modest increase in renal NaPi-IIa levels seen in this study. Moreover, the bone phosphate pool is also known to contribute to the maintenance of phosphate balance, and since the dietary iron regime lasted for only 2 weeks, this homeostatic mechanism may have contributed to the unchanged serum phosphate levels in response to diet-induced iron deficiency observed in the current study. In comparison, chronic iron deficiency in humans [337,380] and severe iron deficiency in rats following a 4-week administration of an iron deficient diet [338] have been associated with loss of bone mineral and osteoporosis. This effect of iron deficiency on bone health may be a consequence of increased osteoclast activity to break down bone minerals in order to release phosphate into the circulation, in response to reduced intestinal phosphate absorption. Although previous findings in neonatal mice, children, and patients with genetic mineral disorders and CKD have linked iron deficiency with the regulators of phosphate homeostasis [305–308,310,312,376,381], iron deficiency in normal

adult animals did not affect phosphate regulators in this study, which is consistent with previous findings in healthy adults [305,309]. The moderate changes in renal NaPi-IIa and urinary phosphate levels observed in this study, in addition to reports on changes in renal phosphate excretion following reduced intestinal phosphate absorption in NaPi-IIb knock-out mice [31,145,251], suggest that the impact of iron deficiency on phosphate homeostasis depends on the degree of inhibition of intestinal phosphate absorption. Therefore, it is possible that chronic or a more severe iron deficiency than what was observed in the current study, may result in a long-term and a more prominent inhibition of intestinal phosphate absorption in the proximal small intestine. This may therefore lead to a significant fall in postprandial phosphate levels in the circulation, serum PTH and urinary phosphate excretion, which were not seen in this study. This speculation is in agreement with previous data showing that 4-week administration of an iron deficient diet resulted in a moderate decrease in the levels of PTH and $1,25(OH)_2D_3$ [338]. Although the levels of active intact FGF-23 following a 4-week administration of an iron deficient diet was not investigated in these animals [338], its levels might be affected via the previously reported regulatory feedback pathways involving dietary phosphate absorption, PTH and $1,25(OH)_2D_3$ [7,382–384]. Future experiments to investigate the effect of long-term administration of an iron deficient diet will be required to ascertain whether serum phosphate levels are affected under this dietary condition and whether the regulators of phosphate homeostasis are significantly altered.

In summary, iron deficiency induced by a 2-week dietary regime inhibits intestinal phosphate absorption by mechanisms that are independent of the systemic phosphate regulators, FGF-23, PTH and $1,25(OH)_2D_3$. The moderate increase in

renal NaPi-IIa and a consequent fall in the rate of renal phosphate excretion observed in this study, in addition to the release of phosphate from bone mineral via bone resorption, are both speculated to be responsible for the maintenance of normal phosphate homeostasis observed in the iron deficient animals (Figure 6.4).

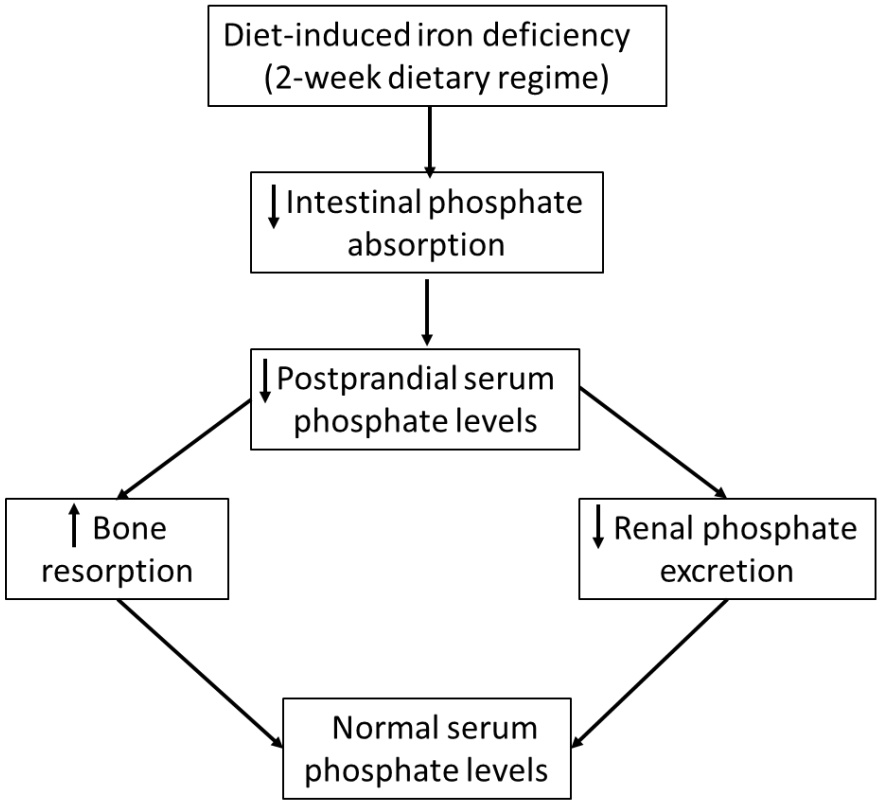


**Figure 6.4. Effect of diet-induced iron deficiency on phosphate homeostasis**. Iron deficiency causes the inhibition of intestinal phosphate absorption, which results in a potential fall in postprandial serum phosphate levels. This fall in serum phosphate levels stimulates the release of phosphate from bone mineral and also stimulates the kidneys to conserve phosphate, thus, restoring phosphate balance.

### 6.4. Effect of diet-induced iron deficiency on the mechanisms of intestinal phosphate absorption

Evidence from this study demonstrates for the first time that diet-induced iron deficiency inhibits phosphate absorption in the duodenum and jejunum via different mechanisms. Iron deficiency inhibited phosphate absorption via the $Na^+$-independent phosphate transport pathway in the duodenum, while both NHE3-regulated phosphate transport and the $Na^+$-independent phosphate transport pathways were inhibited in the jejunum. Since previous reports suggest that the $Na^+$-independent phosphate transport mechanism and NHE3-regulated phosphate transport are both mediated via the paracellular pathway [45,77,319,330], it is likely that iron deficiency inhibits paracellular phosphate absorption. To support this hypothesis, the result of this study showed that the upregulation of DMT1 in the duodenum may be responsible for the increased levels of claudin 3, and this may reduce the permeability of tight junctions since claudin 3 is a pore-sealing claudin. Unlike the duodenum, reduced NHE3 activity in the jejunum of iron deficient rats may inhibit paracellular phosphate absorption via the alteration of tight junction conformation in the jejunum as suggested by King et al. [77]. Changes in duodenal claudin 3 levels or jejunal tight junction conformation are speculated to inhibit paracellular phosphate absorption in iron deficiency in the current study. In addition, the iron deficiency-induced upregulation of claudin 3 levels in the duodenum may be contributing to the more striking inhibition of paracellular phosphate absorption in this segment, in comparison to the less striking effect observed in the jejunum where claudin 3 levels were unchanged.

Interestingly, evidence from this study suggests that iron deficiency had no impact on NaPi-IIb-mediated transcellular phosphate transport in the rat proximal small

intestine and in the mouse small intestine. In iron deficiency, even though changes in NaPi-IIb mRNA was observed in the duodenum of rats, uptake experiments using PFA showed that NaPi-IIb-mediated phosphate transport pathway was not affected. Similarly, in the proximal small intestine of mice, iron deficiency downregulated NaPi-IIb protein levels, but had no effect on phosphate absorption in this segment. Even though changes in NaPi-IIb mRNA or protein was observed in the proximal small intestine of mice and duodenum of rats, evidence from chapter 3 and previous findings on intestinal NaPi-IIb profile [38,39] have demonstrated low levels of NaPi-IIb mRNA and protein in these intestinal regions. The low levels of NaPi-IIb in these intestinal segments of rats and mice, and the unchanged NaPi-IIb mediated phosphate uptake data in response to iron deficiency, indicate that the changes in the mRNA or protein levels of NaPi-IIb in response to iron deficiency are not physiologically relevant. Importantly, in the rat jejunum and mouse ileum where NaPi-IIb is highly expressed, iron deficiency had no effect on both NaPi-IIb levels and NaPi-IIb-mediated phosphate uptake. These findings confirm that NaPi-IIb plays no role in the inhibition of phosphate absorption by iron deficiency in the rat proximal small intestine.

In comparison to NaPi-IIb, NHE3-regulated phosphate absorption appears to be responsible for most of the phosphate absorption via the $Na^+$-dependent pathway in the rat jejunum. However, unlike in the jejunum, evidence from this study showed that the NHE3-regulated pathway has no contribution to phosphate absorption in the duodenum. Based on the lack of contribution of NHE3 to duodenal phosphate absorption, it is very likely that NHE3 plays no role in the marked inhibition of phosphate absorption by iron deficiency in this segment. In contrast, the inhibition of jejunal phosphate absorption by iron deficiency involves

at least in part the $Na^+$-dependent NHE3-regulated phosphate transport pathway. The inhibition of this phosphate transport pathway in the rat jejunum by tenapanor has recently been reported to involve changes in intracellular pH and TEER, both affecting paracellular phosphate diffusion [77]. Although changes in intracellular pH and TEER were not monitored in the current study, it is possible that iron deficiency affects paracellular phosphate absorption via similar mechanisms in the rat jejunum.

In response to iron deficiency, the $Na^+$-independent phosphate transport mechanism was demonstrated to be inhibited mostly in the duodenum where dietary iron is mainly absorbed, with only a minor inhibition of this pathway observed in the jejunum. This finding indicates that the adaptation of the rat proximal small intestine to low dietary iron content interferes with phosphate absorption. In this regard, the upregulation of duodenal and jejunal DMT1 was seen in the iron deficient animals and this is speculated to impact the $Na^+$-independent mechanism of phosphate transport in these segments. As previously described in the jejunum following tenapanor inhibition, it is possible that increased DMT1 levels result in changes in intracellular pH, claudin 3 levels or TEER and these mechanisms may be responsible for the inhibition of the $Na^+$-independent paracellular phosphate transport pathway in the proximal small intestine of iron deficient rats.

It is worth noting that the relatively higher levels of DMT1 in the duodenum compared to the jejunum may be the reason for the substantial inhibition of the $Na^+$-independent pathway in the duodenum in comparison to the moderate inhibition of this pathway in the jejunum in response to iron deficiency. Based on the higher levels of DMT1 protein in the duodenum and the fact that NHE3

inhibition had no effect on duodenal phosphate absorption in this study, increased iron and $H^+$ transport by DMT1 in the duodenum potentially caused the upregulation of claudin 3. In contrast, the inhibition of NHE3 activity possibly resulted in changes in claudin 3 conformation at jejunal tight junctions as reported by King et al. [77] rather than expression levels. These findings implicate NHE3 activity, DMT1 and claudin 3 as potential regulators of the paracellular pathway for phosphate transport in the rat proximal small intestine.

Based on the findings of this study that increased DMT1 function in iron deficiency affects intestinal phosphate absorption in rats, and since DMT1-induced iron absorption occurs in both the duodenum and jejunum of rats [385,386] and humans [387], iron absorption via DMT1 may affect phosphate absorption in humans. Therefore, increased intestinal iron absorption following oral intake of ferric citrate [388] or iron-containing phosphate binders [389–391] by CKD patients may be affecting claudin 3 and other tight junction proteins and this might result in reduced paracellular phosphate absorption. This mechanism may potentially be responsible for the enhanced efficacy of ferric citrate and other iron-containing phosphate binders in the inhibition of intestinal phosphate absorption in CKD patients, even though these therapies are thought to chelate phosphate to reduce its absorption [392].

The hypothesis of the current study is that DMT1-induced iron and $H^+$ hyperabsorption in the duodenum of iron deficient rats leads to an increase in intracellular acidification, which stimulates increased claudin 3 expression within the tight junctions between enterocytes, leading to the sealing of the paracellular pores and subsequent inhibition of $Na^+$-independent paracellular phosphate absorption (Figure 6.5). To test this hypothesis, future studies could be designed

to investigate the role of claudin 3 in paracellular phosphate transport, and whether iron deficiency-induced changes in claudin 3 affect phosphate uptake in epithelial monolayers, for example, in Caco-2 cells, rat small intestinal epithelial cell line (IEC-6) [393] or the recently described intestinal epithelial stem cell monolayers [77]. Additionally, to test the role of DMT1 in the hypothesised pH-induced inhibition of intestinal phosphate absorption in iron deficiency, the effect of DMT1 overexpression or knockdown on intracellular pH could be monitored and this could be correlated with changes in phosphate transport across the monolayers. Further experiments to measure the TEER following DMT1 overexpression or knockdown could also be carried out, and whether changes in TEER are linked to the expression of pore-sealing claudins (e.g. claudin 3 and 4) could be assessed. It is also possible that changes in claudin 3 levels occur in iron deficient enterocytes by a mechanism that is independent of DMT1. This possibility could be investigated to completely unravel the cellular mechanisms underlying the inhibition of paracellular phosphate transport in iron deficient enterocytes.

Of note in the current study is the fact that diet-induced iron deficiency impacts NHE3 activity only in the jejunum, a segment where the inhibition of this transporter has been demonstrated to inhibit paracellular phosphate absorption via a pH-sensitive conformational change within the tight junction [77,247]. Reduced NHE3 activity in the jejunum in response to iron deficiency is speculated to mainly impact intracellular pH, with a smaller contribution by DMT1, due to the low expression profile of this transporter in the jejunum. Therefore, in iron deficiency, the combined effect of reduced NHE3 activity and the upregulation of DMT1 is speculated to increase intracellular $H^+$ and this results in the reduction of paracellular phosphate absorption in the jejunum (Figure 6.6). Unlike the jejunum,

the high levels of duodenal DMT1 and the unchanged duodenal NHE3 activity in response to iron deficiency, suggest that there is a major difference between the mechanisms underlying paracellular phosphate absorption in these segments of the proximal small intestine of rats. Further studies are required to better understand the segmental differences that exist in the mechanisms of paracellular phosphate absorption in the rat duodenum and jejunum.

Importantly, while the current study speculates that iron deficiency affects different mechanisms (DMT1 and NHE3) in the duodenum and jejunum - both generating increased intracellular $H^+$, the cellular signalling pathway linking intracellular $H^+$ and paracellular phosphate transport requires further investigation. To identify potential cellular contributors to the signalling pathway underlying the effect of iron deficiency and/or intracellular $H^+$ on paracellular phosphate transport via tight junctions, proteomic analysis of cell lysates obtained from the duodenum and jejunum of iron deficient and tenapanor-treated rats could be carried out. These experiments will identify differentially expressed tight junction proteins in both segments in response to the different treatments, and may identify protein enzymes that are known to regulate tight junction permeability, for example; PKA, PKC-theta and Rho-activated protein kinases.

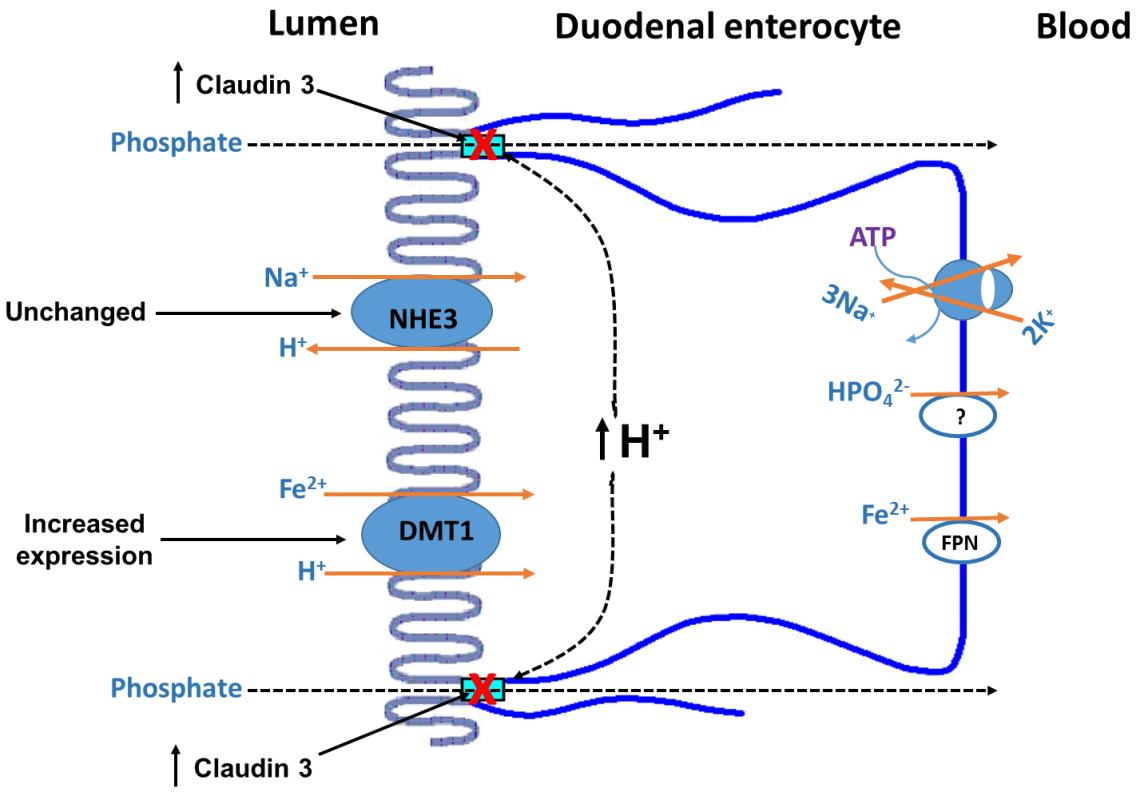


**Figure 6.5. Proposed model depicting the effect of diet-induced iron deficiency on duodenal phosphate absorption in rats**. Increased expression of DMT1 in response to iron deficiency causes intracellular acidification because of increased transport of $H^+$ into the enterocyte. This leads to increased claudin 3 expression resulting in the sealing of the paracellular pathway, thus, inhibiting phosphate absorption.

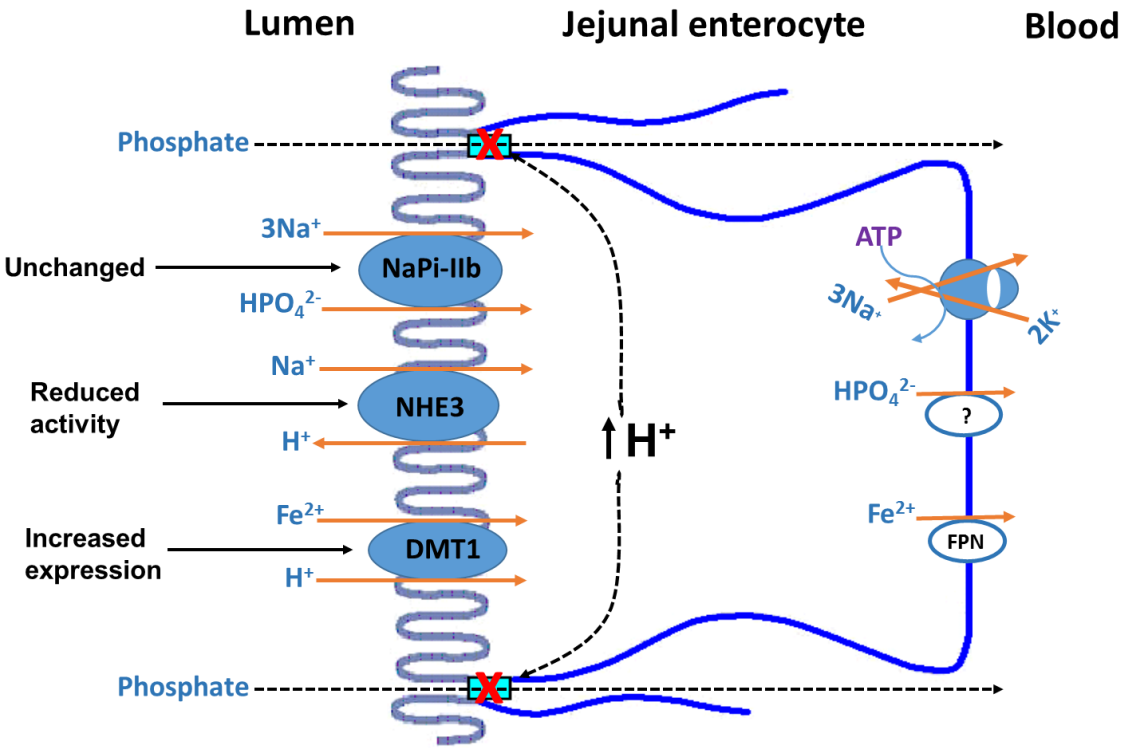


**Figure 6.6. Proposed model depicting the effect of diet-induced iron deficiency on jejunal phosphate absorption in rats**. Reduced NHE3 activity in response to iron deficiency is the major cause of intracellular acidification due to the reduction in the transport of $H^+$ out of the enterocyte. In addition, the upregulated DMT1 is likely to play a minor role in the accumulation of intracellular $H^+$ due to its low expression profile in this segment. The resultant acidification of the intracellular compartment leads to changes in tight junction conformation and the consequent inhibition of paracellular phosphate absorption.

## 6.5. Conclusion

The findings of this thesis provide evidence that intestinal NaPi-IIb is the major transporter responsible for transepithelial phosphate absorption in mice, while in rats, this transporter plays little or no role. NHE3-regulated and the $Na^+$-independent paracellular mechanisms for phosphate transport are likely to be mainly responsible for phosphate absorption in the proximal small intestine of rats. Since tenapanor is known to be effective in inhibiting intestinal phosphate absorption in humans, NHE3-regulated paracellular phosphate absorption is therefore likely to be a key mechanism in mediating $Na^+$-dependent phosphate absorption in humans. Moreover, the similar regional expression profile of intestinal NHE3 in rats and humans, and the fact that tenapanor inhibits phosphate absorption only in these species, suggest that the rat is a better model than the mouse to study phosphate absorption in the human small intestine. Additionally, this is the first study to provide evidence that diet-induced iron deficiency inhibits phosphate absorption in the duodenum and jejunum of rats, an effect that is not dependent on NaPi-IIb or the recognised systemic regulators of phosphate homeostasis. The results of this study suggest that increased DMT1 function mainly in the duodenum and reduced NHE3 activity in the jejunum may be responsible for the inhibition of phosphate absorption in iron deficient rats. This inhibition of intestinal phosphate absorption may be the cause of bone disease in individuals with chronic iron deficient conditions.

**Presentations at scientific meetings**

1. Asowata E.O., Srai S.K.S., Unwin R.J., Walsh S.B., Marks J. (2016). Effect of iron-deficiency on phosphate homeostasis (oral presentation). British Renal Society, UK Kidney Week 2016, Birmingham, UK.
2. Asowata E.O., Casselbrant A., Fandriks L., Unwin, R.J. Marks, J. (2016). Regional Expression of NaPi-IIb, PiT-1 and NHE3 mRNA in the Proximal Small Intestine of Rats and Humans (poster presentation). American Society of Nephrology (ASN) 2016 meeting, Chicago, IL, USA.
3. Asowata E.O., Srai S.K.S., Unwin R.J., Marks J. (2017). Dietary-induced iron deficiency inhibits intestinal phosphate absorption by a NaPi-IIb independent mechanism (poster presentation). American Society of Nephrology (ASN) 2017 meeting, New Orleans, LA, USA.

## References


1. Gattineni, J. & Baum, M. Genetic disorders of phosphate regulation. *Pediatr. Nephrol.* **27,** 1477–1487 (2012).

2. Hruska, K. A., Mathew, S., Lund, R., Qiu, P. & Pratt, R. Hyperphosphatemia of chronic kidney disease. *Kidney Int.* **74,** 148–157 (2008).

3. Hruska, K. A., Mathew, S. & Lund, R. Osteoporosis and cardiovascular disease: lessons from chronic kidney disease. *Clin. Cases Miner. Bone Metab.* **5,** 35–9 (2008).

4. Dhingra, R., Sullivan, L. M., Fox, C. S. & Wang, T. J. Relations of Serum Phosphorus and Calcium Levels to the Incidence of Cardiovascular Disease in the Community. *Am. Med. Assoc.* **167,** 879–885 (2007).

5. Hill, N. R. *et al.* Global Prevalence of Chronic Kidney Disease – A Systematic Review and Meta-Analysis. *PLoS One* **11,** e0158765 (2016).

6. Sharon M. Moe. Disorders Involving Calcium, Phosphorus, and Magnesium. *Prim Care* **35,** 215–vi (2008).

7. Burnett-Bowie, S. A. M., Henao, M. P., Dere, M. E., Lee, H. & Leder, B. Z. Effects of hPTH(1-34) infusion on circulating serum phosphate, 1,25-dihydroxyvitamin D, and FGF23 levels in healthy men. *J. Bone Miner. Res.* **24,** 1681–1685 (2009).

8. Shiguang Liu, Wen Tang, Jianping Zhou, Jason R. Stubbs, Qiang Luo, Min Pi, A. & Quarles, L. D. Fibroblast Growth Factor 23 Is a Counter-Regulatory Phosphaturic Hormone for Vitamin D. *J. Am. Soc. Nephrol.* **17,** 1305–1315 (2006).

9. Saito, H. *et al.* Circulating FGF-23 is regulated by 1α,25-dihydroxyvitamin D3and phosphorus in vivo. *J. Biol. Chem.* **280,** 2543–2549 (2005).

10. Kawata, T. *et al.* Parathyroid hormone regulates fibroblast growth factor-23 in a mouse model of primary hyperparathyroidism. *J. Am. Soc. Nephrol.* **18,** 2683–2688 (2007).

11. Lavi-Moshayoff, V., Wasserman, G., Meir, T., Silver, J. & Naveh-Many, T. PTH increases FGF23 gene expression and mediates the high-FGF23 levels of experimental kidney failure: a bone parathyroid feedback loop. *AJP Ren. Physiol.* **299,** F882–F889 (2010).

12. Forster, I. C., Hernando, N., Biber, J. & Murer, H. Phosphate transporters of the SLC20 and SLC34 families. *Mol. Aspects Med.* **34,** 386–395 (2013).

13. Forster, I. C., Hernando, N., Biber, J. & Murer, H. Phosphate transport kinetics and structure-function relationships of SLC34 and SLC20 proteins. *Curr. Top. Membr.* **70,** 313–356 (2012).

14. Villa-Bellosta, R. & Sorribas, V. Compensatory regulation of the sodium/phosphate cotransporters NaPi-IIc (SCL34A3) and Pit-2 (SLC20A2) during Pi deprivation and acidosis. *Pflugers Arch. Eur. J. Physiol.* **459,** 499–508 (2010).

15. Bourgeois, S. *et al.* The phosphate transporter NaPi-IIa determines the rapid renal adaptation to dietary phosphate intake in mouse irrespective of persistently high FGF23 levels. *Pflugers Arch. Eur. J. Physiol.* **465,** 1557–1572 (2013).

16. Capuano, P. *et al.* Expression and regulation of the renal Na/phosphate cotransporter NaPi-IIa in a mouse model deficient for the PDZ protein PDZK1. *Pflugers Arch. Eur. J. Physiol.* **449,** 392–402 (2005).

17. Giral, H. *et al.* Regulation of rat intestinal Na-dependent phosphate transporters by dietary phosphate. *Am. J. Physiol. Renal Physiol.* **297,** F1466–F1475 (2009).

18. Sabbagh, Y., Giral, H., Caldas, Y., Levi, M. & Schiavi, S. C. Intestinal Phosphate Transport. *Advances in Chronic Kidney Disease* **18,** 85–90 (2011).

19. Capuano, P. *et al.* Intestinal and renal adaptation to a low-P i diet of type II NaP i cotransporters in vitamin D receptor- and 1-alpha-OHase-deficient mice. *Am J Physiol Cell Physiol 288* **288,** 429–434 (2005).

20. Marks, J., Debnam, E. S. & Unwin, R. J. Phosphate homeostasis and the renal-gastrointestinal axis. *Am J Physiol Ren. Physiol* **299,** 285–296 (2010).

21. Ohnishi, M. & Razzaque, M. S. Osteo-renal cross-talk and phosphate metabolism by the FGF23-Klotho system. *Phosphate Vitam. D Chronic Kidney Dis.* **180,** 1–13 (2013).

22. Berndt, T. *et al.* Evidence for a signaling axis by which intestinal phosphate rapidly modulates renal phosphate reabsorption. *Proc. Natl. Acad. Sci. U.S.A.* **104,** 11085–11090 (2007).

23. Thomas, L. *et al.* Acute Adaption to Oral or Intravenous Phosphate Requires Parathyroid Hormone. *J. Am. Soc. Nephrol.* **28,** 903–914 (2017).

24. Lee, G. J., Mossa-Al Hashimi, L., Debnam, E. S., Unwin, R. J. & Marks, J. Postprandial adjustments in renal phosphate excretion do not involve a gut-derived phosphaturic factor. *Exp. Physiol.* **102,** 462–474 (2017).

25. Razzaque, M. S. Osteo-renal regulation of systemic phosphate metabolism. *IUBMB Life* **63,** 240–247 (2011).

26. Albano, G. *et al.* Sodium-dependent phosphate transporters in osteoclast differentiation and function. *PLoS One* **10,** e0125104 (2015).

27. Murer, H., Forster, I. & Biber, J. The sodium phosphate cotransporter family SLC34. *Pflugers Arch. Eur. J. Physiol.* **447,** 763–767 (2004).

28. Collins, J. F., Bai, L. & Ghishan, F. K. The SLC20 family of proteins: Dual functions as sodium-phosphate cotransporters and viral receptors. *Pflugers Arch. Eur. J. Physiol.* **447,** 647–652 (2004).

29. Bergwitz, C. *et al.* SLC34A3 mutations in patients with hereditary hypophosphatemic rickets with hypercalciuria predict a key role for the sodium-phosphate cotransporter NaPi-IIc in maintaining phosphate homeostasis. *Am. J. Hum. Genet.* **78,** 179–92 (2006).

30. Tomoe, Y. *et al.* Phosphaturic action of fibroblast growth factor 23 in Npt2 null mice. *Am. J. Physiol. Physiol.* **298,** F1341–F1350 (2010).

31. Sabbagh, Y. *et al.* Intestinal npt2b plays a major role in phosphate absorption and homeostasis. *J. Am. Soc. Nephrol.* **20,** 2348–2358 (2009).

32. Wagner, C. A., Hernando, N., Forster, I. C. & Biber, J. The SLC34 family of sodium-dependent phosphate transporters. *Pflugers Arch. Eur. J. Physiol.* **466,** 139–153 (2014).

33. Custer, M. *et al.* Expression of Na-Pi cotransport in rat kidney : localization by RT-PCR and immunohistochemistry. *J. Am. Physiol. Physiol.* **266,** F767–F774 (1994).

34. Biber, J., Hernando, N., Forster, I. & Murer, H. Regulation of phosphate transport in proximal tubules. *Pflugers Arch. Eur. J. Physiol.* **458,** 39–52 (2009).

35. Mulroney, S. E. *et al.* Central control of renal sodium-phosphate (NaPi-2) transporters. *Am. J. Physiol. Renal Physiol.* **286,** F647-52 (2004).

36. Khadeer, M. A. *et al.* Na+-dependent phosphate transporters in the murine osteoclast: cellular distribution and protein interactions. *AJP Cell Physiol.* **284,** C1633–C1644 (2003).

37. Jyothsna Gattineni, P. A. F. Regulation of Hormone-Sensitive Renal Phosphate Transport. *Vitam. Horm.* **58,** 249–306 (2015).

38. Radanovic, T., Wagner, C. A., Murer, H. & Biber, J. Regulation of intestinal phosphate transport. I. Segmental expression and adaptation to low-P(i) diet of the type IIb Na(+)-P(i) cotransporter in mouse small intestine. *Am. J. Physiol. Gastrointest. Liver Physiol.* **288,** 496–500 (2005).

39. Marks, J. *et al.* Intestinal phosphate absorption and the effect of vitamin D: A comparison of rats with mice. *Exp. Physiol.* **91,** 531–537 (2006).

40. Hilfiker, H. *et al.* Characterization of a murine type II sodium-phosphate cotransporter expressed in mammalian small intestine. *Proc. Natl. Acad. Sci. U. S. A.* **95,** 14564–14569 (1998).

41. Muscher-Banse, A. S. & Breves, G. Mechanisms and regulation of epithelial phosphate transport in ruminants: approaches in comparative physiology. *Pflügers Arch. - Eur. J. Physiol.* (2018).

42. Traebert, M. *et al.* Distribution of the sodium/phosphate transporter during postnatal ontogeny of the rat kidney. *J. Am. Soc. Nephrol.* **10,** 1407–1415 (1999).

43. Arar, M., Zajicek, H. K., Elshihabi, I. & Levi, M. Epidermal growth factor inhibits Na-Pi cotransport in weaned and suckling rats. *Am. J. Physiol.* **276,** F72-8 (1999).

44. Levi, M. *et al.* Cellular mechanisms of acute and chronic adaptation of rat renal P(i) transporter to alterations in dietary P(i). *Am. J. Physiol.* **267,** F900–F908 (1994).

45. Marks, J., Lee, G. J., Nadaraja, S. P., Debnam, E. S. & Unwin, R. J. Experimental and regional variations in Na+-dependent and Na+-independent phosphate transport along the rat small intestine and colon. *Physiol. Rep.* **3,** e12281 (2015).

46. Walton, J. & Gray, T. K. Absorption of inorganic phosphate in the human small intestine. *Clin. Sci. (Lond).* **56,** 407–12 (1979).

47. Arima, K. *et al.* Glucocorticoid regulation and glycosylation of mouse intestinal type IIb Na-P(i) cotransporter during ontogeny. *Am. J. Physiol. Gastrointest. Liver Physiol.* **283,** G426–G434 (2002).

48. Xu, H., Bai, L., Collins, J. F. & Ghishan, F. K. Age-dependent regulation of rat intestinal type IIb sodium-phosphate cotransporter by 1,25-(OH)(2) vitamin D(3). *Am. J. Physiol. Cell Physiol.* **282,** C487-93 (2002).

49. Virkki, L. V, Biber, J., Murer, H. & Forster, I. C. Phosphate transporters: a tale of two solute carrier families. *Am. J. Physiol. Renal Physiol.* **293,** F643–F654 (2007).

50. Hernando, N., Forster, I. C., Biber, J. & Murer, H. Molecular characteristics of phosphate transporters and their regulation. *Exp. Nephrol.* **8,** 366–75 (2000).

51. Lambert, G., Forster, I. C., Biber, J., Murer, H. Cysteine Residues and the Structure of the Rat Renal Proximal Tubular Type II Sodium Phosphate Cotransporter (Rat NaPi IIa). *J. Membr. Biol* **176,** 133–141 (2000).

52. Lituiev, D. S. & Kiyamova, R. G. Mutations in the gene of human type IIb sodium-phosphate cotransporter SLC34A2. *Biopolymers* **26,** 13–22 (2010).

53. Radanovic, T., Gisler, S. M., Biber, J. & Murer, H. Topology of the type IIa Na+/Pi cotransporter. *J. Membr. Biol.* **212,** 41–49 (2006).

54. Forster, I. C., Hernando, N., Biber, J. & Murer, H. Proximal tubular handling of phosphate: A molecular perspective. *Kidney Int.* **70,** 1548–1559 (2006).

55. Karim-Jimenez, Z., Hernando, N., Biber, J. & Murer, H. Molecular determinants for apical expression of the renal type IIa Na+/Pi-cotransporter. *Pflugers Arch. Eur. J. Physiol.* **442,** 782–790 (2001).

56. Karim-Jimenez, Z., Hernando, N., Biber, J. & Murer, H. A dibasic motif involved in parathyroid hormone-induced down-regulation of the type IIa NaPi cotransporter. *Proc. Natl. Acad. Sci. U. S. A.* **97,** 12896–12901 (2000).

57. Villa-Bellosta, R. *et al.* Interactions of the growth-related, type IIc renal sodium/phosphate cotransporter with PDZ proteins. *Kidney Int.* **73,** 456–464 (2008).

58. Giral, H. *et al.* NHE3 Regulatory Factor 1 (NHERF1) modulates intestinal sodium-dependent phosphate transporter (NaPi-2b) expression in apical microvilli. *J. Biol. Chem.* **287,** 35047–35056 (2012).

59. Yin, B. W. T. *et al.* Monoclonal antibody MX35 detects the membrane transporter NaPi2b (SLC34A2) in human carcinomas. *Cancer Immun.* **8,** 1–9 (2008).

60. Ghezzi, C., Murer, H. & Forster, I. C. Substrate interactions of the electroneutral Na+-coupled inorganic phosphate cotransporter (NaPi-IIc). *J. Physiol.* **587,** 4293–4307 (2009).

61. Virkki, L. V., Murer, H. & Forster, I. C. Voltage Clamp Fluorometric Measurements on a Type II Na + -coupled P i Cotransporter: shedding light on substrate binding order. *J. Gen. Physiol.* **127,** 539–555 (2006).

62. Ehnes, C. *et al.* Structure–Function Relations of the First and Fourth Extracellular Linkers of the Type IIa Na+/Pi Cotransporter. *J. Gen. Physiol.* **124,** 489–503 (2004).

63. Murer, H., Hernando, N., Forster, I. & Biber, J. Regulation of Na/Pi Transporter in the Proximal Tubule. *Annu. Rev. Physiol.* **65,** 531–542 (2003).

64. Bacconi, A., Virkki, L. V, Biber, J., Murer, H. & Forster, I. C. Renouncing electroneutrality is not free of charge: switching on electrogenicity in a Na+-coupled phosphate cotransporter. *Proc. Natl. Acad. Sci. U. S. A.* **102,** 12606–11 (2005).

65. Segawa, H. *et al.* Growth-related renal type II Na/Pi cotransporter. *J. Biol. Chem.* **277,** 19665–19672 (2002).

66. Virkki, L. V., Forster, I. C., Bacconi, A., Biber, J. & Murer, H. Functionally important residues in the predicted 3rd transmembrane domain of the type IIa sodium-phosphate cotransporter (NaPi-IIa). *J. Membr. Biol.* **206,** 227–238 (2005).

67. Kohler, K., Forster, I. C., Lambert, G., Biber, J. & Murer, H. The functional unit of the renal type IIa Na+/P(i) cotransporter is a monomer. *J. Biol. Chem.* **275,** 26113–26120 (2000).

68. Forster, I. C., Biber, J. & Murer, H. Proton-sensitive transitions of renal type II Na+-coupled phosphate cotransporter kinetics. *Biophys. J.* **79,** 215–230 (2000).

69. Amstutz, M., Mohrmann, M., Gmaj, P. & Murer, H. Effect of pH on phosphate transport in rat renal brush border membrane vesicles. *Am. J. Physiol.* **248,** F705–F710 (1985).

70. Forster, I. C., Virkki, L., Bossi, E., Murer, H. & Biber, J. Electrogenic kinetics of a mammalian intestinal type IIb Na +/Pi cotransporter. *J. Membr. Biol.* **212,** 177–190 (2006).

71. Villa-Bellosta, R. & Sorribas, V. Different effects of arsenate and phosphonoformate on P(i) transport adaptation in opossum kidney cells. *Am. J. Physiol. Cell Physiol.* **297,** C516–C525 (2009).

72. Eto, N., Miyata, Y., Ohno, H. & Yamashita, T. Nicotinamide prevents the development of hyperphosphataemia by suppressing intestinal sodium-dependent phosphate transporter in rats with adenine-induced renal failure. *Nephrol. Dial. Transplant.* **20,** 1378–1384 (2005).

73. Miyagawa, A. *et al.* The sodium phosphate cotransporter family and nicotinamide phosphoribosyltransferase contribute to the daily oscillation of plasma inorganic phosphate concentration. *Kidney Int.* **93,** 1073–1085 (2018).

74. Villa-Bellosta, R. & Sorribas, V. Arsenate transport by sodium/phosphate cotransporter type IIb. *Toxicol. Appl. Pharmacol.* **247,** 36–40 (2010).

75. Filipski, K. J. *et al.* Discovery of Orally Bioavailable Selective Inhibitors of the Sodium-Phosphate Cotransporter NaPi2a (SLC34A1). *ACS Med. Chem. Lett.* **9,** 440–445 (2018).

76. Taniguchi K, Terai K, Terada Y, *et al*. Novel NaPi-IIb Inhibitor ASP3325 Inhibits Phosphate Absorption in Intestine and Reduces Plasma Phosphorus Level in Rats with Renal Failure. *J Am Soc Nephrol.* **582A,** FR-PO936 (2015).

77. King, A. J. *et al.* Inhibition of sodium / hydrogen exchanger 3 in the gastrointestinal tract with tenapanor reduces paracellular phosphate permeability. *J. Transl. Med.* **10,** eaam6474 (2018).

78. Lanske, B. & Razzaque, M. S. Molecular interactions of FGF23 and PTH in phosphate regulation. *Kidney Int* **86,** 1072–1074 (2014).

79. Habener, J. F. & Kronenberg, H. M. Parathyroid hormone biosynthesis: structure and function of biosynthetic precursors. *Fed Proc* **37,** 2561–2566 (1978).

80. Bacic, D. *et al.* The renal Na+/phosphate cotransporter NaPi-IIa is internalized via the receptor-mediated endocytic route in response to parathyroid hormone. *Kidney Int.* **69,** 495–503 (2006).

81. Kempson, S. A. *et al.* Parathyroid hormone action on phosphate transporter mRNA and protein in rat renal proximal tubules. *Am. J. Physiol.* **268,** F784-91 (1995).

82. Mannstadt, M., Juppner, H. & Gardella, T. J. Receptors for PTH and PTHrP: their biological importance and functional properties. *J. Am. Physiol. Soc.* **277,** F665–F675 (1999).

83. Capuano, P. *et al.* Defective coupling of apical PTH receptors to phospholipase C prevents internalization of the Na+-phosphate cotransporter NaPi-IIa in Nherf1-deficient mice. *Am. J. Physiol. Cell Physiol.* **292,** C927–C934 (2007).

84. Weinman, E. J. *et al.* Parathyroid hormone inhibits renal phosphate transport by phosphorylation of serine 77 of sodium-hydrogen exchanger regulatory factor-1. *J. Clin. Invest.* **117,** 3412–3420 (2007).

85. Yamada, F. *et al.* Role of serine 249 of ezrin in the regulation of sodium-dependent phosphate transporter NaPi-IIa activity in renal proximal tubular cells. *J. Med. Investig.* **60,** 27–34 (2013).

86. Reshkin, S. J., Forgo, J. & Murer, H. Apical and basolateral effects of PTH in OK cells: Transport inhibition, messenger production, effects of pertussis toxin, and interaction with a PTH analog. *J. Membr. Biol.* **124,** 227–237 (1991).

87. Traebert, M., Völkl, H., Biber, J., Murer, H. & Kaissling, B. Luminal and contraluminal action of 1-34 and 3-34 PTH peptides on renal type IIa Na-Pi cotransporter. *Am. J. Physiol. Renal Physiol.* **278,** F792–F798 (2000).

88. Collazo, R. *et al.* Acute regulation of Na+/H+exchanger NHE3 by parathyroid hormone via NHE3 phosphorylation and dynamin-dependent endocytosis. *J. Biol. Chem.* **275,** 31601–31608 (2000).

89. Pfister, M. F. *et al.* Parathyroid hormone leads to the lysosomal degradation of the renal type II Na/Pi cotransporter. *Proc. Natl. Acad. Sci.* **95,** 1909–1914 (1998).

90. Segawa, H. *et al.* Parathyroid hormone-dependent endocytosis of renal type IIc Na-Pi cotransporter. *Am J Physiol Ren. Physiol* **292,** F395-403 (2007).

91. Picard, N. *et al.* Acute parathyroid hormone differentially regulates renal brush border membrane phosphate cotransporters. *Pflugers Arch. Eur. J. Physiol.* **460,** 677–687 (2010).

92. Andrukhova, O., Streicher, C., Zeitz, U. & Erben, R. G. Fgf23 and parathyroid hormone signaling interact in kidney and bone. *Mol. Cell. Endocrinol.* **436,** 224–239 (2016).

93. Kuntziger, H., Amiel, C., Roinel, N. & Morel, F. Effects of parathyroidectomy and cyclic AMP on renal transport of phosphate, calcium, and magnesium. *Am. J. Physiol.* **227,** 905–911 (1974).

94. Horiuchi, N., Suda, T., Shigematsu, T., Ogura, Y. & Miyahara, T. Human parathyroid hormone inhibits renal 24-hydroxylase activity of 25-hydroxyvitamin d3by a mechanism involving adenosine 3′,5′-monophosphate in rats. *Endocrinology* **118,** 1583–1589 (1986).

95. Flanagan, J. N. *et al.* Regulation of the 25-hydroxyvitamin D-1alpha-hydroxylase gene and its splice variant. *Recent Results Cancer Res* **164,** 157–167 (2003).

96. Yamashita, T., Yoshioka, M. & Itoh, N. Identification of a novel fibroblast growth factor, FGF-23, preferentially expressed in the ventrolateral thalamic nucleus of the brain. *Biochem. Biophys. Res. Commun.* **277,** 494–498 (2000).

97. Fukumoto, S. & Martin, T. J. Bone as an endocrine organ. *Trends Endocrinol. Metab.* **20,** 230–236 (2009).

98. Shimada, T. *et al.* Mutant FGF-23 Responsible for Autosomal Dominant Hypophosphatemic Rickets Is Resistant to Proteolytic Cleavage and Causes Hypophosphatemia in Vivo. *Endocrinology* **143,** 3179–3182 (2002).

99. Saito, H. *et al.* Human fibroblast growth factor-23 mutants suppress Na+-dependent phosphate co-transport activity and 1α,25-dihydroxyvitamin D3 production. *J. Biol. Chem.* **278,** 2206–2211 (2003).

100. Razzaque, M. S. & Lanske, B. The emerging role of the fibroblast growth factor-23 – klotho axis in renal regulation of phosphate homeostasis. *J. Endocrinol.* **194,** 1–10 (2007).

101. Bai, X., Miao, D., Li, J., Goltzman, D. & Karaplis, A. C. Transgenic mice overexpressing human fibroblast growth factor 23 (R176Q) delineate a putative role for parathyroid hormone in renal phosphate wasting disorders. *Endocrinology* **145,** 5269–5279 (2004).

102. Shimada, T. *et al.* Targeted ablation of Fgf23 demonstrates an essential physiological role of FGF23 in phosphate and vitamin D metabolism. *J. Clin. Invest.* **113,** 561–568 (2004).

103. Weber, T. J., Liu, S., Indridason, O. S. & Quarles, L. D. Serum FGF23 Levels in Normal and Disordered Phosphorus Homeostasis. *J. Bone Miner. Res.* **18,** 1227–1234 (2003).

104. Yamazaki, Y. *et al.* Increased circulatory level of biologically active full-length FGF-23 in patients with hypophosphatemic rickets/osteomalacia. *J. Clin. Endocrinol. Metab.* **87,** 4957–4960 (2002).

105. White, K. E. *et al.* Autosomal-dominant hypophosphatemic rickets (ADHR) mutations stabilize FGF-23. *Kidney Int.* **60,** 2079–2086 (2001).

106. Erben, R. G. & Andrukhova, O. FGF23-Klotho signaling axis in the kidney. *Bone* **100,** 62–68 (2017).

107. Han, X. *et al.* Conditional Deletion of Fgfr1 in the Proximal and Distal Tubule Identifies Distinct Roles in Phosphate and Calcium Transport. *PLoS One* **11,** e0147845 (2016).

108. Ide, N. *et al.* In vivo evidence for a limited role of proximal tubular Klotho in renal phosphate handling. *Kidney Int.* **90,** 348–362 (2016).

109. Andrukhova, O. *et al.* FGF23 acts directly on renal proximal tubules to induce phosphaturia through activation of the ERK1/2-SGK1 signaling pathway. *Bone* **51,** 621–628 (2012).

110. Li, H., Martin, A., David, V. & Quarles, L. D. Compound deletion of Fgfr3 and Fgfr4 partially rescues the Hyp mouse phenotype. *Am. J. Physiol. - Endocrinol. Metab.* **300,** E508–E517 (2011).

111. Umbach, A. T. *et al.* Janus kinase 3 regulates renal 25-hydroxyvitamin D 1α-hydroxylase expression, calcitriol formation, and phosphate metabolism. *Kidney Int.* **87,** 728–737 (2015).

112. Urakawa, I. *et al.* Klotho converts canonical FGF receptor into a specific receptor for FGF23. *Nature* **444,** 770–774 (2006).

113. Kurosu, H. *et al.* Regulation of fibroblast growth factor-23 signaling by Klotho. *J. Biol. Chem.* **281,** 6120–6123 (2006).

114. Dërmaku-Sopjani, M. *et al.* Downregulation of NaPi-IIa and NaPi-IIb Na + -coupled Phosphate Transporters by Coexpression of Klotho. *Cell Physiol Biochem* **28,** 251–258 (2011).

115. Imura, A. *et al.* a-Klotho as a Regulator of Calcium Homeostasis. *Science* **316,** 1615–1619 (2007).

116. Smith, R. C. *et al.* Circulating αKlotho influences phosphate handling by controlling FGF23 production. *J. Clin. Invest.* **122,** 4710–4715 (2012).

117. Hu, M. C. *et al.* Klotho: a novel phosphaturic substance acting as an autocrine enzyme in the renal proximal tubule. *FASEB J.* **24,** 3438–3450 (2010).

118. Ben-Dov, I. Z. *et al.* The parathyroid is a target organ for FGF23 in rats. *J. Clin. Invest.* **117,** 4003–4008 (2007).

119. Meir, T. *et al.* Parathyroid hormone activates the orphan nuclear receptor Nurr1 to induce FGF23 transcription. *Kidney Int.* **86,** 1106–1115 (2014).

120. Olauson, H. *et al.* Parathyroid-Specific Deletion of Klotho Unravels a Novel Calcineurin-Dependent FGF23 Signaling Pathway That Regulates PTH Secretion. *PLoS Genet.* **9,** 4–13 (2013).

121. Kuro-o, M. *et al.* Mutation of the mouse klotho gene leads to a syndrome resembling ageing. *Nature* **390,** 45–51 (1997).

122. Khundmiri, S. J., Murray, R. D. & Lederer, E. PTH and Vitamin D. *Compr. Physiol.* **6,** 561–601 (2016).

123. Garabedian, M., Holick, M. F., Deluca, H. F. & Boyle, I. T. Control of 25-hydroxycholecalciferol metabolism by parathyroid glands. *Proc Natl Acad Sci U S A* **69,** 1673–1676 (1972).

124. Y. Tanaka & H. F. Deluca. The Control of 25-Hydroxyvitamin D Metabolism by Inorganic Phosphorus. *Arch. Biochem. Biophys.* **164,** 566–574 (1973).

125. Kurnik, B. R. C. & & Hruska, K. A. Effects of I,25-dihydroxycholecalciferol on phosphate transport in vitamin D-deprived rats. *Am. J. Physiol. Physiol.* **241,** F177–F184 (1984).

126. Lee, D. B., Walling, M. W. & Corry, D. B. Phosphate transport across rat jejunum: influence of sodium, pH, and 1,25-dihydroxyvitamin D3. *Am. J. Physiol.* **251,** G90-5 (1986).

127. Segawa, H. *et al.* Intestinal Na-P(i) cotransporter adaptation to dietary P(i) content in vitamin D receptor null mice. *Am. J. Physiol. Renal Physiol.* **287,** F39–F47 (2004).

128. Slater, S. J. *et al.* Direct Activation of Protein Kinase C by 1α,25-Dihydroxyvitamin D3. *J. Biol. Chem.* **270,** 6639–6643 (1995).

129. de Boland, A. R. & Norman, A. W. 1 , 25 ( O H ) 2 -Vitamin D 3 Signaling in Chick Enterocytes : Enhancement of Tyrosine Phosphorylation and Rapid Stimulation of M itogen-Activated Protein ( M AP ) Kinase. *J. Cell. Biochem.* **69,** 470–482 (1998).

130. Haussler, M. R., Jurutka, P. W., Mizwicki, M. & Norman, A. W. Vitamin D receptor (VDR)-mediated actions of 1α,25(OH)2vitamin D3: Genomic and non-genomic mechanisms. *Best Pract. Res. Clin. Endocrinol. Metab.* **25,** 543–559 (2011).

131. Khare, S. *et al.* 1 , 25-Dihydroxyvitamin D 3 but not TPA activates PLD in Caco-2 cells via pp60 c- src and RhoA 1 , 25-Dihydroxyvitamin D 3 but not TPA activates PLD in Caco-2 cells via pp60 c-src and RhoA. *Am. J. Physiol.* **276,** G1005-1015 (1999).

132. Yamamoto, H. *et al.* Alternative promoters and renal cell-specific regulation of the mouse type IIa sodium-dependent phosphate cotransporter gene. *Biochim. Biophys. Acta - Gene Struct. Expr.* **1732,** 43–52 (2005).

133. Barthel, T. K. *et al.* 1,25-Dihydroxyvitamin D3/VDR-mediated induction of FGF23 as well as transcriptional control of other bone anabolic and catabolic genes that orchestrate the regulation of phosphate and calcium mineral metabolism. *J. Steroid Biochem. Mol. Biol.* **103,** 381–388 (2007).

134. Friedlaender, M. M. *et al.* Vitamin D reduces renal NaPi-2 in PTH-infused rats: complexity of vitamin D action on renal P(i) handling. *Am. J. Physiol. Renal Physiol.* **281,** F428–F433 (2001).

135. Saito, H. *et al.* Circulating FGF-23 is regulated by 1α,25-dihydroxyvitamin D3 and phosphorus in vivo. *J. Biol. Chem.* **280,** 2543–2549 (2005).

136. Kaneko, I. *et al.* Hypophosphatemia in vitamin D receptor null mice: Effect of rescue diet on the developmental changes in renal Na+-dependent phosphate cotransporters. *Pflugers Arch. Eur. J. Physiol.* **461,** 77–90 (2011).

137. Keusch, I. *et al.* Parathyroid hormone and dietary phosphate provoke a lysosomal routing of the proximal tubular Na/Pi-cotransporter type II. *Kidney Int.* **54,** 1224–1232 (1998).

138. Segawa, H. *et al*. Internalization of renal type IIc Na-Pi cotransporter in response to a high-phosphate diet. *AJP Ren. Physiol.* **288,** F587–F596 (2005).

139. Berndt, T. & Kumar, R. Novel Mechanisms in the Regulation of Phosphorus Homeostasis. *Physiology* **24,** 17–25 (2009).

140. Biber, J., Hernando, N. & Forster, I. Phosphate Transporters and Their Function. *Annu. Rev. Physiol.* **75,** 535–550 (2013).

141. Giral, H. *et al.* Role of PDZK1 protein in apical membrane expression of renal sodium-coupled phosphate transporters. *J. Biol. Chem.* **286,** 15032–15042 (2011).

142. Weinman, E. J. *et al.* NHERF-1 is required for renal adaptation to a low phosphate diet. *Am. J. Physiol. Renal Physiol.* **285,** 1225–1232 (2003).

143. Hattenhauer, O., Traebert, M., Murer, H. & Biber, J. Regulation of small intestinal Na-P(i) type IIb cotransporter by dietary phosphate intake. *Am. J. Physiol.* **277,** G756–G762 (1999).

144. Katai, K. *et al.* Regulation of intestinal Na+-dependent phosphate co-transporters by a low-phosphate diet and 1,25-dihydroxyvitamin D3. *Biochem. J.* **343 Pt 3,** 705–12 (1999).

145. Knöpfel, T. *et al.* The intestinal phosphate transporter NaPi-IIb (Slc34a2) is required to protect bone during dietary phosphate restriction. *Sci. Rep.* **7,** (2017).

146. Candeal, E., Caldas, Y. A., Guillen, N., Levi, M. & Sorribas, V. Intestinal phosphate absorption is mediated by multiple transport systems in rats. *Am J Physiol Gastrointest Liver Physiol* **312,** G355–G366 (2017).

147. Gray, R. W. & Napoli, J. L. Dietary phosphate deprivation increases 1,25-dihydroxyvitamin D3 synthesis in rat kidney in vitro. *J. Biol. Chem.* **258,** 1152–1155 (1983).

148. Zhang, M. Y. H. *et al.* Dietary Phosphorus Transcriptionally Regulates 25-Hydroxyvitamin D-1_-Hydroxylase Gene Expression in the Proximal Renal Tubule. *Endocrinology* **143,** 587–595 (2002).

149. Danisi, G., Caverzasio, J., Trechsel, U., Bonjour, J. P. & Straub, R. W. Phosphate transport adaptation in rat jejunum and plasma level of 1,25-dihydroxyvitamin D3. *Scand. J. Gastroenterol.* **25,** 210–215 (1990).

150. Hegan, P. S., Giral, H., Levi, M. & Mooseker, M. S. Myosin VI is required for maintenance of brush border structure, composition, and membrane trafficking functions in the intestinal epithelial cell. *Cytoskeleton* **69,** 235–251 (2012).

151. Stauber, A. *et al.* Regulation of intestinal phosphate transport. II. Metabolic acidosis stimulates Na(+)-dependent phosphate absorption and expression of the Na(+)-P(i) cotransporter NaPi-IIb in small intestine. *Am. J. Physiol. Gastrointest. Liver Physiol.* **288,** G501–G506 (2005).

152. Ambühl, P. M. *et al.* Regulation of renal phosphate transport by acute and chronic metabolic acidosis in the rat. *Kidney Int.* **53,** 1288–1298 (1998).

153. Nowik, M. *et al.* Renal phosphaturia during metabolic acidosis revisited: Molecular mechanisms for decreased renal phosphate reabsorption. *Pflugers Arch. Eur. J. Physiol.* **457,** 539–549 (2008).

154. Lemann, J., Bushinsky, D. A. & Hamm, L. L. Bone buffering of acid and base in humans. *Am. J. Physiol. - Ren. Physiol.* **285,** F811–F832 (2003).

155. Feld, S. & Hirschberg, R. Growth Hormone, the Insulin-Like Growth Factor System, and the Kidney. *Endocr. Rev.* **17,** 423–480 (1996).

156. Caverzasio, J, Montessuit, C. & Bonjour, J. P. Stimulatory Effect of Insulin-Like Growth Factor-1 on Renal Pi Transport and Plasma 1,25-Dihydroxyvitamin D3. *Endocrinology* **127,** 453–459 (1990).

157. Jehle, A. W. *et al.* IGF-I and vanadate stimulate Na/P(i)-cotransport in OK cells by increasing type II Na/P(i)-cotransporter protein stability. *Pflugers Arch. Eur. J. Physiol.* **437,** 149–154 (1998).

158. Weinman, E. J. *et al.* Increased renal dopamine and acute renal adaptation to a high-phosphate diet. *Am. J. Physiol. Physiol.* **300,** F1123–F1129 (2011).

159. Bacic, D. *et al.* Activation of dopamine $D_1$-like receptors induces acute internalization of the renal $Na^+$/phosphate cotransporter NaPi-IIa in mouse kidney and OK cells. *Am. J. Physiol. Physiol.* **288,** F740–F747 (2005).

160. Weinman, E. J. *et al.* Sodium-hydrogen exchanger regulatory factor 1 (NHERF-1) transduces signals that mediate dopamine inhibition of sodium-phosphate co-transport in mouse kidney. *J. Biol. Chem.* **285,** 13454–13460 (2010).

161. Hammond, T. G., Yusufi, A. N. K., Knox, F. G. & Dousa, T. P. Administration of atrial natriuretic factor inhibits sodium-coupled transport in proximal tubules. *J. Clin. Invest.* **75,** 1983–1989 (1985).

162. Bacic, D. *et al.* Regulation of the renal type IIa Na/Pi cotransporter by cGMP. *Pflugers Arch. Eur. J. Physiol.* **443,** 306–313 (2001).

163. Burris, D. *et al.* Estrogen directly and specifically downregulates NaPi-IIa through the activation of both estrogen receptor isoforms (ERα and ERβ) in rat kidney proximal tubule. *Am. J. Physiol. - Ren. Physiol.* **308,** F522–F534 (2015).

164. Faroqui, S., Levi, M., Soleimani, M. & Amlal, H. Estrogen downregulates the proximal tubule type IIa sodium phosphate cotransporter causing phosphate wasting and hypophosphatemia. *Kidney Int.* **73,** 1141–1150 (2008).

165. Xu, H. *et al.* Regulation of intestinal NaPi-IIb cotransporter gene expression by estrogen. *Am. J. Physiol. Gastrointest. Liver Physiol.* **285,** G1317–G1324 (2003).

166. Ash, S. L. & Goldin, B. R. Effects of age and estrogen on renal vitamin D metabolism in the female rat. *Am. J. Clin. Nutr.* **47,** 694–699 (1988).

167. Guner, Y. S., Kiela, P. R., Xu, H., Collins, J. F. & Ghishan, F. K. Differential regulation of renal sodium-phosphate transporter by glucocorticoids during rat ontogeny. *Am. J. Physiol.* **277,** C884-90 (1999).

168. Levi, M. *et al.* Dexamethasone modulates rat renal brush border membrane phosphate transporter mRNA and protein abundance and glycosphingolipid composition. *J. Clin. Invest.* **96,** 207–216 (1995).

169. Euzet, S. C. *et al.* Effect of 3,5,3'-Triiodothyronine on Maturation of Rat Renal Phosphate Transport: Kinetic Characteristics and Phosphate Transporter Messenger Ribonucleic Acid and Protein Abundance. *Endocrinology* **137,** 3522–3530 (1996).

170. Alcalde, A. I. *et al.* Role of thyroid hormone in regulation of renal phosphate transport in young and aged rats. *Endocrinology* **140,** 1544–1551 (1999).

171. Cai, Q. *et al.* Brief report: inhibition of renal phosphate transport by a tumor product in a patient with oncogenic osteomalacia. *N Engl J Med* **330,** 1645–1649 (1994).

172. Bowe, A. E. *et al.* FGF-23 inhibits renal tubular phosphate transport and is a PHEX substrate. *Biochem. Biophys. Res. Commun.* **284,** 977–981 (2001).

173. Shimada, T. *et al.* Cloning and characterization of FGF23 as a causative factor of tumor-induced osteomalacia. *Proc. Natl. Acad. Sci.* **98,** 6500–6505 (2001).

174. Rowe, P. S. N. *et al.* MEPE, a new gene expressed in bone marrow and tumors causing osteomalacia. *Genomics* **67,** 54–68 (2000).

175. Dobbie, H., Unwin, R. J., Faria, N. J. R. & Shirley, D. G. Matrix extracellular phosphoglycoprotein causes phosphaturia in rats by inhibiting tubular phosphate reabsorption. *Nephrol. Dial. Transplant.* **23,** 730–733 (2008).

176. Marks, J., Churchill, L. J., Debnam, E. S. & Unwin, R. J. Matrix extracellular phosphoglycoprotein inhibits phosphate transport. *J. Am. Soc. Nephrol.* **19,** 2313–2320 (2008).

177. Rowe, P. S. N. The Wrickkened Pathways Of FGF23, MEPE and PHEX. *Crit Rev Oral Biol Med.* **15,** 264–281 (2004).

178. Jain, A. *et al.* Serum levels of Matrix Extracellular Phosphoglycoprotein (MEPE) in normal humans correlate with serum phosphorus, parathyroid hormone and bone mineral density. *J. Clin. Endocrinol. Metab.* **89,** 4158–4161 (2004).

179. Berndt, T. *et al.* Secreted frizzled-related protein 4 is a potent tumor-derived phosphaturic agent. *J. Clin. Invest.* **112,** 785–794 (2003).

180. Berndt, T. J. *et al.* Secreted frizzled-related protein-4 reduces sodium-phosphate co-transporter abundance and activity in proximal tubule cells. *Pflugers Arch. Eur. J. Physiol.* **451,** 579–587 (2006).

181. Sommer, S., Berndt, T., Craig, T. & Kumar, R. The phosphatonins and the regulation of phosphate transport and vitamin D metabolism. *J. Steroid Biochem. Mol. Biol.* **103,** 497–503 (2007).

182. Carpenter, T. O. *et al.* Fibroblast growth factor 7: An inhibitor of phosphate transport derived from oncogenic osteomalacia-causing tumors. *J. Clin. Endocrinol. Metab.* **90,** 1012–1020 (2005).

183. Lederer, E. D., Sohi, S. S., Mathiesen, J. M. & Klein, J. B. Regulation of expression of type II sodium-phosphate cotransporters by protein kinases A and C. *Am. J. Physiol.* **275,** F270-7 (1998).

184. Mahon, M. J., Donowitz, M., Yun, C. C. & Segre, G. V. $Na^+/H^+$ exchanger regulatory factor 2 directs parathyroid hormone 1 receptor signalling. *Nature* **417,** 858–861 (2002).

185. Wang, B. *et al.* Ezrin-anchored protein kinase A coordinates phosphorylation-dependent disassembly of a NHERF1 ternary complex to regulate hormone-sensitive phosphate transport. *J. Biol. Chem.* **287,** 24148–24163 (2012).

186. Gisler, S. M. *et al.* Interaction of the Type IIa Na/PiCotransporter with PDZ Proteins. *J. Biol. Chem.* **276,** 9206–9213 (2001).

187. Gisler, S. M. *et al.* Monitoring Protein-Protein Interactions between the Mammalian Integral Membrane Transporters and PDZ-interacting Partners Using a Modified Split-ubiquitin Membrane Yeast Two-hybrid System. *Mol. Cell. Proteomics* **7,** 1362–1377 (2008).

188. McWilliams, R. R. *et al.* Shank2E binds NaP(i) cotransporter at the apical membrane of proximal tubule cells. *Am. J. Physiol. Cell Physiol.* **289,** C1042-51 (2005).

189. Shenolikar, S., Voltz, J. W., Minkoff, C. M., Wade, J. B. & Weinman, E. J. Targeted disruption of the mouse NHERF-1 gene promotes internalization of proximal tubule sodium-phosphate cotransporter type IIa and renal phosphate wasting. *Proc Natl Acad Sci U S A* **99,** 11470–11475 (2002).

190. Karim, Z. *et al*. NHERF1 Mutations and Responsiveness of Renal Parathyroid Hormone. *N Engl J Med* **359,** 1128–35 (2008).

191. Hatano, R. *et al.* Ezrin, a membrane cytoskeletal cross-linker, is essential for the regulation of phosphate and calcium homeostasis. *Kidney Int.* **83,** 41–49 (2013).

192. Tanimura, A. *et al.* Analysis of different complexes of type 2a sodium-dependent phosphate transporter in rat renal cortex using blue-native polyacrylamide gel electrophoresis. *J. Med. Investig.* **58,** 140–147 (2011).

193. Nashiki, K. *et al.* Role of membrane microdomains in PTH-mediated down-regulation of NaPi-IIa in opossum kidney cells. *Kidney Int.* **68,** 1137–1147 (2005).

194. Dobrinskikh, E. *et al.* Shank2 contributes to the apical retention and intracellular redistribution of NaPiIIa in OK cells. *Am. J. Physiol. Cell Physiol.* **304,** C561-73 (2013).

195. Han, W. S. *et al.* Shank2 associates with and regulates Na+/H+exchanger. *J. Biol. Chem.* **281,** 1461–1469 (2006).

196. Okamoto, P. M., Gamby, C., Wells, D., Fallon, J. & Vallee, R. B. Dynamin Isoform-specific Interaction with the Shank/ProSAP Scaffolding Proteins of the Postsynaptic Density and Actin Cytoskeleton. *J. Biol. Chem.* **276,** 48458–48465 (2001).

197. Reining, S. C. *et al.* GABARAP deficiency modulates expression of NaPi-IIa in renal brush-border membranes. *Am. J. Physiol. Renal Physiol.* **296,** F1118-28 (2009).

198. Reining, S. C. *et al.* Expression of renal and intestinal Na/Pi cotransporters in the absence of GABARAP. *Pflugers Arch. Eur. J. Physiol.* **460,** 207–217 (2010).

199. Pathare, G. *et al.* OSR1-sensitive renal tubular phosphate reabsorption. *Kidney Blood Press. Res.* **36,** 149–161 (2012).

200. Fezai, M. *et al.* Up-Regulation of Intestinal Phosphate Transporter NaPi-IIb (SLC34A2) by the Kinases SPAK and OSR1. *Kidney Blood Press. Res.* **40,** 555–564 (2015).

201. Pathare, G. *et al.* Enhanced FGF23 serum concentrations and phosphaturia in gene targeted mice expressing WNK-resistant spak. *Kidney Blood Press. Res.* **36,** 355–364 (2012).

202. Xiao, F. *et al.* Rescue of epithelial $HCO_3^-$ secretion in murine intestine by apical membrane expression of the cystic fibrosis transmembrane conductance regulator mutant F508del. *J. Physiol.* **590,** 5317–5334 (2012).

203. Ito, M. *et al.* Characterization of inorganic phosphate transport in osteoclast-like cells. *Am. J. Physiol. Cell Physiol.* **288,** C921-31 (2005).

204. Togawa, N., Miyaji, T., Izawa, S., Omote, H. & Moriyama, Y. A Na+-phosphate cotransporter homologue (SLC17A4 protein) is an intestinal organic anion exporter. *AJP Cell Physiol.* **302,** C1652–C1660 (2012).

205. Reimer, R. J. & Edwards, R. H. Organic anion transport is the primary function of the SLC17/type I phosphate transporter family. *Pflugers Arch. Eur. J. Physiol.* **447,** 629–635 (2004).

206. Werner, A. *et al.* Cloning and expression of cDNA for a Na/Pi cotransport system of kidney cortex. *Proc. Natl. Acad. Sci. USA* **88,** 9608–9612 (1991).

207. Biber, J., Custer, M., Werner, A., Kaissling, B. & Murer, H. Localization of NaPi-1, a Na/Pi cotransporter, in rabbit kidney proximal tubules - II. Localization by immunohistochemistry. *Pflügers Arch. Eur. J. Physiol.* **424,** 210–215 (1993).

208. Yabuuchi, H. *et al.* Hepatic sinusoidal membrane transport of anionic drugs mediated by anion transporter Npt1. *J Pharmacol Exp Ther* **286,** 1391–1396 (1998).

209. Busch, A. E. *et al.* Expression of a renal type I sodium/phosphate transporter (NaPi-1) induces a conductance in Xenopus oocytes permeable for organic and inorganic anions. *Proc. Natl. Acad. Sci.* **93,** 5347–5351 (1996).

210. Soumounou, Y., Gauthier, C. & Tenenhouse, H. S. Murine and human type I Na-phosphate cotransporter genes: structure and promoter activity. *Am. J. Physiol. Renal Physiol.* **281,** F1082-91 (2001).

211. Cheret, C., Doyen, A., Yaniv, M. & Pontoglio, M. Hepatocyte nuclear factor 1 α controls renal expression of the Npt1-Npt4 anionic transporter locus. *J. Mol. Biol.* **322,** 929–941 (2002).

212. Jin, H. *et al.* A high inorganic phosphate diet perturbs brain growth, alters Akt-ERK signaling, and results in changes in cap-dependent translation. *Toxicol. Sci.* **90,** 221–229 (2006).

213. Breusegem, S. Y. *et al.* Differential regulation of the renal sodium-phosphate cotransporters NaPi-IIa, NaPi-IIc, and PiT-2 in dietary potassium deficiency. *Am. J. Physiol. Renal Physiol.* **297,** F350–F361 (2009).

214. Villa-Bellosta, R. *et al.* The Na+-Pi cotransporter PiT-2 (SLC20A2) is expressed in the apical membrane of rat renal proximal tubules and regulated by dietary Pi. *AJP Ren. Physiol.* **296,** F691–F699 (2009).

215. Bøttger, P. & Pedersen, L. Mapping of the minimal inorganic phosphate transporting unit of human PiT2 suggests a structure universal to PiT-related proteins from all kingdoms of life. *BMC Biochem.* **12,** 21 (2011).

216. Farrell, K. B., Tusnady, G. E. & Eiden, M. V. New structural arrangement of the extracellular regions of the phosphate transporter SLC20A1, the receptor for gibbon ape leukemia virus. *J. Biol. Chem.* **284,** 29979–29987 (2009).

217. Bai, L., Collins, J. F. & Ghishan, F. K. Cloning and characterization of a type III Na-dependent phosphate cotransporter from mouse intestine. *Am. J. Physiol. Cell Physiol.* **279,** C1135-43 (2000).

218. Kavanaugh, M. P. & Kabat, D. Identification and characterization of a widely expressed phosphate transporter/retrovirus receptor family. *Kidney Int.* **49,** 959–963 (1996).

219. Ravera, S., Virkki, L. V, Murer, H. & Forster, I. C. Deciphering PiT transport kinetics and substrate specificity using electrophysiology and flux measurements. *Am. J. Physiol. Cell Physiol.* **293,** C606–C620 (2007).

220. Inden, M. *et al.* The type III transporters (PiT-1 and PiT-2) are the major sodium-dependent phosphate transporters in the mice and human brains. *Brain Res.* **1637,** 128–136 (2016).

221. Inden, M., Iriyama, M., Takagi, M., Kaneko, M. & Hozumi, I. Localization of type-III sodium-dependent phosphate transporter 2 in the mouse brain. *Brain Res.* **1531,** 75–83 (2013).

222. Hernando, N. *et al.* Intestinal depletion of NaPi-IIb/Slc34a2 in mice: Renal and hormonal adaptation. *J. Bone Miner. Res.* **30,** 1925–1937 (2015).

223. Segawa, H. *et al.* Npt2a and Npt2c in mice play distinct and synergistic roles in inorganic phosphate metabolism and skeletal development. *Am. J. Physiol. Renal Physiol.* **297,** F671–F678 (2009).

224. Prasad, N. & Bhadauria, D. Renal phosphate handling: Physiology. *Indian J. Endocrinol. Metab.* **17,** 620–7 (2013).

225. Pastoriza-Munoz, E., Colindres, R. E., Lassiter, W. E. & Lechene, C. Effect of parathyroid hormone on phosphate reabsorption in rat distal convolution. *Am. J. Physiol.* **235,** F321-30 (1978).

226. Amiel, C., Kuntziger, H., Couette, S., Coureau, C. & Bergounioux, N. Evidence for a parathyroid hormone independent calcium modulation of phosphate transport along the nephron. *J. Clin. Invest.* **57,** 256–263 (1976).

227. Murer, H., Hernando, N., Forster, I. & Biber, J. Proximal Tubular Phosphate Reabsorption : Molecular Mechanisms. *Physiol. Rev.* **80,** 1373–1409 (2000).

228. Haramati, A. Tubular capacity for phosphate reabsorption in superficial and deep nephrons. *Am. J. Physiol.* **248,** F729–F733 (1985).

229. Beck, L. *et al.* Targeted inactivation of Npt2 in mice leads to severe renal phosphate wasting, hypercalciuria, and skeletal abnormalities. *Proc. Natl. Acad. Sci.* **95,** 5372–5377 (1998).

230. Madjdpour, C., Bacic, D., Kaissling, B., Murer, H. & Biber, J. Segment-specific expression of sodium-phosphate cotransporters NaPi-IIa and -IIc and interacting proteins in mouse renal proximal tubules. *Pflügers Arch. Eur. J. Physiol.* **448,** 402–

410 (2004).

231. Miyamoto, K. I. *et al.* Sodium-dependent phosphate cotransporters: Lessons from gene knockout and mutation studies. *J. Pharm. Sci.* **100,** 3719–3730 (2011).

232. Segawa, H., Aranami, F., Kaneko, I., Tomoe, Y. & Miyamoto, K. The roles of Na/Pi-II transporters in phosphate metabolism. *Bone* **45,** S2–S7 (2009).

233. Lorenz-Depiereux, B. *et al.* Hereditary Hypophosphatemic Rickets with Hypercalciuria Is Caused by Mutations in the Sodium-Phosphate Cotransporter Gene SLC34A3. *Am. J. Hum. Genet.* **78,** 193–201 (2006).

234. Lapointe, J. Y. *et al.* NPT2a gene variation in calcium nephrolithiasis with renal phosphate leak. *Kidney Int.* **69,** 2261–7 (2006).

235. Schlingmann, K. P. *et al.* Autosomal-Recessive Mutations in SLC34A1 Encoding Sodium-Phosphate Cotransporter 2A Cause Idiopathic Infantile Hypercalcemia. *J. Am. Soc. Nephrol.* **27,** 604–614 (2016).

236. Magen, D. *et al.* A Loss-of-Function Mutation in NaPi-IIa and Renal Fanconi's Syndrome. *N Engl J Med* **362,** 1102–1109 (2010).

237. Blaine, J., Chonchol, M. & Levi, M. Renal Control of Calcium, Phosphate, and Magnesium Homeostasis. *Clin. J. Am. Soc. Nephrol.* **10,** 1257–1272 (2015).

238. Farrow, E. G., Davis, S. I., Summers, L. J. & White, K. E. Initial FGF23-mediated signaling occurs in the distal convoluted tubule. *J. Am. Soc. Nephrol.* **20,** 955–60 (2009).

239. Lee, D. B., Walling, M. W., Gafter, U., Silis, V. & Coburn, J. W. Calcium and inorganic phosphate transport in rat colon: dissociated response to 1,25-dihydroxyvitamin D3. *J. Clin. Invest.* **65,** 1326–1331 (1980).

240. Mchardy, G. J. R. & Parsons, D. S. The absorption of inorganic phosphate from the small intestine of the rat. *Exp. Physiol.* 398–409 (1956).

241. Danisi, G., Bonjour, J. P. & Straub, R. W. Regulation of Na-dependent phosphate influx across the mucosal border of duodenum by 1,25-dihydroxycholecalciferol. *Pflugers Arch. J. Physiol.* **388,** 227–232 (1980).

242. Hunter, M. F. *et al.* Hyperphosphataemia after enemas in childhood: Prevention and treatment. *Arch. Dis. Child.* **68,** 233–234 (1993).

243. Bronner, F. Mechanisms of intestinal calcium absorption. *J. Cell. Biochem.* **88,** 387–393 (2003).

244. Danisi, G. & Straub, R. W. Unidirectional influx of phosphate across the mucosal membrane of rabbit small intestine. *Pflügers Arch. Eur. J. Physiol.* **385,** 117–122 (1980).

245. Williams, K. B. & DeLuca, H. F. Characterization of intestinal phosphate absorption using a novel in vivo method. *Am. J. Physiol. Endocrinol. Metab.* **292,** E1917–E1921 (2007).

246. Candeal, E., Caldas, Y. A., Guillen, N., Levi, M. & Sorribas, V. Na+-independent phosphate transport in Caco2BBE cells. *AJP Cell Physiol.* **307,** C1113–C1122 (2014).

247. Labonte, E. D. *et al.* Gastrointestinal Inhibition of Sodium-Hydrogen Exchanger 3 Reduces Phosphorus Absorption and Protects against Vascular Calcification in CKD. *J. Am. Soc. Nephrol.* **26,** 1138–1149 (2015).

248. Katai, K. *et al.* Nicotinamide inhibits sodium-dependent phosphate cotransport activity in rat small intestine. *Nephrol. Dial. Transplant.* **14,** 1195–1201 (1999).

249. Takahashi, Y. *et al.* Nicotinamide suppresses hyperphosphatemia in hemodialysis patients. *Kidney Int.* **65,** 1099–1104 (2004).

250. Xu, H., Inouye, M., Missey, T., Collins, J. F. & Ghishan, F. K. Functional characterization of the human intestinal NaPi-IIb cotransporter in hamster fibroblasts and Xenopus oocytes. *Biochim. Biophys. Acta - Biomembr.* **1567,** 97–105 (2002).

251. Ikuta, K. *et al.* Effect of Npt2b deletion on intestinal and renal inorganic phosphate (Pi) handling. *Clin. Exp. Nephrol.* **22,** 517–528 (2018).

252. Danisi, G. & Murer, H. Inorganic Phosphate Absorption in Small Intestine - Comprehensive Physiology - Wiley Online Library. Handbook of Physiology: The Gastrointestinal system IV, 323–336 (1991).

253. Xu, H., Bai, L., Collins, J. F. & Ghishan, F. K. Molecular cloning, functional characterization, tissue distribution, and chromosomal localization of a human, small intestinal sodium-phosphate (Na+-Pi) transporter (SLC34A2). *Genomics* **62,** 281–4 (1999).

254. Fordtran, J. S., Rector, F. C., Ewtont, M. F., Soter, N. & Kinney, J. Permeability Characteristics of the Human Small Intestine. *J. Clin. Invest.* **44,** 1935–44 (1965).

255. Eto, N., Tomita, M. & Hayashi, M. NaPi-mediated transcellular permeation is the dominant route in intestinal inorganic phosphate absorption in rats. *Drug Metab. Pharmacokinet.* **21,** 217–221 (2006).

256. Tamura, A. *et al.* Loss of claudin-15, but not claudin-2, causes Na+deficiency and glucose malabsorption in mouse small intestine. *Gastroenterology* **140,** 913–923 (2011).

257. Fujita, H. *et al.* Tight junction proteins claudin-2 and -12 are critical for vitamin D-dependent Ca2+ absorption between enterocytes. *Mol. Biol. Cell* **19,** 1912–21 (2008).

258. Wongdee, K., Teerapornpuntakit, J., Siangpro, C., Chaipai, S. & Charoenphandhu, N. Duodenal villous hypertrophy and upregulation of claudin-15 protein expression in lactating rats. *J. Mol. Histol.* **44,** 103–109 (2013).

259. Rosenthal, R. *et al.* Claudin-2, a component of the tight junction, forms a paracellular water channel. *J. Cell Sci.* **123,** 1913–1921 (2010).

260. Chiba, H., Osanai, M., Murata, M., Kojima, T. & Sawada, N. Transmembrane proteins of tight junctions. *Biochim. Biophys. Acta Biomembr.* **1778,** 588–600 (2008).

261. Saitou, M. *et al.* Complex Phenotype of Mice Lacking Occludin, a Component of Tight Junction Strands. *Mol. Biol. Cell* **11,** 4131–4142 (2000).

262. Riazuddin, S. *et al.* Tricellulin Is a Tight-Junction Protein Necessary for Hearing. *Am. J. Hum. Genet.* **79,** 1040–1051 (2006).

263. Woodfin, A. *et al.* Junctional adhesion molecule-C (JAM-C) regulates polarized neutrophil transendothelial cell migration in vivo. *Nat. Immunol.* **12,** 761–769 (2011).

264. Lal-Nag, M. & Morin, P. The claudins. *Genome Biol.* **10,** 235 (2009).

265. Findley, M. K. & Koval, M. Regulation and roles for claudin-family tight junction proteins. *IUBMB Life* **61,** 431–437 (2009).

266. Krause, G. *et al.* Structure and function of claudins. *Biochim. Biophys. Acta - Biomembr.* **1778,** 631–645 (2008).

267. Amasheh, S., Fromm, M. & Günzel, D. Claudins of intestine and nephron - a correlation of molecular tight junction structure and barrier function. *Acta Physiol.* **201,** 133–140 (2011).

268. Markov, A. G., Veshnyakova, A., Fromm, M., Amasheh, M. & Amasheh, S. Segmental expression of claudin proteins correlates with tight junction barrier properties in rat intestine. *J. Comp. Biochem. Physiol. B* **180,** 591–598 (2010).

269. Alexandre, M. D., Lu, Q. & Chen, Y. H. Overexpression of claudin-7 decreases the paracellular Cl- conductance and increases the paracellular Na+ conductance in LLC-PK1 cells. *J. Cell Sci.* **118,** 2683–2693 (2005).

270. Luettig, J. *et al.* Claudin-2 as a mediator of leaky gut barrier during intestinal in fl ammation Claudin-2 as a mediator of leaky gut barrier during intestinal in fl ammation. *Tissue Barriers* **3,** e9771 (2014).

271. Rahner, C., Mitic, L. L. & Anderson, J. M. Heterogeneity in expression and subcellular localization of claudins 2, 3, 4, and 5 in the rat liver, pancreas, and gut. *Gastroenterology* **120,** 411–422 (2001).

272. Fujita, H. *et al.* Differential Expression and Subcellular Localization of Claudin-7, −8, −12, −13, and −15 Along the Mouse Intestine. *J. Histochem. Cytochem.* **54,** 933–944 (2006).

273. Lu, Z., Ding, L., Lu, Q. & Chen, Y. H. Claudins in intestines. *Tissue Barriers* **1,** e24978 (2013).

274. Zheng, G. *et al.* Chronic stress and intestinal barrier dysfunction: Glucocorticoid receptor and transcription repressor HES1 regulate tight junction protein Claudin-1 promoter. *Sci. Rep.* **7,** 4502 (2017).

275. Lameris, A. L. *et al.* Expression profiling of claudins in the human gastrointestinal tract in health and during inflammatory bowel disease. *Scand. J. Gastroenterol.* **48,** 58–69 (2013).

276. Holmes, J. L., Van Itallie, C. M., Rasmussen, J. E. & Anderson, J. M. Claudin profiling in the mouse during postnatal intestinal development and along the gastrointestinal tract reveals complex expression patterns. *Gene Expr. Patterns* **6,** 581–588 (2006).

277. Milatz, S. *et al.* Claudin-3 acts as a sealing component of the tight junction for ions of either charge and uncharged solutes. *Biochim. Biophys. Acta - Biomembr.* **1798,** 2048–2057 (2010).

278. Amasheh, S. *et al.* Contribution of claudin-5 to barrier properties in tight junctions of epithelial cells. *Cell Tissue Res.* **321,** 89–96 (2005).

279. Angelow, S., Kim, K. J. & Yu, A. S. L. Claudin-8 modulates paracellular permeability to acidic and basic ions in MDCK II cells. *J. Physiol.* **571,** 15–26 (2006).

280. Van Itallie, C., Rahner, C. & Anderson, J. M. Regulated expression of claudin-4 decreases paracellular conductance through a selective decrease in sodium permeability. *J. Clin. Invest.* **107,** 1319–1327 (2001).

281. Hou, J., Gomes, A. S., Paul, D. L. & Goodenough, D. A. Study of claudin function by RNA interference. *J. Biol. Chem.* **281,** 36117–36123 (2006).

282. Günzel, D. & Yu, A. S. L. Claudins and the Modulation of Tight Junction Permeability. *Physiol. Rev.* **93,** 525–569 (2013).

283. Garcia-hernandez, V., Quiros, M. & Nusrat, A. Intestinal epithelial claudins : expression and regulation in homeostasis and inflammation. *Ann. N. Y. Acad. Sci.* **1397,** 66–79 (2017).

284. Teerapornpuntakit, J., Wongdee, K., Thongbunchoo, J., Krishnamra, N. & Charoenphandhu, N. Proliferation and mRNA expression of absorptive villous cell markers and mineral transporters in prolactin-exposed IEC-6 intestinal crypt cells. *Cell Biochem. Funct.* **30,** 320–327 (2012).

285. Kutuzova, G. D. & DeLuca, H. F. Gene expression profiles in rat intestine identify pathways for 1,25-dihydroxyvitamin D 3 stimulated calcium absorption and clarify its immunomodulatory properties. *Arch. Biochem. Biophys.* **432,** 152–166 (2004).

286. Miyoshi, Y., Tanabe, S. & Suzuki, T. Cellular zinc is required for intestinal epithelial barrier maintenance via the regulation of claudin-3 and occludin expression. *Am. J. Physiol. - Gastrointest. Liver Physiol.* **311,** G105–G116 (2016).

287. Amasheh, M. *et al.* Quercetin enhances epithelial barrier function and increases claudin-4 expression in Caco-2 cells. *J Nutr* **138,** 1067–1073 (2008).

288. Amasheh, S. *et al.* Tight junction proteins as channel formers and barrier builders: Claudin-2, -5, and -8. *Ann. N. Y. Acad. Sci.* **1165,** 211–219 (2009).

289. Furuse, M. *et al.* Claudin-based tight junctions are crucial for the mammalian epidermal barrier: A lesson from claudin-1-deficient mice. *J. Cell Biol.* **156,** 1099–1111 (2002).

290. Tanaka, H. *et al.* Intestinal deletion of claudin-7 enhances paracellular organic solute flux and initiates colonic inflammation in mice. *Gut* **64,** 1529–1538 (2015).

291. Poon, C. E., Madawala, R. J., Day, M. L. & Murphy, C. R. Claudin 7 is reduced in uterine epithelial cells during early pregnancy in the rat. *Histochem. Cell Biol.* **139,** 583–593 (2013).

292. Günzel, D. Claudins: vital partners in transcellular and paracellular transport coupling. *Pflugers Arch. Eur. J. Physiol.* **469,** 35–44 (2017).

293. Wada, M., Tamura, A., Takahashi, N. & Tsukita, S. Loss of claudins 2 and 15 from mice causes defects in paracellular Na+flow and nutrient transport in gut and leads to death from malnutrition. *Gastroenterology* **144,** 369–380 (2013).

294. Pan, W. *et al.* The epithelial sodium/proton exchanger, NHE3, is necessary for renal and intestinal calcium (re)absorption. *AJP Ren. Physiol.* **302,** F943–F956 (2012).

295. Van Itallie, C. M. & Anderson, J. M. Claudins and Epithelial Paracellular Transport. *Annu. Rev. Physiol.* **68,** 403–429 (2006).

296. D'Souza, T., Agarwal, R. & Morin, P. J. Phosphorylation of Claudin-3 at threonine 192 by cAMP-dependent protein kinase regulates tight junction barrier function in ovarian cancer cells. *J. Biol. Chem.* **280,** 26233–26240 (2005).

297. Banan, A. *et al.* theta Isoform of protein kinase C alters barrier function in intestinal epithelium through modulation of distinct claudin isotypes: a novel mechanism for regulation of permeability. *J. Pharmacol. Exp. Ther.* **313,** 962–982 (2005).

298. Guillemot, L. & Citi, S. Cingulin Regulates Claudin-2 Expression and Cell Proliferation through the Small GTPase RhoA. *Mol. Biol. Cell* **17,** 3569–3577 (2006).

299. Murata, M. *et al.* Down-regulation of survival signaling through MAPK and Akt in occludin-deficient mouse hepatocytes in vitro. *Exp. Cell Res.* **310,** 140–151 (2005).

300. Shen, L., Weber, C. R., Raleigh, D. R., Yu, D. & Turner, J. R. Tight Junction Pore and Leak Pathways: A Dynamic Duo. *Annu Rev Physiol* **73,** 283–309 (2011).

301. Colegio, O. R., Van Itallie, C. M., McCrea, H. J., Rahner, C. & Anderson, J. M. Claudins create charge-selective channels in the paracellular pathway between epithelial cells. *Am. J. Physiol. Physiol.* **283,** C142–C147 (2002).

302. Tanaka, H. *et al.* Claudin-21 Has a Paracellular Channel Role at Tight Junctions. *Mol. Cell. Biol.* **36,** 954–964 (2016).

303. Li, J., Zhuo, M., Pei, L., Rajagopal, M. & Yu, A. S. L. Comprehensive cysteine-scanning mutagenesis reveals claudin-2 pore-lining residues with different intrapore locations. *J. Biol. Chem.* **289,** 6475–6484 (2014).

304. Fihn, B. M., Sjoqvist, A. & Jodal, M. Permeability of the rat small intestinal epithelium along the villus-crypt axis: Effects of glucose transport. *Gastroenterology* **119,** 1029–1036 (2000).

305. Wolf, M., Koch, T. A. & Bregman, D. B. Effects of iron deficiency anemia and its treatment on fibroblast growth factor 23 and phosphate homeostasis in women. *J. Bone Miner. Res.* **28,** 1793–1803 (2013).

306. David, V. *et al.* Inflammation and functional iron deficiency regulate fibroblast growth factor 23 production. *Kidney Int.* **89,** 135–146 (2016).

307. Clinkenbeard, E. L. *et al.* Neonatal Iron deficiency causes abnormal phosphate metabolism by elevating FGF23 in normal and ADHR Mice. *J. Bone Miner. Res.* **29,** 361–369 (2014).

308. Li, X. *et al.* Mouse Model of Iron Refractory Iron Deficiency Anemia (IRIDA) Exhibits Disrupted Phosphate Homeostasis, Elevated Circulating FGF23 Levels, and Increased Fgf23 Expression in Bone Marrow. *Blood* **130,** 228 (2017).

309. Imel, E. A. *et al.* Iron modifies plasma FGF23 differently in autosomal dominant hypophosphatemic rickets and healthy humans. *J. Clin. Endocrinol. Metab.* **96,** 3541–3549 (2011).

310. Farrow, E. G. *et al.* Iron deficiency drives an autosomal dominant hypophosphatemic rickets (ADHR) phenotype in fibroblast growth factor-23 (Fgf23) knock-in mice. *PNAS* **108,** E1146–E1155 (2011).

311. Gravesen, E., Hofman-Bang, J., Mace, M. L., Lewin, E. & Olgaard, K. High dose intravenous iron, mineral homeostasis and intact FGF23 in normal and uremic rats. *BMC Nephrol.* **14,** 281 (2013).

312. Jin, H. J., Lee, J. H. & Kim, M. K. The prevalence of vitamin D deficiency in iron-deficient and normal children under the age of 24 months. *Blood Res* **48,** 40–45 (2013).

313. Chan, S. *et al.* Phosphate binders in patients with chronic kidney disease. *Aust. Prescr.* **40,** 9–14 (2017).

314. Cannata-Andía, J. B. & Martin, K. J. The challenge of controlling phosphorus in chronic kidney disease. *Nephrol. Dial. Transplant.* **31,** 541–547 (2016).

315. Marks, J., Carvou, N. J. C., Debnam, E. S., Srai, S. K. & Unwin, R. J. Diabetes Increases Facilitative Glucose Uptake and GLUT2 Expression at the Rat Proximal Tubule Brush Border Membrane. *J. Physiol.* **553,** 137–145 (2003).

316. Bradford, M. M. A rapid and sensitive method for the quantitation of microgram quantities of protein utilizing the principle of protein-dye binding. *Anal. Biochem.* **72,** 248–254 (1976).

317. Forstner, G. G., Tanaka, K. & Isselbacher, K. J. Lipid composition of the isolated rat intestinal microvillus membrane. *Biochem. J.* **109,** 51–59 (1968).

318. Larsson, T. E. *et al.* NPT-IIb Inhibition Does Not Improve Hyperphosphatemia in CKD. *Kidney Int. Reports* **3,** 73–80 (2018).

319. Hernando, N. & Wagner, C. A. Mechanisms and regulation of intestinal phosphate absorption. *Compr. Physiol.* **8,** 1065–1090 (2018).

320. Borowitz, S. M. & Ghishan, F. K. Phosphate transport in human jejunal brush-border membrane vesicles. *Gastroenterology* **96,** 4–10 (1989).

321. Marks, J. The role of SLC34A2 in intestinal phosphate absorption and phosphate homeostasis. *Pflügers Arch* **471,** 165–173 (2018).

322. Wright, R. D., Blair-West, J. R., Nelson, J. F. & Tregear, G. W. Handling of phosphate by a parotid gland (ovine). *Am. J. Physiol.* **246,** F916-26 (1984).

323. Homann, V. *et al.* Sodium-phosphate cotransporter in human salivary glands: Molecular evidence for the involvement of NPT2b in acinar phosphate secretion and ductal phosphate reabsorption. *Arch. Oral Biol.* **50,** 759–768 (2005).

324. Shannon, I. L. & Feller, R. P. Parotid saliva flow rate, calcium, phosphorus, and magnesium concentrations in relation to dental caries experience in children. *Pediatr. Dent.* **1,** 16–20 (1979).

325. Delzer, P. R. & Meyer, R. A. Normal handling of phosphate in the salivary glands of X-linked hypophosphataemic mice. *Arch. Oral Biol.* **29,** 1009–1013 (1984).

326. Olaf, B. Intestinal chemistry: vii. The absorption of calcium and phosphorus in the small and large intestines. *J. Biol. Chem.* **70,** 51–58 (1926).

327. Manghat, P., Sodi, R. & Swaminathan, R. Phosphate homeostasis and disorders. *Ann. Clin. Biochem.* **51,** 631–656 (2014).

328. Ohi, A. *et al.* Inorganic phosphate homeostasis in sodium-dependent phosphate cotransporter Npt2b$^{+/-}$ mice. *Am. J. Physiol. Renal Physiol.* **301,** F1105-13 (2011).

329. Brown, A. J., Zhang, F. & Ritter, C. S. The vitamin D analog ED-71 is a potent regulator of intestinal phosphate absorption and NaPi-IIb. *Endocrinology* **153,** 5150–5156 (2012).

330. Marks, J., Debnam, E. S. & Unwin, R. J. The role of the gastrointestinal tract in phosphate homeostasis in health and chronic kidney disease. *Curr. Opin. Nephrol. Hypertens.* **22,** 481–7 (2013).

331. Nemeth, E. *et al.* Hepcidin Regulates Cellular Iron Efflux by Binding to Ferroportin and Inducing Its Internalization. *Science* **306,** 2090–2093 (2004).

332. De Domenico, I. *et al.* The molecular mechanism of hepcidin-mediated ferroportin down-regulation. *Mol. Biol. Cell* **18,** 2569–78 (2007).

333. Brasselagnel, C. *et al.* Intestinal DMT1 cotransporter is down-regulated by hepcidin via proteasome internalization and degradation. *Gastroenterology* **140,** 1261–1271 (2011).

334. McLean, E., Cogswell, M., Egli, I., Wojdyla, D. & De Benoist, B. Worldwide prevalence of anaemia, WHO Vitamin and Mineral Nutrition Information System, 1993-2005. *Public Health Nutr.* **12,** 444–454 (2009).

335. Bailey, R. L., West, K. P. & Black, R. E. The epidemiology of global micronutrient deficiencies. *Ann. Nutr. Metab.* **66,** 22–33 (2015).

336. de Benoist, B., McLean, E., Egli, I. & Cogswell, M. *Worldwide Prevalence of Anaemia 1993– 2005: WHO Global Database on Anaemia*. (2008).

337. Toxqui, L. & Vaquero, M. P. Chronic iron deficiency as an emerging risk factor for osteoporosis: A hypothesis. *Nutrients* **7,** 2324–2344 (2015).

338. Katsumata, S. I., Katsumata-Tsuboi, R., Uehara, M. & Suzuki, K. Severe iron deficiency decreases both bone formation and bone resorption in rats. *J. Nutr.* **139,** 238–243 (2009).

339. Katsumata, S. I., Tsuboi, R., Uehara, M. & Suzuki, K. Dietary Iron Deficiency Decreases Serum Osteocalcin Concentration and Bone Mineral Density in Rats. *Biosci. Biotechnol. Biochem.* **70,** 2547–2550 (2006).

340. Díaz-Castro, J. *et al.* Severe nutritional iron-deficiency anaemia has a negative effect on some bone turnover biomarkers in rats. *Eur. J. Nutr.* **51,** 241–247 (2012).

341. Medeiros, D. M., Stoecker, B., Plattner, A., Jennings, D. & Haub, M. Iron deficiency negatively affects vertebrae and femurs of rats independently of energy intake and body weight. *J Nutr* **134,** 3061–3067 (2004).

342. Hryszko, T., Rydzewska-Rosolowska, A., Brzosko, S., Koc-Zorawska, E. & Mysliwiec, M. Low Molecular Weight Iron Dextran Increases Fibroblast Growth Factor-23 Concentration, Together With Parathyroid Hormone Decrease in Hemodialyzed Patients. *Ther. Apher. Dial.* **16,** 146–151 (2012).

343. Schouten, B. J., Hunt, P. J., Livesey, J. H., Frampton, C. M. & Soule, S. G. FGF23 elevation and hypophosphatemia after intravenous iron polymaltose: A prospective study. *J. Clin. Endocrinol. Metab.* **94,** 2332–2337 (2009).

344. Smith, E. M. *et al.* High-dose vitamin D3 reduces circulating hepcidin concentrations: A pilot, randomized, double-blind, placebo-controlled trial in healthy adults. *Clin. Nutr.* **36,** 980–985 (2017).

345. Zughaier, S. M., Alvarez, J. A., Sloan, J. H., Konrad, R. J. & Tangpricha, V. The role of vitamin D in regulating the iron-hepcidin-ferroportin axis in monocytes. *J. Clin. Transl. Endocrinol.* **1,** e19–e25 (2014).

346. Collins, J. F., Franck, C. A., Kowdley, K. V. & Ghishan, F. K. Identification of differentially expressed genes in response to dietary iron deprivation in rat duodenum. *Am. J. Physiol. Gastrointest. Liver Physiol.* **288,** G964-71 (2005).

347. Collins, J. F. Gene chip analyses reveal differential genetic responses to iron deficiency in rat duodenum and jejunum. *Biol Res.* **39,** 25–37 (2006).

348. Walling, M. W. Intestinal Ca and phosphate transport: differential responses to vitamin D3 metabolites. *Am.J.Physiol.* **233 Vol. 6,** E488–E494 (1977).

349. Gómez-Ayala, A. E. *et al.* Effect of source of iron on duodenal absorption of iron, calcium, phosphorus, magnesium, copper and zinc in rats with ferropoenic anaemia. *Int. J. Vitam. Nutr. Res.* **67,** 106–114 (1997).

350. Bhattacharyya, N. *et al.* Mechanism of FGF23 processing in fibrous dysplasia. *J. Bone Miner. Res.* **27,** 1132–1141 (2012).

351. Bai, X. *et al.* CYP24 inhibition as a therapeutic target in FGF23-mediated renal phosphate wasting disorders. *J. Clin. Invest.* **126,** 667–680 (2016).

352. Hagag, A. A., El-shanshory, M. R. & El-enein, A. M. A. Parathyroid function in children with beta thalassemia and correlation with iron load. *Adv. Pediatr. Res.* 3–8 (2015).

353. Murer, H., Hernando, N., Forster, L. & Biber, J. Molecular mechanisms in proximal tubular and small intestinal phosphate reabsorption (plenary lecture). *Mol Membr Biol* **18,** 3–11 (2001).

354. Van Itallie, C. M. & Anderson, J. M. Architecture of tight junctions and principles of molecular composition. *Semin. Cell Dev. Biol.* **36,** 157–165 (2014).

355. Natoli, M. *et al.* Mechanisms of defence from Fe(II) toxicity in human intestinal Caco-2 cells. *Toxicol. Vitr.* **23,** 1510–1515 (2009).

356. Tandy, S. *et al.* Nramp2 expression is associated with pH-dependent iron uptake across the apical membrane of human intestinal Caco-2 cells. *J. Biol. Chem.* **275,** 1023–1029 (2000).

357. Mackenzie, B., Ujwal, M. L., Chang, M. H., Romero, M. F. & Hediger, M. A. Divalent metal-ion transporter DMT1 mediates both H+ -coupled Fe2+ transport and uncoupled fluxes. *Pflugers Arch. Eur. J. Physiol.* **451,** 544–558 (2006).

358. Gunshin, H. *et al.* Cloning and characterization of a mammalian proton-coupled metal-ion transporter. *Nature* **388,** 482–488 (1997).

359. Gabor Kottra & Eberhard Fromter. Functional properties of the paracellular pathway in some leaky epithelia. *J. exp. Biol* **106,** 217–229 (1983).

360. Masyuk, A. I., Marinelli, R. A. & LaRusso, N. F. Water transport by epithelia of the digestive tract. *Gastroenterology* **122,** 545–562 (2002).

361. Alexander, R. T., Rievaj, J. & Dimke, H. Paracellular calcium transport across renal and intestinal epithelia. *Biochem. cell Biol.* **92,** 467–80 (2014).

362. Diaz de Barboza, G., Guizzardi, S. & Tolosa de Talamoni, N. Molecular aspects of intestinal calcium absorption. *World J. Gastroenterol.* **21,** 7142–54 (2015).

363. Khanal, R. C. & Nemere, I. Regulation of intestinal calcium transport. *Annu. Rev. Nutr.* **28,** 179–196 (2008).

364. Christakos, S., Dhawan, P., Porta, A., Mady, L. J. & Seth, T. Vitamin D and intestinal calcium absorption. *Mol. Cell. Endocrinol.* **347,** 25–29 (2011).

365. Charoenphandhu, N. *et al.* Na+/H+exchanger 3 inhibitor diminishes hepcidin-enhanced duodenal calcium transport in hemizygous β-globin knockout thalassemic mice. *Mol. Cell. Biochem.* **427,** 201–208 (2017).

366. Kraidith, K. *et al.* Hepcidin and 1,25(OH) 2 D 3 effectively restore Ca 2+ transport in β-thalassemic mice: reciprocal phenomenon of Fe 2+ and Ca 2+ absorption. *Am. J. Physiol. - Endocrinol. Metab.* **311,** E214–E223 (2016).

367. Jiang, L., Garrick, M. D., Garrick, L. M., Zhao, L. & Collins, J. F. Divalent metal transporter 1 (Dmt1) Mediates Copper Transport in the Duodenum of Iron-Deficient Rats and When Overexpressed in Iron-Deprived HEK-293 Cells. *J. Nutr.* **143,** 1927–1933 (2013).

368. Charoenphandhu, N., Wongdee, K., Tudpor, K., Pandaranandaka, J. & Krishnamra, N. Chronic metabolic acidosis upregulated claudin mRNA expression in the duodenal enterocytes of female rats. *Life Sci.* **80,** 1729–1737 (2007).

369. Ogihara, H. *et al.* Immuno-localization of H+/peptide cotransporter in rat digestive tract. *Biochem. Biophys. Res. Commun.* **220,** 848–852 (1996).

370. Liao, Z. C. *et al.* Ferrous bisglycinate increased iron transportation through DMT1 and PepT1 in pig intestinal epithelial cells compared with ferrous sulphate. *J. Anim. Feed Sci.* **23,** 153–159 (2014).

371. Davis, G. R. *et al.* Absorption of phosphate in the jejunum of patients with chronic renal failure before and after correction of vitamin D deficiency. *Gastroenterology* **85,** 908–16 (1983).

372. Borowitz, S. M. & Granrud, G. S. Ontogeny of intestinal phosphate absorption in rabbits. *Am. J. Physiol.* **262,** G847-53 (1992).

373. Berner, W., Kinne, R. & Murer, H. Phosphate transport into brush-border membrane vesicles isolated from rat small intestine. *Biochem. J.* **160,** 467–474 (1976).

374. Kommalapati, A., Singhi, R. & Tella, S. H. Association Between Iron-Deficiency Anemia and Hypophosphatemia. *Am. J. Med.* **131,** e103–e104 (2018).

375. Kumar, A., Wermers, R. A. & Tebben, P. J. Iron Replacement As a Therapeutic Approach for Renal Phosphate Wasting With Associated Iron Deficiency. *AACE Clin. Case Reports* **3,** e260–e263 (2017).

376. Kapelari, K., Köhle, J., Kotzot, D. & Högler, W. Iron supplementation associated with loss of phenotype in autosomal dominant hypophosphatemic rickets. *J. Clin. Endocrinol. Metab.* **100,** 3388–3392 (2015).

377. Campos, M. S. *et al.* Interactions among iron, calcium, phosphorus and magnesium in the nutritionally iron-deficient rat. *Exp. Physiol.* **83,** 771–781 (1998).

378. Juan, D., Liptak, P. & Kenneygray, T. Absorption of inorganic phosphate in the human jejunum and its inhibition by salmon calcitonin. *J. Clin. Endocrinol. Metab.* **43,** 517–522 (1976).

379. Kiela, P. R. & Ghishan, F. K. Physiology of intestinal absorption and secretion. *Best Pr. Res Clin Gastroenterol.* **30,** 145–159 (2016).

380. Pan, M. L., Chen, L. R., Tsao, H. M. & Chen, K. H. Iron Deficiency Anemia as a Risk Factor for Osteoporosis in Taiwan: A Nationwide Population-Based Study. *Nutrients* **9,** 616: 10.3390/nu9060616 (2017).

381. Wolf, M. & White, K. E. Coupling fibroblast growth factor 23 production and cleavage: iron deficiency, rickets, and kidney disease. *Curr. Opin. Nephrol. Hypertens.* **23,** 411–9 (2014).

382. Fukumoto, S. Phosphate metabolism and vitamin D. *Bonekey Rep.* **3,** 497 (2014).

383. Bergwitz, C. & Jüppner, H. Regulation of phosphate homeostasis by PTH, vitamin D, and FGF23. *Annu. Rev. Med.* **61,** 91–104 (2010).

384. Aniteli, T. M. *et al.* Effect of variations in dietary Pi intake on intestinal Pi transporters (NaPi-IIb, PiT-1, and PiT-2) and phosphate-regulating factors (PTH, FGF-23, and MEPE). *Pflugers Arch. Eur. J. Physiol.* **470,** 623–632 (2018).

385. Terato, K., Hiramatsu, Y. & Yoshino, Y. Studies on Iron Absorption II. Transport Mechanism of Low Molecular Iron Chelate in Rat Intestine. *Acta Med. Scand.* **18,** 129–134 (1973).

386. Duthe, H. L. The Relative Importance of the Duodenum in the Intestinal Absorption of Iron. **10,** 59–68 (1964).

387. Fuqua, B. K., Vulpe, C. D. & Anderson, G. J. Intestinal iron absorption. *J. Trace Elem. Med. Biol.* **26,** 115–119 (2012).

388. Lewis, J. B. *et al.* Ferric Citrate Controls Phosphorus and Delivers Iron in Patients on Dialysis. *J. Am. Soc. Nephrol.* **26,** 493–503 (2015).

389. Floege, J. *et al.* One-year efficacy and safety of the iron-based phosphate binder sucroferric oxyhydroxide in patients on peritoneal dialysis. *Nephrol. Dial. Transplant.* **32,** 1918–1926 (2017).

390. Floege, J. *et al.* A phase III study of the efficacy and safety of a novel iron-based phosphate binder in dialysis patients. *Kidney Int.* **86,** 638–647 (2014).

391. Nakanishi, T., Hasuike, Y., Nanami, M., Yahiro, M. & Kuragano, T. Novel iron-containing phosphate binders and anemia treatment in CKD: Oral iron intake revisited. *Nephrol. Dial. Transplant.* **31,** 1588–1594 (2016).

392. Locatelli, F. & Del Vecchio, L. Iron-based phosphate binders: a paradigm shift in the treatment of hyperphosphatemic anemic CKD patients? *J. Nephrol.* **30,** 755–765 (2017).

393. Thomas, C. & Oates, P. S. IEC-6 Cells Are an Appropriate Model of Intestinal Iron Absorption in Rats. *J. Nutr.* **132,** 680–687 (2002).